Dissertation

submitted to the

Combined Faculty of Natural Sciences and Mathematics

of the Ruperto Carola University Heidelberg, Germany

for the degree of

Doctor of Natural Sciences

Presented by

M.Sc. Lorenzo Bulli

born in: Firenze, Italy

Oral examination: 10/04/2019

The role of nuclear envelope associated proteins in early HIV-1 infection steps

Referees: Prof. Dr. med. Hans-Georg Kräusslich

Dr. Marina Lusic

To my parents

1. Summary

There is increasing evidence that HIV-1 may interact with components associated with the nuclear envelope (NE) during the infection of dividing and non-dividing cells. This ensures correct nuclear import and integration, suggesting that NE may be of greater importance than is currently appreciated. Previous studies have shown that HIV-1 interacts with the nuclear pore complex, followed by nuclear import of the pre-integration complex and preferential integration into genomic areas that are topologically in close proximity to the inner nuclear membrane. To identify host proteins that may contribute to these processes, we performed an overexpression screen of known membrane-associated NE proteins. Two nuclear membrane associated proteins SUN1/UNC84A and SUN2/UNC84B, members of the Linker of Nucleoskeleton and Cytoskeleton complex, were shown to efficiently block nuclear import of certain HIV-1 laboratory strains (HIV-1NL4.3 and HIV-1IIIB) as well as natural strains upon overexpression. The amino-terminal 85-90 amino acid residues were identified as being required for the SUN1-mediated block and it was further demonstrated that the amino-terminal domains of SUN1 and SUN2 interact with HIV-1 in a capsid (CA)-specific way. To test whether depletion of endogenous SUN proteins causes differences in HIV-1 infection, SUN1-/- and SUN2-/- cells were generated with CRISPR/Cas9 and it was found that SUN1 absence did not have any detectable effect on HIV-1 infectivity, whereas the loss of SUN2 resulted in a modest suppressive effect in the accumulation of viral cDNA in the nucleus. The analysis with HIV-2 and other retroviruses suggests that *SUN2* gene disruption affects HIV-1 specifically and does not involve any unspecific block to nuclear import. This block to infection was further analyzed in U87MG CD4 / CXCR4 cells with shRNA-reduced SUN2 expression. In this case, the reduction of SUN2 levels resulted in a 5-fold decrease in HIV-1 infection after 24h, in comparison to control cells while infection increased to wild type levels 48h post infection. Overall, the data suggest that SUN2 may help promote the early stages of HIV-1 infection, while the contribution of SUN1 needs to be further investigated.

The role of the CA protein and its connection to IFN-α-induced suppression was also investigated, by analyzing the infectivities of HIV-1 CA mutants N74D,

A105T, as well as P90A. Despite their relative resistance to ectopically expressed MX2, these CA mutants showed an increased sensitivity to the IFN-α-induced post entry block, which was not dependent on MX2 antiviral activity. The data suggests that CA protein and the capsid core may protect incoming HIV-1 nucleic acids not only from being detected by cytoplasmic DNA sensors, but also from IFN-α-induced effectors, thereby providing dual protection against host defense mechanism.

2. Zusammenfassung

Es gibt immer mehr Hinweise darauf, dass das humane Immundefizienzvirus Typ 1 (HIV-1) während der Infektion von sich-teilenden, sowie ruhenden Zellen mit Komponenten der nuklearen Membran interagiert um den sicheren Kernimport, sowie die korrekte Integration seines Genoms zu gewährleisten. Frühere Studien zeigten bereits die Interaktion von HIV-1 Proteinen mit Proteinen des Kernporenkomplexes, gefolgt vom nuklearen Import, sowie Integration in transkriptionell aktiven Genomregionen, welche topologisch in der Nähe der Kernmembran lokalisieren. Um Wirtsproteine zu identifizieren, die dabei eine Rolle spielen könnten, haben wir einen Überexpressions-Screen von Proteinen durchgeführt, welche mit der Kernmembran assoziiert sind. Dabei identifizierten wir zwei Proteine der inneren Kernmembran, SUN1/UNC84A, sowie SUN2/UNC84B, Komponenten des sogenannten LINC Komplexes, welche sehr effizient die Infektion mit HIV-1 Laborstämmen NL4.3 und IIIB, sowie einigen natürlich vorkommenden Stämmen nach Überexpression blockieren. Die aminoterminalen 85-90 Aminosäuren waren dabei essentiell für den Block durch SUN1 und wir zeigen weiterhin, dass diese Domainen von SUN1 und SUN2 mit HIV-1 CA interagieren können. Um zu testen ob endogenes SUN1 oder SUN2 wichtig sind für die frühen Infektionsschritte von HIV-1, generierten wir SUN1-/-, sowie SUN2-/- knock-out Zelllinien durch CRISPR/Cas9 Technologie. Das Fehlen von SUN1 hatte keinen detektierbaren Effekt auf die ersten Infektionsschritte von HIV-1, wobei das Fehlen von SUN2 die HIV-1 Infektion und insbesondere die Akkumulation von viraler DNA im Nukleus moderat reduzierte. Dieser Effekt konnte in verschiedenen Zellmodellen gezeigt werden, z.B. THP-1 und U87MG, über knock-out durch CRISPR/Cas9, sowie shRNAs-induzierte Reduktion der Expression. Die

Resultate schliessen auf einen Defekt im Kerntransport von HIV-1 wenn SUN2 abwesend ist, sowie eine dadurch resultierende Reduktion von Integrationsereignissen. Zusammenfassend scheint SUN2 die HIV-1 Infektion zu fördern, wobei die Rolle von SUN1 im Moment noch unklar ist und weiterer Studien bedarf.

Die Rolle des CA Proteins von HIV-1, sowie eine mögliche Verbindung zur IFN-alpha induzierten frühen Suppression der HIV-1 Infektion wurde ebenfalls untersucht. Dabei wurden verschiedene CA Mutanten (P90A, N74D, sowie A105T) analysiert. Erstaunlicherweise, trotz ihrer relative Resistenz gegenüber ektopischer Expression des IFN-induzierten Restriktionsfaktors MX2, waren all diese CA Mutanten hypersensitiv gegenüber IFN-alpha Behandlung, unabhängig von MX2. Die Resultate lassen darauf schliessen, dass CA nicht nur, wie bereits vorher beschrieben das virale Genom vor Wirtszellfaktoren schützt, welche die virale Nukleinsäure erkennen und eine antivirale Reaktion der Zellen hervorrufen, sondern auch beteiligt daran ist, das Virus vor eben diesen IFN-induzierten Restriktionsfaktoren zu schützen. Zukünftige Studien sollten darauf zielen, diese Wirtsfaktoren zu identifizieren und Strategien zu entwickeln, wie diese anti-HIV Faktoren als therapeutisches Mittel genutzt werden können.

Table of contents

1. Summary ..... **I**

2. Zusammenfassung ..... **II**

Table of contents **1**

3. Introduction **1**

3.1. Human immunodeficiency virus (HIV) 1

3.1.1. Discovery of HIV as the cause of AIDS 1

3.1.2. Retroviridae family and HIV classification 3

3.1.3. Genome organization and structure of HIV-1 4

3.2. HIV-1 replication 9

3.2.1. Attachment of HIV-1 and cell entry 11

3.2.3. Trafficking toward the nucleus and reverse transcription of HIV-1 13

3.2.4. Nuclear import of HIV-1 PICs 14

3.2.5. Integration of HIV-1 DNA into the host genome 18

3.3. HIV-1 and host immunity 21

3.3.1. Innate immunity against retroviruses 21

3.4. Nuclear envelope: structure and function 25

3.4.1. Nuclear envelope and HIV-1 25

4. Objective of the study **27**

5. Materials and Methods **29**

5.1. Materials 29

5.1.1. Laboratory equipment 29

5.1.2. Laboratory materials 30

5.1.3. Kits 31

5.1.4. Chemicals and reagents 31

5.1.5. Buffers and solutions 33

5.1.6. Bacterial Strains and bacterial culture media 34

5.1.7. Cells and cell culture media 35

5.1.8. Enzymes 36

5.1.9. Plasmid 36

5.1.10. Primers 39

5.1.11. TaqMan qPCR primer/ probes/ standards 44

5.1.12. Generated plasmids 44

5.1.13. Antibodies 48

5.1.14. Software 49
5.2. Molecular biology methods 49
5.2.1. Bacteria and DNA preparation 49
5.2.2. Polymerase Chain Reaction (PCR) 50
5.2.3. PCR-based mutagenesis 51
5.2.4. Separation of DNA by agarose gel electrophoresis 52
5.2.5. Analysis of DNA with restriction enzymes 52
5.2.6. Ligation 53
5.2.7. Cloning of shRNAs into retroviral vector pSIREN RetroQ 53
5.2.8. Cloning of gRNAs into retroviral vector plentiCRISPRv2 53
5.3. Cell biology and virology methods 54
5.3.1. Cell culture and freezing/thawing of cell lines 54
5.3.2. Virus and vector preparation 55
5.3.3. Transduction of cells with VSV-G-pseudotyped HIV-1 LV 56
5.3.4. Infectivity assays 57
5.3.5. Measurement of RT activity: SG-PERT 58
5.3.6. TaqMan qPCR 58
5.4. Biochemistry methods 60
5.4.1. SDS-polyacrylamide-gel electrophoresis (SDS-PAGE) 60
5.4.2. Western Blot 61
5.4.3. CANC pulldown 61
5.5. Imaging methods 62
5.5.1. Immunofluorescence and confocal microscopy 62
6. Results 63
6.1. The role of inner nuclear membrane proteins SUN1 and SUN2 in early HIV-1 infection steps 63
6.1.1. An overexpression screen of NE-associated proteins identifies SUN1 and SUN2 as HIV-1 interactors 63
6.1.2. Overexpression of SUN1 or SUN2 block full-length HIV-1 NL4.3GFP 67
6.1.3. Overexpression of SUN1 and SUN2 reduces HIV-1 2-LTR circle accumulation 68
6.1.4. Overexpression of SUN1 and SUN2 inhibits HIV-1 and HIV-2 infection but not other lentiviruses 70
6.1.5. Differential susceptibility of HIV-1 strains to SUN1 and SUN2 mediated inhibition. 71
6.1.6. HIV-1 capsid protein determines sensitivity to SUN1-mediated inhibition 73
6.1.7. *In vitro*-assembled HIV-1 CANC complexes interact with SUN1 and SUN2 76
6.1.8. The amino-terminal domain of SUN1 mediates HIV-1 inhibition 78
6.1.9. The amino-terminal domain of SUN2 mediates HIV-1 inhibition 84

6.1.10. CRISPR/Cas9-mediated *SUN2* but not *SUN1* gene disruption decreases HIV-1 infectivity in THP-1 cells 88
6.1.11. Nuclear import is impaired in SUN2 CRISPR/Cas9 THP-1 cells 91
6.1.12. SUN2 shRNA-mediated knockdown in CRISPR/Cas9 *SUN1*-depleted THP-1 cells decreases HIV-1 infectivity 92
6.1.13. SUN2 shRNA-mediated knockdown in U87MG CD4/CXCR4 cells decreases HIV-1 infectivity after 24h 93
6.1.14. CRISPR/Cas9-mediated *SUN1* or *SUN2* gene disruption does not decreases HIV-1 infectivity in Jurkat TAg cells 93
6.1.15. SUN1 and SUN2 are not required for the CypA Restriction in THP-1 cells and Jurkat TAg cells 96
6.2. The role of CA protein during IFN-α-induced suppression of HIV-1 infection 99
6.2.1. Determinants of the MX2 antiviral activity and the role of GTPase domain 99
6.2.2. HIV-1 CA mutants N74D or P90A display enhanced sensitivity to IFN-α-induced blocks 101
6.2.3. The increased sensitivity of HIV-1 CA mutants to IFN-α induced blocks is independent of MX2 102
6.2.4. IFN-α induces an enhanced block to reverse transcription and nuclear import of HIV-1 CA N74D 104
7. Discussion and perspectives 106
7.1. The role of inner nuclear membrane proteins SUN1 and SUN2 in early HIV-1 infection steps 106
7.2. The role of CA protein during IFN-α-induced suppression of HIV-1 infection 114
8. Conclusion 116
9. Abbreviations 117
10. Index 121
10.1. Figures 121
10.2 Tables 123
11. Publications and contributions 124
11.1. Publications 124
11.2. Conference contributions 124
12. References 125
13. Acknowledgements 144

3. Introduction

3.1. Human immunodeficiency virus (HIV)

3.1.1. Discovery of HIV as the cause of AIDS

Human immunodeficiency virus (HIV) is the etiologic agent of acquired immunodeficiency syndrome (AIDS), a condition characterized by a progressive failure of the immune system that leads to opportunistic infections and even cancer. HIV infection occurs by body fluid contact, i.e., blood, semen, vaginal fluid, pre-ejaculate and breast milk, where the virus is present as both free virus particles and within infected cells. For this reason, the main routes of transmission are unsafe sex, contaminated needles, breastfeeding and perinatal transmission [1]. AIDS was first clinically recognized in 1981 in the USA, when an increasing numbers of young homosexual men died following unusual opportunistic infections and rare malignancies [2].

In 1983, Francoise Barré-Sinoussi, Jean-Claude Chermann and Luc Montagnier from the Institute Pasteur in Paris identified and isolated, from the lymph node of a patient suffering from persistent generalized lymphadenopathy, a T-lymphotropic retrovirus [3]. The isolate, named as LAV_{BRU}, replicated very poorly in cell culture and was contaminated by a more rapidly and robustly replicating second AIDS isolate, named LAV_{LAI}. Without knowing about this contamination, Luc Montagnier sent his first isolate LAV_{BRU} to other labs including the lab of Robert Gallo at the U.S. National Institute of Health. On May 4, 1984, Gallo and his collaborators reported the isolation of a T-cell tropic retrovirus robustly replicating in cell culture, named human T-cell lymphotropic virus type III (HTLV-III), which subsequently was identified to be identical to the isolate LAV_{LAI} [4]. Assignment of priority for the discovery of HIV has been controversial. Montagnier's group had published their discovery a year and a half earlier than Gallo, but they reported that HIV's role in causing AIDS "remains to be determined”[5], whereas Gallo's group also demonstrated that the virus was the cause of AIDS. Furthermore, Gallo's lab developed the techniques for growing T cells and for virus isolation in the lab, used also by Montagniers’s lab [6] and that made the discovery possible. Subsequently, the chain of events was reconstructed by Simon Wain-Hobson’s lab [7] and in 2008 Barré-Sinoussi and Montagnier obtained the Nobel Prize for Medicine for their

discovery. In 1986, the new virus was called human immunodeficiency virus because of its relatedness with a group of known lentiviruses. In 1986, a second distantly related human immunodeficiency virus (HIV-2) was isolated from AIDS patients in West Africa. HIV-2 displayed the same modes of transmission as HIV-1 and was also associated with the development of AIDS and similar opportunistic infections, however in fewer numbers of infected people compared to HIV-1. Since HIV-1 is more virulent and has a higher transmission rate, it is the primary agent of AIDS worldwide while HIV-2 is restricted to Western and Central Africa [8].

HIV infection is now at a pandemic scale and a major global public health issue (Fig. 1). By the end of 2017, HIV affected approximately 36.9 million people and caused more than 35 million deaths worldwide. In the same year, 1.8 million new infections were reported and a total of 940000 people died due to HIV-related causes. Of all the HIV-infected patients, 17 million were on antiretroviral treatment [9]. The treatment relies on highly active antiretroviral therapy (HAART), which is a cocktail of at least three drugs targeting early stages of HIV-1 replication, thereby decreasing the viral load of the patient [10]. Due to its impact on human health and society, HIV-1 is the most extensively studied lentivirus today but is still only partially understood.

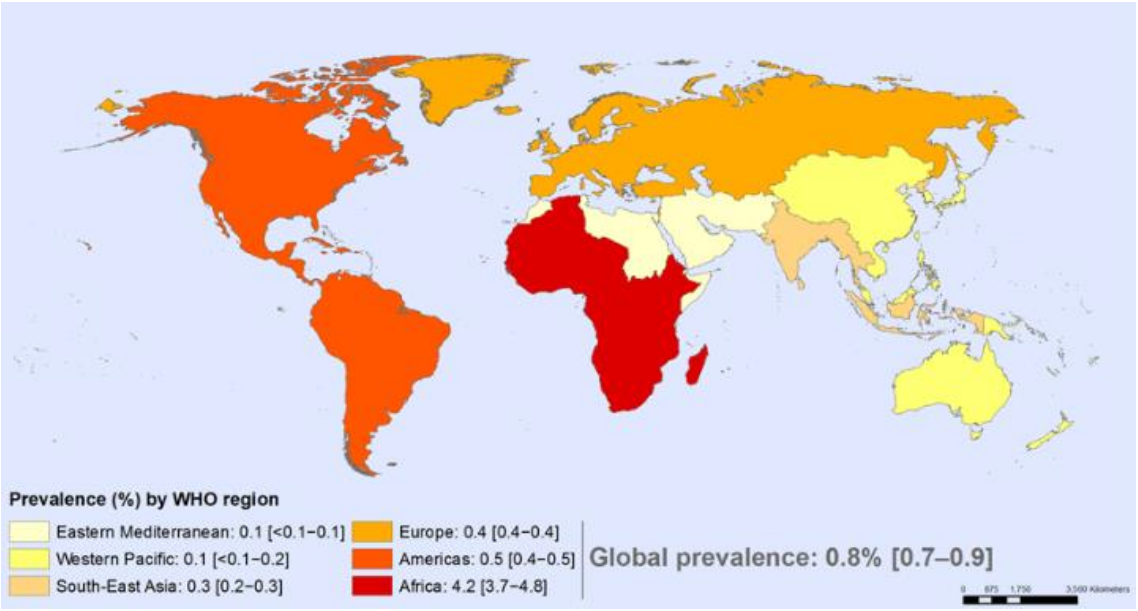

Figure 1. *Worldwide Human Immunodeficiency Virus (HIV) prevalence in adults aged 15 to 49, in 2017*. Figure adapted from [9]

3.1.2. Retroviridae family and HIV classification

HIV is an enveloped retrovirus, belonging to *Lentivirus* subgroup of the *Retroviridae* family. Viruses from the *Retroviridae* family display genomes that vary in complexity (Table 1). The *Alpharetrovirus*, *Betaretrovirus*, *Epsilonretrovirus* and *Gammaretrovirus* subgroups are characterized by a simple genome composed of the three main coding regions: *gag* (group specific antigen), *pol* (polymerase) and *env* (envelope), whereas *Lentiviruses, Spumaviruses* and *Deltaretrovirus* subgroups display more complex genomes that additionally code for a series of accessory proteins that are generated by multiple splicing [11-13]. Reverse transcription of the viral RNA genome by the viral enzyme Reverse Transcriptase (RT) represents the uniting feature of the family of *Retroviridae* [14, 15]. HIV-1 strains are classified in four groups: group M (main), group O (outlier), group N (non-M/non O) and group P. HIV-1 group M occurs worldwide and responsible for the majority of the global HIV epidemic, whereas HIV-1 groups N, O and P are confined to West-Central Africa. Similarly, HIV-2 strains are also classified in groups A-H [2], all confined to Western and Central Africa [8]. Each group of HIV-1 originated from independent transmission events across species from simian immunodeficiency virus (SIV) to humans [16]. A recently published study suggests that transmission of the HIV-1 group M to humans probably happened in the early 1900s and the origin of the AIDS pandemic has been traced to the 1920s in the city of Kinshasa, Democratic Republic of Congo [17]. This area is known for many of the first registered cases of AIDS and for having a large genetic diversity in HIV strains, suggesting that SIV was transmitted to humans a number of different times [18]. Around 1960s, rapid population growth, rail link developments and emigration enabled the virus to spread to different regions. It is believed that the HIV-1 epidemic crossed the Atlantic and entered the USA around 1970s, via New York City, from a pre-existing Caribbean epidemic [19]. Although its relatedness to HIV-1 was only discovered in 1986 [20], one of the oldest known lentiviruses is the equine infectious anaemia virus (EIAV), discovered in 1904 as a filterable agent causing autoimmune haemolytic anaemia in horses [21]. After the discovery of HIV, similar lentiviruses were identified in cats and in diverse non-human primates, respectively named feline

immunodeficiency virus (FIV) [22] and simian immunodeficiency virus (SIV) [23-26].

Table 1. Classification of retroviruses by genera and genome type. *Simple genome retroviruses have gag, pol and env genes, which encode matrix, capsid, nucleoprotein, integrase, protease, reverse transcriptase and Env proteins. Complex genome retroviruses additionally have regulatory and accessory genes, which encode proteins that increase their infection and replication abilities. Gag expression vectors from bold highlighted viruses have been analyzed in this study*

Genera	Species	Genome type
Alpharetrovirus	Avian leukosis virus Rous sarcoma virus	Simple
Betaretrovirus	Mouse mammary tumour virus Mazon-Pfizer monkey virus	Simple
Deltaretrovirus	Human T-Lymphotropic virus Bovine leukaemia virus	Complex
Epsilonretrovirus	Wallabee dermal sarcoma virus	Simple
Gammaretrovirus	**Murine leukaemia virus** Feline leukaemia virus	Simple
Lentivirus	**Human immunodeficiency virus 1** **Human immunodeficiency virus 2** **Simian immunodeficiency virus** **Equine infectious anemia virus** **Feline immunodeficiency virus**	Complex
Spumavirus	Human foamy virus	Complex

3.1.3. Genome organization and structure of HIV-1

The HIV-1 genome consists of two copies of positive sense unspliced single stranded RNA. Like cellular mRNAs, both viral RNA molecules are 5’ capped with 7-methylguanosine and possess a 3’ polyA tail. They are around 10kb in length and able to dimerize through their dimer initiation sites [27]. The viral genomic RNAs are packaged into the nascent HIV-1 particles during replication and are the template for reverse transcription in infected cells, generating viral DNA that is integrated into the host genome establishing a provirus. They contain *cis*-acting elements like the trans-activating responsive region (TAR), the Rev responsive element (RRE), the primer binding site (PBS), packaging signal (Ψ), a 3’ and the central polypurine tracts (PPT), that are required for different steps during the virus life cycle. The viral genome (Fig. 2) consists of three structural genes (*gag*, *pol* and *env*), two regulatory genes (*tat*, *rev*) and four accessory genes (*nef*, *vif*, *vpr* and *vpu*). There are two long terminal repeat sequences (LTRs) of about 600 nucleotides at the 5' and 3' ends, each

composed of three subregions (U3, R, and U5), which have an essential role in reverse transcription and integration of the viral genome into host DNA. The 5' LTR also contains promoter elements that drive transcription, while both the sequences are characterized by complementary regions at the 5' and 3' termini that serve as self-priming sequences during the reverse transcription process [28]. All the proteins are expressed from different splice forms of a single RNA transcript and are important for a natural occurring infection.

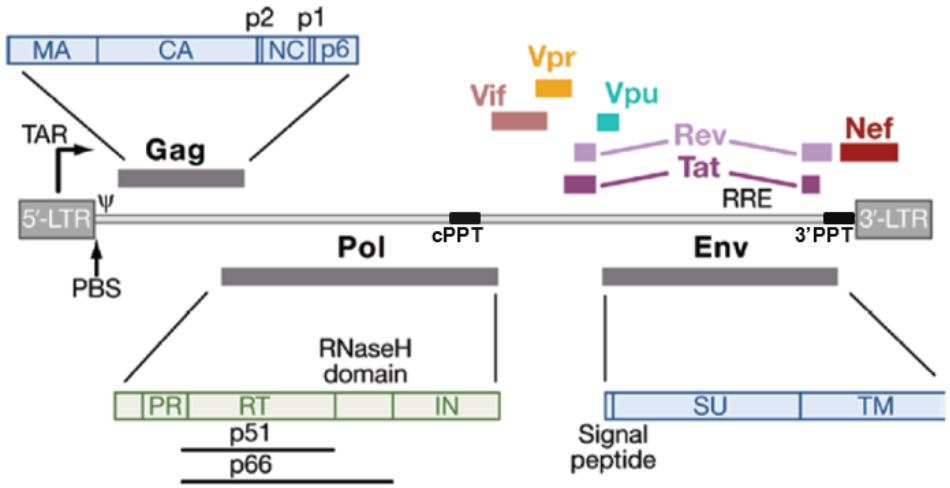

Figure 2. Genome organization of HIV-1. *Structural genes (gag, pol and env), two regulatory genes (tat, rev) and four accessory genes (nef, vif, vpr and vpu). The gag gene comprises MA (p17), CA (p24), NC (p7) and p6. The pol gene comprises RT (p66/51), RNAse H (p15) and IN (p31). The env gene comprises SU (gp120) and TM (gp41), the two components of viral Env protein. Viral cis acting elements include the two long terminal repeats (LTR's), the trans-activating responsive region (TAR) required for Tat binding and transcription activation, the Rev responsive element (RRE) required for Rev binding and nuclear export of partially spliced and unspliced RNAs, the primer binding site (PBS), RNA packaging signal (Ψ), a 3' and the central polypurine tracts (PPT).* Figures derived from [28]

The *gag* gene encodes a 55kDa precursor polyprotein Gag (group-specific antigen) that comprises independently folded domains connected by flexible linkers: matrix (MA), capsid (CA), nucleocapsid (NC) and p6. Two spacer peptides are located between CA and NC (SP1) and between NC and p6 (SP2) (Fig 3A) [29]. Every domain of Gag fulfills a variety of functions during the viral replication cycle. MA protein (p17) contains a highly basic region (HBR) [30, 31] and a co-translationally attached myristoyl residue, both required for membrane targeting and binding [32-35]. Furthermore, MA is also responsible for the incorporation of the Env glycoprotein spikes into viral particles [36-38]. CA protein (p24) drives Gag assembly, builds the viral core in mature particles and regulates the import of the viral genome into the nucleus of infected cells [39]. The protein is composed of two domains, the amino-terminal domain (CA-NTD)

and the carboxy-terminal domain (CA-CTD) connected by a flexible hinge region. The CA-NTD is formed by six to seven α-helices and a flexible loop region involved in binding of cellular host factors, like cyclophilin A (CypA) [40]. The CA-CTD is constituted by four α-helices and contains the major homology region (MHR), a stretch of approximately 20 well conserved residues that represents the second most conserved region of retroviruses after RT [41]. NC (p7) is a nucleic acid binding protein composed of a domain containing positively charged regions and one or two zinc-finger like motifs required for recruiting and binding of viral RNA [42]. It also has a nucleic acid chaperone activity [43]. Phosphoprotein p6 is responsible for the recruitment of the ESCRT (endosomal complex required for transport) machinery during particle release and incorporates Vpr into the virion [44].

The *pol* gene encodes enzymes that are necessary for viral replication: protease (PR), reverse transcriptase (RT) and integrase (IN). For the expression of the *pol* gene, HIV-1 utilizes a programmed ribosomal frameshifting that occurs at the slippery site in the p6 sequence, allowing the translation to continue to *pol* and generate the 160kDa GagPol polyprotein. This mechanism permits the virus to translate structural and enzymatic domains in a defined proportion required for replication [45]. PR is active as a dimer and mediates the proteolytic maturation of newly formed HIV-1 particles by cleaving Gag at five and GagPol at nine distinct positions, leading to a complete remodelling of the virus architecture [46, 47]. The order of cleavage is conserved and starts with processing between SP1 and NC and ends with removal of the SP1 peptide from CA [48, 49], which triggers rearrangement of an immature lattice into the final mature conical shape (Fig. 3B) [50]. Proteolytic processing of viral polyproteins is essential for HIV-1 infectivity [32, 51, 52]. RT is the enzyme essential for generating viral double-stranded cDNA from the single-stranded genomic RNA template, in a process named reverse transcription. This enzyme acts as an asymmetric p51/ p66 heterodimer and has three activities: RNA-dependent DNA polymerase activity, RNaseH activity for RNA digestion and DNA-dependent DNA polymerase activity [53]. IN is the enzyme required for the viral genomic cDNA to be integrated into the host cell genome, establishing the provirus. The enzyme acts as tetramer and consists of an amino-terminal zinc-binding domain that probably supports the

multimerisation, a central catalytic domain and a carboxy-terminal DNA binding domain that associates non-specifically with DNA [54].

The *env* gene encodes the precursor polyprotein gp160, which is synthesised in the rough endoplasmic reticulum where it is heavily glycosylated at asparagine residues. Gp160 then transits the Golgi apparatus where the mannose glycosylation is further refined [55, 56] and is cleaved by cellular protease furin into surface glycoprotein (SU or gp120) and transmembrane protein (TM or gp41) [57, 58]. Mutations that alter the cleavage of the precursor polyprotein gp160 or that alter the association of the gp120 and gp41 subunits render HIV 1 non infectious [59]. Both proteins remain non-covalently attached and are transferred to the plasma membrane where three gp120 and two gp41 glycoproteins combine in a trimer of heterodimers to form the envelope spike (Fig. 3B). Each newly formed virion incorporates between 10 and 100 trimers of gp120/gp41, depending on the isolate [60]. Gp120 protein domain is responsible for target-cell recognition and viral tropism and was one of the first targets of HIV vaccine research, but the conserved regions shielded by variable loops and the extensive glycosylation makes the neutralization by antibodies extremely difficult [61]. The glycoprotein gp41 anchors Env in the viral membrane and promotes fusion of the viral and target cell membranes [62].

In addition to the structural proteins and viral enzymes, HIV-1 encodes accessory proteins Vpu, Vif, Vpr and Nef, which interact with diverse host factors at different stages of the viral life cycle (Fig. 9) with the aim to contrast their antiviral activity and promote the infection [63]. Furthermore, Tat and Rev are encoded which are required for viral transcription and export of mRNA from the cellular nucleus, respectively [64].

HIV forms spherical particles with a diameter of about 120-140 nm that are enveloped by a phospholipid bilayer membrane derived from the host cell plasma membrane. Viral particles released from infected cells are in an immature and non-infectious state, where together with GagPol forms a curved hexameric lattice underneath the viral envelope, in which MA interacts with the membrane, CA forms important protein–protein lattice contacts and NC, bound to the viral genome, is located toward the center of the particle. The released immature Gag shell comprises a large gap that define the shape of a truncated spherical structure (Fig. 3B) [65-67]. Proteolytic processing of Gag and Gag-Pol

during viral maturation, leads to a rearrangement of the single structural proteins where MA remains associated with the viral envelope, whereas NC and the vRNA form a condensed ribonucleoprotein complex surrounded by the CA cone-shaped core (Fig. 3B) [46, 47]. Only through the maturation process the HIV-1 particle acquires infectivity and a new virion is born [32, 51, 52].

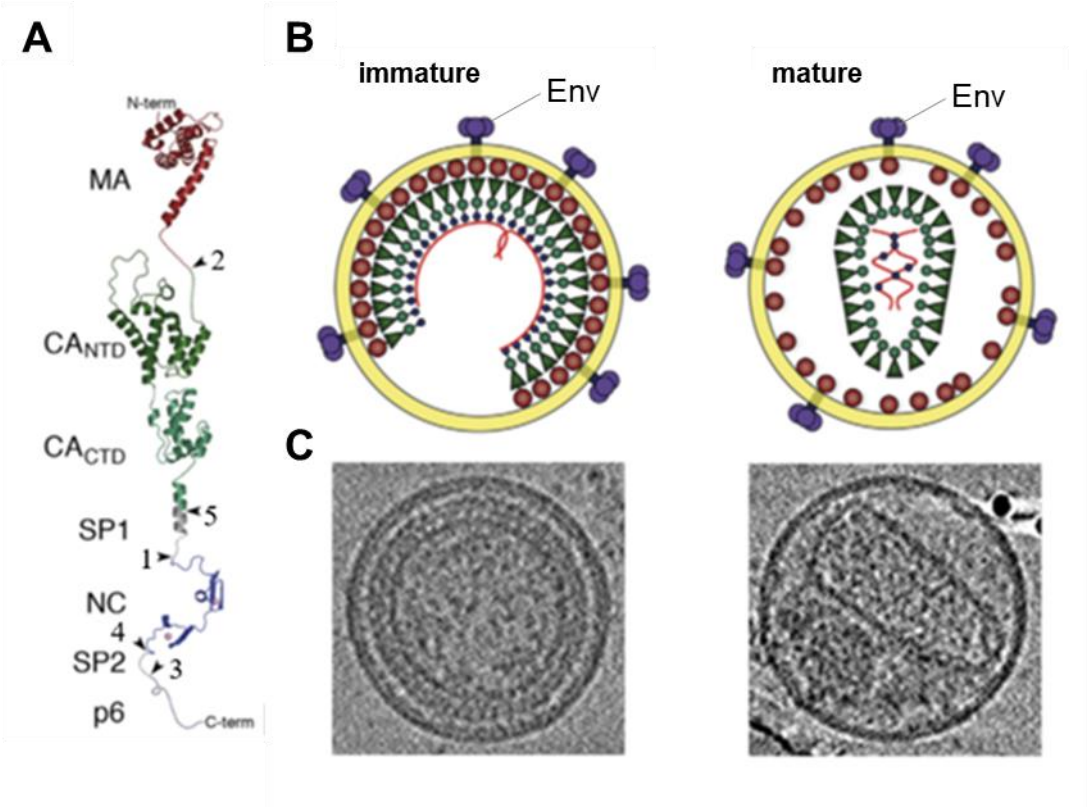

Figure 3. Structure of HIV-1. A) *HIV-1 Gag polyprotein domain structure, showing the locations of MA, CANTD, CACTD, SP1, NC, SP2, and p6. Arrows indicate the PR cleavage sites and numbers show the order of cleavage.* **B)** *After budding from the plasma membrane, immature HIV-1 particles contain uncleaved Gag and GagPol proteins. The viral RNA dimer is associated with the NC domain of Gag. In mature virions, MA remains associated with the viral lipid envelope, NC coats the viral RNA genome, and the liberated CA proteins reassemble into the mature conical capsid enclosing viral genomic RNA and enzymes.* **C)** *Cryo-EM tomograms showing the central slice of an immature and mature HIV-1 particle* [47]. *Gag subunits in illustrations are color-coded according to (A).* Figure adapted from [68]

3.2. HIV-1 replication

The life cycle of HIV-1 (Fig. 4) can be divided in an early and a late phase. During the early phase, the virus infects and integrates the viral genomic DNA into the target cell genome establishing the provirus. In the subsequent late phase, the virus employs and manipulates the transcriptional and translational machinery of the host cell to produce the progeny virus particles. The typical characteristic of lentiviruses is that they cause persistent infections, characterized by a latent state between the two life cycle phases during which the integrated virus genome is silenced but conserves the potential to reactivate, resume replication and produce new infective viral particles.

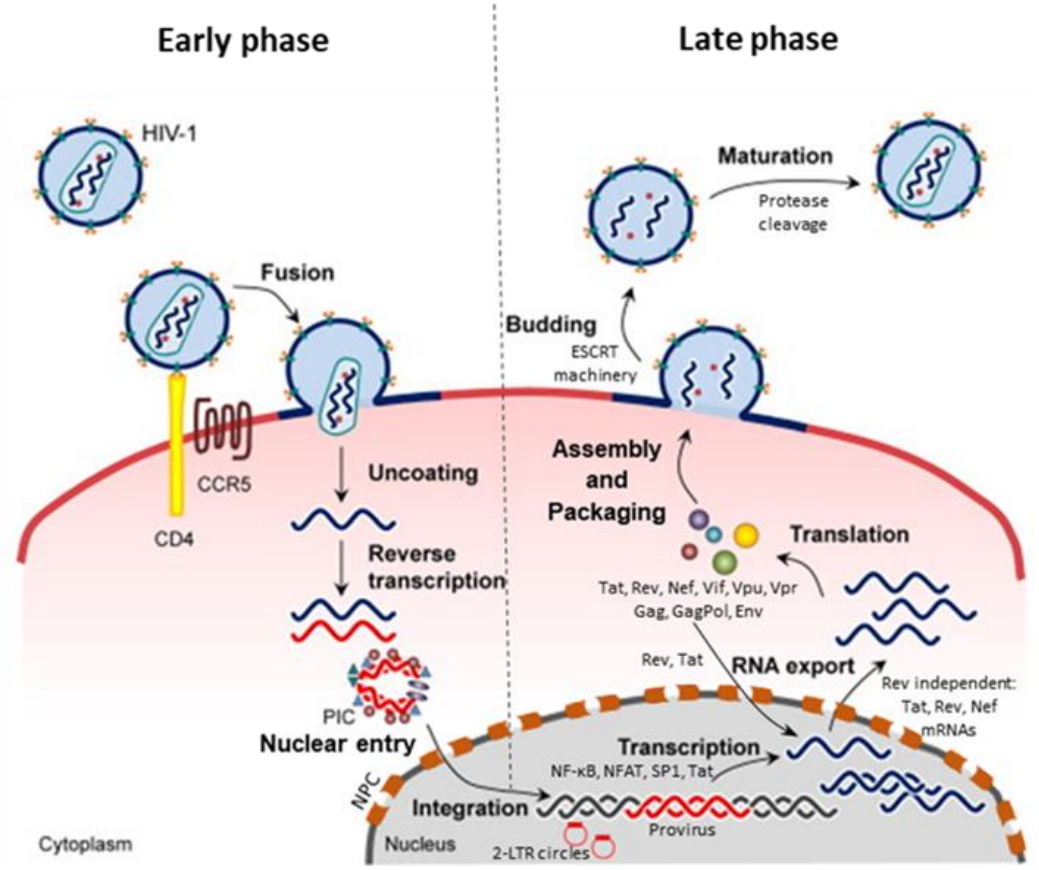

Figure 4. HIV-1 life cycle. *Schematic representation of HIV-1 infection. In the early phase, after fusion of the HIV-1 virion via CD4 and CXCR4 or CCR5 co-receptor engagement, the viral core is released into the cytoplasm where it initiates its trafficking toward the nucleus, during which the capsid core starts disassembling (uncoating) and the RNA genome is reverse transcribed by RT in double stranded DNA. Subsequently, the established PIC enters the nucleus through the NPCs and integrates the viral DNA into cellular chromatin. In addition, circularised viral DNA (2-LTR circles) is found. Integrated viral DNA can be silenced through various epigenetic mechanisms, leading to the creation of silent viral reservoirs (proviral latency). Alternatively, in the subsequent late phase, viral transcription is followed by splicing and nuclear export of viral mRNAs with the aid of Rev (Rev independent: Tat, Rev, Nef), which are translated into Gag, GagPol and Env proteins. Full-length viral genome RNAs are also packaged into new viral particles during assembly at the plasma membrane. Budding of new viral particles from the plasma membrane is mediated by the host ESCRT-I/II/III and is followed by a maturation process during which the viral particles become infectious following the proteolytic cleavage of Gag.* Figure modified from [69]

The HIV-1 life cycle starts with the interaction of gp120 viral proteins with CD4+ receptor of the target cell. Upon binding to one of the two co-receptors, CXCR4 or CCR5, the fusion of viral and cellular membranes is promoted and is followed by the entry of the viral core in the cytoplasm, where the viral RNA genome (vRNA) is reverse-transcribed to proviral cDNA by the viral RT. Once synthetized, the viral cDNA is transported to the nucleus and is integrated into the cellular genome with the help of the viral IN [69]. Integrated viral DNA can be silenced through various epigenetic mechanisms, leading to the creation of silent viral reservoirs (proviral latency). Alternatively, upon cell activation, transcription factors may be recruited to the promotor in the 5'LTR and initiate the expression of proviral genes [70]. Early transcription leads to expression of Tat and Rev regulatory proteins. Tat is essential for efficient LTR-dependent expression of all HIV-1 proteins and the unspliced genomic RNA, whereas Rev is required for the nuclear export of both unspliced viral mRNAs encoding Gag or Gag-Pol, and singly spliced viral mRNAs encoding the viral Env or the singly accessory proteins Vif, Vpr and Vpu [71, 72]. Env is synthesized on ER-associated ribosomes and is transported to the plasma membrane via the secretory pathway [73], while Gag and Gag-Pol are synthesized on free ribosomes in the cytoplasm and are targeted to the plasma membrane after myristoylation and selective binding of two copies of the single stranded RNA genome [74]. HIV-1 assembly occurs predominantly in cholesterol and sphingolipid rich lipid rafts [75], where the interaction of highly HBR region of Gag with phosphatidylinositol 4,5- bisphosphate (PI(4,5)P2) leads to an exposition of the N-terminal myristoyl group that gets anchored in the plasma membrane [35]. Extensive multimerization of Gag and GagPol proteins drives the formation of a hexameric lattice with small irregular defects that defines the shape of the the nascent HIV-1 bud at the cell membrane [67]. Further viral and cellular components including the viral Pol and Env proteins as well as the accessory proteins Vif, Nef and Vpr are recruited to the assembly sites [47]. The release of the the newly assembled HIV-1 particles from the plasma membrane is mediated by the cellular ESCRT machinery through a fission process, following the direct interaction between the C-terminal p6 domain of HIV-1 Gag with the proteins Tsg101 and Alix [76]. Cellular proteins, such as CypA [77] and APOBEC3G [78-82] are also packaged into HIV-1 budding virions. Initially, the

newly formed particles have a non-infectious immature morphology where Gag shell is only 70% complete, forming a truncated sphere (Fig. 3B), presumably derived from the ESCRT mediated particle release prior to assembly of the complete sphere [65-67]. During or concomitant with viral particle release from the infected cell, PR is activated and cleaves Gag as well as Gag- into their components *(as described in 3.1.3.)* leading to the dramatic morphological changes required for creation of a mature, infectious virion (Fig. 3B) [46, 47].

Since the early steps of HIV-1 life cycle represent the major focus of this thesis, the following sections give a more detailed introduction.

3.2.1. Attachment of HIV-1 and cell entry

HIV-1 infects CD4+ T cells and, to a lesser extent, macrophages using CD4 as a receptor [83]. In addition to CD4, the binding to either CCR5 or CXCR-4 as co-receptor is required for infection [84, 85]. CD4 is a type I transmembrane glycoprotein of 58 kDa member of the immunoglobulin (Ig) superfamily and contains four immunoglobulin domains (D1 to D4) that are exposed on the extracellular surface of the cell. CD4 acts as a co-receptor that amplifies the intracellular signal coming from the T cell receptor (TCR) when it binds to the peptide antigen bound to major histocompatibility (MHC) class II molecule on an antigen-presenting cell (APC) [86]. The role of CD4 in the life cycle of HIV-1 was first identified when CD4+ Jurkat T cells developed very large multinucleated syncytia in response to HIV-1 glycoproteins [83, 87]. The role of HIV-1 co-receptors CXCR-4 and CCR5 was later recognized in 1996 [84, 85]. CXCR-4 and CCR5 are integral membrane proteins that belong to the chemokine receptor family [88]. Furthermore, the chemokine receptor CCR3 has also been suggested as co-receptor for HIV-1 [89]. Depending on which co-receptor is used for the entry, the viruses can be differentiated as CCR5 tropic and CXCR-4 tropic or as dual tropic. The importance of the co-receptor for HIV-1 infection is highlighted by the findings that a homozygous 32 bp deletion in the coding region of CCR5 genes leads to a truncated and non-functional receptor, which render some people partially resistant to HIV-1 infection [90, 91].

HIV-1 cell entry involves binding of the trimeric viral envelope glycoprotein gp120/gp41 *(as described in 3.1.3)* to the cellular receptor/co-receptor complex.

During the first step gp120 binds to CD4 (Fig. 5A), which causes a conformation change in gp120 and exposes a binding V3 loop that attaches to the co-receptor (Fig. 5B). Binding to the co-receptor induces a series of conformational changes, which lead to the exposure of the gp41 fusion peptide and the formation of a gp41 helix bundle intermediate that permits the annealing of virus and target cell membranes (Fig. 5C). The gp41 fusion peptide inserts into the cell membrane, leading to the fusion of the virus membrane with the target cell membrane and formation of a fusion pore [92]. The fusion of viral and target cell membranes has been shown to occur in endosomes and not directly at the plasma membrane [93]. However, endocytosis does not significantly contribute to productive infection in T cells [94].

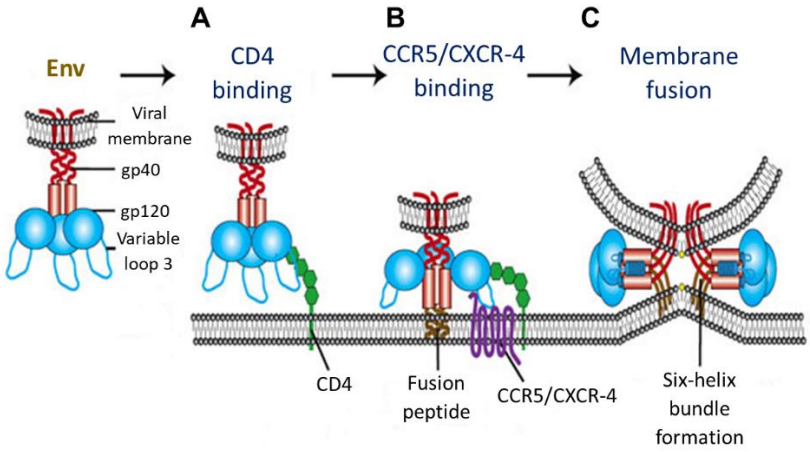

Figure 5. HIV-1 entry. A) *HIV-1 attaches to cell membrane associated CD4 via the gp120 protein.* **B)** *Attachment brings the virus closer to the cell membrane and induces a conformational change in the gp120 protein allowing coreceptor binding, mediated in part by the V3 loop of gp120, and the subsequent exposure of the gp41 fusion peptide that inserts into the target cell membrane.* **C)** *Formation of a helix bundle leads to annealing of virus and cell membranes causing membrane fusion, which may occur after endocytosis.* Figure modified from [95]

Host factors can also negatively influence HIV-1 entry. Serine incorporator 3 and 5 (SERINC3/5) [96, 97] and interferon-induced transmembrane (IFITM) [98-100] proteins are incorporated into budding HIV-1 virions and prevents fusion of the viral envelope with the plasma membrane (Fig. 9). SERINC3/5 are counteracted by HIV-1 accessory protein Nef [96, 97].

3.2.3. Trafficking toward the nucleus and reverse transcription of HIV-1

The fusion of the viral and cellular membrane leads to the release of the viral core into the cytoplasm where reverse transcription occurs. In this process, viral RNA genome is transcribed by the viral RT into double-stranded cDNA [14, 15]. During its trafficking toward the nucleus, the viral core follows a highly ordered disassembly process, named uncoating, which is essential for an optimal delivery of viral DNA to the nucleus in target cells. This process is characterized by an accurate and balanced stability of the viral core, which ensures a structural opening for an efficient reverse transcription [101], as well as a proper shielding from host factors, such as innate sensor cGAS [102-104] or cytosolic exonuclease TREX1 [105], which can detect viral RNA/DNA intermediates and induce an antiviral response with production of type I interferons (IFN) [102-104]. Evidence suggest that the HIV-1 core likely interacts with multiple host cell factors capable to benefit the uncoating process and ensure a proper trafficking of the viral core to the nucleus. Cyclophilin A (CypA) is a peptidyl-prolyl ci-trans isomerase that has been shown to promote HIV-1 replication in some target cell types through its direct interaction with CA [77, 106, 107]. CypA binds a conserved proline rich NTD loop on HIV-1 CA [40, 108, 109] and catalyzes the cis-trans isomerization of the peptide bond between residues G89 and P90 [110]. The inhibition of CypA binding to CA through treatment of infected cells with cyclosporin A (CsA) reduces HIV-1 reverse transcribed DNA levels, indicating that CypA may influence uncoating and hence reverse transcription [111, 112]. Interestingly, infection by the closely related virus HIV-2 induces type 1 IFN production in DCs [103, 113] but the introduction of a HIV-1 CypA-binding loop in HIV-2 CA suppressed its IFN activation [103]. The cyclophilin-binding loop CA mutant P90A binds with lower affinity to CypA, and is resistant to CypA-mediated isomerization of the G89-P90 peptide bond in CA [114-116].

Reverse transcription occurs in a complex of viral and cellular RNA and proteins, referred to as the reverse transcription complex (RTC) that is thought to arise as a result of the viral core uncoating [117]. During this process an aberrant circularised form with a single LTR (1-LTR circle) can form through recombination of the LTRs. In addition, cellular DNA repair enzymes of the non-homologous end-joining pathway can join ends of the linear DNA molecule and

generate a second circular form denoted as 2-LTR circles. The formation of 2-LTR circles is considered a marker for nuclear entry since it involves ligases Ku70 and Ku80, which are nuclear enzymes [118].

The host factor apolipoprotein B mRNA editing enzyme, catalytic polypeptide-like 3G (APOBEC3G) can prevent production of functional viral proteins by inducing G to A hypermutations during reverse transcription process, whereas sterile α motif and histidine-aspartate domain-containing protein 1 (SAMHD1) is a deoxynucleotide-triphosphohydrolase that inhibits reverse transcription by depleting the pool of cellular deoxynucleotide triphosphates (dNTPs). APOBEC3G is counteracted by HIV-1 accessory protein Vif [119-121] whereas SAMDH1 is counteracted by HIV-2/SIV accessory protein Vpx [122, 123] (Fig. 9).

3.2.4. Nuclear import of HIV-1 PICs

After HIV reverse transcription, an integration-competent nucleoprotein complex, named pre-integration complex (PIC), is established. Viral elements associated with the PIC, such as MA [124], IN [125, 126] and Vpr [127-129], contain nuclear localization signals (NLS) and have been proposed to mediate nuclear localization of the HIV-1 complex.

HIV-1 and other lentiviruses are able to productively infect non-dividing cells nearly as well as dividing cells by using active transport [130-135]. On the other hand, other retroviruses, such as the murine leukemia virus (MLV), require cell division and the nuclear envelope breakdown to reach the target cell DNA and finalize the infection. Several data indicate that the main determinants for infection of non-dividing cells are mapped in CA [136-138]. Furthermore, it has been observed that nuclear PICs were almost always CA-positive in monocyte-derived macrophages [139, 140], suggesting that even if disassembly of the conical capsid structure takes place before the nuclear import, CA or a CA-like structure remains associated with the PIC likely to facilitate downstream steps in viral replication. Several host factors interacting with CA have been implicated in nuclear translocation of the viral genome. HIV-1 PIC is thought to be actively guided to enter the nucleus by passing through nuclear pore complex (NPC) [141-144] (Fig. 6, Fig. 7). NPCs are large macromolecular channels that span the nuclear envelope (NE) and mediate the bidirectional and

selective transport of cargoes between the nucleus and cytoplasm [145, 146]. NPC consists of an approximately cylindrical central framework, residing within the NE and containing cytoplasmic and nuclear ring moieties, eight cytoplasmic filaments and a nuclear basket that is composed of eight filaments that join into a distal ring (Fig. 6) [147]. Nucleoporins (Nups) are the molecular building blocks of the NPC and comprise ~30 different proteins, a subgroup of which contains phenylalanine-glycine (FG) repeats that project from both the nucleoplasmic and cytoplasmic regions creating a hydrophobic meshwork that functions as a docking platform for receptor-cargo complexes and plays an important role in modulating the selectivity and the kinetics of nucleocytoplasmic transport [148-150].

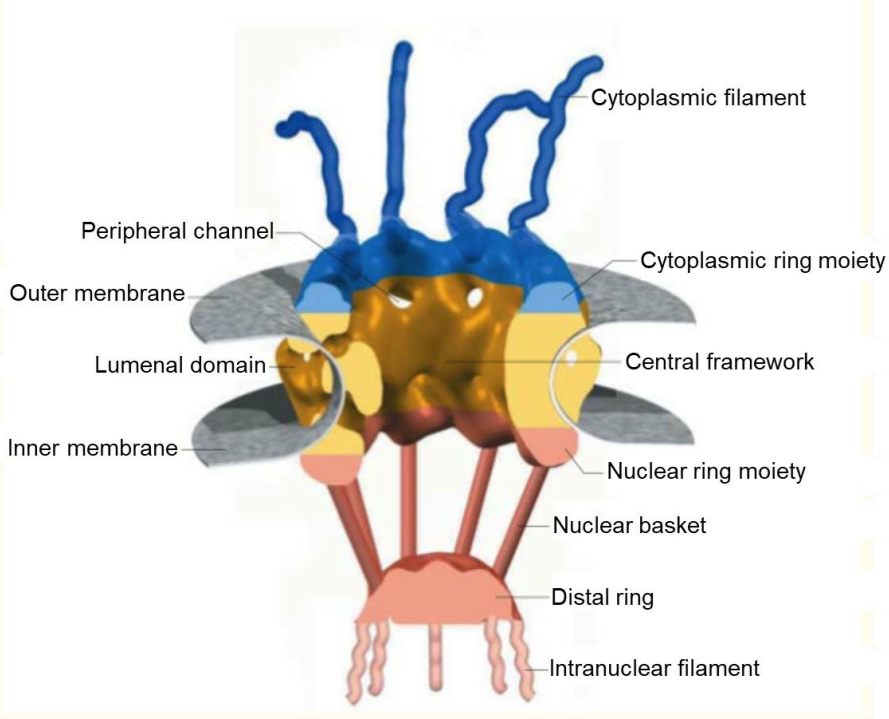

Figure 6. *Structure of the nuclear pore complex (NPC). The main components of the pore include the central framework (yellow), the cytoplasmic ring moiety and attached filaments (blue), the nuclear ring moiety and the distal ring of the nuclear basket (orange). Nuclear membranes are depicted in grey.* Figure derived from [151]

Two components of NPCs, Nup358 and Nup153, were identified by three genome wide screens aiming to identify cellular factors required for HIV-1 infection [152-154]. Nup358 [141-143] is the main cytoplasmically-oriented component of the NPC and possesses a CypA-domain that can bind HIV-1 CA [141] but is not required IN Nup358 for HIV-1 infection [155]. Knockdown

studies have revealed that depletion of Nup358 lead to a 6 to 8-fold reduction of HIV-1 infectivity with unaltered reverse transcription and reduced 2-LTR circle formation, suggesting that the anti-viral effect is linked to nuclear entry of the virus [141, 156, 157]. Interestingly, immunofluorescence analysis based on CA staining at 6 hpi showed that depletion of Nup358 leads to a decrease in perinuclear CA signal, suggesting that this cytoplasmically-oriented nucleoporin may be involved in HIV-1 docking at the nuclear envelope [156]. Nup153 localizes to the nucleoplasmic side and directly binds CA through its FG repeats [144]. In addition, Nup153 shRNA-mediated depletion led to a reduction of HIV-1 infectivity with reduction of of 2-LTR circles formation and unalterated reverse transcription [156, 158, 159], indicating that this nucleoporin also plays a role in viral nuclear entry. Thus, it is suggested that both Nup358 and Nup153 play distinct roles in HIV-1 nuclear entry. While Nup358 may mediate HIV-1 PIC docking at the nuclear pore, Nup153 may play an active role required for HIV-1 PIC to enter the nucleus and finalize the infection [160]. Other NPC related proteins Nup98 and Nup214 have also been proposed to have a role in HIV-1 infection [156, 158, 161]. Interestingly, the knockdown of Nups 98 and 214 leads to reduction of HIV-1 infectivity but doesn't affect nuclear entry, as assessed by measuring 2-LTR circles in infected cells [156, 158]. However, the exact mechanism for nuclear transport of PIC through the NPC remains to be investigated.

The importin-β-like karyopherin TNPO3 and the cleavage and polyadenylation specific factor 6 (CPSF6) (Fig. 7, Fig. 8) are other host factors that have been shown to be involved in HIV-1 infection and whose viral determinants have been mapped to the CA protein [152, 162-166]. TNPO3 is a karyopherin that binds arginine/serine-rich splicing factors (SR proteins) promoting their nuclear import. Studies have suggested that TNPO3 binds to HIV-1 CA [167, 168] and that TNPO3 depletion restricts HIV-1 infection with a decrease of 2-LTR circle formation [141, 157, 169], indicating a role of this karyopherin in the nuclear translocation of the viral PIC. However, it has been suggested that TNPO3 might promote HIV-1 nuclear import only indirectly [167, 169]. CPSF6 is a pre-mRNA splicing factor that shuttles between nucleus and cytoplasm [170] with a carboxy-terminal nuclear-targeting arginine/serine-rich (SR) domain [140, 164]. CPSF6 was found to be involved in HIV-1 infection through a cDNA expression

screen for host restriction factors [163]. The screen identified a carboxy-terminally truncated CPSF6 lacking the SR domain (CPSF6-358). This protein accumulated largely in the cytoplasm and was a strong inhibitor of HIV-1 infection with reduction of of 2-LTR circles formation, indicating impairment of the viral nuclear entry. Additionally, this phenotype was observed also against other primate lentiviruses, such as HIV-2 and SIV but not against MLV [163], suggesting that CPSF6 plays a role in the ability of primate lentiviruses to infect non-dividing cells. Of particular interest, the HIV-1 CA mutation N74D disrupt the interaction between CA and CPSF6-358 and the consequent viral restriction is abolished [163, 164]. N74D CA mutant infectivity is unaffected by TNPO3 depletion, Nu358 depletion and Nup153 depletion [163, 167, 168, 171, 172], suggesting that this CA mutant may enter the nucleus using another pathway. Additionally, A105T CA mutantion has been shown to render HIV-1 resistant to inhibition by CPSF6-358 [169]. Intriguingly, CPSF6 depletion had no effect in HIV-1 infectivity, suggesting that endogenous CPSF6 is not fully essential for HIV infection [163, 173].

The roles of TNPO3 and CPSF6 in HIV-1 infection are now considered interconnected: CPSF6-mediated import of the PIC to the nucleus requires TNPO3, which transports CPSF6 and other SR-family proteins to the nucleus. It has been showed that, in TNPO3 depleted cells, endogenous CPSF6 does not localize at the nuclear envelope and remains mostly cytoplasmic, such as its truncated mutant. However, in this cells HIV-1 infectivity is rescued when ectopically-expressed CPSF6 is retargeted to the nuclear envelope, suggesting that infectivity decrease in TNPO3-depleted cells may be a consequence of the cytoplasmic re-localization of endogenous CPSF6 [169]. CPSF6 is indeed capable of inhibiting HIV-1 replication only when it accumulates in the cytosol, where it binds to CA via the pocket where N74 and A105 are located [163], thus stabilizing the HIV-1 CA core and inducing a delay in uncoating and in nuclear import of the PIC. Therefore, it is conceivable that TNPO3 promotes HIV-1 infectivity indirectly, by shifting the CA-binding protein CPSF6 to the nucleus thus preventing its interaction with HIV-CA.

Since viral nuclear entry is reduced and not entirely suppressed, it is possible that other host partners besides Nups, CPSF6 and TNPO3 may be involved during this stage.

3.2.5. Integration of HIV-1 DNA into the host genome

For a productive infection the viral double stranded linear DNA molecule has to integrate into the host genome establishing a provirus. The HIV-1 PIC does not integrate randomly into the host genome but prefers transcriptionally active regions [174], in close correspondence with the NPC [175] (Fig. 8). Particularly, it has been demonstrated that Nup98, Nup153 [156, 158] and Nup358 [141, 176] influence HIV-1 integration by favouring the integration in transcriptional units and in regions characterized by an open chromatin configuration [141, 156, 158, 176]. Furthermore, translocated promoter region (TPR) (Fig. 8), a protein of the inner basket of the NPC, has been suggested to be involved in regulating the expansion of heterochromatic regions in proximity to the NPC and depositing open chromatin marks on HIV-1 target genes [177, 178]. Therefore, HIV-1 nuclear import pathway seems to be directly linked to integration site selection [141]. Additionally, depletion of endogenous CPF6 resulted in a redistribution of HIV-1 integration sites away from transcriptionally active genes, thus providing clear evidence for an important role for endogenous CPSF6 (Fig. 7 and Fig. 8) in directing HIV-1 integration into actively transcribing genes, despite there were not relevant change in infection [179, 180].

Another important factor that dictates the target site preferences of HIV integration is the host chromatin binding protein lens epithelium-derived growth factor p75 (LEDGF/p75) product of the *PSIP1* gene (Fig. 7 and Fig. 8), which binds lentiviral IN [181, 182] and mediates IN-chromatin binding [183, 184]. Studies showed that in the absence of LEDGF/p75, HIV integration in transcription units is severely compromised [185-187]. Furthermore, TPR stabilizes LEDGF/p75 in the nuclear periphery [177], suggesting that the two proteins may work together to direct HIV-1 DNA preferentially into regions of open chromatin and transcriptionally active sites in the outer shell of the nucleus, in proximity to the NPC

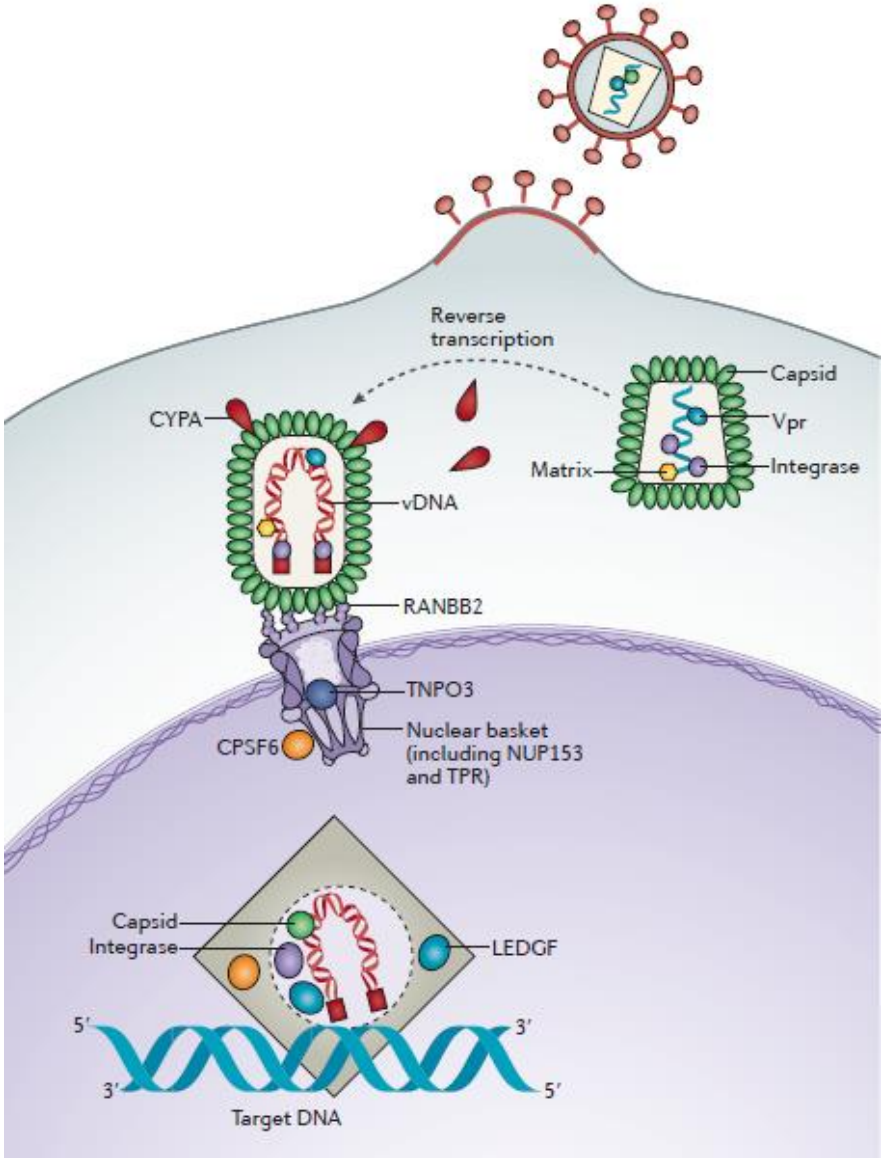

Figure 7. HIV-1 nuclear import of pre-integration complex (PIC). *The capsid of HIV-1 is an important viral factor for both uncoating and nuclear entry of the PIC. Other viral factors like Vpr, MA and IN are also involved in entry of PIC into the nucleus. Different cellular factors such as CypA, NUP358 (RANBP2), NUP153 and CPSF6 play also roles in the nuclear entry of the PIC on the cytosolic side of the NPC. TNPO3 is involved in shuttling through the NPC. NUP153 and CPSF6 have a role in target site selection, together with LEDGF, which is the most important chromatin-tethering factor involved in HIV-1 integration.* Figure derived from [188]

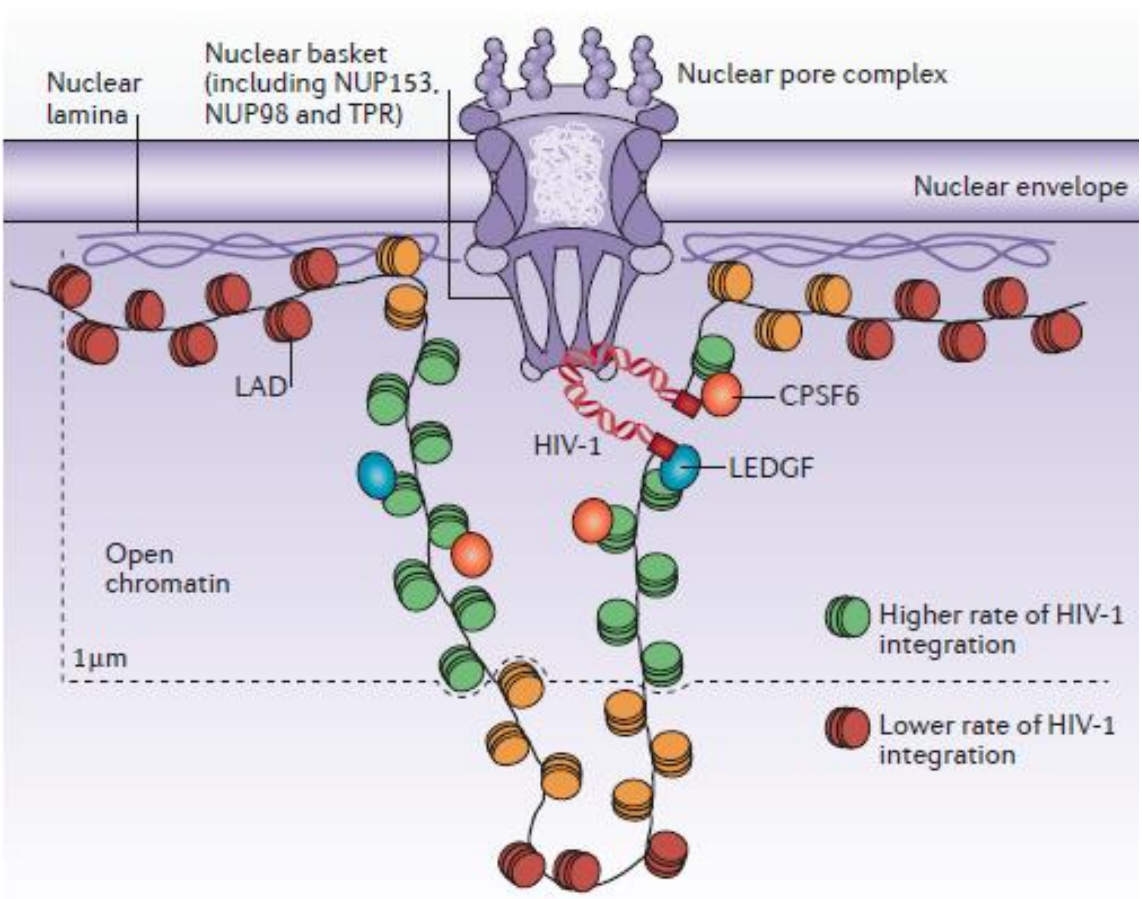

Figure 8. HIV-1 integration at the nuclear periphery. *Binding of the chromatin-tethering factor LEDGF to HIV-1 IN and binding of CPSF6 to the CA lead to HIV-1 integration into transcriptionally active genes and regions of open chromatin. Furthermore, NUP153, NUP98 and TPR also play an important role in HIV-1 integration, which preferentially occurs in the outer shell of the nucleus in proximity to the NPC. Intriguingly, TPR is a protein of the inner basket of the NPC that regulates the expansion of heterochromatic regions in proximity to the NPC and deposits open chromatin marks on HIV-1 target genes. 1 µm beneath the nuclear envelope. LAD, lamin-associated domain.* Figures derived from [188]

Viral DNA integration occurs with the activity of the viral enzyme IN *(see paragraph 3.1.3)*, which promotes two distinct reactions. First, the enzyme removes di- or trinucleotides from double stranded viral DNA ends to expose 3′-hydroxyls from the conserved CA dinucleotides (3′-processing reaction). Second, in a reaction named strand transfer, a phosphodiester bond in the host genomic DNA is attacked by the two reactive hydroxyl-groups previously created. Subsequently, IN ligates the viral DNA into the host DNA, generating a five base pairs single-stranded DNA segment at each end of the host DNA and a two nucleotide 5’ viral DNA flap. After that, the cellular DNA repair machinery

fills the gaps and ligates the synthesised DNA into the host genome [189]. In addition, tetrameric IN complexes have been shown *in vitro* to cleave the junction sequence between two LTRs leading to the linearization of 2-LTRc circles [190].

3.3. HIV-1 and host immunity

The mammalian immune system comprises an adaptive and an innate component and both are essential for efficient protection from infection by pathogens, such as viruses or bacteria.The innate immunity is the first line of host defense and involves multiple mechanisms and cells (macrophages, DCs and natural killer cells (NKs)) that act rapidly to restrict virus replication and to provide time for the organism to activate the second arm of defense, the adaptive immune system. This operates through selection and expansion of T and B cells and the production of specific antibodies directed against the invading pathogen. Furthermore, it prepares the host for future challenges by generating an immunological memory that enhances the host response to subsequent encounter with the same pathogen [191]. Activation of B and T lymphocytes relies on antigen-presentation, a process that is taken by professional antigen-presenting cells (APCs) such as DCs, macrophages and B cells. These cells internalize and process exogenous antigens into peptides and display them complexed with MHC class II on the surface, which are recognized via TCR expressed by helper CD4+ T cells that have the crucial role of assisting other leukocytes, as it is the case of antibody secretion by B cells [192]. Whereas all nucleated cell types can present on their surface antigens originating inside the cell and complexed with MHC class I, which are then recognized by TCR expressed on the surface of CD8+ cytotoxic T lymphocytes (CTLs), that induces programmed cell death to the target cells [193].

3.3.1. Innate immunity against retroviruses

The main innate immune response is inflammation, which is initiated by the recognition of pathogen-associated molecular patterns (PAMPs), by the pattern recognition receptors (PRRs), such as toll-like receptors (TLRs), receptors present on macrophages and DCs. This recognition allows cell activation and release of inflammatory cytokines, like TNF-α, IL-1 and the production of IFNs,

small molecules that are able to induce an antiviral state in the proximity of an infection [194].The innate immune system of mammals also comprises a diverse group of intracellular factors, named restriction factors, which are able to efficiently counteract viral infection in several ways. These factors are generally interferon inducible and their expression is upregulated during early infection. They often operate in a species-specific way; however, they may also block viruses from related species. Since host restriction factors present a major hurdle to incoming virions, it is not surprising that virus species have evolved measures to counteract host restriction factors. The simultaneous evolution of host-encoded restriction factors and the corresponding viral counter measures causes host and pathogen to co-evolve and leads to an evolutionary arms race.

Studies on retroviruses have revealed many of the molecular mechanisms that underpin our understanding of these viral countermeasures. By understanding the antagonistic relationship between restriction factors and their viral countermeasures is not just an academic exercise, but has also enabled the development of drug targets for diseases like AIDS [195]. Known retroviral restriction factors and viral countermeasures to prevent or inhibit these factors are depicted in Fig. 9.

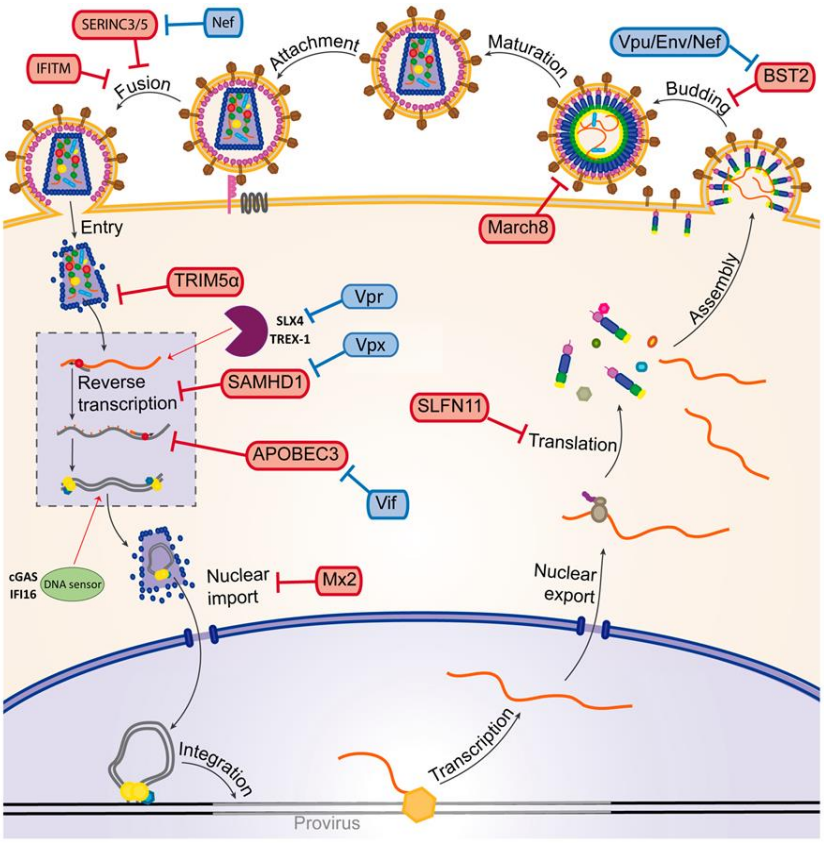

Figure 9. Host retroviral restriction factors and countermeasures by viral accessory proteins. *Cellular antiviral factor are highlighted in red, while countermeasures by viral accessory proteins are highlighted in blue. Innate DNA sensor (cGas, IFI16) and the cytosolic exonuclease TREX1 and SLX4 endonuclease complex are also shown.* Figure modified from [196]

3.3.1.1. Type I interferon responses in HIV Infection

Acute HIV-1 infection starts with a marked decrease of CD4+ T cells and the production of considerable quantities of cytokines [197, 198], which contribute to initial restriction of viral spread and facilitates the partial recovery of CD4+ T cell counts [199]. Type I IFNs, , such as IFN-α and IFN-β, are a group of cytokines expressed and secreted by plasmacytoid dendritic cells in response to recognition of pathogen-associated molecular patterns (PAMPs) during the acute phase of viral infection [200]. Within the first week of HIV infection, endogenous type I IFN production stimulates the expression of a large number of interferon-stimulated genes (ISGs) that limit viral replication in MDMs and CD4+ T cells by operating at multiple stage of the viral replicative cycle, from reverse transcription (SAMHD1 and APOBEC3) to nuclear entry (MX2) to transcription (Schlafen 11) and budding (tetherin), leading to the establishment of generalized antiviral state [201-206]. Therapies combining IFN-α treatment has therefore been examined as a treatment strategy for HIV-1 infection and

other human pathogens infections, like hepatitis C virus (HCV). Despite a considerable reduction in viral load was detected in chronic infection, viral rebound over time indicates that HIV-1 may overcome IFNα-induced antiviral response [207, 208]. It is therefore important to identify the host cell effectors induced by type I IFNs and the viral determinants associated to the overcome the IFN-α- induced blocks. Transmitted founder (T/F) viruses, which are the selected viral strains that establish de novo infections, replicate more efficiently in the presence of type I IFNs than their viral counterparts from chronic infection [209, 210], indicating that some HIV-1 strains have evolved to escape type I IFNs inhibition, emphasizing IFNs physiological importance during the early course of HIV-1 infection [199].

The GTPase myxovirus resistance 2 (MX2 [also called MXB]) is a recently discovered type I IFN-induced factor able to inhibit HIV-1 infection after reverse transcription at the level of nuclear entry [204, 205, 211]. Certain T / F viruses show some degree of resistance to the antiviral activity of MX2, indicating a functional role of MX2 in restricting HIV-1 transmission [212]. Interestingly, MX2 restriction of HIV-1 seems to be sensitive to changes in the HIV-1 CA protein [204, 205, 211, 213]; P90A and N74D CA mutants were less sensitive to inhibition by overexpressed MX2 than wild type HIV-1, suggesting that the CypA binding [211] as well as CPSF6 binding [204, 205] to the HIV-1 capsid may also be involved in the MX2 antiviral mechanism. However some of these CA mutants are still strongly inhibited by type I IFNs [214]. Consistent with this, *In vitro* studies suggest direct binding of MX2 to CA [215, 216]. Two different human MX proteins have been identified, MX1 and MX2 that are different in localization and activity. While it has been shown that MX1 possesses a broad antiviral activity towards certain RNA and DNA viruses [217, 218], different studies have found MX2 to be restrictive only against few viruses such as Vesicular stomatitis virus (VSV), mouse herpes virus type 68 (MHV-68), and HIV-1 [206, 219, 220]. MX2 localizes to the cytoplasmic part of NPCs [221, 222]. Although MX2 antiviral activity is clearly dependent upon Nups, knockdown data suggest that nuclear localization is not essential for antiviral activity [223, 224]. Contrarily to MX1, the antiviral activity of MX2 against HIV-1 is independent of its GTPase domain [204, 205] and requires higher order structures and oligomerization [225]. Additionally, the determinant for MX2

antiviral effect maps to the first 25 amino acids in the amino-terminal region of the protein, in which a triple-arginine motif is required for interaction with the CA and consequent restriction [223, 226].

3.4. Nuclear envelope: structure and function

NE is the double membrane surrounding the eukaryotic cell nucleus, composed of two lipid bilayer membranes: an inner nuclear membrane (INM) and an outer nuclear membrane (ONM), a continuum of the endoplasmic reticulum (ER). A 20–50 nm perinuclear space (PNS) separates the two membranes, which are connected to each other at annular junctions that form aqueous channels between the nucleoplasm and cytoplasm, and which are occupied by NPCs [227]. The INM encloses the nucleoplasm and contains a unique spectrum of integral membrane proteins, at least 50–60 of which have been identified [228]. Furthermore, INM is covered by the nuclear lamina, a network of intermediate filaments important in stabilizing the nuclear membrane and involved in chromatin function. The major components of the nuclear lamina are the A- and B-type lamins (LMNA/B), a group of type-V intermediate filament proteins [145]. The ONM is invariably studded with ribosomes and contains nesprin (Nesp) proteins, which connect cytoskeletal filaments to the nucleoskeleton [229], contributing to nuclear positioning and to the cell's mechanosensory function [230].

3.4.1. Nuclear envelope and HIV-1

HIV and other lentiviruses possess a mechanism to bypass the intact NE to ensure correct nuclear import and integration, and accordingly are able to productively infect most non-dividing cells nearly as well as dividing cells, while *Gammaretroviruses* such as the MLV and spleen necrosis virus (SNV) require mitosis and the NE breaking down for productive infection and are blocked from integrating into non-dividing cells [137]. CA has been revealed as the dominant determinant of retroviral infectivity in non-dividing cells [136-138] and HIV-1 PIC is thought to be actively guided to enter the nucleus by passing through NPC [141-144] and to integrate in actively transcribed chromatin regions [174], in close correspondence with the NPC [175]. Of note, NE-associated proteins have been implicated in transcriptional memory processes [231, 232]. Nup98

and Nup153 were shown to confer cell identity by interacting with super-enhancers and modulating cell-specific transcription [233]. It is therefore possible that HIV-1 uses a distinct nuclear import pathway that leads to integration into chromatin areas that are under control by such transcriptional memory processes to better facilitate reactivation from latency. Components of the INM, including SUN proteins, LMNs or emerins (EMDs), have functions in chromatin organization and decondensation after mitosis [234-241], suggesting that dysregulation of these proteins could affect orderly HIV-1 integration or gene expression from integrated provirus . Previous studies examined whether HIV-1 uses INM components during infection, and indicated that EMD interacts with the host protein BAF in the HIV-1 pre-integration complex through its LEM domain, promoting HIV-1 infection [242]. Conversely, other studies have shown that EMD and lamina-associated polypeptide 2α (LAP2α) are not important for HIV-1 infection [243, 244]. However, the molecular details of how HIV-1 targets preferred sites for provirus establishment and the consequences of site selection for virus replication or latency, as well as the identity and functions of other involved host proteins, are mostly unknown.

Finally, there are also evidences for IFNs modulating the NE composition and proteins in the NE. The IFN-inducible protein IFI16 interacts with the NPC component TPR [245], possibly affecting its function in nuclear transport. Likewise the type I IFN-induced nuclear envelope-associated protein MX2, recently identified as an inhibitor of HIV-1 infection, partially co-localizes with NPC components, suggesting a possible link with its antiviral function [204, 205, 211, 213]. Furthermore, expression of some nucleoporins, such as Nup96 and Nup98, is modulated directly by IFNs [233] and an involvement of Nup98 in HIV-1 nuclear import has been suggested [158, 161]. Furthermore a recent screen to identify ISGs affecting HIV-1 infection, showed that overexpression of inner nuclear membrane protein SUN2 blocke HIV-1 infection moderately [206], to similar level observed for the IFN-induced protein MX2. It is therefore possible that the inhibition of HIV-1 infection by type I IFNs involves NE-associated proteins.

4. Objective of the study

There is an estimated that 36.9 million people worldwide are HIV-positive. Every year another 1.8 million new infections occur and close to a million people will go on to die from AIDS [9]. This indicates that HIV, more than 30 years after its discovery, still impacts a significant health burden on the human population.

The intial steps of HIV infection, involving numerous interactions between incoming virions and host proteins, represent a vulnerable phase that is critical for virus spead. This is underlined by the observation that type 1 IFN treatment of macrophages and CD4+ T cells, both natural targets for HIV-1, causes a potent block at multiple post-entry stages. There is increasing evidence that implicates components of the NE as an important interaction partners for HIV-1 during the early stages of infection. This includes the CA-dependent engagement of NPC specific proteins [141-144, 174, 175] in contrast to antiviral effects of NE-associated proteins such as MX2 [204, 205, 211] and SUN2 [206].

To address the potential role of the NE during the early steps of HIV-1 infection, the current thesis investigated several NE-associated proteins. Thus, the following objectives were established:

1. Identification of NE membrane-associated proteins that potentially affect HIV infection by performing an overexpression screen.
2. Determination of the ability of the identified proteins to affect different retroviruses as well as different strains of HIV-1.
3. Determination and characterization of viral determinants by generating chimeras between sensitive and insensitive viruses.
4. Determination and characterization of cellular determinants by generating multiple deletion mutants of the identified proteins.
5. Determination of the physiological relevance of the identified endogenous proteins in HIV-1 infection. On this purpose, shRNA-mediated protein expression reduction and CRISPR/Cas9-mediated gene disruption in different cell lines were achieved.

Besides understanding the NE-HIV interaction, the current thesis also aimed to elucidate the role of the CA protein in IFN-α-induced suppression of HIV-1

infection. Thus, the sensitivity of HIV-1 CA mutants N74D, A105T, and P90A, to IFN-α-induced blocks was analyzed.

Together the proposed research will likely advance our understanding of the early steps of HIV-1 infection. The results may uncover some host cell barrier, which could contribute to the low permissivity for HIV-1 infection in certain cell types, e.g. CD4+ resting T cells, and may reveal novel targets for therapeutic intervention.

5. Materials and Methods

5.1. Materials

5.1.1. Laboratory equipment

Name	Company
Analogue tube rollers SRT6 Stuart®	Cole-Parmer, Vernon Hills, USA
Biological Safety Cabinet Class II SterilGARD® III Advance°	The Baker Company, Sanford, USA
Centrifuge Heraeus™ Megafuge™ 40R	Heraeus, Kleinostheim, Germany
Centrifuge J2HS with rotor JA-10	Beckman Coulter, Brea, USA
CO2 incubator Heracell™ 150i	Thermo Fisher Scientific, Waltham, USA
Confocal Laser Scanning Microscope Leica TCS SP5	Leica Microsystems, Wetzlar, Germany
Confocal Laser Scanning Microscope Leica TCS SP8	Leica Microsystems, Wetzlar, Germany
ECL ChemoCam Imager	INTAS Science Imaging, Göttingen, Germany
Electrophoretic Transfer Cell Mini Trans-Blot®	BioRad, Hercules, USA
Flow cytometer BD FACSVerse™	Becton Dickinson, Franklin Lakes, USA
Gel iX Imager (Agarose gel UV-imager)	INTAS Science Imaging, Göttingen, Germany
Horizontal Electrophoresis Unit MIDI Standard	Carl Roth, Karlsruhe, Germany
Incubator Shaker Multitron Pro	Infors AG, Basel, Switzerland
Inverted Laboratory Microscope Leica DM IL LED	Leica Microsystems, Wetzlar, Germany
Magnetic Stirring Hotplate Mr 3001	Heidolph Instruments, Schwabach, Germany
Microcentrifuge Heraeus™ Biofuge Fresco™	Heraeus, Kleinostheim, Germany
NanoPhotometer P300	Implen, München, Germany
Power Supply PowerPac™ Basic	BioRad, Hercules, USA
Real Time PCR detector CFX96 Touch™	BioRad, Hercules, USA
Tetra Vertical Electrophoresis Cell Mini-PROTEAN®	BioRad, Hercules, USA
Thermal Cycler C1000 Touch™	BioRad, Hercules, USA
Thermoblock Eppendorf ThermoMixer® comfort	Eppendorf, Hamburg, Germany
Ultracentrifuge L8-60M with SW28 rotor	Beckman Coulter, Brea, USA
Vortex Mixer Reax Top	Heidolph Instruments, Schwabach, Germany
Water bath Type 1008	GFL mBH, Burgwedel, Germany
Wide-field fluorescence microscope Zeiss Axiovert 200M	Carl Zeiss Imaging Solutions GmbH, München, Germany

Table 2. Equipment used in this work

5.1.2. Laboratory materials

Name	Company
Blotting paper 3MM Chr	Whatman, Dassel, Germany
Cell Culture Flasks (25, 75 and 175 cm^2) CELLSTAR®	Greiner Bio-One, Kremsmünster, Austria
Cell Culture Multiwell Plates (6, 12, 24, 48 well) CELLSTAR®	Greiner Bio-One, Kremsmünster, Austria
Cell Culture Dishes (100 x 20 mm) CELLSTAR®	Greiner Bio-One, Kremsmünster, Austria
Counting Chamber Neubauer-improved	Paul Marienfeld GmbH & Co.KG, Lauda-Königshofen, Germany
Cover glasses thickness No. 1 circular	Paul Marienfeld GmbH & Co.KG, Lauda-Königshofen, Germany
Disposable Nitrile Gloves TouchNTuff® 92-600	Ansell, Richmond, Australia
Filtered Tips AvantGuard™ (20 µl)	Midwest Scientific, Valley Park, USA
Filtered Tips OneTouch™ (10 µl, 200 µl, 1000 µl)	Sorenson BioScience, Salt Lake City, USA
Fluid aspiration system BVC professional	VACUUBRAND, Wertheim, Germany
Microscope slides thickness approx. 1 mm	Paul Marienfeld GmbH & Co.KG, Lauda-Königshofen, Germany
Multichannel Pipettes 8- and 12-channel (10 µl, 100 µl, and 300 µl) Eppendorf® Research® plus	Eppendorf, Hamburg, Germany
Nitrocellulose Transfer Membran Rolls Protran® BA85	Whatman, Dassel, Germany
Plastic paraffin film Parafilm®	Bemis Company, Neenah, USA
PCR Tubes (0,2 mL) Eppendorf tubes®	Eppendorf, Hamburg, Germany
PIPETBOY acu 2	INTEGRA Biosciences AG, Zizers, Switzerland
Pipetting Reservoirs (25 mL)	Argos Technologies, Vernon Hills, USA
Polypropylene Tubes (15 ml, 50 ml) CELLSTAR®	Greiner Bio-One, Kremsmünster, Austria
Tubes (0,5 ml, 1.5 ml, 2 ml) SafeSeal	Sarstedt, Nürnbrecht, Germany
Serological pipette (5 ml, 10 ml, 25 ml, 50 ml)	Sarstedt, Nürnbrecht, Germany
Single Channel Pipettes (P2µl, P10µl, P20µl, P200µl, P1000µl) PIPETMAN Neo®	Gilson Inc., Middleton, USA
Surgical Disposable Scalpels	B. Braun Melsungen, Melsungen, Germany
Syringes (1ml, 3ml, 5 ml, 10 ml, 60 ml) BD Luer-Lok™	Becton Dickinson, Franklin Lakes,USA
Syringe filters units (0.22 µm, 0.45 µm) Millex®	Merck Millipore, Billerica, USA
Syringe filters units (0.45 µm) Rotilabo® KH55.1	Carl Roth, Karlsruhe, Germany

Table 3. Materials used in this work

5.1.3. Kits

Name	Company
CD4+ T Cell Enrichment Cocktail RosetteSep™	Stemcell Technologies, Vancouver, Canada
CD4+ T Cell Isolation Kit - T cells, human	Miltenyi Biotec, Bergisch Gladbach, Germany
Monocyte Isolation Kit II, human	Miltenyi Biotec, Bergisch Gladbach, Germany
NucleoBond® Xtra Midi EF	Macherey-Nagel, Dueren, Germany
NucleoSpin® Gel and PCR Clean-up	Macherey-Nagel, Dueren, Germany
QIAamp® DNA Mini Kit	Qiagen, Hilden, Germany
QIAprep® Spin Miniprep Kit	Qiagen, Hilden, Germany
QuikChange Site-Directed Mutagenesis Kit	Agilent Technologies, Santa Clara, USA

Table 4. Kits used in this work

5.1.4. Chemicals and reagents

Name	Company
Acrylamide Solutions TGX™ FastCast™	BioRad, Hercules, USA
Ammonium Persulfate (APS)	Sigma-Aldrich, St. Louis, USA
Ampicillin	Carl Roth, Karlsruhe, Germany
Agarose	Janssen-Pharmaceuticalaan, Geel, Belgium
Aqua ad iniectabilia Braun	B. Braun Melsungen, Melsungen, Germany
β-Mercaptoethanol	Sigma-Aldrich, St. Louis, USA
Biocoll Separating Soultion	Biochrom GmbH, Berlin, Germany
Boric acid (H_3BO_3)	Carl Roth, Karlsruhe, Germany
Bromophenolblue	Chroma, Furstenfeldbruck, Germany
BSA 100X	New England Biolabs, Ipswich, USA
Cyclosporine (Sandimmune®)	Novartis International AG, Basel, Switzerland
Clarity™ Western ECL substrates	BioRad, Hercules, USA
Dimethyl sulfoxide (DMSO)	Merck Millipore, Darmstadt, Germany
DNA ladder 1kb Plus	Thermo Fisher Scientific, Waltham, USA
dNTP Set 100 mM Solutions	Thermo Fisher Scientific, Waltham, USA
Dulbecco's Modified Eagle Medium (DMEM), High Glucose, GlutaMAX™ Supplement	Gibco, Life Technologies, Carlsbad, USA
EDTA	Carl Roth, Karlsruhe, Germany
Efavirenz SUSTIVA® 30 mg/ml oral solution	Bristol-Myers Squibb Pharma EEIG, Uxbridge, UK
Ethanol (99 %) (EtOH)	Zentralbereich INF, Heidelberg, Germany
Fetal Calf Serum (FCS)	Biochrom GmbH, Berlin, Germany
Gel Loading Dye, Purple (6x) for DNA	New England Biolabs, Ipswich, USA

Glycerol	Sigma-Aldrich, St. Louis, USA
Glycine	Carl Roth, Karlsruhe, Germany
Granulocyte-macrophage colony-stimulating factor (GM-CSF), human recombinant	R & D Systems, Minneapolis, USA
Hoechst 33258	Thermo Fisher Scientific, Waltham, USA
Interferon α-2a Roferon®-A	Roche Holding AG, Basel, Switzerland
Interleukin-2, human recombinant (rHuIL-2)	Biomol, Hamburg, Germany
Isopropanol (C_3H_8O)	Sigma-Aldrich, St. Louis, USA
Kanamycin	Carl Roth, Karlsruhe, Germany
LB Broth (Lennox)	Sigma-Aldrich, St. Louis, USA
Methanol (MeOH)	Sigma-Aldrich, St. Louis, USA
Mowiol 4-88	Sigma-Aldrich, St. Louis, USA
DNA/RNA stain MIDORI^{Green} Advance	Nippon Genetics Europe GmbH, Dueren, Germany
Opti-MEM™ I Reduced Serum Medium	Gibco, Life Technologies, Carlsbad, USA
Paraformaldehyde (PFA)	Merck, Darmstadt, Germany
PBS Dulbecco Powder	Biochrom GmbH, Berlin, Germany
Penicillin Streptomycine (PenStrep)	Biochrom GmbH, Berlin, Germany
Phytohemagglutinin-M (PHA-M)	Sigma-Aldrich, St. Louis, USA
Phorbol 12-myristate 13-acetate (PMA)	Sigma-Aldrich, St. Louis, USA
Plasmocin™ - Mycoplasma Elimination Reagent	InvivoGen, San Diego, USA
Polyethylenimine (PEI)	Sigma-Aldrich, St. Louis, USA
Powdered milk	Carl Roth, Karlsruhe, Germany
Precision Plus Protein™ WesternC™ Standards	BioRad, Hercules, USA
Protease Inhibitor Cocktail EDTA-free cOmplete™	Roche Holding AG, Basel, Switzerland
Puromycin dihydrochloride	Santa Cruz Biotechnology, Dallas, USA
Ribonuclease Inhibitor RiboLock™	Thermo Fisher Scientific, Waltham, USA
RNA from bacteriophage MS2	Roche Holding AG, Basel, Switzerland
RPMI 1640 Medium, GlutaMAX™ Supplement	Gibco, Life Technologies, Carlsbad, USA
Sodium azide (NaN3)	Sigma-Aldrich, St. Louis, USA
Sodium chloride (NaCl)	Sigma-Aldrich, St. Louis, USA
Sodium dodecyl sulfate (SDS)	Applichem, Karlsruhe, Germany
Sodium Hydroxide (NaOH)	Sigma-Aldrich, St. Louis, USA
Sucrose	Sigma-Aldrich, St. Louis, USA
SYBR Green , 10000X concentrate	Thermo Fisher Scientific, Waltham, USA
Tetramethylethylenediamine (TEMED)	Carl Roth, Karlsruhe, Germany
Trypsin/EDTA solution	Biochrom GmbH, Berlin, Germany
Tris[(1-benzyl-1H-1,2,3-triazol-4yl)methyl]amine	Sigma-Aldrich, St. Louis, USA
Triton X-100	Sigma-Aldrich, St. Louis, USA
Tween 20	Carl Roth, Karlsruhe, Germany

Table 5. Chemical and reagents used in this work

5.1.5. Buffers and solutions

Name	Component	Concentration
PBS 10x	ddH2O NaCl KCl $N_{a2}HPO_4$ KH_2PO_4	 1,4 M 27 mM 80 mM 18 mM
TBE Electrophoresis Buffer 10x	ddH2O Tris base Boric acid EDTA pH 8	 890 mM 890 mM 20 mM
SDS Running Buffer 10x	ddH2O Glycine Tris base SDS	 1,92 M 250 mM 1%
SDS Blotting Buffer 10x	ddH2O Glycine Tris base	 1,92 M 250 mM
SDS Blotting Buffer 1x	ddH2O Glycine Tris base Methanol	 192 mM 25 mM 10% (v/v)
SG-PERT dilution buffer 1x, pH 8.0	ddH2O $(NH_4)2SO_4$ KCl Tris-HCl	 5 mM 20 mM 20 mM
SG-PERT lysis buffer 2x, pH 7.4	ddH2O KCl Tris-HCl Glycerol Triton X-100	 50 mM 100 mM 40 % 0.25 %
SG-PERT PCR reaction buffer 2x	SG-PERT dilution buffer MgCl2 BSA dNTPs Primer RT-Assay-fwd Primer RT-Assay-rev MS2 RNA SYBR Green GoTaq Hotstart Polymerase	 10 mM 0.2 mg/ml 400 µM 1 pmol 1 pmol 8 ng 1:10000 0.5 U
Hypotonic lysis buffer	Tris-HCl KCl protease inhibitor cocktail	10 mM 10 mM 1x
CANC binding buffer	Tris-HCl [pH 8] NaCl	50 mM 100 mM

CANC washing buffer	Tris-HCl NaCl KCl	50 mM 50 mM 5 mM
Laemmli Sample Buffer 2X	Tris-HCl pH 6.8 SDS Glycerol Bromophenol blue	120 mM 4% (w/v) 20% (w/v) 0.02% (w/v)
WB Stripping Buffer	ddH2O NaOH	 0.5 M
WB Wash Buffer for membranes and Dilution Buffer for antibodies	PBS Tween 20	 0.05% (v/v)
WB Blocking Buffer	PBS Milk powder	 5% (w/v)
Mowiol embedding medium	PBS Mowiol 4-88	 8mM

Table 6. Buffer and solutions used in this work

5.1.6. Bacterial Strains and bacterial culture media

For plasmid preparation and amplification, the chemo-competent *E. coli* strain Stbl2 was used. Genotype: F- mcrA Δ(mcrBChsdRMSmrr) recA1 endA1 lon gyrA96 thi supE44 relA1 λ- Δ(lac-proAB). They are characterized by high transformation efficiencies and low recombination rates.

Bacterial culture media

Name	**Component**	**Concentration**
LB	ddH2O NaCl Tryptone Yeast extract adjust to pH 7.2 and autoclave	 5 g/l 10 g/l 5 g/l
LB agar plates	Agar LB	12.5 g/l

Table 7. Bacterial culture media used in this work

For selection, Ampicillin (0.1 mg/ml) or Kanamycin (0.1 mg/ml for liquid culture and 0.06 mg/ml for plates) was added to the medium.

5.1.7. Cells and cell culture media

Cell lines

Name	Description	References
HEK-293T	Human embryonic kidney (HEK) stem cell line expressing a large Simian Vacuolating Virus 40 TAg (SV40 T) antigen on their cell surface	[246-248]
U87MG-CD4/CXCR4	Uppsala 87 Malignant Glioma (U87MG) CD4/CXCR4 is a human glioblastoma-astrocytoma cell line expressing HIV-1 receptors CD4 and CXCR4	[204, 249-255]
THP-1	Tohoku Hospital Pediatrics-1 (THP-1) is a human acute monocytic leukemia cell line	[204, 256-266]
Jurkat-TAg	Human acute lymphoblastic leukemia T-cell line expressing a large Simian Vacuolating Virus 40 TAg (SV40 T) antigen on their cell surface	[267-271]

Table 8. Cells used in this work

Adherent cell lines were routinely grown in Dulbecco's modified eagle's medium Dulbecco's Modified Eagle Medium (DMEM), High Glucose GlutaMAX™ supplemented with 100 U/ml of penicillin and 100 µg/ml of streptomycin and 10% fetal calf serum (FCS) previously heat-inactivated (heated to 56°C for 30 minutes in water-bath). Suspension cell lines were normally grown in RPMI 1640 Medium GlutaMAX™ supplemented with 100 U/ml of penicillin and 100 µg/ml of streptomycin and 10 % FCS.

Adherent cell lines were cryopreserved in liquid nitrogen by using FCS containing 10% DMSO as freezing medium, whereas suspension cell lines FCS containing 10% glycerol.

Primary cells

Human primary $CD4^+$ T cells and monocyte-derived macrophages (MDMs) were obtained from peripheral blood mononuclear cells (PBMCs) of healthy volunteer donors and grown in RPMI 1640 Medium GlutaMAX™ supplemented with 100 U/ml of penicillin and 100 µg/ml of streptomycin and 10% heat-inactivated FCS.

5.1.8. Enzymes

Name	Company
GoTaq® Hot Start DNA Polymerase	Promega, Madison, USA
Phusion® High-Fidelity DNA Polymerase	New England Biolabs, Ipswich, USA
PfuTurbo DNA Polymerase	Agilent Technologies, Santa Clara, USA
Restriction Endonucleases (*Apa*I, *BamH*I, *Bgl*II, *Bsmb*I, *BssH*II, *Dpn*I, *Eco*RI, *Mfe*I, *Mlu*I, *Not*I, *PspOM*I, *Xho*I)	New England Biolabs, Ipswich, USA
RQ1 RNase-Free DNase	Promega, Madison, USA
TaqMan® Universal PCR Master Mix	Applied Biosystems, Foster City, USA
T4 DNA Ligase	New England Biolabs, Ipswich, USA

Table 9. Enzymes used in this work

5.1.9. Plasmid

Plasmid	Notes	Reference
HIV-1 pCMV-ΔR8.91	NL4.3 gag pol, tat and rev expression plasmid. ΔvifΔvprΔvpuΔenvΔnef.	Torsten Schaller (Universitätsklinikum Heidelberg) [141, 272]
HIV-1 pCMV-ΔR8.91Ex	NL4.3 gag pol, tat and rev expression plasmid modified. ΔvifΔvprΔvpuΔenvΔnef	Torsten Schaller (Universitätsklinikum Heidelberg) [273, 274]
HIV-1 pCMV-ΔR8.91Ex-SCA	NL4.3 gag pol, tat and rev expression plasmid encoding SIV_{MAC} CA. ΔvifΔvprΔvpuΔenvΔnef	Torsten Schaller (Universitätsklinikum Heidelberg) [274]
HIV-1 pCMV-ΔR8.91-N74D	NL4.3 gag pol, tat and rev expression plasmid harboring CA mutation N74D. ΔvifΔvprΔvpuΔenvΔnef.	Torsten Schaller (Universitätsklinikum Heidelberg) [141, 163]
HIV-1 pCMV-ΔR8.91-P90A	NL4.3 gag pol, tat and rev expression plasmid harboring CA mutation P90A. ΔvifΔvprΔvpuΔenvΔnef.	Torsten Schaller (Universitätsklinikum Heidelberg) [114, 141]
HIV-1 pCMV-ΔR8.91-A105T	NL4.3 gag pol, tat and rev expression plasmid harboring CA mutation A105T. ΔvifΔvprΔvpuΔenvΔnef.	Torsten Schaller (Universitätsklinikum Heidelberg) [169]
HIVac-1	NL4-3 gag pol, tat and rev expression plasmid encoding GFP in place of nef and harboring V86I-IAP91LPA-M96L CA mutations. ΔvifΔvprΔvpuΔenvΔnef.	Nicolas Manel (Institut Curie, Paris) [103]
HIV-1 pCSxW	HIV-1 vector	Torsten Schaller (Universitätsklinikum Heidelberg) [275]
HIV-1 pCSxW-HA	HIV-1 vector hemagglutinin (HA)- tagged	Torsten Schaller (Universitätsklinikum Heidelberg) [275]
HIV-1 pCSGW	HIV-1 vector encoding GFP	Torsten Schaller (Universitätsklinikum Heidelberg) [141, 276]
VSV-G Env pMD.G	VSV-G expression plasmid	Torsten Schaller (Universitätsklinikum Heidelberg) [274, 277]

MLV pCNCG	MLV vector encoding GFP	Torsten Schaller (Universitätsklinikum Heidelberg) [274, 278]
MLV-N/B pCIG3 N/B	MoMLV gag pol expression plasmid	Torsten Schaller (Universitätsklinikum Heidelberg) [274, 279]
HIV-2pack	HIV-2 gag pol expression plasmid	Torsten Schaller (Universitätsklinikum Heidelberg) [274, 280]
HIV-2GFP	HIV-2 vector encoding GFP	Torsten Schaller (Universitätsklinikum Heidelberg) [274, 280]
FIV pFP93	FIV gag pol expression plasmid	Torsten Schaller (Universitätsklinikum Heidelberg) [274, 281]
FIV pGinSin	FIV vector encoding GFP	Torsten Schaller (Universitätsklinikum Heidelberg) [274, 281]
EIAV pONY3.0	EIAV gag pol expression plasmid	Torsten Schaller (Universitätsklinikum Heidelberg) [274, 282]
EIAV pONY8.7GFP	EIAV vector encoding GFP	Torsten Schaller (Universitätsklinikum Heidelberg) [274, 283]
SIV pSIV3+	SIV gag pol expression plasmid	Torsten Schaller (Universitätsklinikum Heidelberg) [274, 284]
pSIVRMES4	SIV vector encoding GFP	Torsten Schaller (Universitätsklinikum Heidelberg) [274, 284]
pNL4.3	Full-length NL4.3 molecular clone	Torsten Schaller (Universitätsklinikum Heidelberg) [204, 285]
pNL4.3-GFP	Full-length NL4.3 encoding GFP in place of Nef followed by an IRES-Nef cassette	Torsten Schaller (Universitätsklinikum Heidelberg) [141, 286]
pNL4.3-N74D-GFP	Full-length NL4.3 encoding GFP in place of Nef followed by an IRES-Nef cassette harboring CA mutation N74D.	Torsten Schaller (Universitätsklinikum Heidelberg) [141, 163]
pNL4.3-P90A-GFP	Full-length NL4.3 encoding GFP in place of Nef followed by an IRES-Nef cassette harboring CA mutation P90A.	Torsten Schaller (Universitätsklinikum Heidelberg) [114, 141]
pNL4.3-A105T-GFP	Full-length NL4.3 encoding GFP in place of Nef followed by an IRES-Nef cassette harboring CA mutation A105T.	Torsten Schaller (Universitätsklinikum Heidelberg) [169]
pIIIB	Full-length IIIB molecular clone	Torsten Schaller (Universitätsklinikum Heidelberg) [204, 287]
pRHPA	Full-length T/F HIV-1-RHPA molecular clone	Torsten Schaller (Universitätsklinikum Heidelberg) [204, 288]
pWITO	Full-length T/F HIV-1-WITO molecular clone	Torsten Schaller (Universitätsklinikum Heidelberg) [204, 288]

pTHRO	Full-length T/F HIV-1-THRO molecular clone	Torsten Schaller (Universitätsklinikum Heidelberg) [204, 288]
pSUMA	Full-length T/F HIV-1-SUMA molecular clone	Torsten Schaller (Universitätsklinikum Heidelberg) [204, 288]
pZM247	Full-length T/F HIV-1-ZM247 molecular clone	Torsten Schaller (Universitätsklinikum Heidelberg) [204, 288]
pLVX-Puro-MX2	Lentiviral vector encoding Mx2 wild type	Mirjam Schilling (Universitätsklinikum Freiburg) [220]
pLVX-Puro-MX2(K131A)	Lentiviral vector encoding Mx2 mutant devoid of GTPase activity	Mirjam Schilling (Universitätsklinikum Freiburg) [220]
pLVX-Puro-MX2(T151A)	Lentiviral vector encoding Mx2 mutant devoid of GTPase activity	Mirjam Schilling (Universitätsklinikum Freiburg) [220]
pLVX-Puro-MX2(D297N)	Lentiviral vector encoding Mx2 mutant devoid of GTPase activity	Mirjam Schilling (Universitätsklinikum Freiburg) [220]
pLVX-Puro-MX2(D300N)	Lentiviral vector encoding Mx2 mutant devoid of GTPase activity	Mirjam Schilling (Universitätsklinikum Freiburg) [220]
pLVX-Puro-MX2(M574D)	Lentiviral vector encoding Mx2 mutant that prevents oligomerization	Mirjam Schilling (Universitätsklinikum Freiburg) [220]
pLVX-Puro-MX2(-NLS)	Lentiviral vector encoding Mx2 mutant lacking the first 25 amino-terminus aminoacids (NLS)	Mirjam Schilling (Universitätsklinikum Freiburg) [220]
pLVX-Puro-MX1	Lentiviral vector encoding Mx1 wild type	Mirjam Schilling (Universitätsklinikum Freiburg) [220]
pLVX-Puro-MX1(K83A)	Lentiviral vector encoding Mx1 mutant devoid of GTPase activity	Mirjam Schilling (Universitätsklinikum Freiburg) [595]
TopoTA pCR2.1-LUC	Cloning vector harboring *firefly* luciferase (LUC) cDNA	Torsten Schaller (Universitätsklinikum Heidelberg) [289]
TopoTA pCR2.1-SUN1	Cloning vector harboring SUN1 cDNA	Torsten Schaller (Universitätsklinikum Heidelberg) [289]
TopoTA pCR2.1-SUN2	Cloning vector harboring SUN2 cDNA	Torsten Schaller (Universitätsklinikum Heidelberg) [289]
TopoTA pCR2.1-LMNA	Cloning vector harboring LMNA cDNA	Torsten Schaller (Universitätsklinikum Heidelberg) [289]
TopoTA pCR2.1- EMD	Cloning vector harboring EMD cDNA	Juan Martin-Serrano (King's College London) [289]
TopoTA pCR2.1-EMDΔLEM	Cloning vector harboring EMDΔLEM cDNA	Juan Martin-Serrano (King's College London) [289]
pBudCE4.1-NET26	Cloning vector harboring NET26 cDNA	Rose Goodchild (KU Leuven) [290]

pBudCE4.1-NET31	Cloning vector harboring NET31 cDNA	Rose Goodchild (KU Leuven) [290]
pBudCE4.1-NET39	Cloning vector harboring NET39 cDNA	Rose Goodchild (KU Leuven) [290]
pBudCE4.1-LUMA	Cloning vector harboring LUMA cDNA	Rose Goodchild (KU Leuven) [290]
pBudCE4.1-LBR	Cloning vector harboring LBR cDNA	Rose Goodchild (KU Leuven) [290]
pBudCE4.1-LULL1	Cloning vector harboring LULL1 cDNA	Rose Goodchild (KU Leuven) [290]
pBudCE4.1-NET3	Cloning vector harboring NET3 cDNA	Rose Goodchild (KU Leuven) [290]
pBudCE4.1-TSPAN5	Cloning vector harboring TSPAN5 cDNA	Rose Goodchild (KU Leuven) [290]
pBudCE4.1-TMEM53	Cloning vector harboring TMEM53 cDNA	Rose Goodchild (KU Leuven) [290]
pBudCE4.1-LAP2 β	Cloning vector harboring LAP2β cDNA	Rose Goodchild (KU Leuven) [290]
pBudCE4.1-TORSA	Cloning vector harboring TORSA cDNA	Rose Goodchild (KU Leuven) [290]
pBudCE4.1-TORSA-EQ	Cloning vector harboring g TORSA-EQ cDNA	Rose Goodchild (KU Leuven) [290]
pBudCE4.1-NURIM	Cloning vector harboring NURIM cDNA	Rose Goodchild (KU Leuven) [290]
plentiCRISPRv2	Retroviral vector with a puromycin resistance marker to express guide RNAs (gRNAs) constructs for CRISPR-mediated genome editing.	Addgene, Cambridge, USA
pSIREN RetroQ vector (pSRQ)	Retroviral vector with a puromycin resistance marker to express short hairpin RNAs (ShRNAs) constructs for targeted gene silencing.	Clontech, Mountain View, USA

Table 10. Plasmids used in this work

5.1.10. Primers

OTS1	ATCGAATTCATGGATTTTTCTCGGCTTCACATGTAC
OTS2	ATCAGATCTCACCATGGATTTTTCTCGGCTTCACATGTAC
OTS3	GATGCGGCCGCTCACTTGACAGGTTCGCCATGAACTCTG
OTS4	ATGCGAATTCATGTCCCGAAGAAGCCAGCGCCTCACGCGCTAC
OTS5	ATGCAGATCTATGTCCCGAAGAAGCCAGCGCCTCACGCGCTAC
OTS6	GCATGCGGCCGCCTAGTGGGCGGGCTCCCCATGCACTCTGAAGC
OTS7	ATCGAATTCATGGAAGACGCCAAAAACATAAAGAAAG
OTS8	GATGCGGCCGCTTACACGGCGATCTTTCCGCCCTTC
OTS9	ATCGAATTCTCAGATGCTCTGGATTTTGAGACGGAGC
OTS10	ATCGAATTCACAGCATGCACCCTGGGGGATGGTGAGG
OTS11	ATCGAATTCACAAAACAGCGCAGAAGCACAAACAAATCAG
OTS12	ATCGAATTCGCTTTTAGTATCAACCACGTGTCAAGGCAGGTC
OTS13	ATCGAATTCGGGAAGGCAGCCTCTGGAGTGTTCTGGTG

OTS14	GATGCGGCCGCTCACAGCTGGAGGTGCTCGACTGTGGGCAGGAG
OTS15	ATGGTGACGCCAACTGGGGCTACTCGGATGTGGACCAG
OTS16	TCCACATCCGAGTAGCCCCAGTTGGCGTCACCATGCAG
OTS17	ATCGAATTCATGGTCTCACGGGCGGGCTCCTTACTCTGGATG
OTS18	GATGCGGCCGCTCATGTCACTCCAATCACACCTTCTTTCTG
OTS19	AGCAGCTCTGCCGCCGCGAAGAACCGAGCG
OTS20	TTCTTCGCGGCGGCAGAGCTGCTGGTGCC
OTS21	TCCCTGGCGGCCGCAAGCGCCAGAACAACAAAAC
OTS22	TGTTCTGGCGCTTGCGGCCGCCAGGGAGACAGC
OTS23	AAGAACGCATCGTCCGCAACAACAAAACAGCG
OTS24	GTTGTTGCGGACGATGCGTTCTTCAGGGAGAC
OTS25	CCGAGCGAGCGCAGCAGCAAAACAGCGCAGAAG
OTS26	CTGTTTTGCTGCTGCGCTCGCTCGGTTCTTCAG
OTS27	GCCAGAGCAGCAGCAGCGCGCAGAAGCACA
OTS28	TCTGCGCGCTGCTGCTGCTCTGGCCGCTCG
OTS29	AGGATGCTGTGACGCGTCGGCCTCCTGTATTG
OTS30	AGGCCGACGCGTCACAGCATCCTGCAGGCTG
OTS31	GATACGCGTCGACTCACTGTAGTAGGAGGTGTG
OTS32	ATCGAATTCATCACGCGTATGAATTTCCCACGTGCGCTTGCTGG
OTS33	GATGCGGCCGCTCAGAGTTTTGTAGCTGCTGTTGGC
OTS34	GATGCGGCCGCTCAACGCGTCACAGCATCCTGCAGGCTGAC
OTS35	ATCCAATTGATGGACAACTACGCAGATCTTTCGGATAC
OTS36	ATCCAATTGATGGACAGGCGGCGGCTCTCGCCCCCCAGC
OTS37	GATGCGGCCGCCTAGAAGGGGTTGCCTTCTTCAGCCTGCATG
OTS38	ATCGAATTCATGGAGACCCCGTCCCAGCGGCGCG
OTS39	GATGCGGCCGCTTACATGATGCTGCAGTTCTGGGGGCTC
OTS40	ATCGAATTCATGCAGGACACTGGCTCAGTAGTGCC
OTS41	GATGCGGCCGCCTAATGGGGTCTGTTGAACATACTAAC
OTS42	ATCGAATTCATGATGCAGGGGGAGGCACACCCTAGTG
OTS43	GATGCGGCCGCCTACTCGCCAAAGATCCACAATATATTC
OTS44	ATCGAATTCATGCCAGCTTCCCAGAGCCGGGCCCG
OTS45	GATGCGGCCGCTCACCAGGCAGAGATGAGCATCTGGC
OTS46	ATCGAATTCATGGCCGCGAATTATTCCAGTACCAG
OTS47	GATGCGGCCGCTCACTCCAACTTTTTGGCTGGCACCCG
OTS48	ATCGAATTCATGCCAAGTAGGAAATTTGCCGATGGTG
OTS49	GATGCGGCCGCTTAGTAGATGTATGGAAATATACGGTAGGGC
OTS50	ATCGGATCCACCATGCCAAGTAGGAAATTTGCCGATGG
OTS51	TGAGGGCCCCTACGCATAGTCAGGAACATCGTATGGGTAGGCGGCCGCGTAG ATGTATGGAAATATACGGTAG
OTS52	ATCGAATTCATGGCCGACAGTGGACTTAGGGAACC

OTS53	GATGCGGCCGCTTAGAAAAGGCACCCCTGTTCTTCTATG
OTS54	ATCAGATCTCACCATGGCCGACAGTGGACTTAGGGAACC
OTS55	GATGCGGCCGCGAAAAGGCACCCCTGTTCTTCTATGC
OTS56	ATCGAATTCATGGCCACGGCCGTGAGCCGGCCCTG
OTS57	GATGCGGCCGCCTATTCTTTGAACTCCAAGAACTGTTG
OTS58	ATCGGATCCACCATGGCCACGGCCGTGAGCCGGCCCTG
OTS59	GATGCGGCCGCTTCTTTGAACTCCAAGAACTGTTGAAG
OTS60	ATCGGATCCACCATGTCCGGGAAGCACTACAAGGGTCCTG
OTS61	GATGCGGCCGCCCAGCTCGCCCTGACAGCTTCGATATC
OTS62	ATCGGATCCACCATGGCCTCGGCAGAGCTGGACTACACC
OTS63	GATGCGGCCGCGCAGCGGACGCAGTTGCGCATGAAG
OTS64	ATCGGATCCACCATGCCGGAGTTCCTGGAAGACCCCTC
OTS65	GATGCGGCCGCGTTGGATTTTCTAGGGTCAACATG
OTS66	ATCGAATTCATGAAGCTGGGCCGGGCCGTGCTGGGCCTG
OTS67	GATGCGGCCGCTCAATCATCGTAGTAATAATCTAAC
OTS68	ATCGGATCCACCATGAAGCTGGGCCGGGCCGTGCTGGGCCTG
OTS69	GATGCGGCCGCATCATCGTAGTAATAATCTAACTTG
OTS70	ATCGAATTCATGGCCCCTGCACTGCTCCTGATCCCTG
OTS71	GATGCGGCCGCTCACTCTGCCTCCCCATCCTGGGGCCGAG
OTS72	ATCAGATCTCACCATGGCCCCTGCACTGCTCCTGATCC
OTS73	GATGCGGCCGCCTCTGCCTCCCCATCCTGGGGCCG
OTS74	ATCCAATTGATGTTACCGAGTACTTCAGTGAATTCC
OTS75	GATGCGGCCGCTTATTTCACTCTGTACTTATAGAAAGAAC
OTS76	ATCGGATCCACCATGTTACCGAGTACTTCAGTGAATTC
OTS77	GATGCGGCCGCTTTCACTCTGTACTTATAGAAAGAAC
OTS78	ACTGGAAGGGCTTTAAGACTCCCAACGAAGAC
OTS79	TTCGTTGGGAGTCTTAAAGCCCTTCCAGTCCC
OTS80	ATCCCTCAGACCGAAAAAGTCAGTGTGGAAAATC
OTS81	TCCACACTGACTTTTTCGGTCTGAGGGATCTCTAG
OTS82	ATCGCGGCCGCTGGTGAGAGATGGGTGCGAGAGCGTCGGTATTAAGCGGGGG
OTS83	ACCTGATCATACTGTCTTACTTTGATAAAACC
OTS84	TTGCATCCAGTGCAAGCAGGGCCTATTGCACC
OTS85	TGCAATAGGCCCTGCTTGCACTGGATGCAATC
OTS86	AGGATGGATGACAAATAATCCACCTATCCC
OTS87	ATAGGTGGATTATTTGTCATCCATCCTATTTG
OTS88	AGCATTGGGACCAGCAGCGACACTAGAAG
OTS89	TAGTGTCGCTGCTGGTCCCAATGCTTTTAAAATAG
OTS90	TGCATCCAGTGCACGCAGGCCCTATTGCAC
OTS91	TGCAATAGGGCCTGCGTGCACTGGATGCAATC

OTS92	GCATTACTCCACGGAGGAGAACAAGAAATGGAACCAGTAGATCCTAGAC
OTS93	TGGTTCCATTTCTTGTTCTCCTCCGTGGAGTAATGCCTATTCTGCTATG
OTS94	ATTGGGACCAGGAGCTACACTAGAAGAAATG
OTS95	AGTGTAGCTCCTGGTCCCAATGCTTTTAAG
OTS96	ATCGGATCCACCATGTCTAAGGCCCACAAGCCTTGGCCCTAC
OTS97	GATGCGGCCGCGTGGATCTCTTTGCTGGAGAATTGAC
OTS98	ATCGGATCCACCATGAATTCCTTCCAGCAACAGCCACCGCC
OTS99	ATCGAATTCATGGTTGTTTCCGAAGTGGACATCGCAAAAG
OTS100	GATGCGGCCGCTTAACCGGGGAACTGGGCAAGCCGGCGCCG
OTS101	ATCGGATCCACCATGGAAGACGCCAAAAACATAAAG
OTS102	GATGCGGCCGCCACGGCGATCTTTCCGCCCTTCTTG
OTS103	GATCCGCACAAATTGGACCCTGTATTCAAGAGATACAGGGTCCAATTTGTGCTTTTTTACGCGTG
OTS104	AATTCACGCGTAAAAAAGCACAAATTGGACCCTGTATCTCTTGAATACAGGGTCCAATTTGTGCG
OTS105	GATCCGAGGGAGACTGACTTTATGTTCAAGAGACATAAAGTCAGTCTCCCTCTTTTTTACGCGTG
OTS106	AATTCACGCGTAAAAAAGAGGGAGACTGACTTTATGTCTCTTGAACATAAAGTCAGTCTCCCTCG
OTS107	GATCCGGGACAGTTCACGTATGATTTCAAGAGAATCATACGTGAACTGTCCCTTTTTTACGCGTG
OTS108	AATTCACGCGTAAAAAAGGGACAGTTCACGTATGATTCTCTTGAAATCATACGTGAACTGTCCCG
OTS109	GATCCGTCAGAGCACCCTGTTTAATTCAAGAGATTAAACAGGGTGCTCTGACTTTTTTACGCGTG
OTS110	AATTCACGCGTAAAAAAGTCAGAGCACCCTGTTTAATCTCTTGAATTAAACAGGGTGCTCTGACG
OTS111	GATCCGACGTATGGTGCTTGGTATTTCAAGAGAATACCAAGCACCATACGTCTTTTTTACGCGTG
OTS112	AATTCACGCGTAAAAAAGACGTATGGTGCTTGGTATTCTCTTGAAATACCAAGCACCATACGTCG
OTS113	GATCCGCCGTTACCTTAGAGCATGTTTCAAGAGAACATGCTCTAAGGTAACGGTTTTTTTACGCGTG
OTS114	AATTCACGCGTAAAAAACCGTTACCTTAGAGCATGTTCTCTTGAAACATGCTCTAAGGTAACGGCG
OTS115	GATCCGACTCAGAAGACCTCTTCATTCAAGAGATGAAGAGGTCTTCTGAGTCTTTTTTACGCGTG
OTS116	AATTCACGCGTAAAAAAGACTCAGAAGACCTCTTCATCTCTTGAATGAAGAGGTCTTCTGAGTCG
OTS117	CACCGTACGTGTAGCCCGTGTTCTC
OTS118	AAACGAGAACACGGGCTACACGTAC
OTS119	CACCGTCGTGGCCAGGCGCAAACTA

OTS120	AAACTAGTTTGCGCCTGGCCACGAC
OTS121	CACCGGACTCGACGGCCTCCTGTAT
OTS122	AAACATACAGGAGGCCGTCGAGTCC
OTS123	CACCGCGCCTCACGCGCTACTCCCA
OTS124	AAACTGGGAGTAGCGCGTGAGGCGC
OTS125	CACCGAACTGCATGGTGACGCCAAC
OTS126	AAACGTTGGCGTCACCATGCAGTTC
OTS127	CACCGCTCCTCTGAGGACGACTACG
OTS128	AAACCGTAGTCGTCCTCAGAGGAGC
OTS129	CACCGACACTCTCTGGAGCGGCGTC
OTS130	AAACGACGCCGCTCCAGAGAGTGTC
OTS131	CACCGTATGTCCCGGGTACACTCTC
OTS132	AAACGAGAGTGTACCCGGGACATAC
OTS133	CACCGAATTGACTTCTCCTCCGGTA
OTS134	AAACTACCGGAGGAGAAGTCAATTC
OTS135	CACCGGGCACTGTGCCGAATGGCGG
OTS136	AAACCCGCCATTCGGCACAGTGCCC
OTS137	CACCGACAAGCCTTGGCCCTACCGG
OTS138	AAACCCGGTAGGGCCAAGGCTTGTC
OTS139	CACCGTGTGGTGGCACTGTGCCGAA
OTS140	AAACTTCGGCACAGTGCCACCACAC
OTS141	ACACTGCTGCTGGCCGTGTTTCCTG
OTS142	AGTCACCAGGATGAACAGATTCAG
OTS143	AGTAATAGTTGCTCTTGAAAATCCAC
OTS144	TCGAGACAGGGTGCGGCTTTACAGAC
OTS145	ACAGTGCAGGGGTGCTTCACAGATC
OTS146	TGCTGTGTGCTCATACACATGGAGC
OTS147	TTGTAAAGTTTGAATGTGGC
OTS148	AAGTCCTCGGTGGCCTTGCG
OTS149	TGTTGGCCTTAGGTTGCCATAG
OTS150	AGCACCCACCATGTGTGAGC
OTS151	AGCAAAGGAACATTGAGACTCTACTG
OTS152	TTATTGTGGTGGGCTTACATGACAGC

Table 11. Oligonucleotide sequences used in this study

5.1.11. TaqMan qPCR primer/ probes/ standards

Target	Primer 1 5'-3'	Primer 2 5'-3'	Probe 5'-3' (F: FAM, Ta:TAMRA)	Standard
GFP	GT139 (CAACAGCCACAACGTCTATATCAT)	GT140 (ATGTTGTGGCGGATCTTGAAG)	GFP-P (**F**)-CCGACAAGCAGAAGAACGGCATCAA-(**Ta**)	pCNCG
***2-LTR* circles**	2-LTR Fwd (AACTAGAGATCCCTCAGACCCTTTT)	2-LTR Rev (CTTGTCTTCGTTGGGAGTGAATT)	2-LTR P (**F**)-CTAGAGATTTTCCACACTGAC-(**Ta**)	p2LTR
***2-LTR* circles++**	2-LTR++ Fwd (AACTAGAGATCCCTCAGACCGAAAA)	2-LTR++ Rev (CTTGTCTTCGTTGGGAGTCTTAA)	2-LTR P (**F**)-CTAGAGATTTTCCACACTGAC-(**Ta**)	p2LTR++
MS2 genomic DNA	RT-Assay-fwd (TCCTGCTCAACTTCCTGTCGAG)	RT-Assay-rev (CACAGGTCAAACCTCCTAGGAATG)	**SYBR Green**	HIV-1 RT

Table 12. TaqMan qPCR primer/ probes/ standards

5.1.12. Generated plasmids

Name	Template	Primers (PCR)	Enzymes	Target/ *SDM*
pCSxW-HA-SUN1	TopoTA pCR2.1-SUN1	OTS1 OTS3	*Eco*RI, *Not*I	pCSxW-HA
pCSxW-SUN1	TopoTA pCR2.1-SUN1	OTS2 OTS3	*Bgl*II, *Not*I	pCSxW
pCSxW-HA-SUN2	TopoTA pCR2.1-SUN2	OTS4 OTS6	*Eco*RI, *Not*I	pCSxW-HA
pCSxW-SUN2	TopoTA pCR2.1-SUN2	OTS5 OTS6	*Bgl*II, *Not*I	pCSxW
pCSxW-HA-LUC	TopoTA pCR2.1-LUC	OTS7 OTS8	*Eco*RI, *Not*I	pCSxW-HA
pCSxW-HA-SUN1Δ30	pCSxW-HA-SUN1	OTS9 OTS3	*Eco*RI, *Not*I	pCSxW-HA
pCSxW-HA-SUN1Δ60	pCSxW-HA-SUN1	OTS10 OTS3	*Eco*RI, *Not*I	pCSxW-HA
pCSxW-HA-SUN1Δ90	pCSxW-HA-SUN1	OTS11 OTS3	*Eco*RI, *Not*I	pCSxW-HA
pCSxW-HA-SUN1Δ100	pCSxW-HA-SUN1	OTS12 OTS3	*Eco*RI, *Not*I	pCSxW-HA

pCSxW-HA-SUN1Δ355	pCSxW-HA-SUN1	OTS13 OTS3	*EcoR*I, *Not*I	pCSxW-HA
pCSxW-HA-SUN1-1-583	pCSxW-HA-SUN1	OTS1 OTS14	*EcoR*I, *Not*I	pCSxW-HA
pCSxW- HA-SUN2ΔLBS	pCSxW-HA-SUN2	OTS15 OTS16	-	*SDM* (pCSxW-HA-SUN2)
pCSxW- HA-SUN2Δ157	pCSxW-HA-SUN2	OTS17 OTS6	*EcoR*I, *Not*I	pCSxW-HA
pCSxW-HA-SUN2-1-524	pCSxW-HA-SUN2	OTS4 OTS18	*EcoR*I, *Not*I	pCSxW-HA
pCSxW-HA-SUN1-80SAAA83	pCSxW-HA-SUN1	OTS19 OTS20	-	*SDM* (pCSxW-HA-SUN1)
pCSxW-HA-SUN1-84AAAS87	pCSxW-HA-SUN1	OTS21 OTS22	-	*SDM* (pCSxW-HA-SUN1)
pCSxW-HA-SUN1-86ASSA89	pCSxW-HA-SUN1	OTS23 OTS24	-	*SDM* (pCSxW-HA-SUN1)
pCSxW-HA-SUN1-88SAAA91	pCSxW-HA-SUN1	OTS25 OTS26	-	*SDM* (pCSxW-HA-SUN1)
pCSxW-HA-SUN1-90AAAA93	pCSxW-HA-SUN1	OTS27 OTS28	-	*SDM* (pCSxW-HA-SUN1)
pCSxW- HA-SUN1*MluI*	pCSxW-HA-SUN1	OTS29 OTS30	-	*SDM* (pCSxW-HA-SUN1)
pCSxW-HA-SUN2^{NTD}-SUN1	pCSxW-HA-SUN2	OTS4 OTS31	*EcoR*I, *Mlu*I	pCSxW- HA-SUN1*MluI*
pCSxW HA-Fv1^{n}	Fv1n cDNA	OTS32 OTS33	*EcoR*I-*Mlu*I, *Not*I	pCSxW-HA
pCSxW-HA-SUN1^{NTD}-Fv1^{n}	pCSxW-HA-SUN1	OTS1 OTS34	*EcoR*I, *Mlu*I	pCSxW HA-Fv1^{n}
pCSxW- HA-EMD	EMD cDNA	OTS35 OTS37	*Mfe*I, *Not*I	pCSxW-HA
pCSxW- HA-EMDΔLEM	EMDΔLEM cDNA	OTS36 OTS37	*Mfe*I, *Not*I	pCSxW-HA
pCSxW- HA-LMNA	LMNA cDNA	OTS38 OTS39	*EcoR*I, *Not*I	pCSxW-HA
pCSxW- HA-NET26	pBudCE4.1-NET26	OTS40 OTS41	*EcoR*I, *Not*I	pCSxW-HA
pCSxW- HA-NET31	pBudCE4.1-NET31	OTS42 OTS43	*EcoR*I, *Not*I	pCSxW-HA
pCSxW- HA-NET39	pBudCE4.1-NET39	OTS44 OTS45	*EcoR*I, *Not*I	pCSxW-HA
pCSxW- HA-LUMA	pBudCE4.1-LUMA	OTS46 OTS47	*EcoR*I, *Not*I	pCSxW-HA
pCSxW- HA-LBR	pBudCE4.1-LBR	OTS48 OTS49	*EcoR*I, *Not*I	pCSxW-HA
pCSxW- LBR-HA	pCSxW- HA-LBR	OTS50 OTS51	*BamH*I, *PspOM*I	pCSxW
pCSxW- HA-LULL1	pBudCE4.1-LULL1	OTS52 OTS53	*EcoR*I, *Not*I	pCSxW-HA
pCSxW- LULL1-HA	pBudCE4.1-LULL1	OTS54 OTS55	*Bgl*II, *Not*I	pCSxW- LBR-HA

pCSxW- HA-NET3	pBudCE4.1-NET3	OTS56 OTS57	*EcoR*I, *Not*I	pCSxW-HA
pCSxW- NET3-HA	pBudCE4.1-NET3	OTS58 OTS59	*BamH*I, *Not*I	pCSxW- LBR-HA
pCSxW- TSPAN5-HA	pBudCE4.1-TSPAN5	OTS60 OTS61	*BamH*I, *Not*I	pCSxW- LBR-HA
pCSxW- TMEM53-HA	pBudCE4.1-TMEM53	OTS62 OTS63	*BamH*I, *Not*I	pCSxW- LBR-HA
pCSxW- LAP2β-HA	pBudCE4.1-LAP2β	OTS64 OTS65	*BamH*I, *Not*I	pCSxW- LBR-HA
pCSxW- HA-TORSA	pBudCE4.1-TORSA	OTS66 OTS67	*EcoR*I, *Not*I	pCSxW-HA
pCSxW- TORSA-HA	pBudCE4.1-TORSA	OTS68 OTS69	*BamH*I, *Not*I	pCSxW- LBR-HA
pCSxW- HA-TORSA-EQ	pBudCE4.1-TORSA-EQ	OTS66 OTS67	*EcoR*I, *Not*I	pCSxW-HA
pCSxW- TORSA-EQ-HA	pBudCE4.1-TORSA-EQ	OTS68 OTS69	*BamH*I, *Not*I	pCSxW- LBR-HA
pCSxW- HA-NURIM	pBudCE4.1-NURIM	OTS70 OTS71	*EcoR*I, *Not*I	pCSxW-HA
pCSxW- NURIM-HA	pBudCE4.1-NURIM	OTS72 OTS73	*Bgl*II, *Not*I	pCSxW- LBR-HA
pCSxW- HA-UNCL	pBudCE4.1-UNCL	OTS74 OTS75	*Mfe*I, *Not*I	pCSxW-HA
pCSxW- UNCL-HA	pBudCE4.1-UNCL	OTS76 OTS77	*BamH*I, *Not*I	pCSxW- LBR-HA
pCSGW+	pCSGW	OTS78 OTS79	-	*SDM* (pCSGW)
pCSGW++	pCSGW+	OTS80 OTS81	-	*SDM* (pCSGW+)
p2LTR++	p2LTR	2-LTR Fwd 2-LTR Rev	-	*SDM* (p2LTR)
pCMV-ΔR8.91Ex-NRA	pRHPA	OTS82 OTS83	*Not*I, *Apa*I	pCMV-ΔR8.91Ex
pCMV-ΔR8.91Ex-H87Q	pCMV-ΔR8.91Ex	OTS84 OTS85	-	*SDM* (pCMV-ΔR8.91Ex)
pCMV-ΔR8.91Ex-H120N	pCMV-ΔR8.91Ex	OTS86 OTS87	-	*SDM* (pCMV-ΔR8.91Ex)
pCMV-ΔR8.91Ex-G208A	pCMV-ΔR8.91Ex	OTS88 OTS89	-	*SDM* (pCMV-ΔR8.91Ex)
pCMV-ΔR8.91Ex- H87Q-H120N	pCMV-ΔR8.91Ex-H87Q	OTS86 OTS87	-	*SDM* (pCMV-ΔR8.91Ex-H87Q)
pCMV-ΔR8.91Ex- H87Q-H120N- G208A	pCMV-ΔR8.91Ex-H87Q- H120N	OTS88 OTS89	-	*SDM* (pCMV-ΔR8.91Ex-H87Q-H120N)
pCMV-ΔR8.91Ex-NRA-Q87H	pCMV-ΔR8.91Ex-NRA	OTS90 OTS91	-	*SDM* (pCMV-ΔR8.91Ex-NRA)
pCMV-ΔR8.91Ex-NRA-Q87H-N120H	pCMV-ΔR8.91Ex-NRA-Q87H	OTS92 OTS93	-	*SDM* (pCMV-ΔR8.91Ex-NRA-Q87H)

pCMV-ΔR8.91Ex-NRA-Q87H-N120H-A208G	pCMV-ΔR8.91Ex-NRA-Q87H-N120H	OTS94 OTS95	-	*SDM* (pCMV-ΔR8.91Ex-NRA-Q87H-N120H)
pNL4.3-BRX	pRHPA	-	*BssH*II, *Xho*I	pNL4.3
pNL4.3-BRE	pRHPA	-	*BssH*II, *EcoR*I	pNL4.3
pNL4.3-ERX	pRHPA	-	*EcoR*I, *Xho*I	pNL4.3
pCSxW- MX2-HA	pLVX-Puro-MX2	OTS96 OTS97	*BamH*I, *Not*I	pCSxW- LBR-HA
pCSxW- MX2(K131A)-HA	pLVX-Puro-MX2(K131A)	OTS96 OTS97	*BamH*I, *Not*I	pCSxW- LBR-HA
pCSxW- MX2(T151A)-HA	pLVX-Puro-MX2(T151A)	OTS96 OTS97	*BamH*I, *Not*I	pCSxW- LBR-HA
pCSxW- MX2(D297N)-HA	pLVX-Puro-MX2(D297N)	OTS96 OTS97	*BamH*I, *Not*I	pCSxW- LBR-HA
pCSxW- MX2(D300N)-HA	pLVX-Puro-MX2(D300N)	OTS96 OTS97	*BamH*I, *Not*I	pCSxW- LBR-HA
pCSxW- MX2(M574D)-HA	pLVX-Puro-MX2(M574D)	OTS96 OTS97	*BamH*I, *Not*I	pCSxW- LBR-HA
pCSxW- MX2(-NLS)-HA	pLVX-Puro-MX2(-NLS)	OTS98 OTS97	*BamH*I, *Not*I	pCSxW- LBR-HA
pCSxW- HA-MX1	pLVX-Puro-MX1	OTS99 OTS100	*EcoR*I, *Not*I	pCSxW-HA
pCSxW- HA-MX1(K83A)	pLVX-Puro-MX1(K83A)	OTS99 OTS100	*EcoR*I, *Not*I	pCSxW-HA
pCSxW-LUC-HA	pCSxW-HA-LUC	OTS101 OTS102	*BamH*I, *Not*I	pCSxW- LBR-HA
pSRQ_SUN1_sh1	Primer annealing	OTS103 OTS104	*BamH*I, *EcoR*I	pSRQ
pSRQ_SUN1_sh2	Primer annealing	OTS105 OTS106	*BamH*I, *EcoR*I	pSRQ
pSRQ_SUN1_sh3	Primer annealing	OTS107 OTS108	*BamH*I, *EcoR*I	pSRQ
pSRQ_SUN2_sh1	Primer annealing	OTS109 OTS110	*BamH*I, *EcoR*I	pSRQ
pSRQ_SUN2_sh2	Primer annealing	OTS111 OTS112	*BamH*I, *EcoR*I	pSRQ
pSRQ_SUN2_sh3	Primer annealing	OTS113 OTS114	*BamH*I, *EcoR*I	pSRQ
pSRQ_SUN2_sh4	Primer annealing	OTS115 OTS116	*BamH*I, *EcoR*I	pSRQ
plentiCRISPRv2_SUN1g1	Primer annealing	OTS117 OTS118	*Bsmb*I	plentiCRISPRv 2
plentiCRISPRv2_SUN1g2	Primer annealing	OTS119	*Bsmb*I	plentiCRISPRv

		OTS120		2
plentiCRISPRv2_SUN1g3	Primer annealing	OTS121 OTS122	*Bsmb*I	plentiCRISPRv2
plentiCRISPRv2_SUN2g1	Primer annealing	OTS123 OTS124	*Bsmb*I	plentiCRISPRv2
plentiCRISPRv2_SUN2g2	Primer annealing	OTS125 OTS126	*Bsmb*I	plentiCRISPRv2
plentiCRISPRv2_SUN2g3	Primer annealing	OTS127 OTS128	*Bsmb*I	plentiCRISPRv2
plentiCRISPRv2_SUN2g4	Primer annealing	OTS129 OTS130	*Bsmb*I	plentiCRISPRv2
plentiCRISPRv2_SUN2g5	Primer annealing	OTS131 OTS132	*Bsmb*I	plentiCRISPRv2
plentiCRISPRv2_MX2g1	Primer annealing	OTS133 OTS134	*Bsmb*I	plentiCRISPRv2
plentiCRISPRv2_MX2g2	Primer annealing	OTS135 OTS136	*Bsmb*I	plentiCRISPRv2
plentiCRISPRv2_MX2g3	Primer annealing	OTS 137 OTS138	*Bsmb*I	plentiCRISPRv2
plentiCRISPRv2_MX2g4	Primer annealing	OTS139 OTS140	*Bsmb*I	plentiCRISPRv2

Table 13. Plasmids generated in this work

5.1.13. Antibodies

Name	Antigen	Species	Application	Company
3F10	HA	Rat, monoclonal, HRP linked	1:5000 in WB	Roche Holding AG, Basel, Switzerland
HA.11 16B12	HA	Mouse, monoclonal	1:250 in IF	Covance, Princeton, USA
EPR6554	SUN1	Rabbit, monoclonal	1:1000 in WB 1:250 in IF	GeneTex, Inc., Irvine, USA
EPR6557	SUN2	Rabbit, monoclonal	1:1000 in WB 1:250 in IF	Abcam plc, Cambridge, UK
13750-1-AP	MX1	Rabbit, polyclonal	1:1000 in WB	Proteintech Group, Inc. Chicago, USA
NBP1-81018	MX2	Rabbit, polyclonal	1:1000 in WB	Novus Biological, Littleton, USA
183	HIV-1 CA/p24	Mouse, monoclonal	1:1000 in WB	NIH, Bethesda, USA
137F5	MAPK	Rabbit, monoclonal	1:1000 in WB	Cell Signaling Technology, Inc., Danvers, USA
H-114	HSP90α/β	Rabbit, polyclonal	1:3000 in WB	Santa Cruz Biotechnology, Inc., Dallas, USA
B-5-1-2	Tubulin	Mouse, monoclonal	1:3000 in WB	Sigma-Aldrich, St. Louis, USA

ECL Mouse IgG	Mouse IgG	Goat, polyclonal HRP linked	1:10000 in WB	Thermo Fisher Scientific, Waltham, USA
ECL Rabbit IgG	Rabbit IgG	Goat, polyclonal HRP linked	1:10000 in WB	Cell Signaling Technology, Inc., Danvers, USA
AlexaFluor 488	Mouse IgG	Goat, polyclonal	1:2000 in IF	Thermo Fisher Scientific, Waltham, USA
AlexaFluor 488	Rabbit IgG	Goat, polyclonal	1:2000 in IF	Thermo Fisher Scientific, Waltham, USA

Table 14. Antibodies used in this work

5.1.14. Software

Name	Source
CFX Manager	BioRad, Hercules, USA
Fiji	Open source [291]
FlowJo V10	FlowJo LLC, Ashland, USA
Microsoft Office 2010	Microsoft, Redmond, USA

Table 15. Software used in this work

5.2. Molecular biology methods

5.2.1. Bacteria and DNA preparation

Chemically competent bacteria were transformed using a heat-shock procedure. 80 µl of chemo-competent *E. coli* Stbl2 bacteria suspension was incubated with 1 µg plasmid DNA or 5 µl ligation product for 45 min on ice. Heat shock was performed for 90 sec at 42°C followed by incubation on ice for 5 min. If plasmid DNA with Ampicillin resistance was used, transformed bacteria were directly plated on selective agar plates. In the case of kanamycin resistance, transformed cells were mixed with 800 µl of LB-medium and incubated for a further 30 min at 37 °C while shaking. After centrifugation for 2 min at 6000 rpm, supernatants were removed and cells resuspended in 50 µl of LB medium. After plating the cells onto selective agar plates (50 mg/l ampicillin or kanamycin), colonies were grown overnight at 37 °C. For the amplification of plasmid DNA, single colonies were used to inoculate overnight cultures in LB medium (containing 100 mg/l ampicillin or 50 mg/l kanamycin) on a shaker at 37 °C. For small and medium scale DNA preparations, 2 and 50 ml overnight bacteria

culture were utilized, respectively. Purification of DNA from bacterial cultures was performed using QIAprep® Spin Miniprep Kit or NucleoBond® Xtra Midi EF according to the manufacturer's instructions.

DNA concentration and purity were measured using a nanophotometer. 1 µl of DNA solution was applied to the cuvette top and concentration was measured by optical density at 260 nm against the respective Elution buffer. Purity was controlled by verifying that OD260nm/OD280nm ratio was between 1.8 and 2.0. DNA solutions were adjusted to 1 µg/µl using the respective Elution buffer.

5.2.2. Polymerase Chain Reaction (PCR)

PCR is a method to selectively amplify a defined DNA sequence from a complex template DNA. The flanking sequences of the target DNA are used to generate a sense and an anti-sense oligonucleotide primer (usually 18-30 bp). The primers are used as the starting point by the polymerase for amplification. Chain elongation in 5´ to 3´direction is achieved by addition of dNTPs. The steps of PCR amplification are as follows I) heat denaturation of the double-stranded template DNA at 95 °C, II) primer annealing to the complementary sequences of the single stranded target (45-60 °C), III) extension by the DNA polymerase at 68-72 °C. After primer extension the mixture is heated again to separate the strands. Cooling down the mixture allows the primers to hybridize with the complementary regions of newly synthesized DNA. Each cycle literally doubles the amplicon. The reaction mixture was prepared on ice and the following components were mixed in a 0.2 ml PCR tube:

Name	Component
ddH_2O	32,5 µl
Phusion HF Buffer 5x	10 µl
dNTP (10 mM stock)	1 µl
Forward primer (10 µM)	2.5 µl
Reverse primer (10 µM)	2.5 µl
Template DNA (100 ng/µl)	1 µl
Phusion® High-Fidelity DNA Polymerase	0.5 µl

PCR was performed using Thermal Cycler C1000 Touch™ with the following thermocycling program:

Step	Temperature	Duration
1. Initial denaturation	98°C	30 sec
2. Denaturation	98°C	10 sec
3. Annealing	55°C	30 sec
4. Elongation	72°C	15-30 sec / kb of plasmid length
Repeat steps 2 to 4 for 34 cycles		
5. Final extension	72°C	7 min
6. store	4°C	

Annealing temperature as well as elongation time were set depending on the primer composition and the length of the amplified sequence, respectively. Usually 34 cycles were performed.

Successful DNA amplification was monitored by running 5 µl product on a 1% agarose gel. All nucleotide sequences of PCR products were confirmed by sequencing (GATC Biotech, Konstanz, Germany).

5.2.3. PCR-based mutagenesis

To generate plasmids carrying point mutations, PCR based mutagenesis was performed as described above using two primers with opposite orientation covering the desired point mutation. The reaction mixture was prepared on ice and the following components were mixed in a 0.2 ml PCR tube:

Name	Component
ddH_2O	39,5 µl
PfuTurbo Buffer 10x	5 µl
dNTP (10 mM stock)	1 µl
Forward primer (100 ng/µl)	1.25 µl
Reverse primer (100 ng/µl)	1.25 µl
Template DNA (100 ng/µl)	1 µl
PfuTurbo DNA Polymerase	1 µl

PCR was performed using Thermal Cycler C1000 Touch™ with the following thermocycling program:

Step	Temperature	Duration
1. Initial denaturation	95°C	30 sec
2. Denaturation	95°C	30 sec
3. Annealing	55°C	1 min
4. Elongation	68°C	1 min /kb of plasmid length
	Repeat steps 2 to 4 for 12 cycles	
5. Final extension	72°C	10 min
6. store	4°C	

PfuTurbo DNA Polymerase was used according to the manufacturer's protocol. After the amplification, the template plasmid was digested by adding 2 µl of *Dpn*I directly to the PCR reaction mix and incubation at 37 °C for 2 h. After digestion, 10 µl of the mix were transformed into competent bacteria.

5.2.4. Separation of DNA by agarose gel electrophoresis

0.5-1 µg DNA fragments were separated by electrophoresis using 1% agarose in 1x TBE buffer gels. GelRed was used to stain DNA (diluted 1:10.000 in the gel prior to polymerization). DNA was mixed with DNA loading buffer and loaded into the wells. Gels were run at 80 V for 30-45 min and size of DNA fragments was compared to a size standard (1 kb DNA ladder). Analytical gels were analyzed under UV light at 254 nm, while DNA was excised from preparative gels under 360 nm illumination and purified by NucleoSpin® Gel and PCR Clean-up kit according to manufacturer's instructions.

5.2.5. Analysis of DNA with restriction enzymes

Restriction digests of DNA were performed using 2 µg plasmid DNA, 0.5 µl of each restriction enzyme and 2 µl 10x NEB buffer according to the enzyme used. The reaction was filled up with water to 20 µl. Enzymes and buffers were used as recommended by the manufacturer NEB and reaction conditions were set according to their protocols.

5.2.6. Ligation

For ligation reactions, 100 ng of digested and purified vector was mixed with the digested and purified insert in a 1:3 or 1:5 ratio. Subsequently, 2 µl of 10x T4 ligase buffer and 1 µl of T4 DNA ligase was added, reactions were filled up with water to 20 µl and incubated over night at 4 °C. 5 µl were used for transformation of bacteria *(see paragraph 5.2.1.)*.

5.2.7. Cloning of shRNAs into retroviral vector pSIREN RetroQ

Suitable silencing RNA target sequences for SUN1 or SUN2 were identified using *http://bioinfo.clontech.com/rnaidesigner/sirnaSequenceDesignInit.do*. Oligonucleotide sequences to generate short hairpin RNAs were designed using the website http://bioinfo.clontech.com/rnaidesigner/oligoDesigner.do, and ordered from Eurofins Scientific (Brussel, Belgium).

Overlapping oligonucleotides encoding the shRNA were annealed using the following protocol. 10 µg of each oligonucleotide (1 µg/ µl) were mixed with 2.5 µl of 2 M NaCl solution in a total volume of 50 µl. The mix was boiled for 5 min at 98°C in a PCR block and subsequently cooled down at a rate of 0.1 °C per second. After annealing 350 µl H_2O, 40 µl 3 M NaAc and 1100 µl 100 % ethanol were added and the solution was briefly vortexed and then placed at -80 °C and incubated overnight. To pellet the annealed oligos the solution was spun at 14000 rpm in a bench top centrifuge at 4 °C for 20 min. The DNA pellet was air dried and resuspended in 50 µl H_2O. The annealed oligos with overhanging single strand ends were then cloned into the *EcoR*I and *BamH*I sites in the pSIREN RetroQ vector.

5.2.8. Cloning of gRNAs into retroviral vector plentiCRISPRv2

Suitable CRISPR/Cas9 target sequences within SUN1, SUN2 or MX2 DNA region were identified using the website http://chopchop.cbu.uib.no/ and oligonucleotides encoding guide RNA (gRNA), which contains the ~20-nucleotide targeting sequence and a Cas9 nuclease-recruiting sequence, were designed and ordered from Eurofins Scientific (Brussel, Belgium).

Guide RNA encoding oligonucleotides were annealed following the same protocol of *paragraph 5.2.6.* and cloned into *BsmB*I-linearized plentiCRISPRv2 according to the manufacturer's guidelines.

5.3. Cell biology and virology methods

5.3.1. Cell culture and freezing/thawing of cell lines

All cells were incubated at 37°C at 5 % CO_2 in 95 % humidity.

293T and U87MG CD4/CXCR4 cell lines were kept in DMEM High Glucose GlutaMAX™, supplemented with 10 % FCS, 100 U/ml penicillin and 100 µg/ml streptomycin.

THP-1 and Jurkat TAg cell lines were kept in RPMI 1640 Medium GlutaMAX™ supplemented with 10 % FCS, 100 U/ml penicillin and 100 µg/ml streptomycin. THP-1 cells were differentiated with 25 ng/ml phorbol 12-myristate 13-acetate (PMA) for 24 h.

Peripheral blood mononuclear cells (PBMCs) were isolated from 50 ml of whole blood or from buffy coats of healthy blood donors. To this end, the buffy coats were diluted 1:2 with PBS, prior to loading 35 ml of the diluted buffy coat on a 15 ml Ficoll cushion. Leukocytes were then isolated by gradient. Cells at the interphase of Ficoll and plasma was aspirated and washed twice with PBS. CD4+ T-cells were then enriched from PBMCs by magnetic bead negative selection using the Human CD4+ T Cell Isolation Kit - T cells according to the manufacturer's protocol (Miltenyi Biotec). Alternatively, CD4+ T-cells were directly enriched from buffy coats of healthy blood donors using the Human CD4+ T Cell Enrichment Cocktail RosetteSep™ according to the manufacturer's protocol (Stemcell Technologies). CD14+ monocytes were directly enriched from PMBCs by magnetic bead negative selection using the Monocyte Isolation Kit II according to the manufacturer's protocol (Miltenyi Biotec). Primary CD4+ T cells or CD14+ monocytes were then kept in RPMI 1640 Medium GlutaMAX™ with 10% supplemented with 10 % FCS, 100 U/ml penicillin and 100 µg/ml streptomycin. CD4+ T-cells were activated with 100 IU/ml interleukin-2 (IL-2) and 2 µg/ml phytohemagglutinin (PHA) for 3 days, whereas MDMs were differentiated for 7 days using 100 ng/ml granulocyte-macrophage colony-stimulating factor (GM-CSF).

Cells were passaged every 3 days at ~ 90% confluent cells. For that purpose, adherent cells were briefly washed with PBS, detached with 0.05 % Trypsin/EDTA in PBS for 5 min and reseeded in new medium at a ratio of 1:4. Suspension cells were separated and then passaged in the appropriate

concentration. Cell line stocks were maintained by cryo-conservation in liquid nitrogen. For this purpose, cells were pelleted (1200 rpm, 8 min), resuspended in 1 ml freezing medium (FCS supplemented with 10 % DMSO or glycerol) and transferred into a cryo-conservation tube. Tubes were slowly cooled to -80°C in freezing Styrofoam box and then transferred to liquid nitrogen for long-term storage. Cells were thawed rapidly and transferred to 75 cm^2 flasks or 10 cm dishes containing 20 ml pre-warmed fresh medium. The medium was changed after 24 hrs and cells were split at 90 % confluency.

5.3.2. Virus and vector preparation

Infections and fluorescence activated cell sorting (FACS) were performed as described in earlier studies [185, 293, 480, 481]. Viruses and lentivectors (LVs) were produced by transient transfection of 293T cells [467] with three plasmids using Polyethylenimine (PEI), an organic polymeric polycation that spontaneously forms complexes by binding to the DNA phosphate backbone. These complexes are taken up into the cell, leading to transfection.

For lentiviral vector (LV) production, 4.5 µg of HIV-1 viral plasmid (pCSxW vector, plentiCRISPRv2 or RetroQ vectors encoding respectively the protein, the gRNA or the shRNA of interest; *see paragraph 5.1.9.*) 3 µg of pCMVΔR8.91 GagPol encoding plasmid and 3 µg of VSV-G Env expression plasmid pMD.G *(see paragraph 5.1.9.)* were mixed into a separate reaction tube in which 1 ml OptiMem was pre mixed with 42 µl of PEI (stock 1mg/ml in H_2O). Next, the mixture is homogenised by vortexing for short time, incubated for at least 15 min at room temperature and added drop-wise onto a ~75 % confluent 10 cm dish of 293Ts replaced with new fresh 8 ml media. For VSV-G-pseudotyped full-length HIV-1 production, 8 µg HIV-1 GFP reporter viral plasmid pNLENG-IRES-Nef *(see paragraph 5.1.9.)* and 2 µg pMD.G were transfected per plate. To generate full-length laboratory strains HIV-1NL4.3, HIV-1IIIB, or HIV-1 transmitted/founder RHPA, SUMA, WITO, THRO or ZM247 with a copackaged GFP lentivirus (LV) minigenome, 4.5 µg pCSGW was cotransfected with 3 µg full-length viral plasmid (pNL4.3, pIIIB, pRHPA, pWITO, pTHRO, pSUMA, pZM247; *see paragraph 5.1.9*) and 3 µg pMD.G. For all viral production, medium was replaced 24 h post transfection, the viral supernatant was

harvested at 48 h and 72 h post transfection, and collections were pooled and passed through a 0.45 µm cellulose filters to remove cell debris.

To determine infectious titres, 10^5 cells were plated in 6-well plates and infected the next day with 1 ml of viral supernatant diluted usually in a three-fold serial dilution series to obtain six different concentrations. Infected cells were enumerated 48 h post infection by measuring the GFP expression using FACS. Subsequently, the cleared supernatant was aliquoted and stored at -80 °C or particles were collected by centrifugation through a 20 % (w/v in PBS) sucrose cushion (30 ml supernatant on a 7 ml sucrose cushion) in a SW-28 rotor at 28,000 rpm, at 4°C for 2 h. Pellets were resuspended in 200 µl RPMI and stored at -80°C.

5.3.3. Transduction of cells with VSV-G-pseudotyped HIV-1 LV

5.3.3.1. Generation of stable cell lines ectopically expressing proteins

Cell lines ectopically expressing proteins of interest were generated by transduction of 10^5 cells in 6-well plates with 1 ml VSV-G-pseudotyped HIV-1 LV encoding the individual protein and generated as described in *paragraph 5.3.1*. 48 h post-infection, the newly produced cell lines were usually expanded to 10 cm plates before analysis.

5.3.3.2. Generation of CRISPR/Cas9 knockout stable cell lines

THP-1 and Jurkat Tag CRISPR/Cas9 *SUN1*, *SUN2* or *MX2* knockout cells clones were generated by transduction with VSV-G-pseudotyped HIV-1 LV produced using pCMV-ΔR8.91, pMD.G, and plentiCRISPRv2 *(see paragraph 5.1.9.)*. Transduced cell populations were selected with 2 µg/ml puromycin for 2 weeks. Single-cell clones were generated by limiting dilution in 96-well plates and grown for at least 2 weeks in the absence of puromycin. Subsequently, they were usually expanded first to 24-well plates, then to 6-well plates and lastly to 10 cm plates before analysis. Cell clones without protein expression were determined by immunoblotting using specific antibodies. Gene disruption was validated by PCR amplification and sequencing of the targeted genomic region from isolated total genomic DNA of selected clones. On this purpose, the following primer pairs (forward/reverse) were used: OTS141/OTS142 for

SUN1g1, OTS143/OTS144 for SUN1g2, OTS145/OTS146 for SUN2g1, OTS147/OTS148 for SUN2g2, OTS149/OTS150 for SUN2g3, OTS151/OTS152 for MX2g2 *(see paragraph 5.1.10.)*. As negative controls, we used either a single-cell clone still expressing the protein of interest or parental cells.

5.3.3.3. Generation of ShRNA-mediated knockdowns cells

SUN1, SUN2 ShRNA-mediated knockdowns U87MG CD4/CXCR4 and THP-1 cells were generated by transduction of 10^5 cells in 6-well plates with VSV-G-pseudotyped HIV-1 LV produced using pCMV-ΔR8.91, pMD.G and pSIREN RetroQ vectors *(see paragraph 5.1.9.)* expressing individual specific short hairpin RNAs to silence proteins gene expression via RNA interference (RNAi). Transduced cell populations were selected with 2 µg/ml puromycin for 3 days and were usually expanded to 10 cm plates before analysis. Cells without protein expression were determined by immunoblotting using specific antibodies.

5.3.4. Infectivity assays

For infectivity assays, a total of 8 x 10^4 U87MG CD4/CXCR4, 1 x 10^5 THP-1 or Jurkat TAg cells were plated in 100 µl of medium per well in 96-well plates. In the case of IFN-α titration experiments, a total of 5 x 10^5 THP-1 or CD4+ T cells were plated and treated for 24 h with IFN-α. Next, cells were infected with 100 µl of supernatant containing VSV-G-pseudotyped GFP-reporter lentiviral vectors or full-length GFP-reporter virus for 24 to 72 h and virus titrations were usually performed with 3-fold serial dilutions of the viral supernatant. Cells were fixed in 4% paraformaldehyde (PFA), the infectivities were determined from the percentage of GFP+ cells by flow cytometry using a FACSVerse system (BD Biosciences), and the infectious titers were determined on at least three different virus doses. The average infectious titers were calculated using Excel with standard deviations depicted as error bars. To compare different CA mutants with wild-type GFP reporter vector/virus, viral input was normalized by 293T infectious titers or by units of reverse transcriptase in the supernatant, as determined by SG-PERT assay previously described.

Experiments with MDMs were performed with 48-well plates, seeding 5 x 10^5 monocytes per well prior to differentiation. For analysis by flow cytometry, MDMs were trypsinized for at least 30 min, resuspended and fixed in 4% PFA.

Virus titrations were usually performed by 3-fold serial dilutions of the viral supernatant.

For experiments using Ciclosporin A (CsA), drug was used at 5 µM in DMSO and added at the time of infection with the reporter virus. DMSO was used as the vehicle control at the same concentration.

In the case of IFN-α titration experiments, a single dose of supernatant containing reporter virus was used, aiming for a MOI of ≤1.

5.3.5. Measurement of RT activity: SG-PERT

Analysis of RT activity in supernatants, as a measure of virus release, was performed by SG-PERT (SYBR Green based Product Enhanced Reverse Transcriptase) assay [292].

On this purpose, 5 µl of the virus containing supernatants obtained from virus producing cells *(see paragraph 5.3.1.)* were lysed by incubation with 5 µl 2x SG-PERT lysis buffer (50 mM KCl, 100 mM Tris-HCl, 40 % Glycerol, 0.25 % Triton X-100, pH 7.4), containing 2 U Ribolock RNAse inhibitor. Subsequently, 90 µl SG-PERT PCR buffer (5 mM $(NH_4)_2SO_4$, 20 mM KCl, 20 mM Tris-HCl, pH 8.0) was added. From this mixture, 10 µl were added to 10 µl SG-PERT PCR-reaction mix (PCR buffer containing 10 mM MgCl2, 0.2 mg / ml BSA, 400 µM dNTPs, 1 pmol primer RT-Assay-fwd, 1 pmol RT-Assay-rev, 8 ng MS2 RNA, and 1:10000 SYBR Green), containing 0.5 U GoTaq Hotstart Polymerase.

RT-PCR was performed using Real Time PCR detector CFX96 Touch™ (BioRad) with the following thermocycling program: 42 ºC for 20 minutes, 95 ºC for 2 minutes, 40 cycles of 95 ºC for 5 seconds, 60 ºC for 5 seconds, 72 ºC for 15 seconds and 80 ºC for 7 seconds. A final melting curve step was included. Results were analyzed with the CFX Manager software (BioRad).

5.3.6. TaqMan qPCR

Quantitative TaqMan PCR (qPCR) was performed to determine the copy numbers of *GFP* or *2-LTR* DNA circles, surrogates for early RT products and nuclear import, respectively. Specific primer/probe sets were used *(see paragraph 5.1.11.)*. 2 x 10^5 cells per well (U87MG CD4/CXCR4) or 6 x 10^5 cells per well (THP-1) were seeded in 6-well plates and infected the next day in triplicate for 6 h (*GFP*) or 24 h (*2-LTR* DNA circles) with equal doses of DNase

treated virus (RQ1 RNase-Free DNase; final concentration 70 U/ml for 1h). After the incubation time, total DNA was isolated using the QIAamp® DNA Mini Kit. To enumerate infected cells, the third sample was subjected to FACS analysis 48 h after infection. As a negative control for plasmid contamination cells were incubated with the non-nucleoside reverse transcriptase inhibitor efavirenz (5 µM final concentration). Extracted total DNA (100-500 ng) was subjected to Taqman qPCR and the reaction mixture was prepared on ice. For each reaction, the following components were mixed in a 0.2 ml PCR tube:

Name	Component
ddH_2O	5 µl
TaqMan® Universal PCR Master Mix	12,5 µl
Forward primer (7,5 µM)	1 µl
Reverse primer (7,5 µM)	1 µl
Probe (7,5 µM)	0,5 µl
Diluted plasmid standard/Total DNA sample	5 µl

In every experiment, a standard curve of the respective amplicon was measured in duplicate ranging from 10^1 to 10^5 copies in addition to a no-template control. To measure *GFP* the plasmid CNCG served as standard, whereas for *2-LTR* circles the plasmid 2-LTR was used *(see paragraph 5.1.11.)*, and all dilutions were performed in an equal amount of salmon sperm carrier DNA in water (100 µg/ ml). The PCR cycling program for the GFP and the LRT-P amplicon consisted of initial incubations at 50 °C for 2 min and 95 °C for 10 min, after which 40 cycles of amplification were carried out at 15 s at 95 °C followed by 1 min at 60 °C. For 2-LTR circles usually 50 cycles were performed with 15 s at 95 °C followed by 90 s at 60 °C. For detection the Real Time PCR detector CFX96 Touch™ system (BioRad) was used.

Since LV-mediated transduction was used to express HALUC, HASUN1 or HASUN2 in U87MG CD4/CXCR4 cells, a reporter vector where the 5'- and 3'-LTRs had been engineered was used (referred to as HIV-1 LV++; *see paragraph 5.1.12.*), such that only the 2-LTR circles produced by the reporter virus could be detected by using specific primer (2-LTR++ fwd/rev) and standard sets (pLTR++) *(see paragraph 5.1.11.)*. Results were analyzed with

the CFX Manager software and usually the number of copies of amplicon per 100 ng total DNA was calculated and plotted.

5.4. Biochemistry methods

5.4.1. SDS-polyacrylamide-gel electrophoresis (SDS-PAGE)

Sodium dodecyl sulfate polyacrylamide gel electrophoresis (SDS-PAGE) is a very common method for separating proteins by their molecular weight under denaturing conditions. Cell samples for SDS-PAGE were usually lysed by boiling in protein sample buffer at 95 °C for 5 min. After equilibrating to RT, aliquots of cell lysates were loaded on a 10 % polyacrylamide gel and electrophoresis was performed at 130 V for 90 min in SDS PAGE running buffer using the Tetra Vertical Electrophoresis Cell Mini-PROTEAN® system (Biorad). Precision Plus Protein™ WesternC™ Standards (Biorad) was used as a protein size reference.

Laemmli gels were generated using Acrylamide Solutions TGX™ FastCast™ according to the manufacturer's protocol (Biorad) and an acrylamide concentration of normally 10 % for the separating gel and 6 % for the stacking gel were utilized. Briefly, for each separating gel 3 ml Resolver A, 3 ml of Resolver B, 3 µl of TEMED were mixed in a 50 ml Falcon Tube before starting gel polymerisation by adding 30 µl of 20 % ammonium-persulfate (APS). The separating gel was quickly poured between two glass plates of the Bio-Rad PAGE Gel casting system. To avoid formation of air bubbles, 1 ml of isopropanol was carefully pipetted on top of the separating gel. After polymerisation the isopropanol was washed away with water and the excess water was removed by using Whatman paper strips. To prepare the stacking gel, 1 ml of Stacker A, 1 ml of Stacker B and 2 µl TEMED were mixed in a 50 ml Falcon tube before starting gel polymerisation by adding 10 µl APS. The solution was mixed and carefully added on top of the separating gel avoiding formation of air bubbles. The comb was inserted and the gels were left for 15 min at room temperature for gel polymerisation. The gels were wrapped in wet tissues and could be kept at 4°C for up to 1 week.

5.4.2. Western Blot

After separating by SDS-PAGE, the proteins were blotted onto methanol activated polyvinylidene difluoride (PVDF) membranes using the Electrophoretic Transfer Cell Mini Trans-Blot® system (Biorad) at 100 V for 60 min. Membranes were incubated for 1h in PBS containing 0.05 % Tween 20 (PBS-Tween 20) and 5 % (w/v) non-fat milk powder to saturate non-specific binding sites. The membrane was briefly washed in PBS-Tween 20. The primary antibody was diluted in PBS-Tween 20 and the membrane was incubated shaking for 1 h at room temperature or overnight at 4 C°. After being washed three times with PBS-Tween 20, the membrane was incubated with secondary antibody conjugated with peroxidase in TBS-Tween 20 for 1 h shaking at room temperature and subsequently washed three times as described above. Membrane- bound secondary antibody was detected by chemiluminescence using the reagent Clarity™ Western ECL substrates (Biorad). Chemiluminescence was measured by the ECL ChemoCam Imager system (INTAS Science Imaging).

5.4.3. CANC pulldown

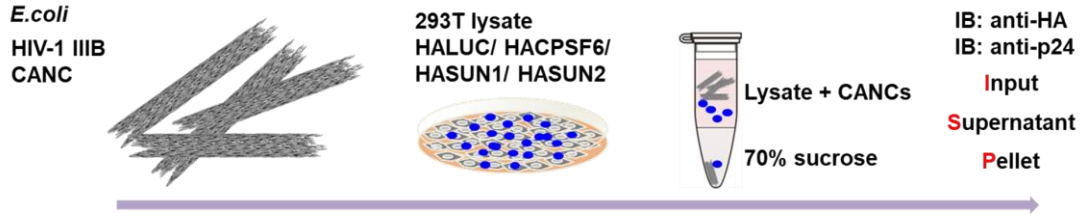

Figure 10. CANC pulldown method data from Malim Lab (KCL, London). *Cell lysates from 293T cells transfected with HALUC, HACPSF6, HASUN1, or HASUN2 were incubated with in vitro-synthesized CANC nanotubes before centrifugation through a sucrose cushion and analysis of supernatants and pellets by immunoblotting using HA- and CA-specific antibodies. I, input; S, supernatant; P, pellet*

To address the question if SUN proteins may interact with the HIV-1 capsid, the Malim lab in London (King's College London) investigated the binding of the different SUN1 or SUN2 mutants to *in vitro* synthesized HIV-1 CANC complexes (capsid-nucleocapsid complexes). 293T cells transfected with pCSxW expressing HA-tagged firefly luciferase, CPSF6, or wild-type SUN1 or SUN2 proteins were lysed with hypotonic lysis buffer using a Dounce homogenizer. Lysates were cleared by centrifugation at 20,000 x g for 15 min. For pulldown

experiments, 200 µl of cell lysate was mixed with either 40 µl of 40 µM assembled CANC (an input sample was taken from this mix) or 40 µl of CANC binding buffer containing 5 µM TG50 and incubated at room temperature for 1 h. The mixture was then overlaid onto a 250 µl 70% sucrose cushion and centrifuged at 15,000 x g for 10 min. A sample of the supernatant was withdrawn for further analysis, and the pellet was washed with 500 µl of wash buffer and centrifuged again at 10,000 x g for 5 min. Finally, the pellet was resuspended in 50 µl of 1x SDS-PAGE loading buffer. Input, supernatant, and pellet fractions were analyzed by immunoblotting using appropriate antibodies.

5.5. Imaging methods

5.5.1. Immunofluorescence and confocal microscopy

Cells lines were seeded on glass cover slips in 24-well cell culture plates at a concentration of 2.5×10^4 cells per well. The cells were washed three times with warm 1 × PBS and fixed with 500 µl of a 4 % paraformaldehyde (w/v) solution for 10 min at room temperature. Subsequently, the cells were washed again three times with 1 × PBS and were then either directly used for further preparation or stored for up to 3 days at 4 °C. For permeabilization the cells were incubated for 5 min with 500 µl of a 0.2 % triton-x-100/ PBS (v/v) solution and washed 3 times with warm 1 × PBS prior to incubation with the primary antibody. The primary antibody was diluted to the desired concentration in a 1 × PBS buffer containing 5 % horse serum (v/v). After 45 min incubation at room temperature the cells were washed 3 times with 1 × PBS for 10 min and incubated with the secondary antibody conjugated with fluorescent dye Alexa 488, diluted 1:2000 in a 1 × PBS buffer containing 5 % horse serum (v/v). After 60 min incubation at room temperature in the dark, the cells were washed three times with 1 × PBS. Counterstaining of nuclei was performed using 1:500 Hoechst 33258 in the secondary antibody solution. Subsequently, cells were washed again 3 times with 1 × PBS, rinsed with H_2O and mounted on glass slides using Mowiol embedding medium (8 mM Mowiol 4-88 in PBS). Immunofluorescence pictures were obtained using a Leica confocal microscope following protocols provided by the manufacturer. In general, pictures were obtained using the 63 × oil immersion objective.

6. Results

6.1. The role of inner nuclear membrane proteins SUN1 and SUN2 in early HIV-1 infection steps

6.1.1. An overexpression screen of NE-associated proteins identifies SUN1 and SUN2 as HIV-1 interactors

SUN2 has recently been described to impact the early stages of HIV-1 infection [173, 206, 293, 294], and to address the question whether other membrane associated NE proteins would exert similar activity, an overexpression screen with a number of HA-tagged human NE-associated proteins (Table 16) was carried out by stably transducing U87MG CD4/CXCR4 cells with lentiviral vectors encoding the individual NE proteins (*see paragraphs 5.1.12. and 5.3.3.1. in Materials and Methods*). The cells were then infected with a VSV-G pseudotyped GFP-encoding HIV-1 LV vector for two days, and measured its infection rate as the percentage of GFP-positive cells. Whereas most of the NE proteins had minimal or null effect, SUN2 overexpression inhibited by 5-fold the HIV-1 LV infection, while SUN1 resulted in a 20-fold decrease of the infection (Fig. 11A). The protein expression level of HASUN1 and HASUN2 was validated by immunoblotting using an HA-specific antibody (Fig. 11B). Particularly, using specific antibodies for SUN1 or SUN2, it was confirmed the ectopically expressed proteins were considerably more abundant than endogenous SUN1/SUN2 (Fig. 12A). Furthermore, subcellular localization of endogenous SUN1 and SUN2 was examined in comparison tothe overexpressed and HA-tagged SUN1 and SUN2 in U87MG CD4/CXCR4 cells. While HA-tagged protein expressions maintained the predominantly perinuclear staining pattern, their expressions were also localized in cytosol unlike endogenous proteins (Fig. 12B).

Table 16. Membrane-associated NE proteins analyzed in the overexpression screen.

NE protein	Species	Tag[a]	Expression in WB assay (antibody)[b]	Cell viability[c] (U87MG CD4/CXCR4)	Block to HIV-1 (U87MG CD4/CXCR4)
SUN1	human	N-term HA	Yes (anti-HA)	++	20- to 50-fold
SUN1	human	untagged	Yes (anti-SUN1)	++	20- to 50-fold
SUN2	human	N-term HA	Yes (anti-HA)	+	3- to 5-fold
SUN2	human	untagged	Yes (anti-SUN2)	+	3- to 5-fold
NET26	human	N-term HA	Yes (anti-HA)	++	-
NET39	human	N-term HA	Yes (anti-HA)	++	-
LUMA	human	N-term HA	Yes (anti-HA)	+	2-fold
LMNA	human	N-term HA	Yes (anti-HA)	++	-
EMD	human	N-term HA	Yes (anti-HA)	+	-
EMDΔLEM	human	N-term HA	Yes (anti-HA)	+	-
LBR	human	N-term HA	Yes (anti-HA)	++	-
LULL1	human	N-term HA	Yes (anti-HA)	++	2-fold
LULL1	human	c-term HA	Yes (anti-HA)	+	-
TORSA	human	N-term HA	No (anti-HA)	++	-
TORSA-EQ	human	N-term HA	No (anti-HA)	++	-
TORSA	human	C-term HA	Yes (anti-HA)	-	-
TORSA-EQ	human	C-term HA	No (anti-HA)	-	-
TSPAN5	human	C-term HA	No (anti-HA)	++	-
TMEM53	human	C-term HA	Yes (anti-HA)	-	-
LAP2β	human	C-term HA	Yes (anti-HA)	-	-
NURIM	human	N-term HA	No (anti-HA)	++	-
NURIM	human	C-term HA	Yes (anti-HA)	-	-
UNCL	rat	N-term HA	Yes (anti-HA)	++	-
UNCL	human	C-term HA	No (anti-HA)	++	-
NET3	human	N-term HA	No (anti-HA)	++	-
NET3	human	C-term HA	No (anti-HA)	+	-
NET31	human	N-term HA	No (anti-HA)	++	-

a N-term HA, N-terminal HA; C-term HA, C-terminal HA.
b WB assay, Western blotting assay to detect protein expression with indicated antibody.
c Cell viability was visually judged by the appearance of cytopathic effect and cell death in culture, in comparison to parental U87MG CD4/CXCR4 cells (response set as 100%). ++, 90 to 100% relative to response in parental cells; +, 50% to 89%; -, 0 to 49%. Proteins for which no expression signal was observed or which showed a strong cytopathic effect were not investigated further.

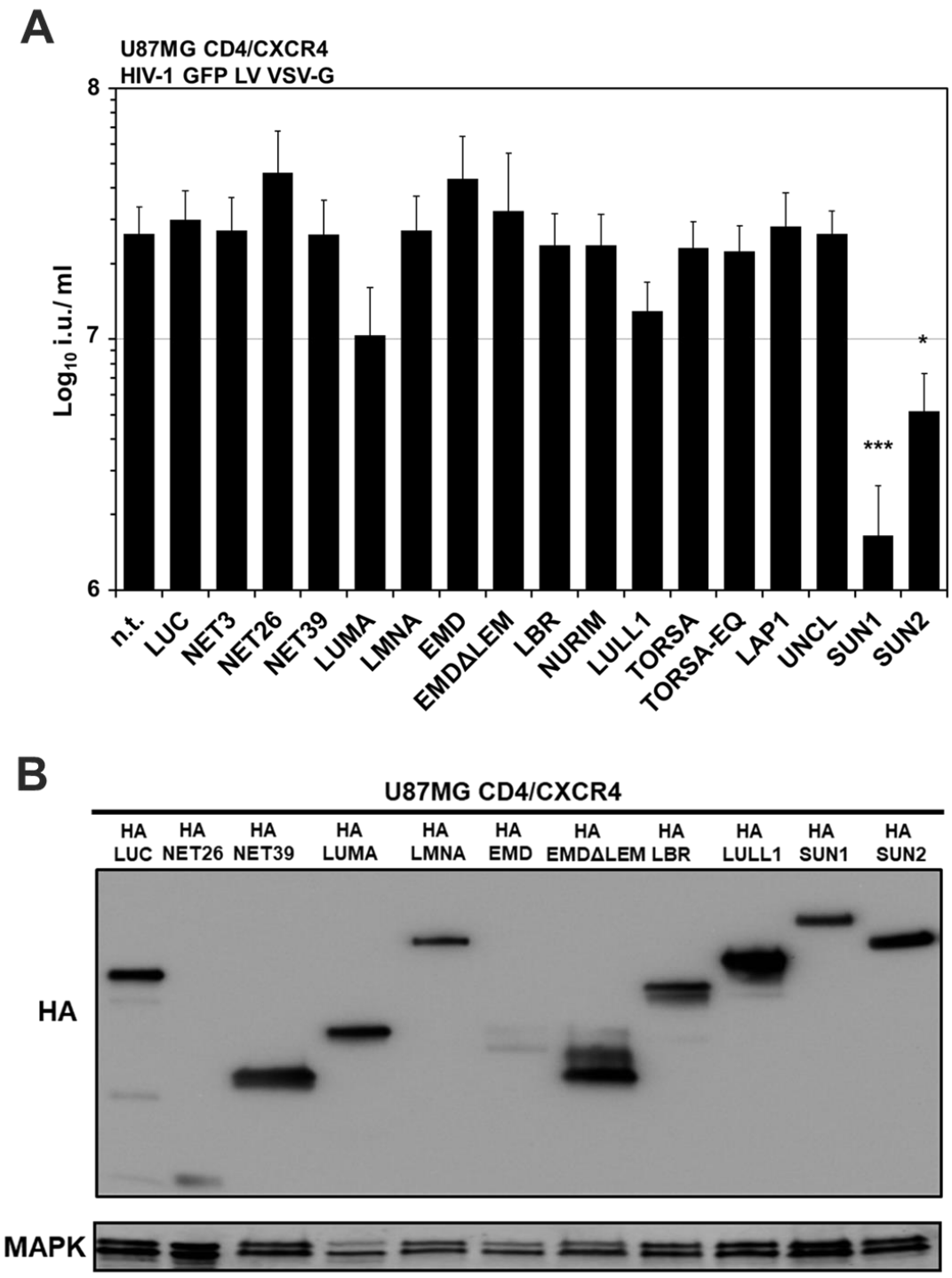

Figure 11. Overexpression of SUN1 or SUN2 inhibits HIV-1 infection. A) *Non-transduced U87MG CD4/CXCR4 cells (n.t.) or cells expressing the indicated HA-tagged membrane-associated NE proteins or luciferase (LUC; negative control) were infected with VSV-G-pseudotyped HIV-1 GFP LV for 48h before harvest, fixed in 4% paraformaldehyde (PFA) and analyzed by flow cytometry. Virus titrations were usually performed by threefold serial dilutions of the viral supernatant. Infectious titers (in infectious units [i.u.] per milliliter) were calculated from at least three virus doses and mean titers are shown. Error bars are standard deviations. Representative results from three independent experiments are shown.* **B)** *Corresponding WB for A). Same numbers of cells were lysed in the same volume of Laemmli buffer and subjected to immunoblotting analysis with antibodies targeting HA. MAPK served as a loading control.*

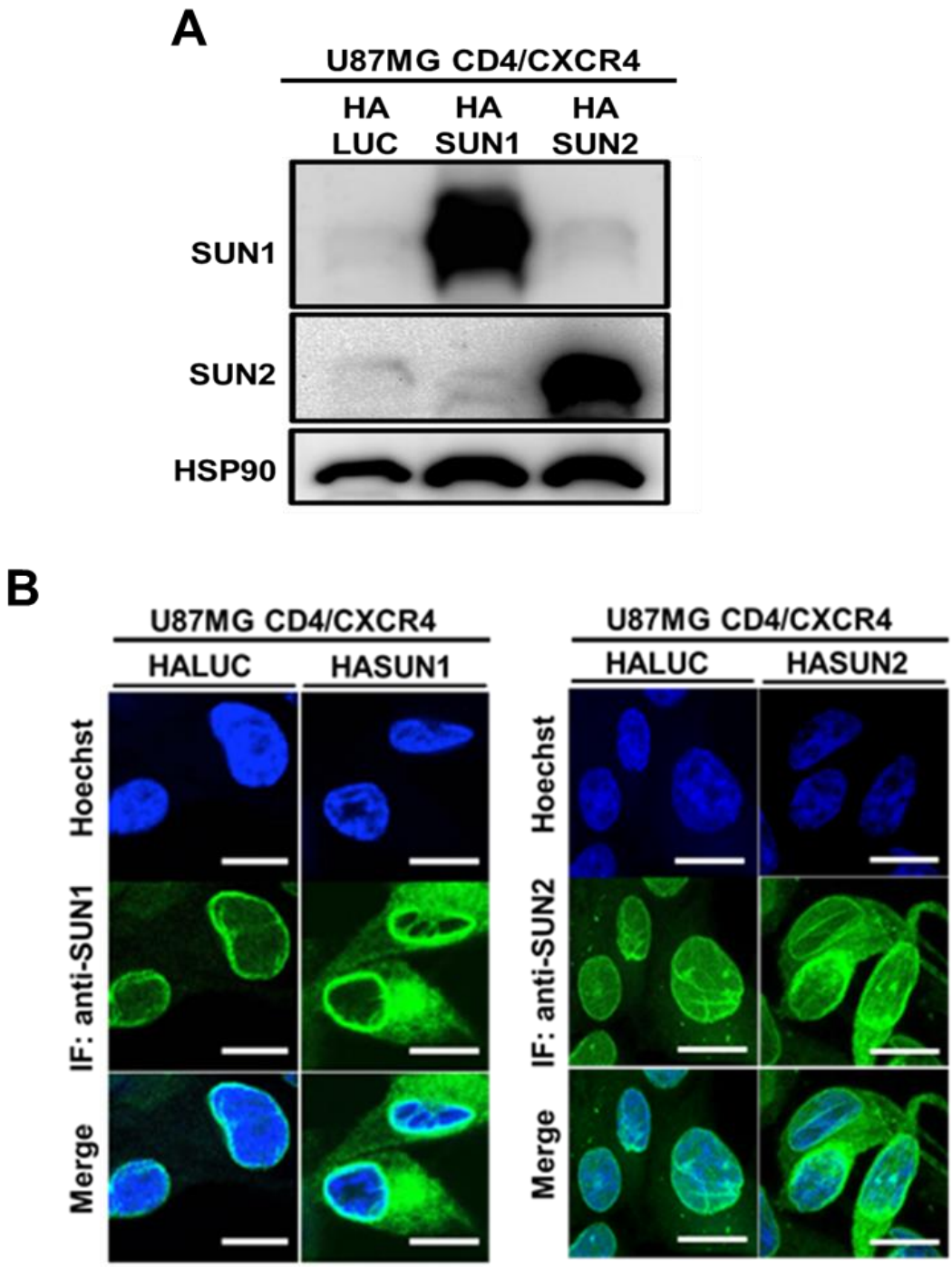

Figure 12. SUN1 and SUN2 expression in U87MG CD4/CXCR4 cells. A) *U87MG CD4/CXCR4 cells expressing HALUC, HASUN1 or HASUN2 were probed with antibodies targeting SUN1 or SUN2. HSP90 served as a loading control.* **B)** *U87MG CD4/CXCR4 cells expressing HALUC, HASUN or HASUN2 were subjected to immunofluorescence microscopy using SUN1 or SUN2-specific antibodies. Nuclei were visualized using Hoechst stain. Scale bar =10 µm*

6.1.2. Overexpression of SUN1 or SUN2 block full-length HIV-1 NL4.3GFP

In order to analyze whether the route of viral entry affects the magnitude of SUN1-mediated suppression, U87MG CD4/CXCR4 cells overexpressing HALUC (negative control), HASUN1 or HASUN2 were infected for two days with a full-length non-pseudotyped CXCR4-tropic HIV-1 GFP reporter virus (NL4.3-GFP: *see paragraph 5.1.9. in Materials and Methods)* [141, 286]. A strong suppression of HIV-1 infection by SUN1 was also observed (Fig. 13A), suggesting that SUN1 has an inhibitory effect in downstream of membrane fusion and independent of viral entry into the cell.

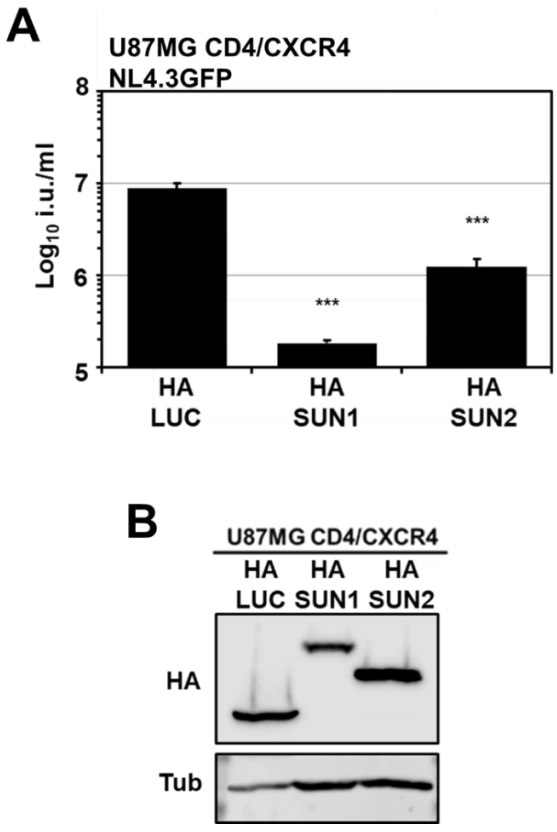

Figure 13. Overexpression of SUN1 or SUN2 inhibits HIV-1 infection. A) *U87MG CD4/CXCR4 cells overexpressing HALUC (negative control), HASUN1 or HASUN2 were infected with full-length non-pseudotyped CXCR4-tropic NL4.3GFP for 48h before harvest, fixed in 4% paraformaldehyde (PFA) and analyzed by flow cytometry. Virus titrations were usually performed by threefold serial dilutions of the viral supernatant. Infectious titers (in infectious units [i.u.] per milliliter) were calculated from at least three virus doses and mean titers are shown. Error bars are standard deviations. Representative results from three independent experiments are shown.* **B)** *Corresponding WB for A). Same numbers of cells were lysed in the same volume of Laemmli buffer and subjected to immunoblotting analysis with antibodies targeting HA. Tubulin served as a loading control.*

6.1.3. Overexpression of SUN1 and SUN2 reduces HIV-1 2-LTR circle accumulation

To determine the stage of the infection block, U87MG CD4/CXCR4 cells expressing HALUC, HASUN1 or HASUN2 were infected with DNase-treated VSV-G-pseudotyped HIV-1 GFP LV++ (*see paragraphs 5.1.12. and 5.3.6. in Materials and Methods*) and total DNA was isolated at various time points of post-infection. Quantitative Taqman PCR was then performed to determine the copy numbers of GFP or 2-LTR circles as surrogates for early reverse transcription products and nuclear import, respectively. To control for plasmid contamination deriving from vector production, analogous samples treated with the allosteric reverse transcriptase inhibitor Efavirenz (+RTinh) were included in the assay. In parallel, infectivities were determined by flow cytometry 48h after infection. Although cells overexpressing HASUN1 or HASUN2 showed considerably reduced susceptibility to HIV-1 LV++ infection (Fig. 14A), similar levels of GFP reverse transcription products were detected in control, HASUN1 or HASUN2-expressing cells (Fig. 14B). In contrast, the amount of HIV-1 2LTR circles was reduced in SUN1 or SUN2 overexpressing cell lines by 10-fold, (Fig. 14C) suggesting that inhibitory effect by over expression of these proteins occurs at the stage of viral nuclear import.

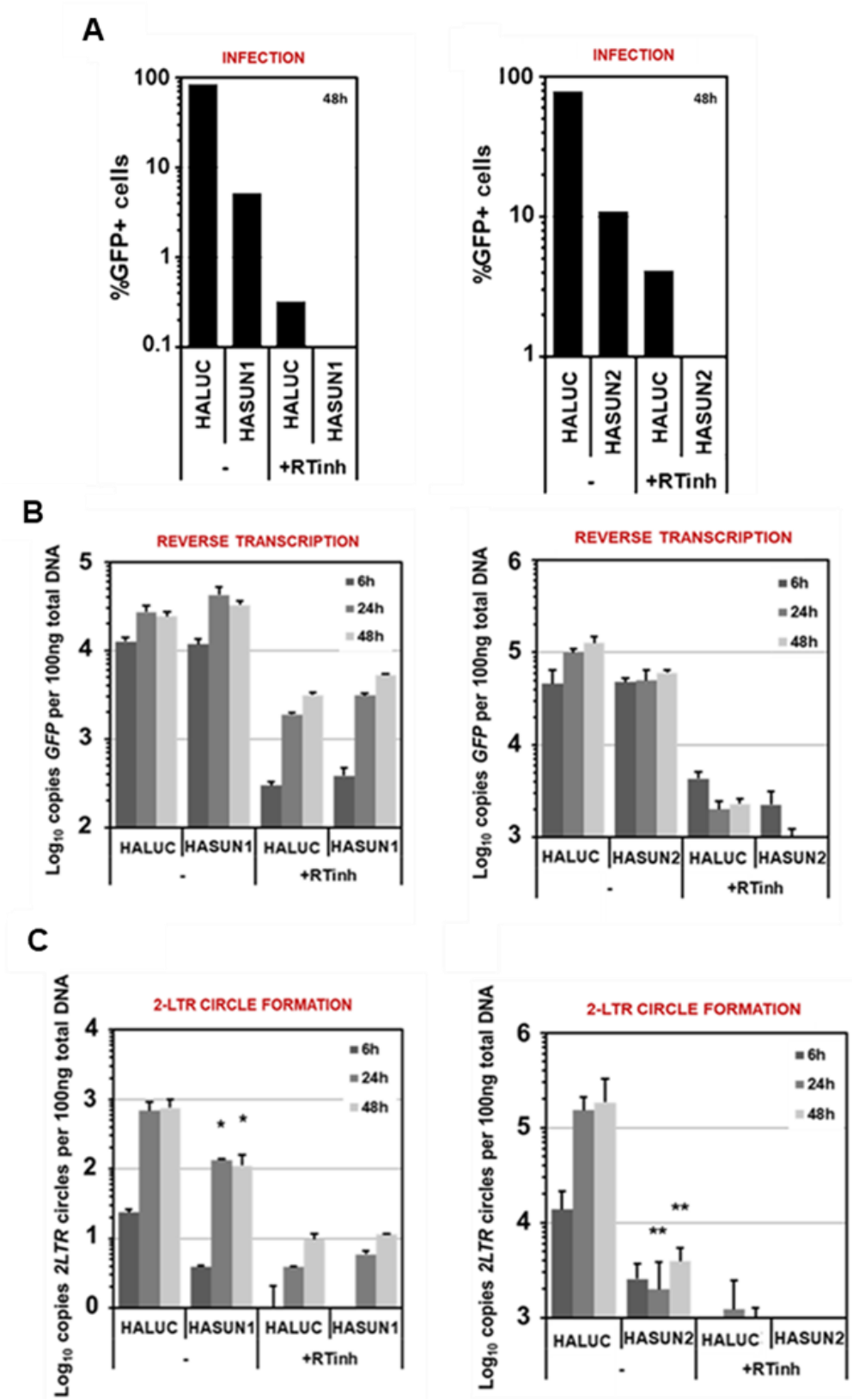

Figure 14. Overexpression of SUN1 and SUN2 inhibits HIV-1 2-LTR circle formation. *U87MG CD4/CXCR4 cells overexpressing HALUC (negative control), HASUN1 or HASUN2 were infected in the presence or absence of 5μM efavirenz (+RTinh) with VSV-G-pseudotyped HIV-1 GFP LV++.* **A)** *Percentages of infected cells (%GFP+ cells) were determined by flow cytometry 48h post infection. Mean infectivities for three samples and standard deviations are shown. Representative results from three independent experiments are shown.* **B-C)** *Total DNA was extracted at the indicated time points, and early reverse transcription products for GFP (B) or 2-LTR circles (C) were measured by qPCR and normalized to total DNA input. Representative results from three independent experiments are shown.*

6.1.4. Overexpression of SUN1 and SUN2 inhibits HIV-1 and HIV-2 infection but not other lentiviruses

In order to investigate the selectivity of the SUN protein-induced inhibitory effect for different retroviruses, U87MG CD4/CXCR4 cells expressing HASUN1, HASUN2, or HALUC as negative control were infected with a diverse set of VSV-G-pseudotyped GFP-encoding retroviral vectors derived from HIV-2_{ROD}, SIV_{MAC}, FIV, EIAV, or Moloney murine leukemia virus (MoMLV) (*see paragraph 5.1.9. in Materials and Methods*). Only HIV-1 and HIV-2_{ROD} were sensitive to the overexpression of SUN proteins compared to the all other retroviral vectors (Fig. 15), suggesting that the inhibitory effect is specific for that 2 retroviruses in terms of nuclear import. Although HASUN1 overexpression inhibited HIV-1 infection by ~20-fold, HIV-2_{ROD} was suppressed by ~5-fold (Fig. 15A), indicating the specificity of virus substrate. A similar profile was observed in cells overexpressing HASUN2 (Fig. 15B).

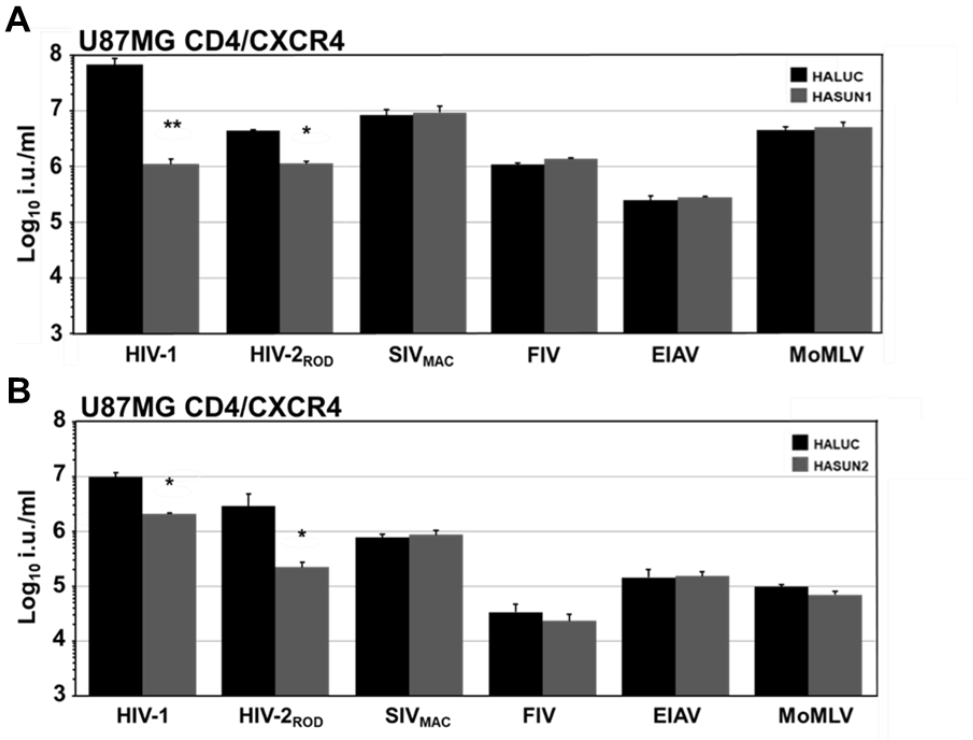

Figure 15. Overexpression of SUN1 and SUN2 inhibits HIV-1 and HIV-2_{ROD} but not SIV_{MAC}, FIV, EIAV, or MoMLV infection. *U87MG CD4/CXCR4 cells overexpressing HALUC (negative control), HASUN1 or HASUN2 were infected with the indicated VSV-G-pseudotyped GFP retroviral vector, for 48h before harvest, fixed in 4% paraformaldehyde (PFA) and analyzed by flow cytometry. Virus titrations were usually performed by threefold serial dilutions of the viral supernatant. Infectious titers (in infectious units [i.u.] per milliliter) were calculated from at least three virus doses and mean titers are shown. Error bars are standard deviations. Representative results from three independent experiments are shown.*

6.1.5. Differential susceptibility of HIV-1 strains to SUN1 and SUN2 mediated inhibition

To understand whether the sensitivity of SUN1- and SUN2-induced inihibitory effect varies among different HIV-1 strains, infection by lab strains virus NL4.3 and IIIB as well as T/F viruses, RHPA, SUMA, WITO, THRO, and ZM247 was tested. To measure infectivity a trans-packaging approach was used, whereby the individual viruses were produced in the presence of a GFP-encoding vector (pCSGW: *see paragraph 5.1.9. in Materials and Methods*) that was transpackaged resulting in GFP expression in infected target cells. The virus preparation obtained through this trans-packaging strategy was compared with the one using a typical GFP reporter virus, and both generated similar infectious titers in 293T cells. Furthermore, the SUN1-mediated inhibitory effect led to a ~20-fold decrease of the infection for both viruses in U87MG CD4/CXCR4 cells (Fig. 16).

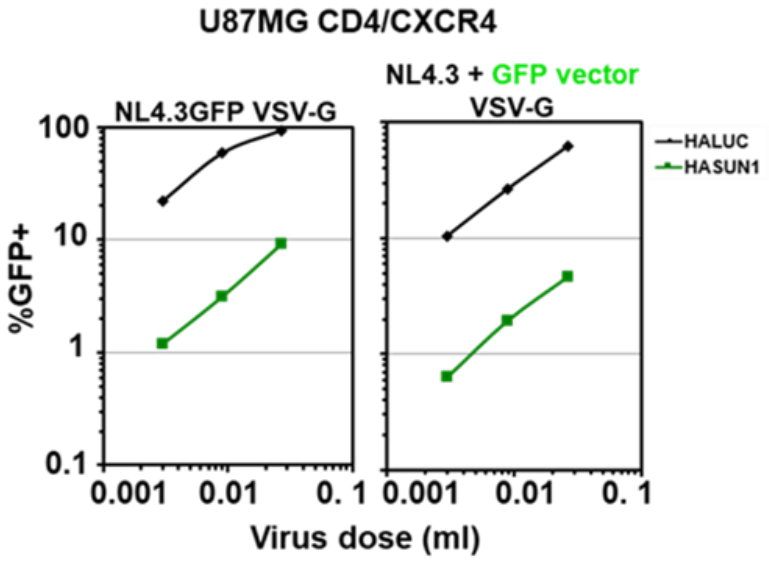

Figure 16. HIV-1 sensitivities to the SUN1-induced block. *U87MG CD4/CXCR4 cells overexpressing HALUC (negative control) or HASUN1 were infected with VSV-G-pseudotyped NL4.3GFP reporter virus or virus derived by co-transfecting NL4.3 with the GFP LV pCSGW for 24h before harvest, fixed in 4% paraformaldehyde (PFA) and analyzed by flow cytometry. Virus titrations were usually performed by threefold serial dilutions of the viral supernatant. Percentages of infected cells (%GFP+ cells) were determined from at least four virus doses. Representative results from three independent experiments are shown.*

NL4.3 and IIIB infectivities were suppressed ~20-fold by SUN1 overexpression, SUMA, WITO, and THRO were all reduced by 6- to 10-fold, whereas RHPA and ZM247 were only mildly affected (Fig. 17A) (hence RHPA served as a good control for adverse overexpression effects). Similar reductions in sensitivities of these T/F viruses to SUN2-mediated inhibition (Fig. 17B) suggested a common mechanism.

These data show that SUN1 and SUN2 efficiently block nuclear import of certain HIV-1 lab strains (NL4.3 and IIIB) as well as natural strains upon overexpression, whereas some naturally occurring HIV-1 strains, in particular T/F viruses RHPA and ZM247 are resistant to that block in a CA-dependent way.

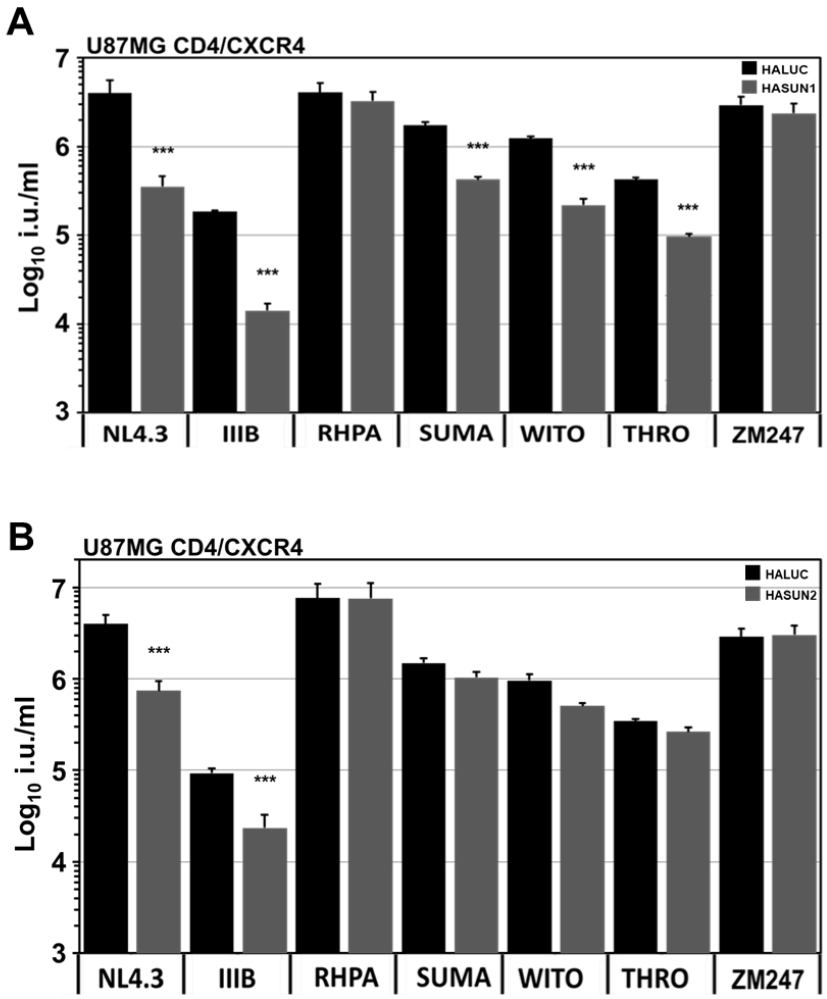

Figure 17. HIV-1 strains have differential sensitivities to the SUN1- and SUN2-induced block. *U87MG CD4/CXCR4 cells overexpressing HALUC (negative control), HASUN1 or HASUN2 were infected with the indicated VSV-G-pseudotyped virus produced by co-transfection with the HIV-1 GFP LV pCSGW, for 24h before harvest, fixed in 4% paraformaldehyde (PFA) and analyzed by flow cytometry. Virus titrations were usually performed by threefold serial dilutions of the viral supernatant. Infectious titers (in infectious units [i.u.] per milliliter) were calculated from at least three virus doses and mean titers are shown. Error bars are standard deviations. Representative results from three independent experiments are shown*

6.1.6. HIV-1 capsid protein determines sensitivity to SUN1-mediated inhibition

Previous works showed that T/F HIV-1 strains were relatively insensitive to MX2 restriction and the viral determinants were mapped to CA [204, 205, 211, 213]. To identify the viral determinants dictating sensitivity to SUN1 mediated restriction, GFP-reporter chimeric viruses between the SUN1-sensitive NL4.3 and the insensitive T/F RHPA were generated by using specific restriction sites present in both the viral genomes; *BssHII* (5=-LTR), *EcoRI* (Vpr), and *XhoI* (Nef) (Fig. 18).

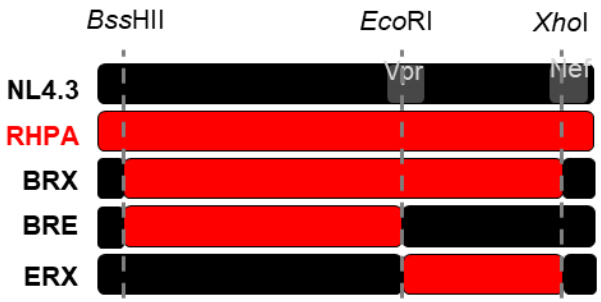

Figure 18. *Schematic of the generation of chimeric viruses between T/F virus RHPA and NL4.3.*

GFP-reporter viruses were therefore produced by co-transfecting pCSGW, and infectivity was tested in U87MG-CD/CXCR4 cells expressing HALUC or HASUN1. The chimeric virus constituted by the replacement of the region between *EcoRI* and *XhoI* sites (encoding part of Vpr, Vpu, Env, Nef, Tat, and Rev) was still sensitive to SUN1-mediated inhibition (ERX) (Fig. 19). In contrast, the chimeric virus BRE, generated by the replacement of the NL4.3 region between *BssH*II and *Eco*RI sites (encoding Gag, Pol, Vif, and part of Vpr) with that of RHPA, was mainly resistant to SUN1-induced suppression (Fig. 19), suggesting that the relative insensitivity of T/F HIV-1 to SUN1 or SUN2 may be dictated by Gag-Pol.

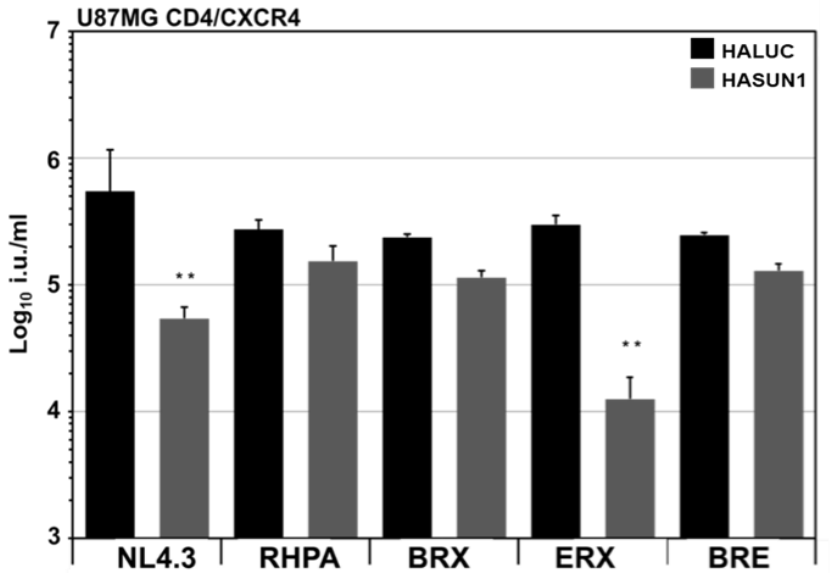

Figure 19. Identification of the HIV-1 determinant for the sensitivity to SUN1-induced inhibition. *VSV-G-pseudotyped GFP reporter viruses were produced by cotransfection with the pCSGW vector, and U87MG CD4/CXCR4 cells overexpressing HALUC (negative control) or HASUN1 were infected for 24h before harvest, fixed in 4% paraformaldehyde (PFA) and analyzed by flow cytometry. Virus titrations were usually performed by threefold serial dilutions of the viral supernatant. Infectious titers (in infectious units [i.u.] per milliliter) were calculated from at least three virus doses and mean titers are shown. Error bars are standard deviations. Representative results from three independent experiments are shown.*

HIV-1 incorporating the CA-p2 of the insensitive SIV_{MAC} (HIV-1 (SCA) chimera) (pCMV-ΔR8.91Ex-SCA: *see paragraph 5.1.9. in Materials and Methods*) [274, 295] was also largely insensitive to SUN1 or SUN2 (Fig. 20), further indicating the CA role in determining sensitivity to SUN-mediated inhibition.

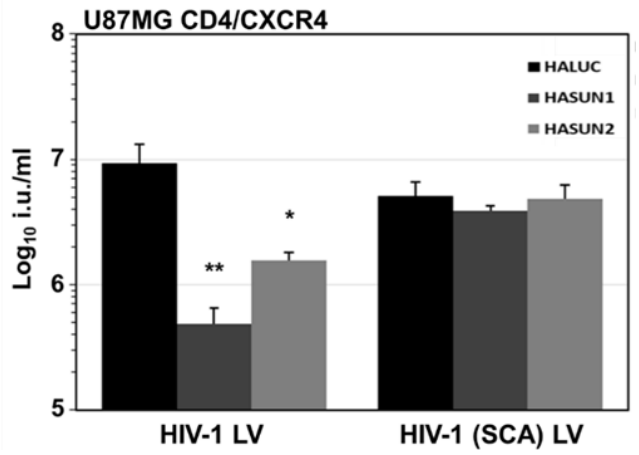

Figure 20. HIV-1 incorporating the CA-p2 of the insensitive SIV_{MAC} (HIV-1 (SCA) chimera) is largely insensitive to SUN1- or SUN2-induced inhibition. *U87MG CD4/CXCR4 cells expressing HALUC (negative control), HASUN1 or SUN2 were infected with VSV-G-pseudotyped HIV-1 SCA GFP LV for 48h before harvest, fixed in 4% paraformaldehyde (PFA) and analyzed by flow cytometry. Virus titrations were usually performed by threefold serial dilutions of the viral supernatant. Infectious titers (in infectious units [i.u.] per milliliter) were calculated from at least three virus doses and mean titers are shown. Error bars are standard deviations. Representative results from three independent experiments are shown.*

CA sequences from sensitive NL4.3 and resistant RHPA show amino acid differences at nine positions, some of which are located in proximity, or inside of the Cyp-binding loop in CA (Fig. 21).

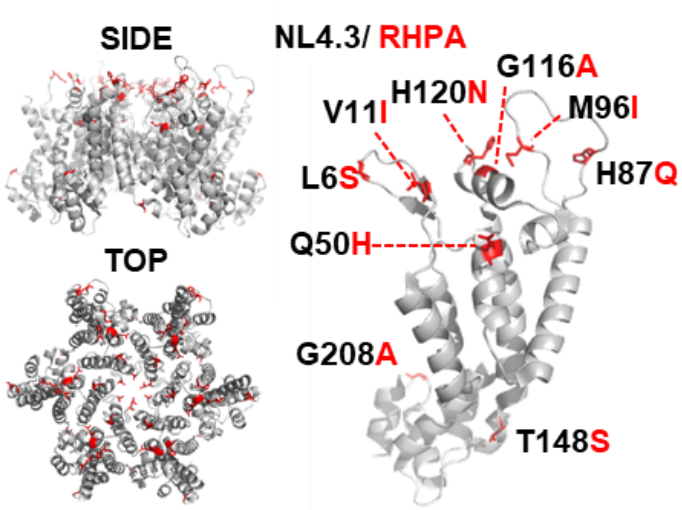

Figure 21. *CA amino acid differences between sensitive HIV-1$_{NL4.3}$ and resistant HIV-1$_{RHPA}$.* Figure adapted from [296]

To further define the specific sequence determinant dictating sensitivity to SUN1 inhibition, Gag-Pol–encoding vector pCMV-ΔR8.91ExNRA was generated (HIV-1 NRA LV; *see paragraph 4.1.12. in Materials and Methods*) by replacing the NL4.3 Gag sequence up to the *Apa*I site in pCMV-ΔR8.91Ex with that of RHPA **(Fig. 22)**.

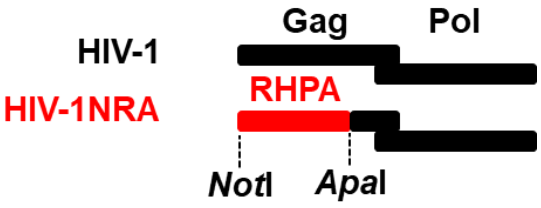

Figure 22. *HIV-1 LV and HIV-1NRA LV: replacement of the sequence of the SUN1-sensitive HIV-1 variant NL4.3 up to the ApaI site with that of RHPA.*

Wild type HIV-1 LV (NL4.3-based) was inhibited >10-fold by SUN1, whereas HIV-1 NRA LV was also largely insensitive (Fig. 23). Subsequently, to further define the specific sequence determinant, single or multiple amino acid CA substitutions were introduced into the NL4.3 CA region and new compound mutants were created, among which the triple mutant H87Q+H120N+G208A

that rendered HIV-1 largely resistant to SUN1-mediated inhibition, phenocopying HIV-1NRA LV (Fig. 23). To address whether the reciprocal was competent, the reverse amino acid substitutions (Q87H+N120N+A208G) were introduced into HIV-1NRA and the infectivity compared to HIV-1NRA in HALUC or HASUN1 overexpressing U87MG-CD4/CXCR4 cells. Indeed, these three changes were sufficient to render HIV-1NRA sensitive to SUN1-induced suppression (Fig. 23).

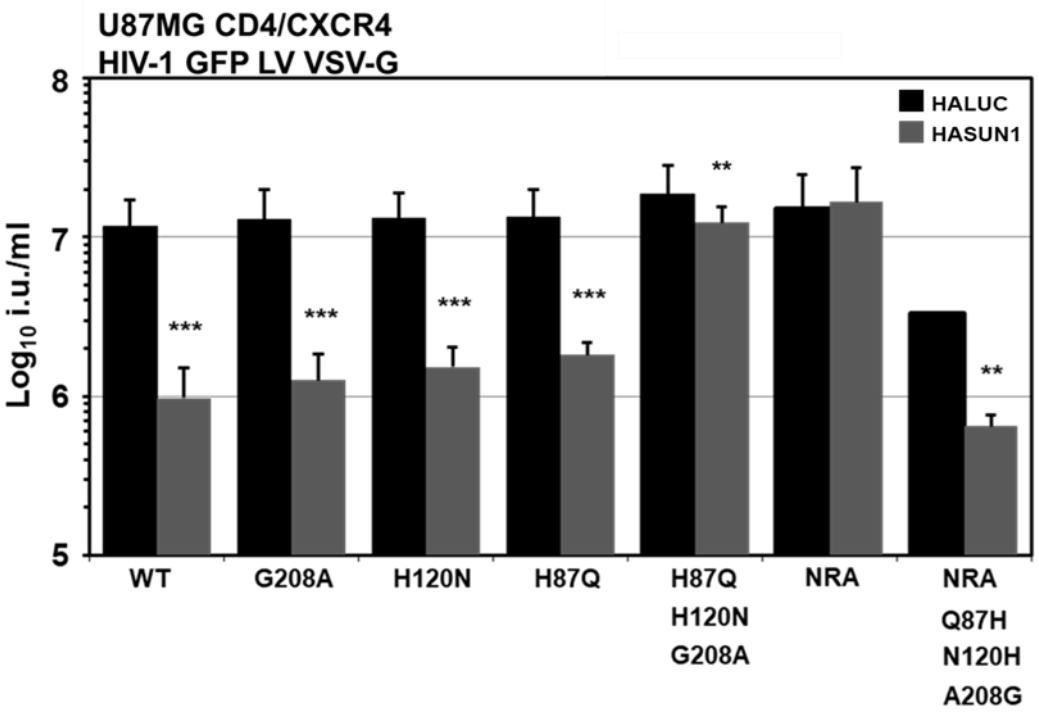

Figure 23. The determinant for the sensitivity to SUN1-induced inhibition maps to CA. *U87MG CD4/CXCR4 cells overexpressing HALUC (negative control) or HASUN1 were infected with VSV-G-pseudotyped HIV-1 GFP LV and with VSV-G-pseudotyped chimeric HIV-1 GFP LV (NL4.3H87Q, NL4.3H120N, NL4.3G208A, NL4.3H87Q+H120N+G208A, NRA, NRAQ87H+N120N+A208G) for 48h before harvest, fixed in 4% paraformaldehyde (PFA) and analyzed by flow cytometry. Virus titrations were usually performed by threefold serial dilutions of the viral supernatant. Infectious titres were calculated from at least three virus doses and mean titres are shown. Error bars are standard deviations. Representative results from three independent experiments are shown.*

These results suggest that specific residues in HIV-1 CA are likely the viral determinant defining the sensitivity to SUN1 or SUN2-mediated restriction after overexpression.

6.1.7. *In vitro*-assembled HIV-1 CANC complexes interact with SUN1 and SUN2

Since HIV-1 sensitivity to SUN1 or SUN2-mediated suppression is determined by specific amino acid residues in CA, the binding of of SUN proteins to *in vitro*

synthesized HIV-1 CANC complexes (capsid-nucleocapsid complexes) was investigated with the Malim lab in London (King's College London).

Synthetic CANC nanotubes derived from SUN1- and SUN2-sensitive HIV-1 strain IIIB or T/F virus RHPA were used to analyze if HASUN1 or HASUN2 could be co-precipitated from 293T cell lysates. Since it was able to interact efficiently with IIIB and RHPA CANC nanotubes, HACPSF6 was used as positive control to compare with the negative control, HALUC. Parallel samples without adding CANCs were also used as control for unspecific precipitation of proteins (Fig. 10). Both HASUN1 and HASUN2 were able to interact with IIIB CANC complexes in cell lysates (Fig. 24A). However, they also interacted with RHPA CANC complexes, despite they couldn't block RHPA infection (Fig. 24B). Therefore, though SUN1 or SUN2 seem to interact with CANCs in vitro, a direct correlation between such interactions and the suppression of virus infection in cultured cells was not identified. It is possible that RHPA and other SUN1- and SUN2-insensitive viruses overcome SUN1 or SUN2-induced restriction in cells because physical interaction is absent due to choice of a different trafficking pathway towards the nucleus. Likewise, it is possible that interaction is necessary but not sufficient for mediating a block to infection.

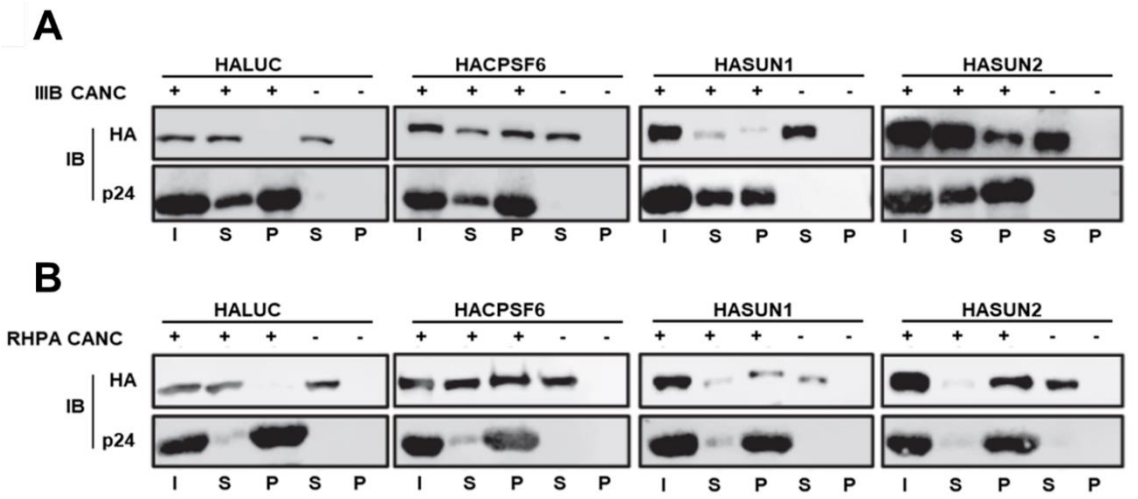

Figure 24. *In vitro*-synthesized HIV-1 CANC nanotubes capture SUN1 and SUN2 from cell lysates. *Cell lysates from 293T cells transfected with HALUC, HACPSF6, HASUN1, or HASUN2 were incubated with in vitro-synthesized CANC nanotubes before centrifugation through a sucrose cushion and analysis of supernatants and pellets by immunoblotting using HA- and CA-specific antibodies. I, input; S, supernatant; P, pellet.* **A)** *In vitro-synthesized CANC complexes from IIIB were mixed with cell lysates and analyzed as described in panel A.* **B)** *In vitro-synthesized CANC complexes from RHPA were mixed with cell lysates and analyzed as described in panel A.* Data from Malim Lab (KCL, London)

6.1.8. The amino-terminal domain of SUN1 mediates HIV-1 inhibition

To identify which regions of SUN1 are involved in HIV-1 infection suppression, amino-terminal and carboxy-terminal deletion mutants (Fig. 25) were generated.

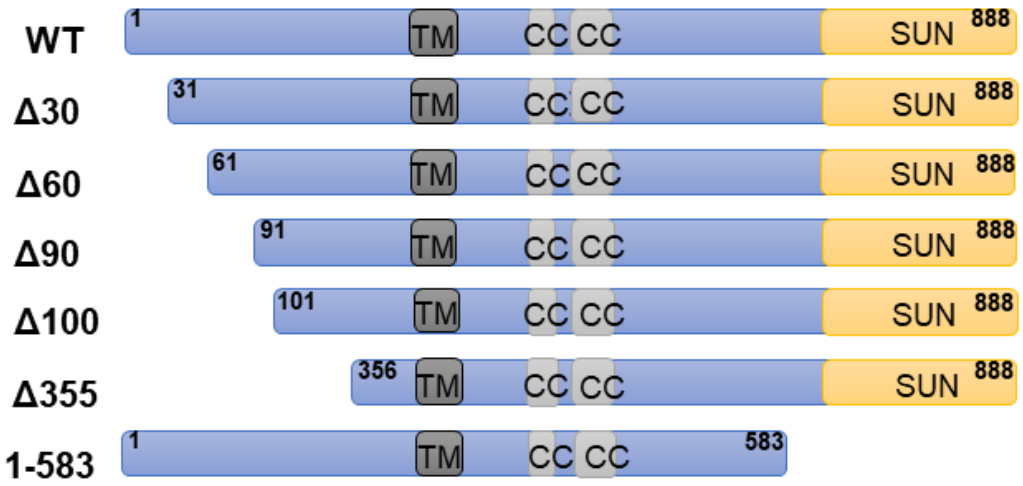

Figure 25. *Schematic of the analyzed SUN1 deletion mutants.*

Among the amino-terminal SUN1 deletions, removing the first 30 (HASUN1Δ30) or 60 (HASUN1Δ60) amino acids had no or minor effects on the SUN1 capacity to block HIV-1 infection (Fig. 26A). In contrast, removing the first 90 (HASUN1Δ90), 100 (HASUN1Δ100) or 355 (HASUN1Δ355) amino acids was abrogating the suppression of HIV-1 infection (Fig. 26A). The expression levels of the amino-terminal SUN1 deletion mutants were generally higher than the wild type protein (Fig. 26B). Deletion of the carboxy-terminal SUN domain (HASUN1-1-583) did not interfere with the inhibition of HIV-1 (Fig. 26B), suggesting that interaction with nesprin proteins in the perinuclear space and LINC complex formation may not be required for the antiviral activity.

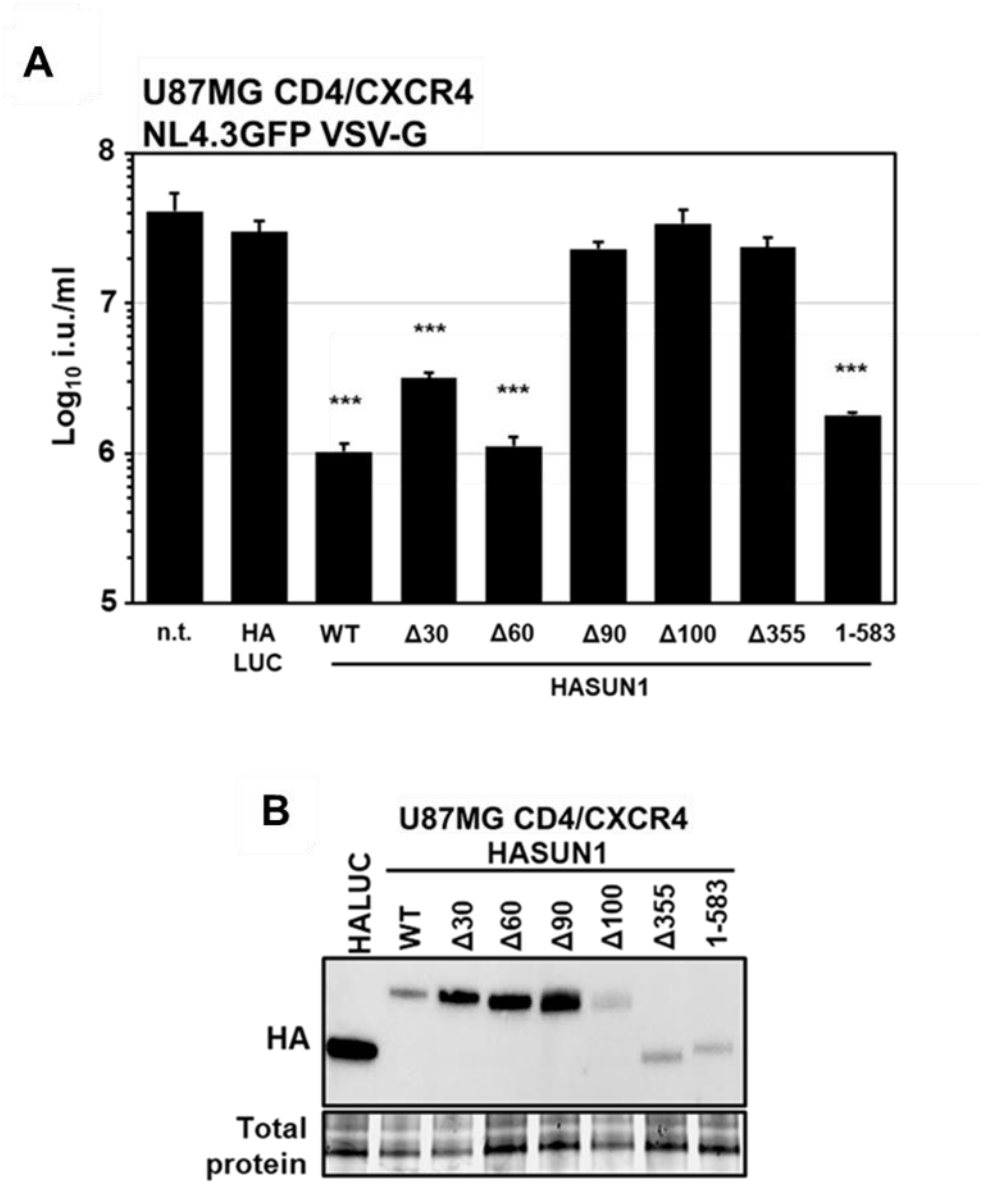

Figure 26. The amino-terminal domain of SUN1 is required for the block to HIV-1.
A) *U87MG CD4/CXCR4 overexpressing HALUC (negative control), HASUN1, HASUN1Δ30, HASUN1Δ60, HASUN1Δ90, HASUN1Δ100, HASUN1Δ355, HASUN1-1-583 were infected with full length VSV-G HIV-1 GFP reporter virus (NL4.3GFP VSV-G) for 48h before harvest, fixed in 4% paraformaldehyde (PFA) and analyzed by flow cytometry. Virus titrations were usually performed by threefold serial dilutions of the viral supernatant. Infectious titres were calculated from at least three virus doses and mean titres are shown. Error bars are standard deviations. Representative results from three independent experiments are shown.*
B) *Corresponding WB for A). Same numbers of cells were lysed in the same volume of Laemmli buffer and subjected to immunoblotting analysis. Total protein was determined by UV-activating the gel and served as loading control.*

Furthermore, by indirect immunofluorescence microscopy, it was shown that the restriction of wild type HASUN1, HASUN1Δ30 or HASUN1Δ60 did not show apparent differences in subcellular localization as compared to the inactive HASUN1Δ90 or HASUN1Δ100, particularly all showed cytoplasmic as well as perinuclear staining (Fig. 27). In contrast, HASUN1Δ355 mutant mainly localizes in a perinuclear cytoplasmic compartment, suggesting that the different localization may contribute to the inactivity of this mutant (Fig. 27).

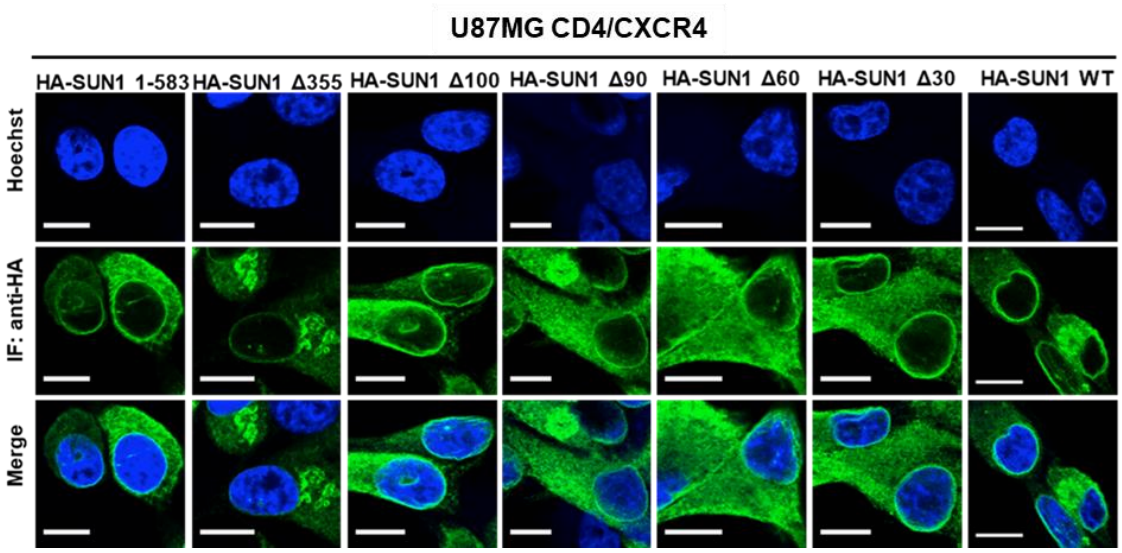

Figure 27. IF of U87MG CD4/CXCR4 cells expressing HASUN1 wild type or HASUN1 amino-terminal and carboxy-terminal deletion mutants. *U87MG CD4/CXCR4 overexpressing HALUC, HASUN1wt, HASUN1Δ30, HASUN1Δ60, HASUN1Δ90, HASUN1Δ100, HASUN1Δ355, HASUN1-1-583 were stained by immunofluorescence for HA, using Alexa Fluor 488 conjugated secondary antibody. Hoechst staining was used to label double stranded DNA and thus visualize nuclei*.

Subsequently, to further define the specific antiviral determinants, different quadruple alanine mutants of SUN1 were created, each one with different four single alanine mutations in the region between 75 to 95 (Fig. 28).

SUN1 wt	75-S G T S S A V S L K N R A A R T T K Q R-95
80SAAA83	75-S G T S S S A A A K N R A A R T T K Q R-95
84AAAS87	75-S G T S S A V S L A A A S A R T T K Q R-95
86ASSA89	75-S G T S S A V S L K N A S S A T T K Q R-95
88SAAA91	75-S G T S S A V S L K N R A S A A A K Q R-95
90AAAA93	75-S G T S S A V S L K N R A A R A A A A R-95

Figure 28. *Schematic of analyzed SUN1 alanin mutants*.

Each mutant was overexpressed in U87MG CD4 / CXCR4 cells and infected with full-length non-pseudotyped NL4.3GFP for 48h. The SUN1 mutants 84AAAS87 and 86ASSA89 lost the capacity to block the HIV-1 infection, suggesting that the amino acids 85-90 are those relevant in SUN1 antiviral activity (Fig. 29A).

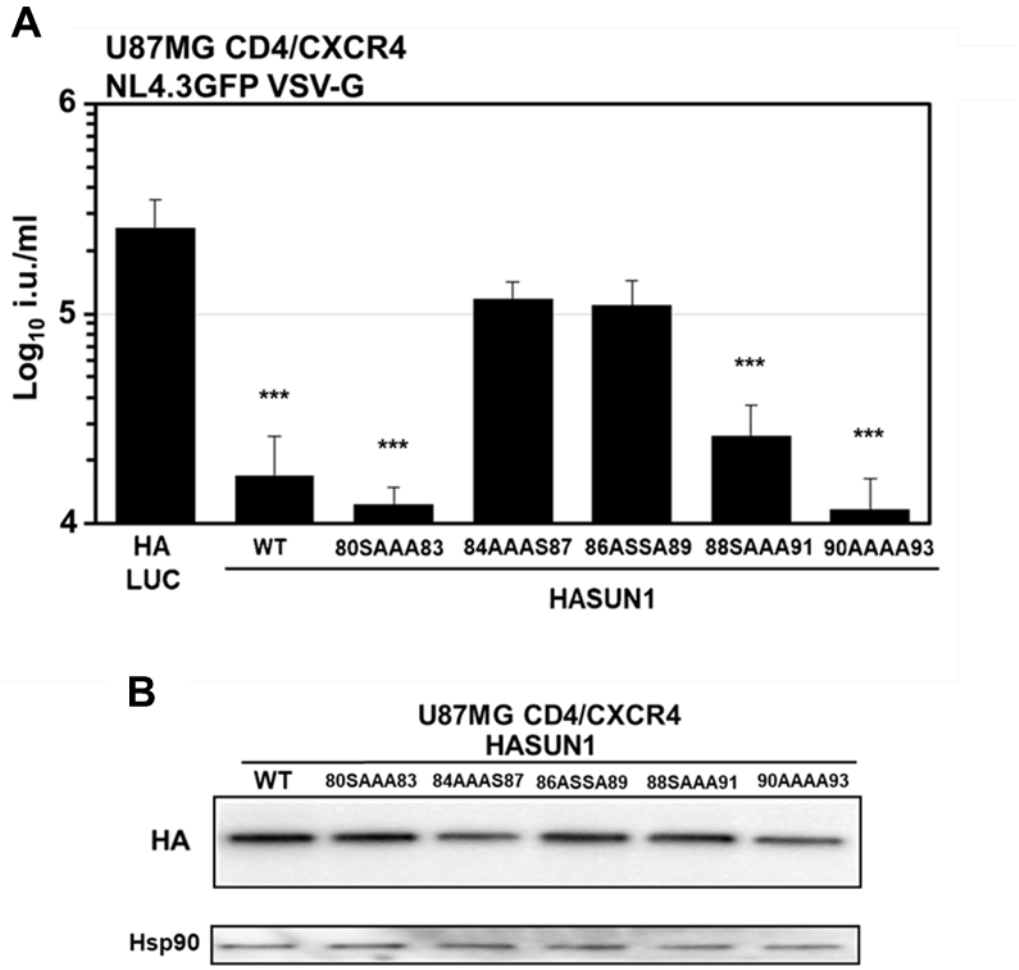

Figure 29. The amino-terminal amino acids 85-90 relevant in SUN1 blocking infection capacity. A) *U87MG CD4/CXCR4 cells overexpressing HALUC (negative control), HASUN1 or the indicated SUN1 alanin mutants were infected with VSV-G-pseudotyped NL4.3GFP for 24h before harvest, fixed in 4% paraformaldehyde (PFA) and analyzed by flow cytometry. Virus titrations were usually performed by threefold serial dilutions of the viral supernatant. Infectious titers (in infectious units [i.u.] per milliliter) were calculated from at least three virus doses and mean titers are shown. Error bars are standard deviations. Representative results from three independent experiments are shown.* **B)** *Corresponding WB for A). Same numbers of cells were lysed in the same volume of Laemmli buffer and subjected to immunoblotting analysis with antibodies targeting HA. HSP90 served as a loading control.*

In order to determine whether SUN1 amino-terminal region would still have the capacity to suppress HIV-1 infection when appended to an entirely unrelated protein, the fusion protein composed of the first 130 amino-terminal SUN1 amino acids fused with the entire $Fv1^N$ protein was created ($HASUN1^{NTD}$-$Fv1^N$; *see paragraph 5.1.12. in Materials and Methods*) **(Fig. 30)**.

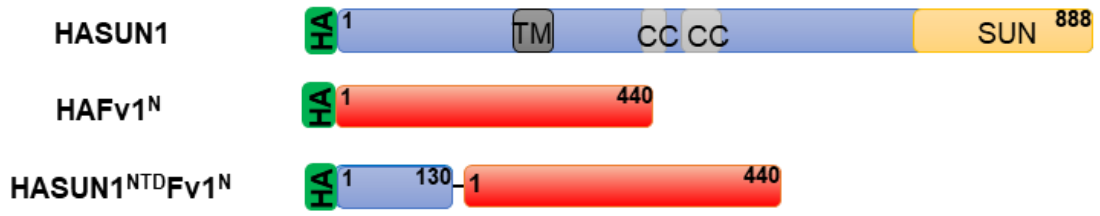

Figure 30. *Schematic of analyzed chimeric protein composed of the amino-terminal 130 amino acids of SUN1 fused to the restriction factor MLV $Fv1^N$ ($HASUN1^{NTD}$-$Fv1^N$).*

$Fv1^N$ was chosen as the substrate since this protein is an inhibitor of retrovirus infection (MLV B-tropic but not HIV-1) [297] and it is naturally oligomeric [298]. Furthermore, this strategy has already been used in previous studies to analyze CA binding and antiviral activity of certain protein domains in the context of a heterologous fusion partner by Fv1-Cyp [299, 300], or $MX2^{NTD}$-Fv1 [226]. As expected, the expression of the control protein $HAFv1^N$ in U87MG CD4/CXCR4 did not suppress HIV-1 infection. In contrast, the fusion protein $HASUN1^{NTD}$-$Fv1^N$ was able to reduce the HIV-1 infection (Fig. 31A), without reaching the same levels of wild type HASUN1, maybe due to reduced expression level (Fig. 31B).

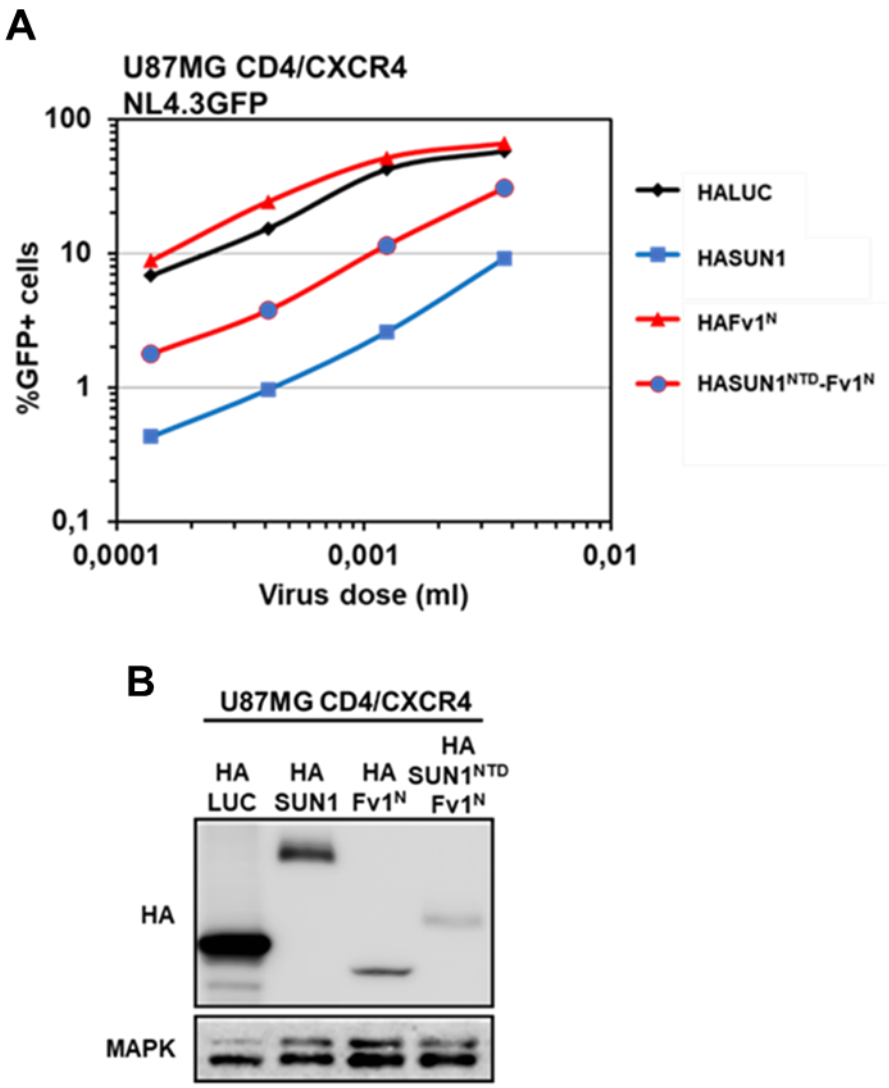

Figure 31. Fusion of the amino-terminal SUN1 domain to Fv1 generates a potent HIV-1-inhibiting factor. A) *U87MG CD4/CXCR4 cells expressing HALUC (negative control), HASUN1 (positive control),HAFv1^{N}, or HASUN1^{NTD}-Fv1^{N} were infected with full-length non-pseudotyped CXCR4-tropic NL4.3GFP for 48h before harvest, fixed in 4% paraformaldehyde (PFA) and analyzed by flow cytometry. Virus titrations were usually performed by threefold serial dilutions of the viral supernatant. Percentages of infected cells (%GFP+ cells) were determined from at least four virus doses. Representative results from three independent experiments are shown.* **B)** *Corresponding WB for A). Same numbers of cells were lysed in the same volume of Laemmli buffer and subjected to immunoblotting analysis with antibodies targeting HA. MAPK served as a loading control.*

In addition, it was confirmed that HASUN1^{NTD}-Fv1^{N} mainly shows a strong perinuclear cytoplasmatic localization, suggesting that incoming HIV-1 CA could interact with the SUN1 amino-terminal domain in the cytoplasm (Fig. 32).

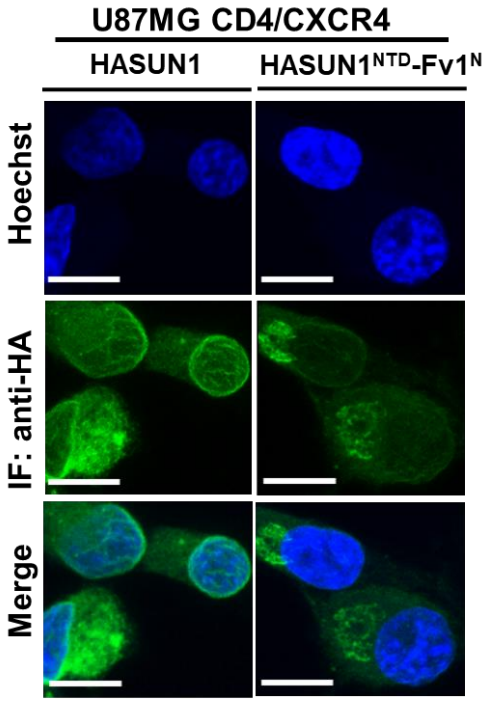

Figure 32. IF U87MG CD4/CXCR4 cells expressing HASUN1 wild type HASUN1^{NTD}-Fv1^{N}. *U87MG CD4/CXCR4 overexpressing HASUN1wt or HASUN1^{NTD}-Fv1^{N} were stained by immunofluorescence for HA, using Alexa Fluor 488 conjugated secondary antibody. Hoechst staining was used to label double stranded DNA and thus visualize nuclei.*

In conclusion, the data confirm that the amino-terminal region of SUN1 is necessary and sufficient for the HIV-1 infection suppression.

6.1.9. The amino-terminal domain of SUN2 mediates HIV-1 inhibition

In order to understand which regions of SUN2 are involved in HIV-1 and HIV-2 infection suppression, amino-terminal and carboxy-terminal deletion mutants were also generated (Fig. 33).

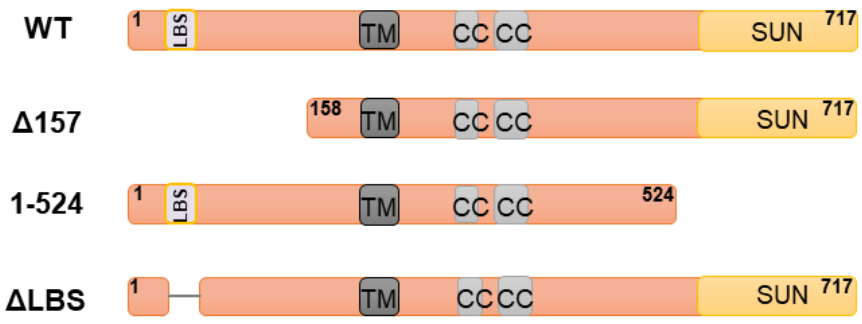

Figure 33. *Schematic of the analyzed SUN2 deletion mutants.*

The results showed that removing the carboxy-terminal SUN domain (HASUN2-1-524) had no effect on the viral infections (Fig. 34A), suggesting that interaction with the nesprin proteins in the perinuclear space may not be required for the antiviral activity. Analysis of the amino-terminal SUN2 deletions indicated that the elimination of the lamin-binding site (LBS) had minor effects on the SUN2 capacity to suppress the viral infections (Fig. 34A), suggesting that interaction of SUN2 with lamins in the nucleus is not important for the antiviral activity. In contrast, the deletion of the first 157 amino acids (HASUN2Δ157) was abrogating the suppression of HIV-1 and HIV-2 infection (Fig. 34A).

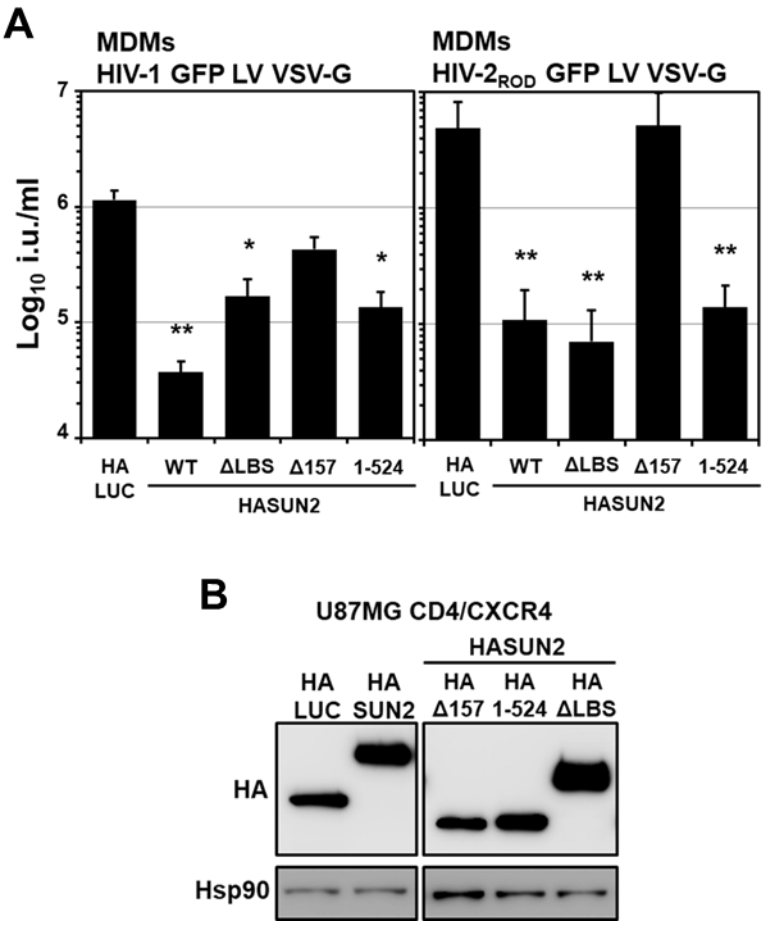

Figure 34. The amino-terminal domain of SUN2 is required for the block to HIV-1. A) *MDMs from three independent donors overexpressing HALUC (negative control), HASUN2, HASUN2ΔLBS, HASUN2Δ157, HASUN1-1-524 were infected with VSV-G-pseudotyped HIV-1 GFP LV or VSV-G-pseudotyped HIV-2ROD GFP LV in presence of Vpx for 48h before harvest, fixed in 4% paraformaldehyde (PFA) and analyzed by flow cytometry. Virus titrations were usually performed by threefold serial dilutions of the viral supernatant. Infectious titres were calculated from at least three virus doses and mean titres are shown. Error bars are standard deviations. Representative results from three independent experiments are shown.* **B)** *Corresponding WB for A). Same numbers of cells were lysed in the same volume of Laemmli buffer and subjected to immunoblotting analysis. HSP90 served as a loading control.*

Subcellular localization between the restricting wild type HASUN2, HASUN2ΔLBS or HASUN2 1-524 and the inactive HASUN1Δ157 displayed all

the variants in cytoplasmic as well as perinuclear staining **(Fig. 35)**, as already seen with SUN1 **(Fig. 27)**.

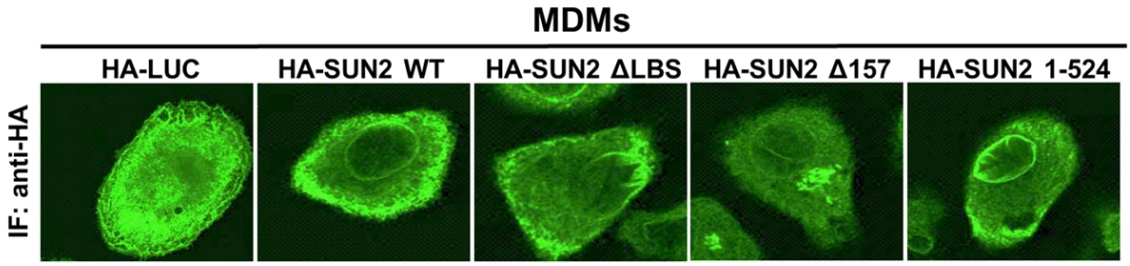

Figure 35. IF of U87MG CD4/CXCR4 cells expressing HASUN1 wild type or HASUN1 amino-terminal and carboxy-terminal deletion mutants. *MDMs from three independent donors overexpressing HALUC (negative control), HASUN2, HASUN2ΔLBS, HASUN2Δ157, HASUN1-1-524 were stained by immunofluorescence for HA, using Alexa Fluor 488 conjugated secondary antibody.*

In order to verify if SUN2 amino-terminal can replace the antiviral activity of SUN1 amino-terminal, a fusion protein of SUN1 and SUN2 was generated in which the first 130 amino-terminal amino acids of SUN1 are replaced with the first 90 amino-terminal amino acids of SUN2 (HASUN2^{NTD}-SUN1; *see paragraph 5.1.12. in Materials and Methods*) (Fig. 36).

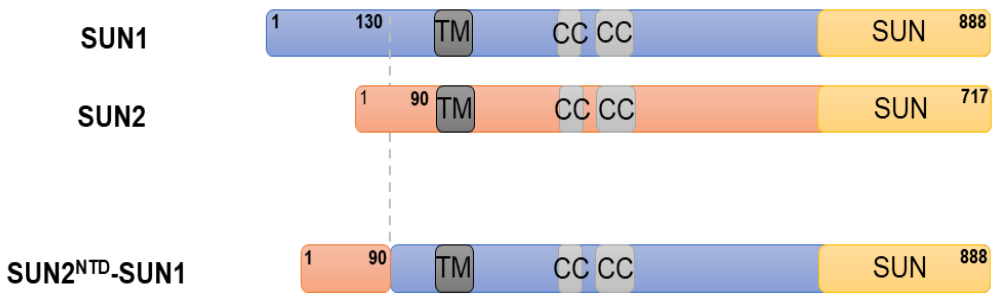

Figure 36. *Schematic of analyzed chimeric protein composed of the SUN2 amino-terminal fused to SUN1 (SUN2^{NTD}-SUN1).*

The chimeric protein, HASUN2^{NTD}-SUN1 was able to reduce the HIV-1 infection when overexpressed in U87MG CD4/CXCR4 cells (Fig. 37A), without reaching to the same levels of wild type HASUN1, maybe due to reduced expression

level (Fig. 37B). Thus, it is confirmed that the amino-terminal region of SUN2 is necessary and sufficient for the HIV-1 infection suppression, as observed in SUN1.

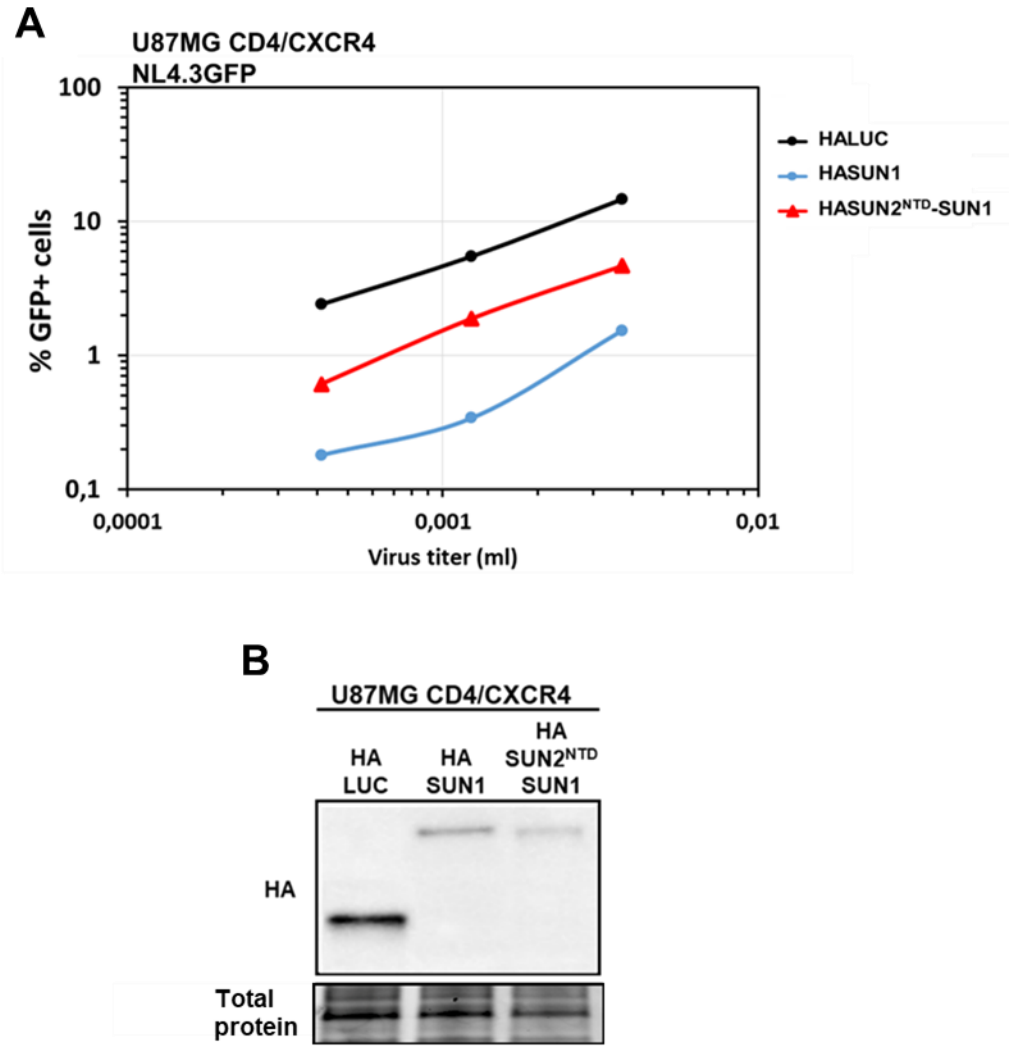

Figure 37. Fusion of the amino-terminal SUN2 domain to SUN1 generates a potent HIV-1-inhibiting factor. A) *U87MG CD4/CXCR4 cells expressing HALUC (negative control), HASUN1 (positive control),HASUN2^{NTD}-SUN1 were infected with full-length non-pseudotyped CXCR4-tropic NL4.3GFP for 48h before harvest, fixed in 4% paraformaldehyde (PFA) and analyzed by flow cytometry. Virus titrations were usually performed by threefold serial dilutions of the viral supernatant. Percentages of infected cells (%GFP+ cells) were determined from at least four virus doses. Representative results from three independent experiments are shown.* **B)** *Corresponding WB for A). Same numbers of cells were lysed in the same volume of Laemmli buffer and subjected to immunoblotting analysis with antibodies targeting HA. MAPK served as a loading control.*

6.1.10. CRISPR/Cas9-mediated *SUN2* but not *SUN1* gene disruption decreases HIV-1 infectivity in THP-1 cells

To verify whether depletion of endogenous SUN proteins have an effect in HIV-1 infection, THP-1 cells were transduced with CRISPR/Cas9 LVs expressing individual specific guide RNAs (gRNA) against SUN1 or SUN2 *(see paragraphs 5.1.12. and 5.3.3.2. in Materials and Methods)*. Two independent THP-1 single-cell knockout clones for each gene with complete loss of SUN1 or SUN2 expression (SUN1g2c5, SUN1g2c7, SUN2g2c1, and SUN2g3c4) were generated, as well as various clones with intact SUN1 or SUN2 expression (Fig. 38A). The knockout was verified by immunoblotting (Fig. 38B) as well as by sequencing over the gRNA target site in the cell genome.

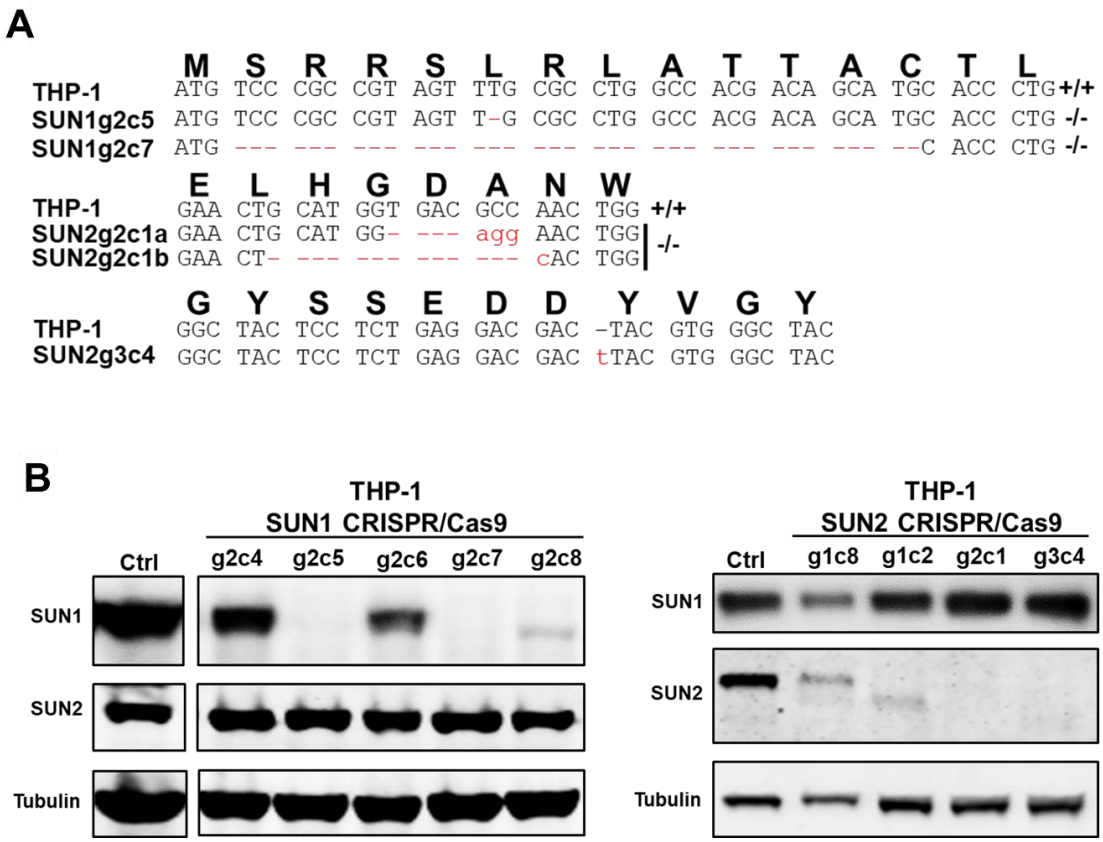

Figure 38. THP-1 single-cell knockout clones for SUN1 or SUN2 genes. A) *THP-1 CRISPR/Cas9 single-cell cloning followed by PCR-based sequencing across the guide RNA target sites identified two clones for each gene in which the open reading frame was disrupted.* **B)** The *SUN1 or SUN2 abrogated expression in the individual single-cell clones was verified by immunoblotting using SUN1- or SUN2-specific antibodies. Tubulin served as the loading control.*

All the clones were tested for their sensitivity to VSV-G pseudotyped NL4.3GFP or chimeric BREGFP reporter virus's infection. BRE chimeric virus (Fig. 18) was used because it was insensitive to SUN1/2 overexpression (Fig. 19), and thus expected to serve as a negative control. The SUN1 gene disruption did not show any detectable effect on infection by either virus, while the depletion of SUN2 reduced HIV-1 infection by 2 to 3-fold in comparison to a CRISPR/Cas9 control cell clone (Fig. 39).

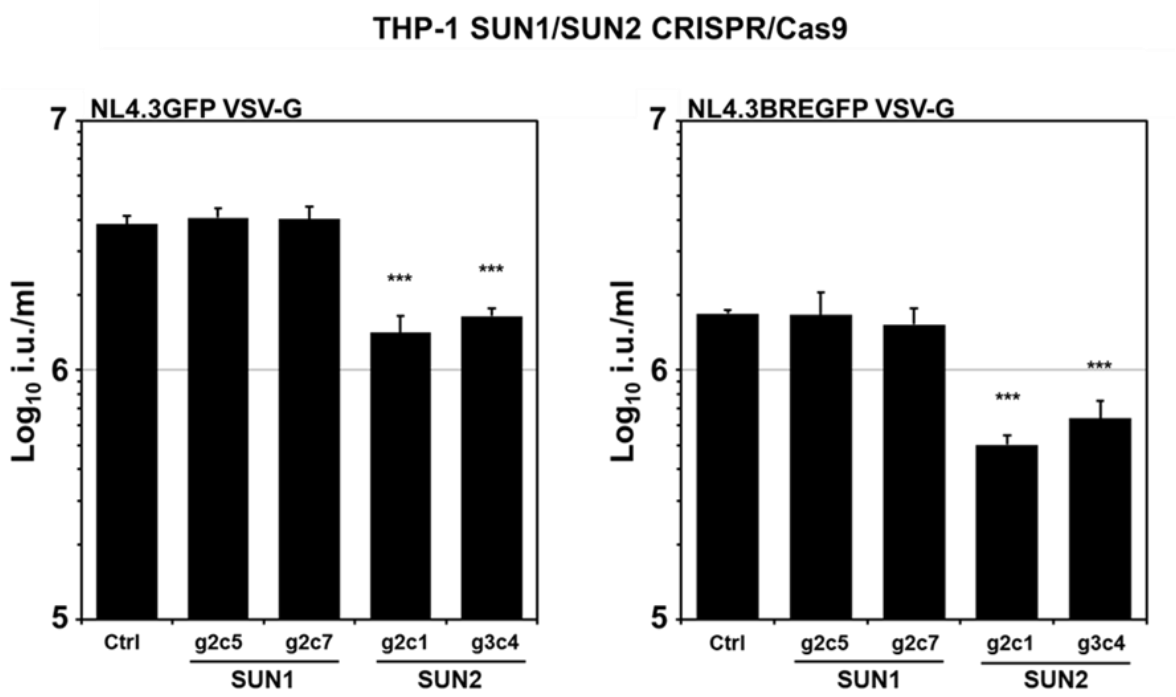

Figure 39. HIV-1 infection is impaired in CRISPR/Cas9 *SUN2*-depleted THP-1 cells. A) The *SUN1 or SUN2 abrogated expression in the individual single-cell clones was verified by immunoblotting using SUN1- or SUN2-specific antibodies. Tubulin served as the loading control.* **B)** *THP-1 CRISPR/Cas9 control, SUN1- or SUN2-depleted cells were infected with VSV-G-pseudotyped NL4.3GFP or BREGFP reporter viruses for 24h before harvest, fixed in 4% paraformaldehyde (PFA) and analyzed by flow cytometry. Virus titrations were usually performed by threefold serial dilutions of the viral supernatant. Infectious titers (in infectious units [i.u.] per milliliter) were calculated from at least three virus doses and mean titers are shown. Error bars are standard deviations. Representative results from three independent experiments are shown.*

Proliferation assay confirmed that the reduction of infectivity in SUN2 knockout clones is independent of cell number (Fig. 40A). The susceptivity of infection by MoMLV-derived-LV and VSV-G-pseudotyped GFP-encoding retroviral vectors derived from HIV-2_{ROD}, SIV_{MAC}, FIV, EIAV was also determined (Fig. 40B, 40C). It was found that only HIV-1 was sensitive to the SUN2 gene depletion.

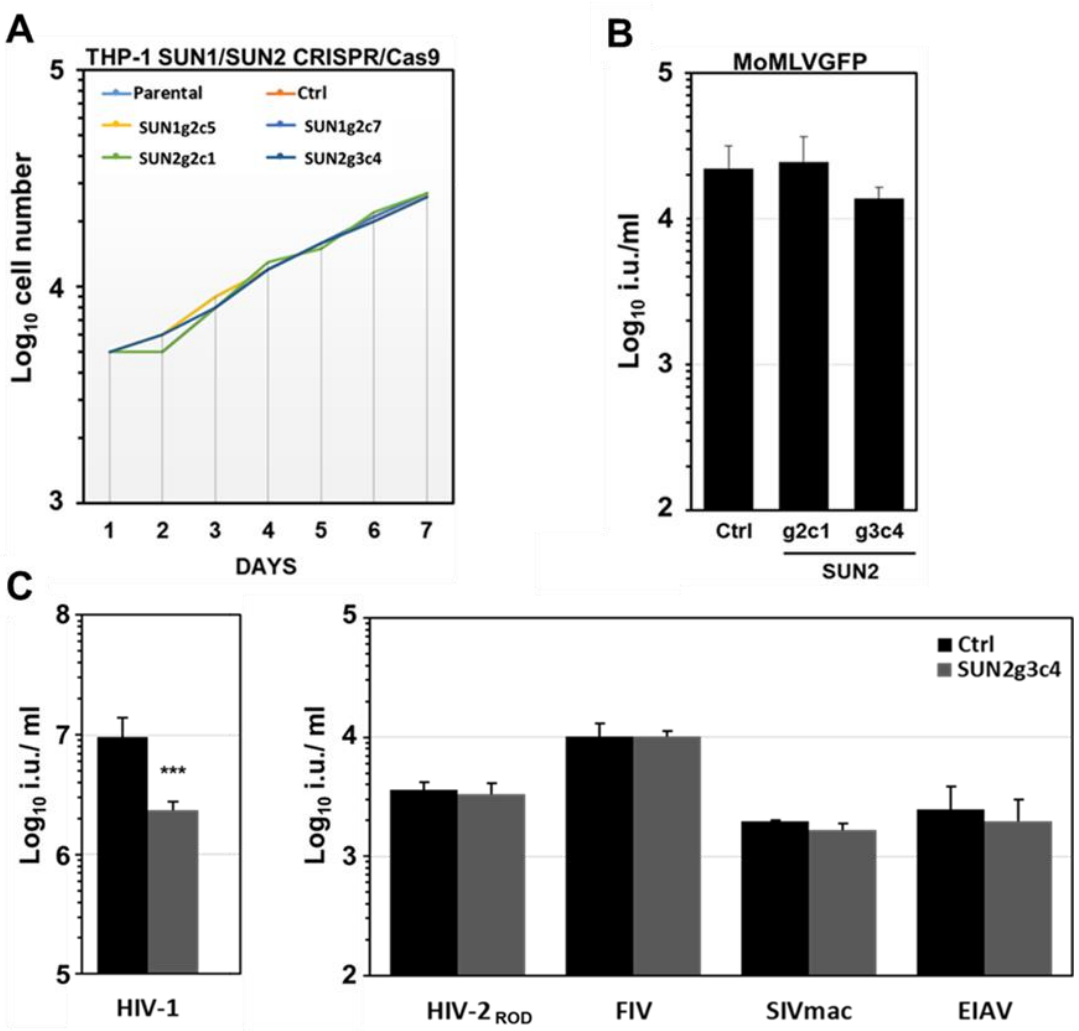

Figure 40. Gene disruption of *SUN2* inhibits HIV-1 but not HIV-2_{ROD}, FIV, SIV_{MAC}, EIAV or MoMLV infection. A) *Growth kinetics of CRISPR/Cas9 SUN2-depleted THP-1 cells in comparison to CRISPR/Cas9 control or THP-1 parental cells. At each time point, THP-1 parental, CRISPR/Cas9 control, SUN1- or SUN2-depleted cells were harvested and counted. Viable cells are represented.* **B)** *THP-1 control, SUN2-depleted cells were infected with VSV-G-pseudotyped MoMLV GFP LV for 48h before harvest, fixed in 4% paraformaldehyde (PFA) and analyzed by flow cytometry. Virus titrations were usually performed by threefold serial dilutions of the viral supernatant. Infectious titers (in infectious units [i.u.] per milliliter) were calculated from at least three virus doses and mean titers are shown. Error bars are standard deviations. Representative results from three independent experiments are shown.* **C)** *THP-1 control, SUN2-depleted cells were infected with the indicated VSV-G-pseudotyped GFP retroviral vector, for 48h before harvest, fixed in 4% paraformaldehyde (PFA) and analyzed by flow cytometry. Virus titrations were usually performed by threefold serial dilutions of the viral supernatant. Infectious titers (in infectious units [i.u.] per milliliter) were calculated from at least three virus doses and mean titers are shown. Error bars are standard deviations. Representative results from three independent experiments are shown.*

6.1.11. Nuclear import is impaired in SUN2 CRISPR/Cas9 THP-1 cells

To determine which stage of HIV-1 infection is affected by the absence of SUN2, THP-1 control cells and SUN2 knockout cells were infected with DNase-treated VSV-G-pseudotyped NL4.3GFP and the production of GFP reverse transcription products or 2-LTR circles was measured by real time PCR as described in *paragraph 6.1.3*. Although SUN2 knockout cells showed reduced susceptibility to HIV-1 infection, similar levels of GFP reverse transcription products were detected in control and SUN2 knockout cells (Fig.41A). In contrast, the amount of 2-LTR circles was reduced by ~3-fold, which correlated with the reduction in infectivity (Fig.41A), suggesting that HIV-1 nuclear import is impaired in in THP-1 lacking SUN2. Similar infection phenotypes were obtained in THP-1 cells previously differentiated by use of phorbol 12-myristate 13-acetate (PMA) (Fig. 41B).

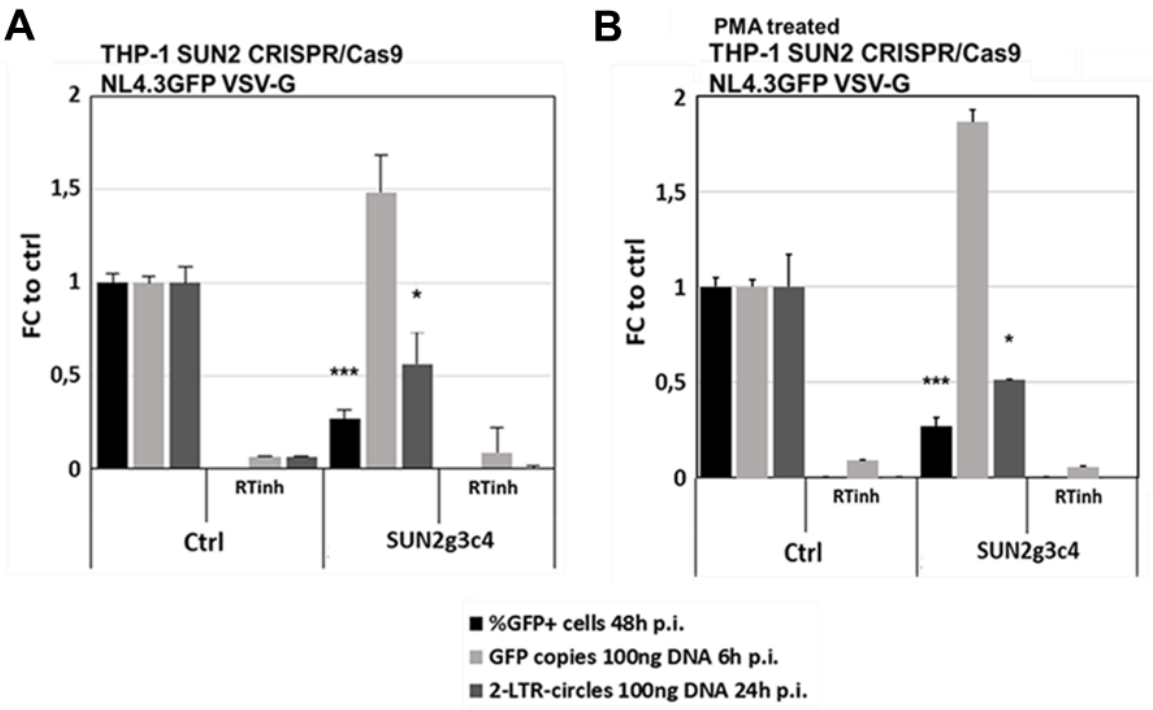

Figure 41. HIV-1 nuclear import is impaired in CRISPR/Cas9 *SUN2*-depleted cells. A) *THP-1 CRISPR/Cas9 control as well as SUN2-depleted cells (SUN2g3c4) were infected with DNase-treated VSV-G-pseudotyped NL4.3GFP in the presence or absence of efavirenz (RTinh), and total DNA was isolated for TaqMan qPCR 6 h (GFP) or 24 h (2-LTR circles) postinfection (p.i.). Parallel samples were used to determine percentages of infected cells (% GFP+) by flow cytometry 48h post infection. Fold changes to control cells in the absence of RTinh were calculated. Representative results from three independent experiments are shown.* **B)** *Same as for panel A, but with PMA treated (24h) THP-1 control cells or SUN2g3c4 knockout cells.*

6.1.12. SUN2 shRNA-mediated knockdown in CRISPR/Cas9 *SUN1*-depleted THP-1 cells decreases HIV-1 infectivity

To examine a possible cooperation of SUN1 and SUN2 in the context of HIV-1 post-entry steps, double-knockout was employed at first using CRISPR/Cas9-mediated depletion. However, the depletion of both genes interrupted in cell survival for sufficient measurement, as reported in previous study [234]. Thus, CRISPR/Cas9 *SUN1*-depleted THP-1 cells were transduced with pSIREN RetroQ vectors expressing individual specific short hairpin RNAs *(see paragraphs 5.1.12. and 5.3.3.3. in Materials and Methods)* to silence SUN2 expression via RNA interference (RNAi). SUN2 knockdown was verified by immunoblotting (Fig. 42B) and resulted in 3 different cell bulks with 3 different shRNAs in which SUN2 protein levels were strongly reduced (Fig. 42B). *SUN1*-depleted THP-1 cells resulted in a 2- to 3-fold decrease in HIV-1 infection by knockdown of SUN2 (Fig. 42A), similar to the results of *SUN2*-depleted THP-1 cells. These findings suggest that SUN2 may work independently from SUN1.

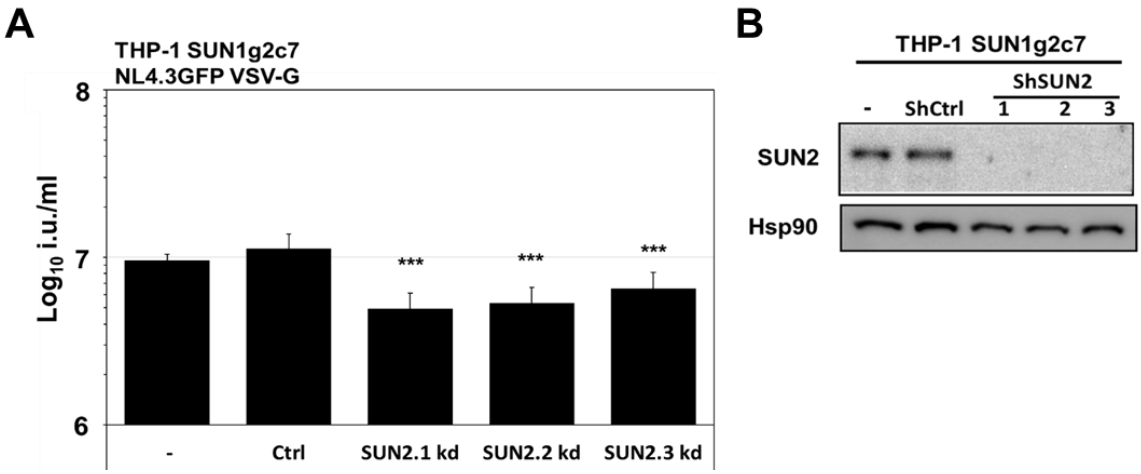

Figure 42. SUN2 shRNA-mediated knockdown decrases HIV-1 infection in CRISPR/Cas9 *SUN1*-depleted THP-1 cells. A) *shRNA-reduced SUN2* CRISPR/Cas9 *SUN1-depleted THP-1 cells were infected with VSV-G-pseudotyped NL4.3GFP or BREGFP reporter viruses for 24h before harvest, fixed in 4% paraformaldehyde (PFA) and analyzed by flow cytometry. Virus titrations were usually performed by threefold serial dilutions of the viral supernatant. Infectious titers (in infectious units [i.u.] per milliliter) were calculated from at least three virus doses and mean titers are shown. Error bars are standard deviations. Representative results from three independent experiments are shown.* **B)** *Corresponding WB for A). Same numbers of cells were lysed in the same volume of Laemmli buffer and subjected to immunoblotting analysis. HSP90 served as a loading control.*

6.1.13. SUN2 shRNA-mediated knockdown in U87MG CD4/CXCR4 cells decreases HIV-1 infectivity after 24h

To clarify the role of endogenous SUN1 and SUN2 proteins in other cell lines, SUN1 or SUN2 shRNA-mediated knockdown in U87MG CD4/CXCR4 cells was investigated. While SUN1 knockdown was too toxic for the U87MG CD4/CXCR4 cells to grow, SUN2 protein levels were efficiently reduced by two different shRNAs (Fig. 43B). These cell populations were infected with VSV-G-pseudotyped NL4.3GFP and resulted in a 5-fold decrease in HIV-1 infection after 24h, while it was recovered after 48h (Fig. 43A). Thus, it is suggested a delay in nuclear early infection steps, possibly leading to reduced integration events.

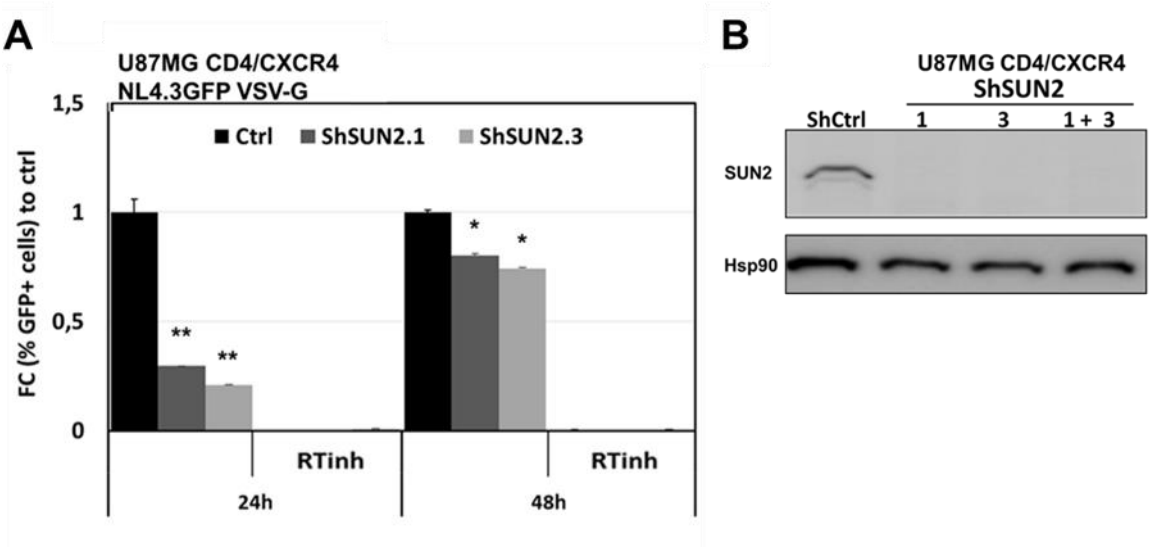

Figure 43. HIV-1 infection is impaired in shRNA-reduced SUN2 U87MG CD4/CXCR4 cells.
A) *shRNA-reduced SUN2 U87MG CD4/CXCR4 cells were infected with VSV-G-pseudotyped HIV-1 GFP LV, in the presence or absence of efavirenz (RTinh). Percentages of infected cells (% GFP+) were determined by flow cytometry 24h and 48h post infection. Fold changes to control cells in the absence of RTinh were calculated. Representative results from three independent experiments are shown.*
B) *Corresponding WB for A). Same numbers of cells were lysed in the same volume of Laemmli buffer and subjected to immunoblotting analysis. HSP90 served as a loading control.*

6.1.14. CRISPR/Cas9-mediated *SUN1* or *SUN2* gene disruption does not decreases HIV-1 infectivity in Jurkat TAg cells

Jurkats TAg cells were transduced with CRISPR/Cas9 LVs expressing individual specific gRNA against SUN1 or SUN2. Independent Jurkats TAg cells single-cell knockout clones for each gene were generated, with complete loss of SUN1 or SUN2 expression (SUN1g2c15, SUN1g2c16, SUN2g1c5, and SUN2g1c15) as well as various clones with intact SUN1 or SUN2 expression

(Fig. 44A). Knockout was verified by immunoblotting (Fig. 44B) as well as by sequencing over the gRNA target site in the cell genome.

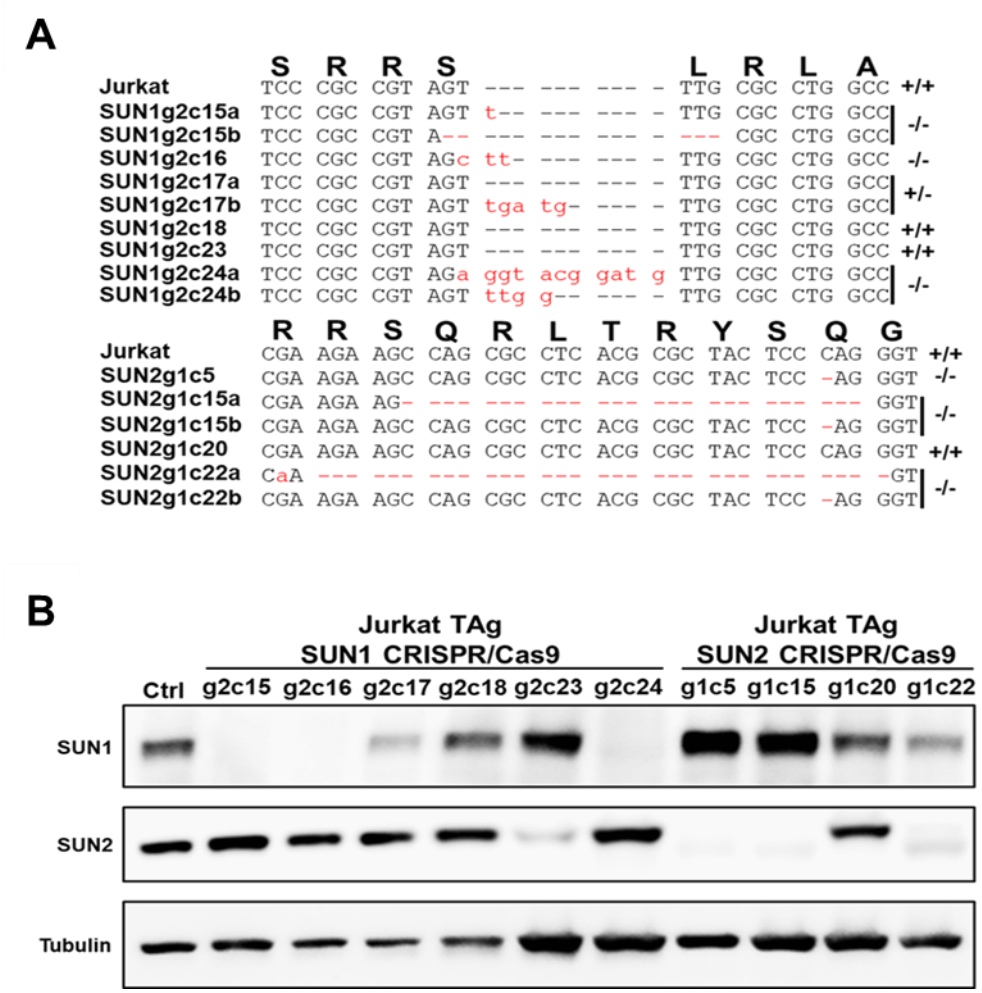

Figure 44. Jurkat Tag single-cell knockout clones for SUN1 or SUN2 genes. A) *Jurkat TAg CRISPR/Cas9 single-cell cloning followed by PCR-based sequencing across the guide RNA target sites identified two clones for each gene in which the open reading frame was disrupted*. **B)** *The SUN1 or SUN2 abrogated expression in the individual single-cell clones was verified by immunoblotting using SUN1- or SUN2-specific antibodies. Tubulin served as the loading control.*

All the clones were tested for their sensitivity to VSV-G pseudotyped NL4.3GFP or full-length non-pseudotyped CXCR4-tropic NL4.3GFP. SUN1 and SUN2 gene knockout did not have any effect on infection by either virus (Fig. 45), in comparison to a CRISPR/Cas9 control cell clone.

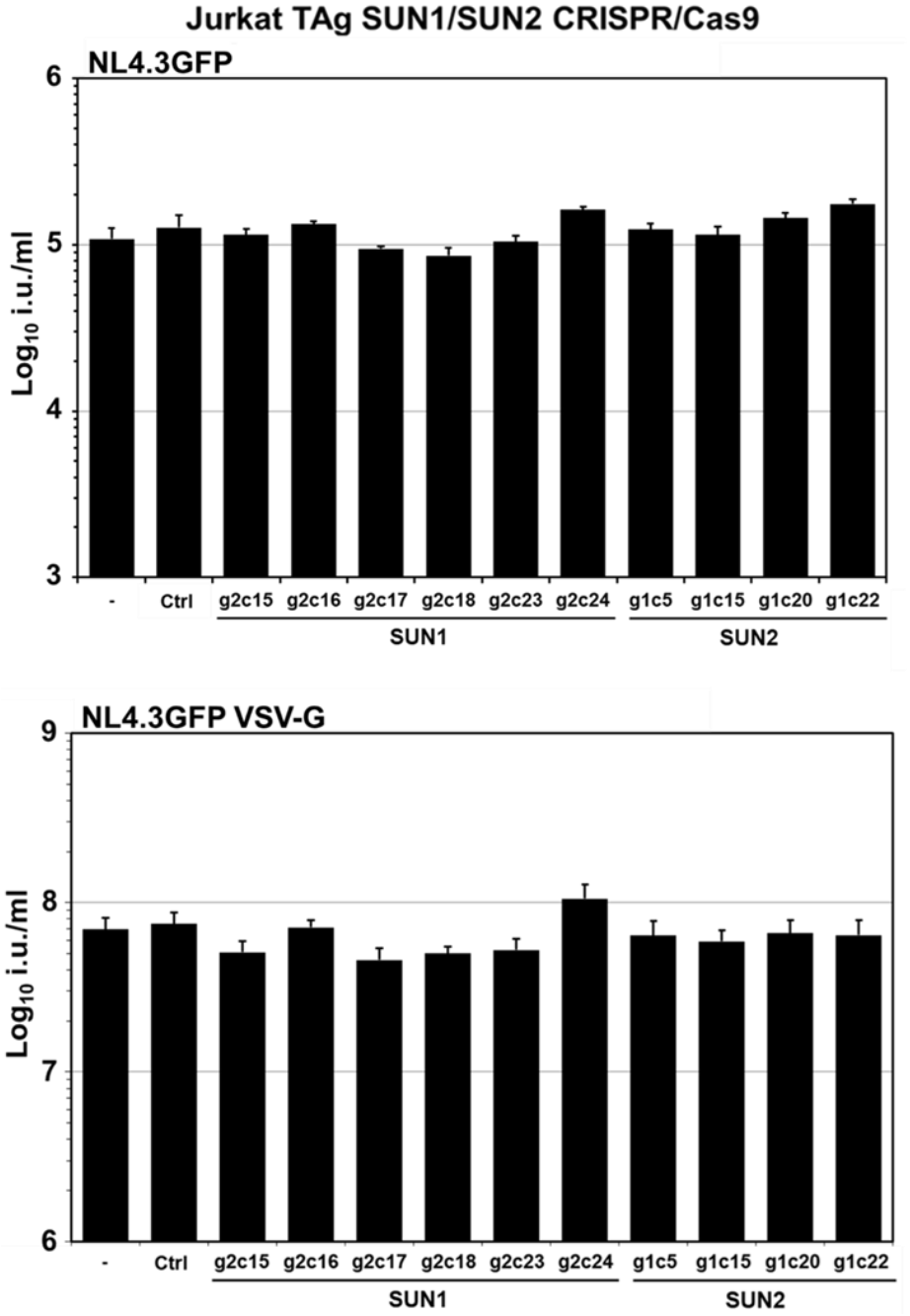

Figure 45. HIV-1 infection is not impaired in CRISPR/Cas9 *SUN1*- or *SUN2*-depleted Jurkat TAg cells. *Jurkat TAg Parental, CRISPR/Cas9 control, SUN1- or SUN2-depleted cells were infected with VSV-G-pseudotyped NL4.3GFP or full-length non-pseudotyped CXCR4-tropic NL4.3GFP for 24h before harvest, fixed in 4% paraformaldehyde (PFA) and analyzed by flow cytometry. Virus titrations were usually performed by threefold serial dilutions of the viral supernatant. Infectious titers (in infectious units [i.u.] per milliliter) were calculated from at least three virus doses and mean titers are shown. Error bars are standard deviations. Representative results from three independent experiments are shown.*

6.1.15. SUN1 and SUN2 are not required for the CypA Restriction in THP-1 cells and Jurkat TAg cells

Lahaye *et al* introduced HIVac-1 as a HIV-1 CA mutant restricted by CypA [173]. It was reported that SUN2 knockdown rescued HIVac-1 from CypA-restiction in bone-marrow derived dendritic cells from mice. Thus, HIVac-1 infectivity was analyzed to compare with HIV-1 wild type in THP-1 cells overexpressing CypA and lacking SUN1 or SUN2 expression. The infectious titer of HIVac-1 was reduced by 10-fold in comparison to HIV-1 wild type in all tested cell lines independently of SUN protein expression (Fig. 46A). HIV-1 wild type was blocked by CypA overexpression and no major differences were detected between control cells and SUN2 knockout cells. In contrast, HIVac-1 was not affected by CypA overexpression, possibly because endogenous CypA levels already substantially reduced the infectious titre. However, addition of cyclosporine A (CsA) increased both HIV-1 and HIVac-1 infectious titres up to wild type levels, independently of SUN protein expressions (Fig. 46A). Similary, SUN1 or SUN2 gene knockout in Jurkat TAg cell lines resulted in no changes for wild-type HIV-1 GFP LV, in the presence or absence of CsA (Fig. 47). The infectivity of HIVac-1 GFP LV was significantly reduced in Jurkat TAg control cells as well as in Jurkat TAg SUN1 or SUN2 knockout cell clones, and CsA treatment rescued infectivity in all cases to the level of wild-type LV (Fig. 47).

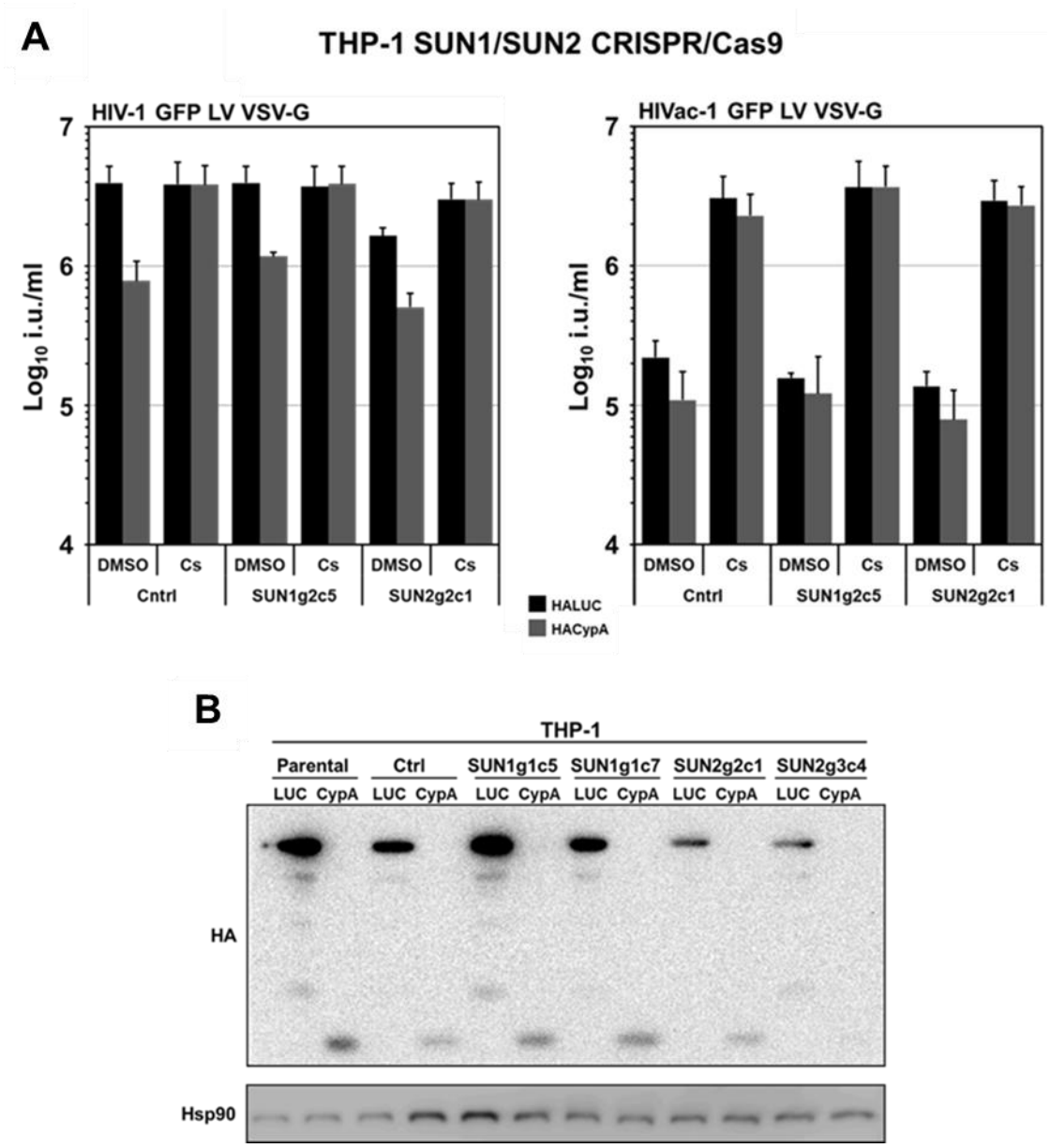

Figure 46. THP-1 CRISPR/Cas9 SUN1- or SUN2-depleted cells and the CypA restriction of HIVac capsids. A) *THP-1 CRISPR/Cas9 control as well as SUN1- or SUN2-depleted cells (SUN1g1c5, SUN2g2c1) overexpressing CypA were infected with VSV-G GFP-reporter wild type HIV-1 LV or with VSV-G pseudotyped GFP-reporter chimearic HIVac-1 LV for 48h before harvest, fixed in 4% paraformaldehyde (PFA) and analyzed by flow cytometry. Virus titrations were usually performed by threefold serial dilutions of the viral supernatant and titres were calculated from at least three virus doses. Mean titres are shown and error bars are standard deviations. Cyclosporine (Cs) was used at 5 µM and added at the time of infection. DMSO was used as vehicle control at the same concentration. Representative results from three independent experiments are shown.* **B)** *Corresponding WB for A). Same numbers of cells were lysed in the same volume of Laemmli buffer and subjected to immunoblotting analysis with antibodies targeting HA. Hsp90 served as the loading control.*

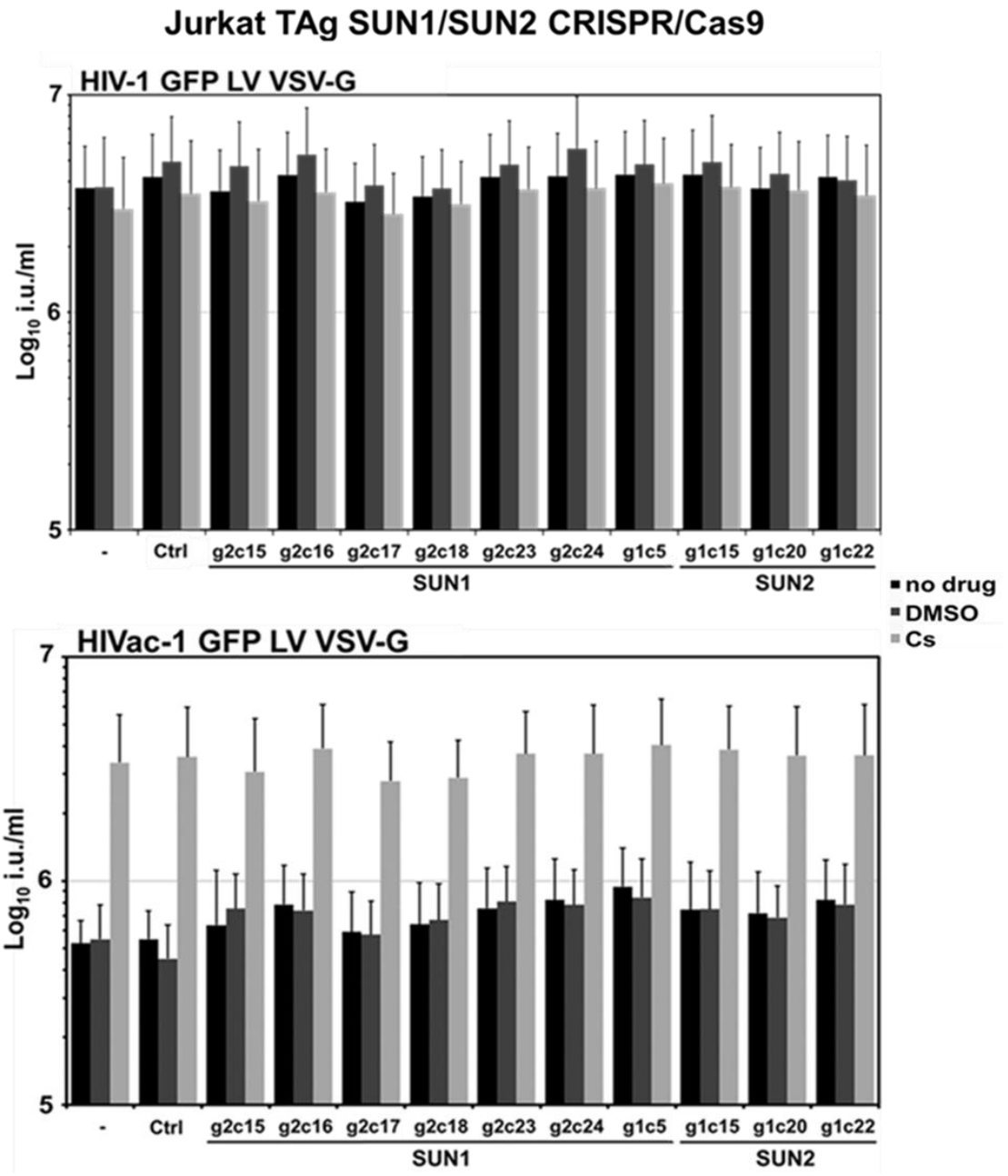

Figure 47. Jurkat TAg CRISPR/Cas9 SUN1- or SUN2-depleted cells and the CypA restriction of HIVac capsids. *Jurkat TAg CRISPR/Cas9 control as well as SUN1- or SUN2-depleted cells were infected with VSV-G GFP-reporter wild type HIV-1 LV or with VSV-G pseudotyped GFP-reporter chimearic HIVac-1 LV for 48h before harvest, fixed in 4% paraformaldehyde (PFA) and analyzed by flow cytometry. Virus titrations were usually performed by threefold serial dilutions of the viral supernatant and titres were calculated from at least three virus doses. Mean titres are shown and error bars are standard deviations. Cyclosporine (Cs) was used at 5 µM and added at the time of infection. DMSO was used as vehicle control at the same concentration. Representative results from three independent experiments are shown.*

6.2. The role of CA protein during IFN-α-induced suppression of HIV-1 infection

6.2.1. Determinants of the MX2 antiviral activity and the role of GTPase domain

To test the role of the G domain in anti-HIV-1 activity of MX2, mutations at key positions in the G domain located in the amino-terminal domain of MX2 were generated based on sequence homologies to MX1 by a collaborator, Mirjam Schilling (University of Freiburg) *(see paragraph 5.1.12. in Materials and Methods)*. There are six MX2 mutants generated as following: K131A, inhibiting GTP binding; T151A, inhibiting GTP hydrolysis; D297A inhibiting GTP binding, D300, binding but not hydrolyzing GTP; M574D, a known mutant that prevents MX2 from oligomerization [220]. The MX2 mutants, along with MX2 wild type and MX2 lacking first 25 amino acids of the amino-terminal region (MX2(ΔNLS)), were then overexpressed in U87MG CD4/CXCR4 cells and infected for 48h with a VSV-G pseudotyped GFP-encoding HIV-1 lentiviral vectors harboring the NL4.3 CA (pCMV-ΔR8.91Ex) or the RHPA CA (pCMV-ΔR8.91ExNRA) *(see paragraph 5.1.10 and 5.1.12 in Materials and Methods)*. U87MG CD4/CXCR4 cells expressing wildtype MX1 or GTPase defective MX1(K83A) were used as controls. As expected, none of the mutations reduced the capacity of MX2 wild type to restrict HIV-1 (Fig. 48A) except for MX2(ΔNLS) and the monomeric MX2(M574D), confirming that the amino-terminal 25 amino acids of MX2 are essential for the antiviral activity [226] as well as oligomerization [225], whereas both GTP binding and hydrolysis are not important for the anti-HIV-1 activity [204, 205]. Intriguingly, MX2 containing the T151A mutation, which render the protein deficient in GTP hydrolysis but not GTP binding, was anti-virally active against RHPA derived lentiviral vector (Fig. 48B), suggesting that it may assume an antiviral conformation capable to recognize RHPA and block the viral target.

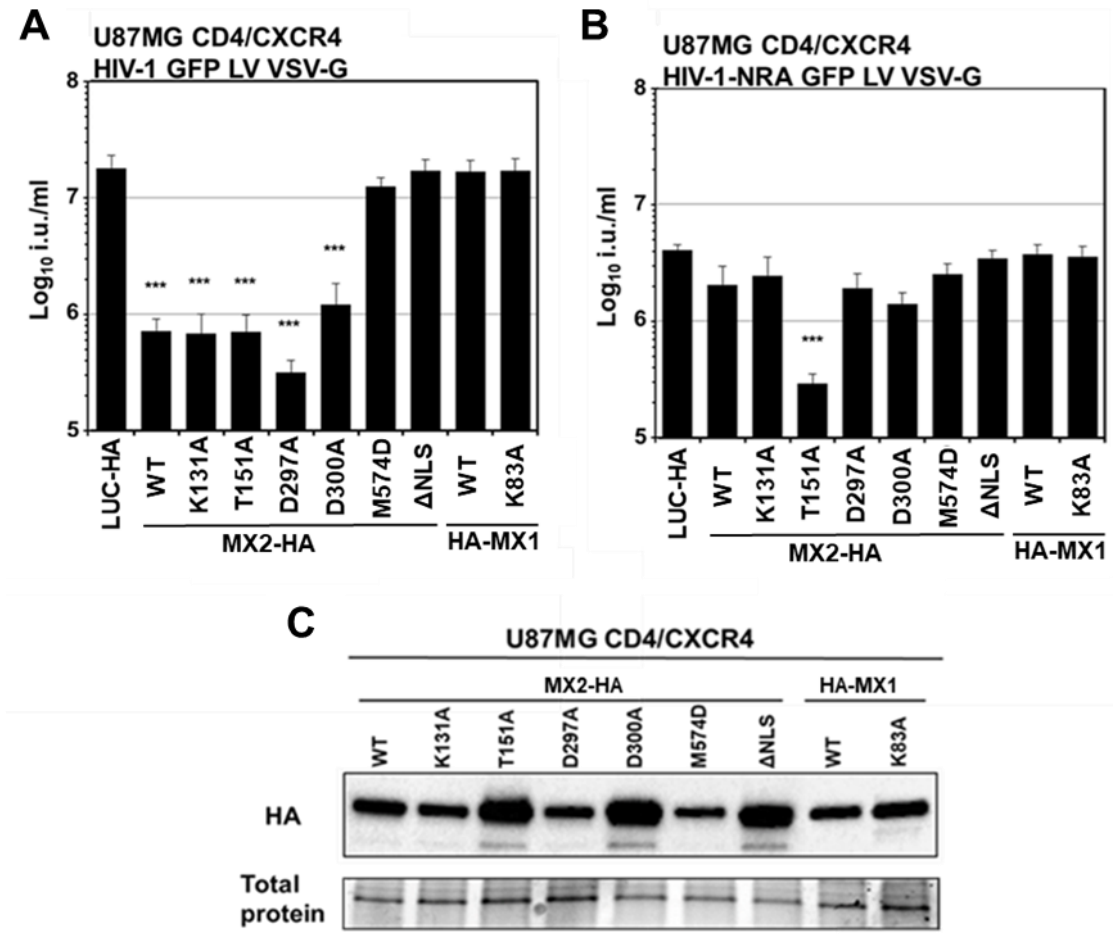

Figure 48. GTP binding and hydrolysis are not important for anti-HIV-1 activity of MX2.
A) *U87MG CD4/CXCR4 cells expressing LUC-HA, HAMX1 wt, HAMX1-K83A (negative controls), MX2-HA or different MX2 amino-terminal mutants were challenged with a VSV-G-pseudotyped HIV-1 GFP LV. At 48h post infection, the cells were harvest, fixed in 4% paraformaldehyde (PFA) and analyzed by flow cytometry. Virus titrations were usually performed by threefold serial dilutions of the viral supernatant. Infectious titres were calculated from at least three virus doses and mean titres are shown. Error bars are standard deviations. Representative results from three independent experiments are shown.* **B)** *Same as for panel A but with VSV-G-pseudotyped chimeric HIV-1-NRA GFP LV* **C)** *Corresponding WB for A) and B). Same numbers of cells were lysed in the same volume of Laemmli buffer and subjected to immunoblotting analysis. Loading was controlled by measuring total protein by UV activation of the gel.*

6.2.2. HIV-1 CA mutants N74D or P90A display enhanced sensitivity to IFN-α-induced blocks

Previous studies showed that the CA amino acids substitutions N74D and P90 reduced the sensitivity of HIV-1 to repression by ectopically expressed MX2 [204, 205, 211, 213]. Hence, it was speculated that these substitutions in the HIV-1 CA could reduce the sensitivity of these viruses to the type I IFN-induced post-entry-blockage. THP-1 cells were infected after treating with increasing doses of type I IFN (subtype IFN-α2A) with HIV-1 wild type or CA mutants N74D or P90A. Surprigingly, infectivities of the CA mutants in THP-1, MDMs and CD4+ cells were strongly reduced following IFN-α treatment, compared to the wild type virus, (Fig. 49A, B, C, D), suggesting an increased sensitivity to the IFN-α-induced post entry blockage.

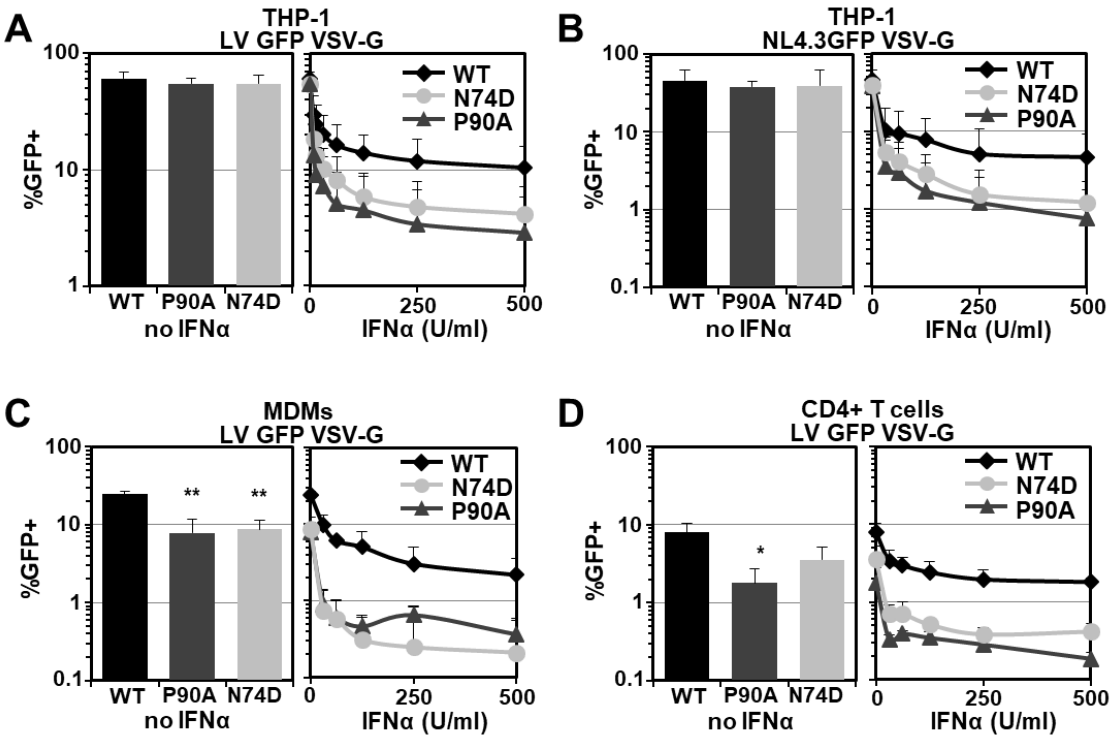

Figure 49. HIV-1 CA mutants N74D and P90A have increased sensitivity to IFN-α-induced suppression in diverse cell types. A) *THP-1 cells were pretreated with increasing doses of IFN-α and infected 24 h later with an equal amount of VSV-G-pseudotyped wild-type HIV-1 GFP lentiviral vector ΔR8.91 or CA mutant N74D or P90A. At 48h post infection, the cells were harvest, fixed in 4% paraformaldehyde (PFA) and percentage of GFP-positive cells (%GFP+ cells) was determined. Error bars indicate the standard deviations. Representative results from three independent experiments are shown.* **B)** *Same as for panel A but with NL4.3GFP-IRES-NEF (NL4.3GFP) viruses.* **C)** *Same as for panel A, but with MDMs from three independent donors.* **D)** *Same as for panel A, but with CD4+ T cells from three independent donors.*

6.2.3. The increased sensitivity of HIV-1 CA mutants to IFN-α induced blocks is independent of MX2

Subsequently, CRISPR/Cas9 MX2 THP-1 knockout cell lines were generated using two independent guide RNAs to examine the possible link with MX2 (MX2g1 and MX2g2; *see paragraph 5.1.12. and 5.3.3.2. in Materials and Methods*). The THP-1 bulk populations expressing either of the two guide RNAs showed a ~5 to 8-fold reduced inhibition to HIV-1 NL4.3GFP VSV-G infection after IFN-α treatment (Fig. 50A). On the other hand, THP-1 parental cells and control cells with minor susceptibility to HIV-1 infection resulted in similar expression levels of MX1 and MX2 upon IFN-α treatment (Fig. 50B). Of note, a MoMLV-derived-LV, which is unaffected by ectopic MX2 overexpression [142], was significantly inhibited by IFN-α in control cells and MX2 CRISPR/Cas9 cells (Fig. 50A). No detectable differences in the absence of IFN-α treatment were found, when comparing the infectivity of the HIV-1 NL4.3GFP VSV-G wild type with that of the CA mutants N74D, P90A, A105T in single cell clones in which MX2 expression was either ablated (MX2g2c4) or reduced (MX2g1c1) (Fig. 50B). The IFN-α signalling pathway remained intact in those clones, as measured by MX1 induction through immunoblot analyzes (Fig. 50B). As expected, the infectivity of wild-type virus in parental THP-1 cells decreased by 10-fold after IFN-α treatment, but only 3- to 5-fold in MX2g1c1 and MX2g2c4 cells (Fig. 50C). In contrast, the infectivity of the N74D mutant decreased by 43-fold in parental THP-1 cells and 20-fold in MX2g1c1 and MX2g2c4 cells (Fig. 50C). SImilary, HIV-1 P90A and A105T showed stronger inhibition by IFN-α treatment in parental THP-1, as well as MX2 CRISPR/Cas9 cells, compared to the wild type virus (Fig. 50C). These data demonstrate that the increased sensitivity of the HIV-1 CA mutants to IFN-α induced blockage was likely to be independent of IFN-induced MX2.

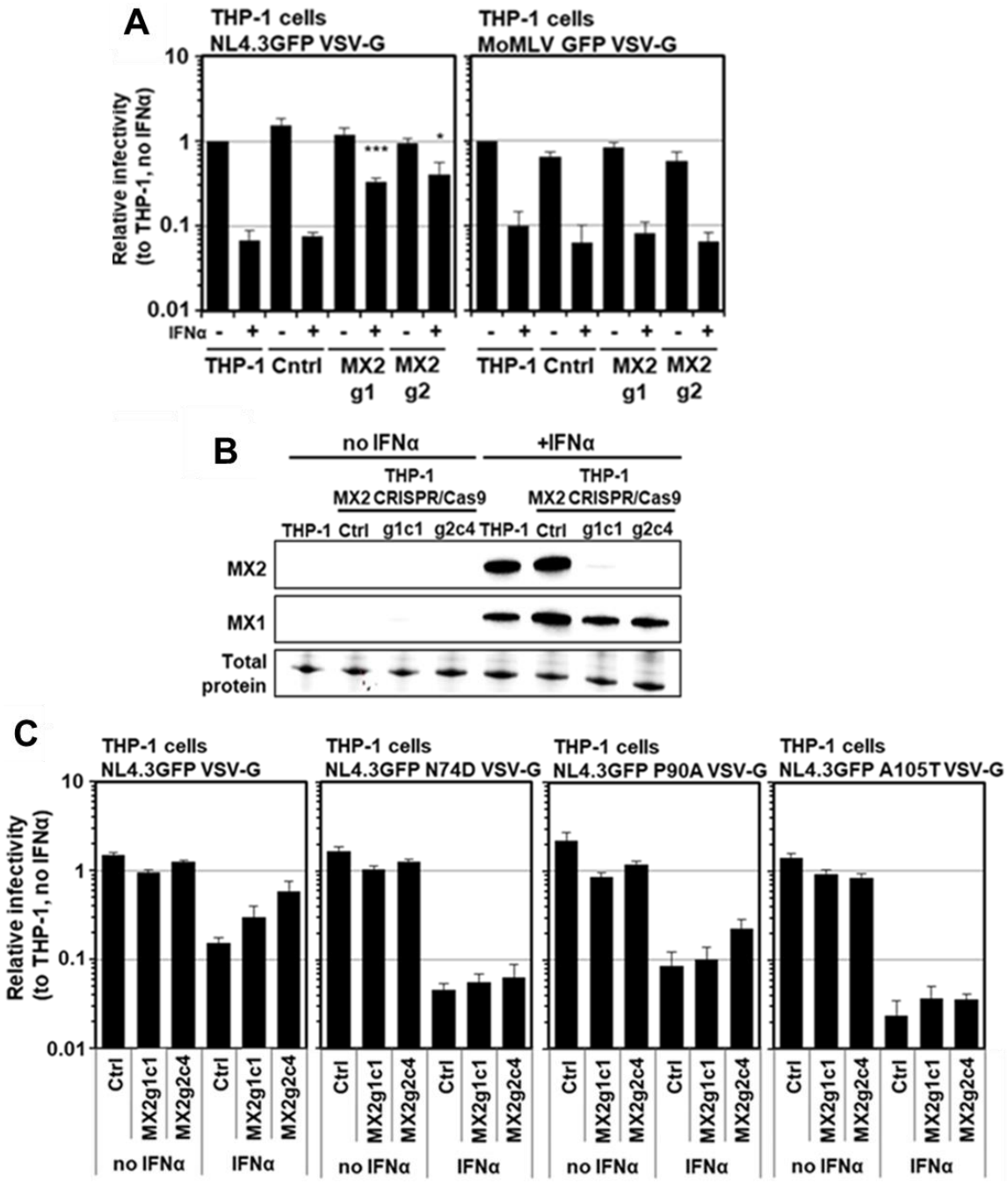

Figure 50. HIV-1 CA mutants are sensitized to MX2-independent IFN-α-induced blocks in THP-1 cells. A) *THP-1 cells were transduced with HIV-1 LVs encoding a control gRNA (Cntrl) or two independent gRNAs against MX2 (g1 and g2) and then puromycin selected for 2 weeks. Parental THP-1 cells or transduced CRISPR/Cas9 cell bulk populations were treated with 500 U/ml IFN-α and infected 24h later with a serial dilution of NL4.3GFP VSV-G reporter virus or Moloney murine leukemia virus GFP VSV-G vector. At 48h post infection, the cells were harvest, fixed in 4% paraformaldehyde (PFA) and percentage of GFP-positive cells (%GFP+ cells) was determined by flow cytometry. The relative infectivities were determined. Bars indicate the average infectious titers determined from at least three independent viral doses normalized to untreated THP-1 cells, and error bars indicate the standard deviations. Representative results from three independent experiments are shown.* **B)** *Wild-type THP-1 cells, a CRISPR/Cas9 control, and two independent MX2 knockout THP-1 single cell clones (g1c1 and g2c4) were treated with 500 U/ml IFN-α2 for 24 h. Immunoblots of untreated or IFN-α-treated cells using antibodies specific for MX1 and MX2 are shown. Loading was controlled by measuring total protein by UV activation of the gel.* ***C)*** *Wild-type THP-1 and the MX2 knockout cell clones (g1c1 and g2c4) were treated for 24 h with 500 U/ml IFN-α and then infected with a serial dilution of VSV-G-pseudotyped NL4.3GFP wild-type, CA N74D or CA P90A or CA A105T mutant viruses. The figure shows infection measured at 48 h as in panel A.*

6.2.4. IFN-α induces an enhanced block to reverse transcription and nuclear import of HIV-1 CA N74D

Parental THP-1 or MX2g2c4 cells were infected with VSV-G-pseudotyped NL4.3GFP wild type or N74D CA mutant to examine the stage of infection blockage in MX2-depleted cells. Total DNA was isolated at 4h and 24h post infection, and Quantitative Taqman PCR was performed to determine the copy numbers of GFP or 2-LTR circles as surrogates for early reverse transcription products and nuclear import, respectively. In parallel, the infectivities by flow cytometry were determined 24h after infection (Fig. 51A). In the IFN-α treated cells, 4h post infection the GFP reverse transcription products from HIV-1 wild-type virus decreased by 4-fold compared to untreated cells with no substantially difference between MX2g2c4 cells and parental THP-1 (Fig. 51B). In comparison, the levels of GFP reverse transcription products in HIV-1 CA N74D infection were reduced by 8-fold and no significant difference was shown between MX2g2c4 cells and parental THP-1 (Fig. 51B). In addition, there was a strong reduction in copy numbers of GFP reverse transcription products for both the wild type and the N74D mutant in IFN-treated cells upon 24h infection (Fig. 51C). After IFN-α pre-treatment and wild-type HIV-1 infection, 2-LTR circles at 24h post infection were reduced by 30-fold in parental THP-1 cells and only ~10-fold in MX2g2c4 cells, associated with MX2 role in blocking nuclear import. In HIV-1 CA N74D, the production of 2-LTR circles was blocked by 2-fold in parental and MX2g2c4 cells (Fig. 51D). Therefore, the increased sensitivity of the HIV-1 CA N74D mutant to IFN-α induced blockage (Fig. 51A) is likely to be explained by a stronger reduction in reverse transcription products as compared to wild type virus (Fig. 51B and C) and consequent reduced accumulation of 2-LTR circles, reflecting the suppression of nuclear import (Fig. 51D).

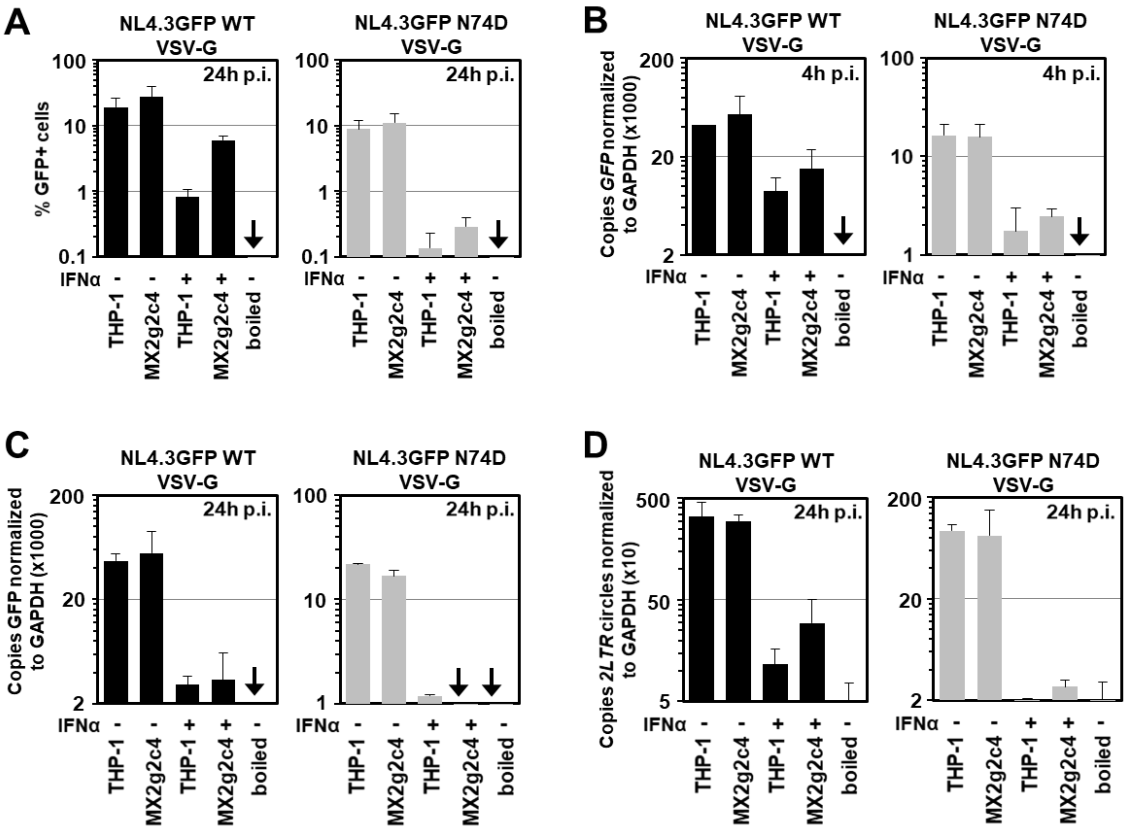

Figure 51. Hypersensitivity of the HIV-1 CA mutant N74D to IFN-α occurs at the stages of reverse transcription and nuclear import. *Parental THP-1 or MX2g2-4 CRISPR/Cas9 cells were treated with 500 U/ml IFN-α and infected 24h later with VSV-G-pseudotyped NL4.3GFP wild-type or N74D CA mutant virus.* **A)** *At 24 h post infection, the cells were harvest, fixed in 4% paraformaldehyde (PFA) and percentage of GFP-positive cells was determined by flow cytometry.* **B-D)** *Total DNA was extracted at the indicated time points. Early reverse transcription products for GFP or 2-LTR circles were measured by qPCR and normalized to total DNA input.*

7. Discussion and perspectives

7.1. The role of inner nuclear membrane proteins SUN1 and SUN2 in early HIV-1 infection steps

The role of different NE proteins during the early stage of HIV-1 infection was analyzed through the development of an overexpression screen with different human NE membrane-associated proteins (Fig. 11). This revealed that most of the NE proteins had minimal or no effect on HIV-1 infection, while both SUN1 and SUN2 were identified as having a significant impact on HIV-1 infection. Specifically, SUN2 overexpression decreased HIV-1 LV infection by 5-fold, while SUN1 resulted in a 20-fold decrease in infection (Fig. 11). The overexpression of both SUN1 and SUN2 were shown to reduce HIV-1 2-LTR circle formation (Fig. 14), a surrogate for nuclear import. However, the ectopically expressed SUN proteins maintained a predominantly perinuclear staining pattern, with a further cytosolic localization not present in the case of the endogenous proteins (Fig. 12) and did not induce alterations in nucleus morphology as previously noted by Donahue et. al.[293]. SUN1 and SUN2 are integral type II transmembrane proteins that are widely expressed and predominantly localised to the INM, where the nucleoplasmic amino-terminal domain interacts with proteins in the nuclear lamina, such as LMNA [301, 302] and EMD [303], whereas the PNS carboxy-terminal SUN domain interacts with the Klarsicht-ANC1-Syne-homology (KASH) domain of Nesp proteins [301, 302, 304-309]. Together with Nesp proteins, SUN proteins represent the core elements of linker of nucleoskeleton and cytoskeleton (LINC) complexes, which span both nuclear membranes and physically connect proteins constituting the cytoskeleton (e.g., actin, microtubules, and intermediate filaments) with proteins of the nuclear skeleton (e.g., nuclear lamins) (Fig. 52). SUN proteins function as transluminal tethers for Nesp proteins in the ONM and seem to have an important role in maintaining the regular space between INM and ONM [229]. SUN1 and SUN2 are also important for various cellular processes, including telomere attachment to the NE during meiosis and for postmitotic cells [310-314], DNA damage response (DDR), removal of membranes from chromatin during mitosis [234], positioning of the nucleus, cell migration and polarization [304, 315-319]. *SUN1* and *SUN2* gene dysfunction has been connected with

cardiomyopathies and skeletal myopathies [303, 320] and has been detected in certain cancer tissues, suggesting possible tumor suppressor activity [321, 322]. SUN1 and SUN2 proteins may also have individual roles, in addition to the many redundant cellular functions: for example, SUN2 has been described as a protein involved in the trafficking of endosomes by its binding to Rab5 [323], while for SUN1 no such role has been described so far.

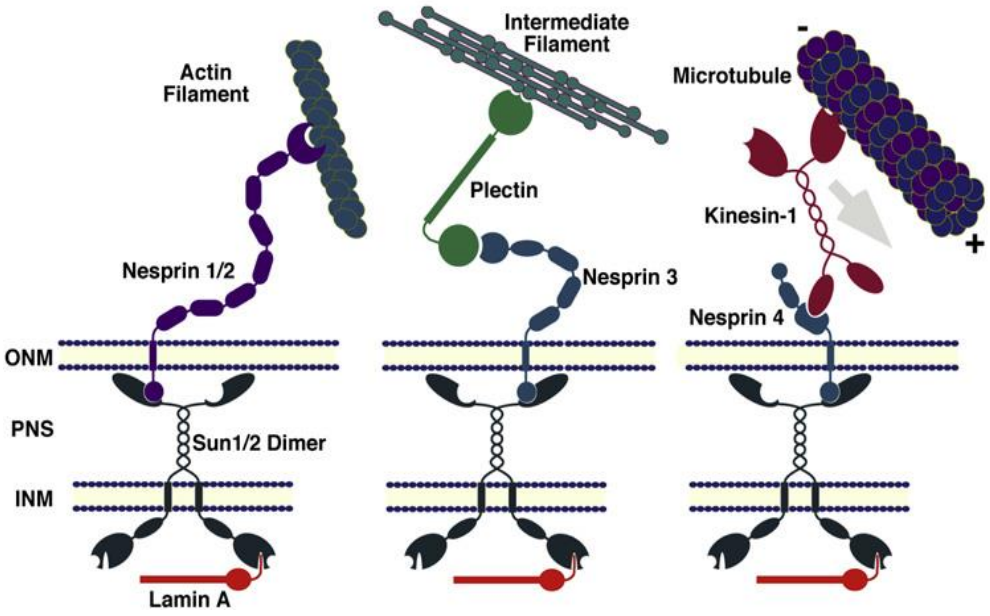

Figure 52. The LINC complex connects nuclear structures to the cytoskeleton. *INM SUN-domain proteins can assemble homodimers or heterodimers and function as transluminal tethers for ONM KASH-domain proteins. The nucleoplasmic domain of SUN proteins binds to lamins and/or other nuclear components. Cytoplasmic KASH domains of nesprins interact with cytoskeletal elements, including actin, plectin, and kinesin.* Figure adapted from [229]

Previous studies reported that both SUN1 and SUN2 interact also with the INM protein Emerin [302], which has been suggested as a cofactor for HIV integration [242]. However, later studies did not validate this and the incapacity of a LEM domain-deleted EMD to affect HIV-1 infection (Fig. 11) can be considered coherent with the latest reports [243, 244]. SUN2 was proposed to be a type I interferon (IFN)-induced gene able to weakly inhibit HIV-1 infection [206]. Other recent studies have also reported a possible role of SUN2 in early infection steps [173, 293, 294], however they did not confirm changes in SUN2 protein levels in type I IFN-treated cells [173, 293]. Here it was shown that overexpression of SUN1 or SUN2 reduces HIV-$1_{NL4.3}$ as well as HIV-2_{ROD} infection but not the other retroviruses that were tested (Fig. 15), suggesting

that the block exerted by the ectopically expressed SUN1 and SUN2 is specific for these two laboratory-adapted lentiviruses and does not involve any unspecific block to nuclear import. Is still unknown why SIV_{MAC} and the other non-primate retroviruses are insensitive to the overexpressed SUN1 and SUN2 human proteins, but one hypothesis might be that these viruses are only able to interact specifically with the SUN proteins of their natural hosts. It has been shown that the amino-terminal of SUN1 might have undergone positive selection processes during evolution, which could refer to historical occurrences of specific species [289]. The establishment of virus infection in a naïve host most often results from the transmission and subsequent propagation of a single virus strain, termed a transmitted/founder (T/F) virus. The extremely diverse HIV-1 population in the blood of infected donors, suggests that during HIV transmission there are one or more strong obstacles that reduce viral infectivity, resulting in the transmission of a single T/F virus. Exploring viral phenotypes that associate with transmission and determinate whether these obstacles are stochastic and restrict all viruses or whether there are selective pressures favouring certain phenotypes in the T/F virus, may therefore clarify the biology of HIV-1 transmission and tell novel prevention approaches. SUN proteins might have exerterted a strong inhibitory pressure on HIV-1 infection *in vivo*, leading to the occurace of SUN-resistant HIV-1 strains. To address this question, the infection by T/F viruses RHPA, SUMA, WITO, THRO, and ZM247 along with that of lab strain viruses IIIB and NL4.3 was tested in this stydy. RHPA, SUMA, THRO and WITO were identified in subjects with early/acute subtype B HIV-1 infection, whereas ZM247 in subjects with early/acute subtype C HIV-1 infection [288, 324]. In the case of SUN1 many T/F viruses were found to be sensitive to some degree except for strains RHPA and ZM247 (Fig. 17A), suggesting that only certain HIV-1 strains (and possibly HIV-2 strains) appear to be sensitive to SUN1 or SUN2 overexpression. A similar antiviral profile was observed for SUN2, despite it being more widely distributed (Fig. 17B). Previous works have shown that some of these T/F viruses, including RHPA and ZM247, are also hyposensitive to overexpressed MX2 [212], suggesting that these viruses may be able to bypass several factors associated with the NE. Infection data obtained with GFP-reporter chimeric viruses between the SUN1-sensitive NL4.3 and the insensitive T/F RHPA (Fig. 19A, Fig. 19B), suggest that HIV-1

CA is likely the viral determinant that is defining the sensitivity to SUN1 or SUN2-mediated restriction after overexpression. Furthermore, the HIV-1 containing the CA from SIV_{MAC} was largely insensitive to SUN1 (Fig. 20) further indicating the CA role in determining sensitivity to SUN-mediated inhibition. Donahue et al. [293] showed that the HIV-1 CA mutant (P207S) was able to overcome the block induced by SUN2 overexpression, but this residue is conserved between NL4.3 and RHPA and for this reason it cannot explain the insensitivity of RHPA in the data presented here. Therefore, to further investigate the insensitivity of RHPA, differences between the insensitive RHPA and sensitive NL4.3 CA sequences were analyzed by using HIV-1 chimeric viruses between NL4.3 and RHPA and it was found that specific residues in HIV-1 CA are likely the viral determinants defining the sensitivity to SUN1 or SUN2-mediated restriction after overexpression, since a combination of the amino acid substitutions H87R,H120N, G208A in NL4.3 made the virus largely insensitive to SUN1 (Fig. 23).

In addition, $HIV\text{-}2_{ROD}$ was also sensitive to both SUN1- and SUN2-induced inhibition of infection (Fig. 15) and its amino acid sequences shares only 69% identity with that of NL4.3 or IIIB. The H87, N120 and G208 amino acid residues in HIV-1 capsid, correspond to P86, R118 and N207 in $HIV\text{-}2_{ROD}$ capsid. However, these residues are also conserved in SIV_{MAC}, which is insensitive to the SUN1- or SUN2-mediated block (Fig. 15); therefore, further analysis is needed to determine whether these residues are critical for the sensitivity of HIV-2 to SUN1- or SUN2-induced inhibition. The RHPA Q87 amino acid residue is located in the CypA binding loop of the CA [108] and it has been shown that the NL4-3 H87Q CA mutant was refractory to MX2 inhibition [325], suggesting a function of CypA in MX2 antiviral response and that some HIV-1 strains have evolved to escape MX2 inhibition at the expense of losing viral capsid binding to CypA. Therefore, CypA may play similar role also in SUN1- or SUN2-mediated restricon of HIV-1 infection, whereas HIV-2 does not require host CypA for efficient replication in human cells [109, 112, 326] and particularly HIV-2 CA binds CypA with a much lower affinity than HIV-1 CA [141, 327], suggesting that this connection needs to be investigated in further studies.

Since HIV-1 sensitivity to SUN1 or SUN2-mediated suppression is determined by amino acid residues in CA, the ability of SUN proteins to physically interact with the HIV-1 capsid was tested in collaboration with Malim lab (King's College London). Specifically, the binding of different SUN1 or SUN2 mutants to *in vitro* synthesized HIV-1 CANC complexes (capsid- nucleocapsid complexes) was investigated. SUN1 as well as SUN2 were able to interact with CANC complexes derived from the susceptible virus strain IIIB (Fig. 24A). However, they also interacted with RHPA CANC complexes (Fig. 24B), suggesting that the insensitivity of RHPA to SUN1 or SUN2 may not be caused by a defect in binding. RHPA and other insensitive viruses may overcome SUN1 or SUN2-induced restriction because the physical interaction is absent due to choice of a different trafficking pathway towards the nucleus. Likewise, it is possible that the interaction is necessary but not sufficient for mediating a block to infection. Comparably, the insensitivity of certain capsid mutants to MX2 restriction could also not be correlated to defects in MX2 binding *in vitro* [215]. SUN1 or SUN2 induced restriction resembled characteristics, reminiscent of the restriction induced by the type I IFN-induced restriction factor MX2, i.e. inhibition of 2LTR circle formation and negative antiviral effect against T/F such as RHPA [204, 205, 212]. Additionally, SUN1 and SUN2 largely localized to the nuclear envelope, like MX2 [328]. For this reason, this connection is attractive and needs to be investigated in further studies by functional assays of MX2 restriction in SUN1 or SUN2 depleted cells as well as testing SUN1 or SUN2-mediated block in MX2 knockout cells. Similar approaches for known or newly identified SUN1 and SUN2 interactors needs to be the subject of further studies.

The domains of SUN1 and SUN2 that are involved in HIV-1 infection suppression were analyzed and it was verified that the removal of the carboxy-terminal region of the proteins had no impact on the block (Fig. 26, Fig. 34), suggesting that SUN interaction with nesprin proteins in the perinuclear space and LINC complex formation may not be required for the antiviral activity [301]. In contrast, by deleting 90 amino acids from the SUN1 amino-terminal and 157 amino acids from SUN2 amino-terminal it completely abrogated the suppression of HIV-1 infection (Fig. 26, Fig. 34). Particularly, amino acids residues 85-90 were shown to be relevant in the SUN1-mediated blocking on infection (Fig. 29). In addition, the SUN1 amino-terminal also showed a potent antiviral activity

when artificially fused to $Fv1^N$ (Fig. 31) and the SUN2 amino-terminal could replace the antiviral activity of the SUN1 amino-terminal (Fig. 37). The chimeric $HASUN1^{NTD}$-$Fv1^N$ showed a strong cytoplasmic localization (Fig. 32), suggesting that the interaction of the SUN1 amino-terminal domain with incoming HIV-1 CA can occur in the cytoplasm. Previous studies suggested that SUN1 interacts with NPC [329] through Nup153 [330], which has shown to be important for the nuclear import of HIV-1 and HIV-2 [144, 163]. Nup153 depletion leads to changes in the localization of SUN1 [331] and POM121 [332], a protein associated with Nup153 and important for its stability. According to these data, overexpression of SUN1 and its subsequent cytoplasmic accumulation may inhibit HIV-1 infection by perturbing the required interaction between incoming HIV-1 capsids and NPC. However, it is unlikely that SUN1 overexpression affects Nup153 activity, since SIVmac is insensitive to SUN1 or SUN2-induced restriction (Fig. 15) but is similarly sensitive to RNA interference-mediated Nup153 depletion as are HIV-2 and HIV-1 [144]. Further analysis is necessary to gain more insights into possible effects of Nup153 and POM121 in SUN1 overexpression, possibly by RNA interference-mediated depletion of these proteins in SUN overexpressing cells.

The role of the endogenous proteins SUN1 and SUN2 in HIV infection in the myeloid cell line THP-1 and in the T cell line Jurkat TAg was analyzed, and single-cell clones with SUN1 and SUN2 knocked out were generated from both the cell lines. In THP-1 cells, SUN2 depletion resulted in a moderate but reproducible reduction in HIV-1 infection (Fig. 39), and is in agreement with published data in which SUN2 levels were reduced by shRNA [173], while SUN1 absence did not show any detectable effect on infection by GFP-reporter viruses or GFP-encoding lentiviral vectors (Fig. 39). Furthermore, the lack of SUN2 reduced the amount of 2-LTR circles (Fig. 41), suggesting a defect in virus nuclear import, and did not affect MoMLV (Fig. 40B) and other retroviral strains (Fig. 40C), indicating that the absence of SUN2 does not involve any unspecific block to nuclear import and may affect specifically HIV-1 infection. In Jurkat TAg cells, SUN1 or SUN2 absence did not have any detectable repercussions on infection (Fig. 45), suggesting possible differences in SUN expression levels between the cell types tested. The same infection pattern was observed with the chimeric virus BRE, which incorporates the T/F RHPA capsid

and shows a reduced sensitivity to overexpressed SUN1 and SUN2. However, since interactions between RHPA CANC complexes and SUN2 were detected *in vitro*, it indicates that the RHPA capsid may still be able to interact with SUN2, regardless of its lack of sensitivity to ectopically expressed SUN2.

Lahaye *et al* introduced HIVac-1 as a HIV-1 CA mutant restricted by CypA and reported that SUN2 knockdown rescued HIVac-1 from CypA-restiction in bone-marrow derived dendritic cells from mice. Furthermore, they showed that combination of SUN2 depletion with CypA inhibition did not lead to a further decrease of HIV-1 infectivity in primary CD4+ T cells, suggesting that SUN2 SUN2 promotes the positive effects of CypA on HIV-1 replication in CD4+ T cells [173]. These results were here challenged and HIVac-1 infectivity was analyzed to compare with HIV-1 wild type in THP-1 cells lacking SUN1 or SUN2 expression and in the presence or absence of CsA. The infectious titer of HIVac-1 was reduced by 10-fold in comparison to HIV-1 wild type in all tested cell lines independently of SUN protein expression (Fig. 46A). Furthermore, addition of cyclosporine A (CsA) increased HIVac-1 infectious titres up to wild type levels, independently of SUN protein expressions (Fig. 46, Fig. 47). A recent study confirmed these results even in primary CD4+ T cells, in which the researchers did not find any connection between SUN2 and CypA [294]. Despite the possible differences between mice and human cells or the different cell types tested, SUN1 or SUN2 gene disruption in the studied cell lines seems to have no impact on the CypA-mediated events during early HIV-1 post-entry steps.

These data support the idea that SUN2 may help promote the early stages of HIV-1 infection, but that the contributions of SUN1 are less clear. ShRNA-mediated SUN2 reduction in SUN1 CRISPR/Cas9 showed a reduction in HIV-1 infectivity comparable to that seen in THP-1 SUN2 knockout cells (Fig. 42), further indicating an independent role for SUN2 in promoting the early stages of HIV-1 infection. However, the CRISPR/Cas9-mediated depletion of both genes interrupted in cell survival for sufficient measurement, as reported in previous study [234]. Thus, further analysis needs to be performed to investigate the possible functional redundancy between SUN1 and SUN2, possibly by applying

a different CRISPR/Cas9 strategy, i.e. by creating SUN2 knockout cell clones in which the SUN1 amino-terminal is also deleted.

This work therefore adressed the question why NL4.3 infection is reduced by either SUN2 overexpression or endogenous gene knockout. This apparent contradiction could be accounted for when one compares the distribution of overexpressed SUN proteins to that of endogenous SUN proteins. Overexpressed SUN proteins are found in the NE and the cytosol, while endogenous SUN proteins are absent from the cytosol. Similar observations have previously been seen for CPSF6, where the mislocalized truncated protein was a strong inhibitor of HIV-1 infection when overexpressed, even while knockdown of the endogenous protein had no effect in most cell types and despite its well-documented role in promoting nuclear entry and integration into actively transcribing genes [163, 164, 169, 173, 179, 180]. Similarly, overexpressed SUN proteins may mislocalize to the cytosol where they interact with incoming HIV-1 (CA-containing) replication complexes and obscure important binding sites for other factors required for HIV infection. This would indicate that endogenous SUN may be relevant, as suggested by the effect of the SUN2 knockout in THP-1 cells, but potentially not by the mechanisms seen upon overexpression. This may also describe the discrepancy that the BRE virus is resistant to overexpression, but still affected by SUN2 knockout. Mapping of the CA-SUN interface would be a consistent aspect to follow.

Previous studies showed that *NUP98* and *NUP153* depletion reduces HIV-1 integration preferences and that the depletion of endogenous expression of another CA binder like CPF6, using CRISPR/Cas technology, changed the integration profile of HIV-1 despite there were not relevant change in infection [180, 185, 186, 243]. In collaboration with the Debyser lab (KU Leuven, Belgium), the integration site selection for HIV-1 in THP-1 cell lines with knocked-out SUN1 or SUN2 is currently being investigated. This will hopefully identify a possible role of the SUN proteins in dictating HIV-1 integration site selection.

7.2. The role of CA protein during IFN-α-induced suppression of HIV-1 infection

Whether the susceptibility of the viral determinants targeted by IFN-α-induced blocks could be sensitive to changes in the HIV-1 CA protein was also investigated in the present study. By analysing the infectivities of previously described HIV-1 CA mutants (N74D, A105T, as well as P90A) that are able to escape the inhibition of ectopically expressed IFN-α-induced MX2 [204, 205, 211]. This analysis suggested that the CypA binding to the HIV-1 capsid [211] as well as CPSF6 binding [204, 205], are also involved in the MX2 antiviral mechanism. Despite their relative resistance to ectopically expressed MX2, the infectivities of HIV-1 CA mutants N74D, A105T, as well as P90A were more reduced after IFN-α treatment of THP-1 cells, MDMs, or CD4+ T-cells as compared to wild type virus (Fig. 49), indicating an increased sensitivity to the IFN-α-induced post entry block. This suggests that the HIV capsid may not solely protect viral nucleic acids from being detected by cytoplasmic DNA sensors such as cGAS [102], but also that the defect of these CA mutants to replicate in MDMs can at least in part be explained by an increased sensitivity to type I IFN-induced effectors.

Furthermore, the knockout data indicate that the HIV-1 CA mutants increased sensitivity does not depend on MX2 (Fig. 50) and takes place during reverse transcription (Fig. 51), suggesting that the interactions between IFN-α-induced antiviral effectors and CA are enhanced by that alterations in CA, possibly as a consequence of slower capsid uncoating [333], leading to disadvantageous exposition of reverse transcription complexes to such effectors. These results confirm that IFN-α induces at least two blocks: the first one, sensitive to changes in CA, at the level of reverse transcription and the second one at the level of nuclear import and involving MX2 [204, 205, 211]. The determinant for MX2 antiviral effect maps to the first 25 amino acids in the amino-terminal region of MX2, in which a triple-arginine motif is required for interaction with the HIV-1 CA and consequent restriction [223] [226].

MX2 is expressed in two isoforms in IFN-treated cells: full-length MX2(1-715) and MX2(26-715), which lacks the first 25 amino-terminal amino acids that function as a nuclear localization signal (NLS) and is essential for the anti-HIV-1

activity [226]. Analysis of MX2 mutants in the N-terminal extension and the G domain reveal that none of the mutations reduced the capacity of full length MX2 to restrict HIV-1 (Fig. 48A), except the truncated MX2(26-715) and MX2(M574D), a mutant that prevents MX2 oligomerization resulting in a monomeric MX2 protein inactive against HIV-1. These data confirm that the antiviral activity of MX2 against HIV-1 is independent of its GTPase domain [204, 205] and requires higher order structures and oligomerization [225]. Intriguingly, all the MX2 mutants, with the exception of G domain mutant MX2(T151A), were inactive against a HIV-1 lentiviral vector harboring the T/F RHPA CA (Fig. 48B), confirming the RHPA resistance phenotype to MX2 inhibition, which was previously mapped to the amino acid positions 87 and 208 in CA [325]. Particularly, the H87Q mutation is located in the CypA binding loop of the CA [108] and it has been shown to render HIV-$1_{NL4.3}$ refractory to MX2 inhibition [325], suggesting a function of CypA in MX2-mediated block and that likely some HIV-1 strains have evolved to escape MX2 inhibition at the expense of losing viral capsid binding to CypA. Attractive is the RHPA sensitivity to the mutant MX2(T151A), which contain a mutation that render the protein deficient in GTP hydrolysis but not in GTP binding, indicating that this mutation renders MX2 active against RHPA, likely by exhibiting an antiviral conformation capable to recognize and block the viral target. Several single amino acid substitutions in CA have been identified that confer resistance to MX2 [204, 205, 211-213] and many of them, such as G89V, N57A/S, A92E as well as N74D, A105T and P90A are also known to affect binding to cellular proteins implicated in HIV-1 nuclear import including CypA, CPSF6, Nup153, and NUP358 [106, 107, 141, 144, 163, 334]. Interactions with cellular factors that help to protect HIV-1 from IFN-α-induced antiviral effectors, as well as the capsid stability and uncoating of incoming viral capsids, are thus affected by these particular mutations, one consequence of which is the greater sensitivity of relevant mutant viruses to IFN-α-induced infectivity blocks. Enhanced interactions between IFN-α-induced antiviral effectors and CA alter the infection non-dividing cells and likely may modulate certain HIVs nuclear entry and possibly target site selection.

Further investigations, not associated with this thesis, showed that disruption of CypA by CRISPR/Cas9 modestly increased the sensitivity of HIV-1 to IFN-α-induced blocks [214], indicating that CypA interactions with incoming capsids

may help to protect HIV-1 from IFN-α-induced antiviral effectors in THP-1. In contrast, genetic disruption of CPSF6 did not increase the sensitivity of wild type or CA mutant HIV-1 to IFN-α-induced effectors in THP-1 cells [214], arguing that CPSF6 does not play a role in protecting infection from IFN-α-induced blocks [163, 169].

8. Conclusion

SUN1 and SUN2 proteins have been identified in the present study as two NE membrane-associated components able to affect HIV-1 infection. The data obtained after knockout of these proteins support the idea that endogenous SUN2 may be relevant during the early stages of HIV-1 infection, but potentially not by the mechanisms seen upon overexpression. The contributions of SUN1 are less clear, as the gene disruption of SUN1 did not yield a different infection phenotype in THP-1, yet overexpression resulted in a potent suppression of infection. SUN1 and SUN2 are proteins required for diverse cellular processes and their role during HIV infection could be involve mediating telomere attachment to the NE and the positioning of the nucleus during cell division, as well as DNA damage response (DDR) and the removal of membranes from chromatin during mitosis. Since the endogenous SUN1 and SUN2 proteins localize to the INM with their amino termini facing the nucleoplasm, one hypothesis suggest that the interaction between SUN1 and SUN2 with the nuclear CA-containing nucleoprotein complexes [139, 140, 335] may contribute to nuclear import and/or possibly dictate the site of HIV-1 integration in the host cell genome. However, this need to be further investigated and further studies are ongoing with the Debyser lab (KU Leuven, Belgium). The CA protein has been showed to be important for HIV-1 nuclear import [138, 141, 163, 336], and this work demonstrated that the amino-terminal domains of SUN1 and SUN2 may interact with HIV-1 in a CA-specific way. Additionally it has also shown that CA protein and the capsid core may protect incoming HIV-1 nucleic acids from detection by innate pattern recognition receptors [102, 103], as well as IFN-α-induced effectors, thereby providing dual protection against host defense mechanism.

Overall, in this project, SUN proteins emerge as critical regulators of HIV infection, both upon over-expression and at the endogenous level and enhance

our understanding of the early post-entry events occurring during HIV-1 infection. Further mechanistic details may advance the insights of the interplay between HIV and host, and reveal a novel target for theraupetic interventation.

9. Abbreviations

A	Alanine
AIDS	Acquired immunodeficiency syndrome
ALIX	Interacting protein X
APC	Antigen-presenting cell
APOBEC	Apolipoprotein B mRNA-editing catalytic polypeptide-like
ART	Antiretroviral therapy
CA	Capsid protein
CCR5	C-C chemokine receptor type 5
cDNA	Complementary DNA
CD	Cluster of differentiation
cGAS	Cyclic GMP-AMP synthase
CPSF6	Cleavage and polyadenylation specificity factor subunit 6
Cryo-EM	Electron cryomicroscopy
CsA	Cyclosporine A
CTD	Carboxy terminal domain
CTL	Cytotoxic T lymphocytes
CypA	Cyclophilin A
CXCR	C-X-C chemokine receptor
DC	Dendritic cell
DDR	DNA damage response
DMEM	Dulbecco's modified eagle's medium
DNA	Deoxyribonucleic acid
dNTP	Deoxynucleotide
EDMD	Emery-Dreifuss muscular dystrophy
EDTA	Ethylenediaminetetraacetic acid
EIAV	Equine infectious anaemia virus
EMD	Emerin
Env	Envelope

FACS	Fluorescence activated cell sorting
FCS	Fetal calf serum
FG	Phenylalanine/glycine
FIV	Feline immunodeficiency virus
Fv1	Friend virus susceptibility 1
Gag	Group specific antigens
GFP	Green fluorescent protein
GM-CSF	Granulocyte-macrophage colony-stimulating factor
Gp	Glycoprotein
gRNA	Guide RNA
h	Hours
HBR	Highly basic region
HIV	Human immunodeficiency virus
HRP	Horse reddish peroxidase
HTLV	Human T-lymphotropic virus
Hu	Human
IFN	Interferon
INM	Inner nuclear membrane
IN	Integrase
IU	Infectious units
ISG	IFN-stimulated gene
KASH	Klarsicht-ANC1-syne-homology
kb	Kilobase
kDa	Kilodalton
L	Late
LB	Lysogeny broth
LINC	Linker of nucleoskeleton and cytoskeleton
LMNA	Lamin
LTR	Long terminal repeat
MA	Matrix
MAPK	Mitogen-activated protein kinase
MARCH	Membrane-associated RING-CH
MHC	major histocompatibility complex
min	Minutes

ml	Millilitre
mM	Millimolar
MLV	Murine leukaemia virus
MX	Myxovirus resistance
NC	Nucleocapsid
NE	Nuclear envelope
Nef	Negative factor
Nesp	Nesprins
NK	Natural killer
NLS	Nuclear localisation signal
nm	Nanometer
NPC	Nuclear pore complex
nt	Nucleotide
NTD	Amino-terminal domain
Nup	Nucleoporin
ONM	Outer nuclear membrane
PAGE	polyacrylamide gel electrophoresis
PAMP	Pathogen-associated molecular pattern
PBL	Peripheral blood lymphocytes
PBS	Phosphate buffered saline
PCR	Polymerase chain reaction
PFA	Paraformaldehyde
PHA	Phytohemagglutinin
pi	Post infection
PIC	Pre-integration complex
PI(4,5)P2	Inositol (4,5) bisphosphate
PNS	Perinuclear space
Pol	Polymerase
PR	Protease
PRR	Pattern recognition receptor
RE	Endoplasmic reticulum
Rb	Rabbit
RPMI	Roswell Park Memorial Institute
RT	Reverse transcriptase

RTC	Reverse transcription complex
s	Seconds
S	Serine
SAMHD	sterile α motif and histidine-aspartate domain-containing protein
SDM	Site directed mutagenesis
SDS	Sodium dodecyl sulfate
SERINC	Serin incorporator
ShRNA	Short hairpin ribonucleic acid
SIV	Simian immunodeficiency virus
SLFN	Schlafen
SLX	Structure-specific endonuclease subunit
SP	Spacer peptide
SR	Arginine/serine
SUN	Sad and UNC domain containing
SG-PERT	SYBR green based product enhanced reverse transcriptase
TBE	Tris-borate-EDTA
TBP	TATA box-binding protein
TCR	T-cell receptor
T/F	Transmitted founder
TM	Transmembrane
TNPO	Transportin
TPR	Translocated promoter region
TREX	Three prime repair exonuclease
tRNA	Transfer RNA
TSG101	Tumour susceptible gene 101
U	Units
Vif	Viral infectivity factor
Vpr	Viral protein R
Vpu	Viral protein U
VSV-G	Vesicular stomatitis virus G
WB	Western blot
wt	Wild type

10. Index

10.1. Figures

Figure 1. Worldwide Human Immunodeficiency Virus (HIV) prevalence in adults aged 15 to 49, in 2017..... 2
Figure 2. Genome organization of HIV-1..... 5
Figure 3. Structure of HIV-1..... 8
Figure 4. HIV-1 life cycle..... 9
Figure 5. HIV-1 entry..... 12
Figure 6. Structure of the nuclear pore complex (NPC)..... 15
Figure 7. HIV-1 nuclear import of pre-integration complex (PIC)..... 19
Figure 8. HIV-1 integration at the nuclear periphery..... 20
Figure 9. Host retroviral restriction factors and countermeasures by viral accessory proteins..... 22
Figure 10. CANC pulldown method data from Malim Lab (KCL, London)..... 61
Figure 11. Overexpression of SUN1 or SUN2 inhibits HIV-1 infection..... 65
Figure 12. SUN1 and SUN2 expression in U87MG CD4/CXCR4 cells..... 66
Figure 13. Overexpression of SUN1 or SUN2 inhibits HIV-1 infection..... 67
Figure 14. Overexpression of SUN1 and SUN2 inhibits HIV-1 2-LTR circle formation..... 69
Figure 15. Overexpression of SUN1 and SUN2 inhibits HIV-1 and HIV-2_{ROD} but not SIVMAC, FIV, EIAV, or MoMLV infection..... 70
Figure 16. HIV-1 sensitivities to the SUN1-induced block..... 71
Figure 17. HIV-1 strains have differential sensitivities to the SUN1- and SUN2-induced block..... 72
Figure 18. Schematic of the generation of chimeric viruses between T/F virus RHPA and NL4.3..... 73
Figure 19. Identification of the HIV-1 determinant for the sensitivity to SUN1-induced inhibition..... 74
Figure 20. HIV-1 incorporating the CA-p2 of the insensitive SIV_{MAC} (HIV-1 (SCA) chimera) is largely insensitive to SUN1- or SUN2-induced inhibition..... 74
Figure 21. CA aminoacid differences between sensitive HIV-$1_{NL4.3}$ and resistant HIV-1_{RHPA}..... 75
Figure 22. HIV-1 LV and HIV-1NRA LV: replacement of the sequence of the SUN1-sensitive HIV-1 variant IIIB up to the ApaI site with that of RHPA..... 75
Figure 23. The determinant for the sensitivity to SUN1-induced inhibition maps to CA..... 76

Figure 24. *In vitro*-synthesized HIV-1 CANC nanotubes capture SUN1 and SUN2 from cell lysates..... 77
Figure 25. Schematic of the analyzed SUN1 deletion mutants..... 78
Figure 26. The amino-terminal domain of SUN1 is required for the block to HIV-1.....79
Figure 27. IF of U87MG CD4/CXCR4 cells expressing HASUN1 wild type or HASUN1 amino-terminal and carboxy-terminal deletion mutants..... 80
Figure 28. Schematic of analyzed SUN1 alanin mutants..... 80
Figure 29. The amino-terminal aminoacids 85-90 relevant in SUN1 blocking infection capacity..... 81
Figure 30. Schematic of analyzed chimeric protein composed of the amino-terminal 130 aminoacids of SUN1 fused to the restriction factor MLV $Fv1^{N}$ ($HASUN1^{NTD}$-$Fv1^{N}$)..... 82
Figure 31. Fusion of the amino-terminal SUN1 domain to Fv1 generates a potent HIV-1-inhibiting factor..... 83
Figure 32. IF U87MG CD4/CXCR4 cells expressing HASUN1 wild type $HASUN1^{NTD}$-$Fv1^{N}$..... 84
Figure 33. Schematic of the analyzed SUN2 deletion mutants..... 84
Figure 34. The amino-terminal domain of SUN2 is required for the block to HIV-1. 85
Figure 35. IF of U87MG CD4/CXCR4 cells expressing HASUN1 wild type or HASUN1 amino-terminal and carboxy-terminal deletion mutants..... 86
Figure 36. Schematic of analyzed chimeric protein composed of the SUN2 amino-terminal fused to SUN1 ($SUN2^{NTD}$-SUN1)..... 86
Figure 37. Fusion of the amino-terminal SUN2 domain to SUN1 generates a potent HIV-1-inhibiting factor..... 87
Figure 38. THP-1 single-cell knockout clones for SUN1 or SUN2 genes..... 88
Figure 39. HIV-1 infection is impaired in CRISPR/Cas9 *SUN2*-depleted THP-1 cells..... 89
Figure 40. Gene disruption of *SUN2* inhibits HIV-1 but not $HIV\text{-}2_{ROD}$, FIV, SIVMAC, EIAV or MoMLV infection..... 90
Figure 41. HIV-1 nuclear import is impaired in CRISPR/Cas9 *SUN2*-depleted cells..... 91
Figure 42. SUN2 shRNA-mediated knockdown decrases HIV-1 infection in CRISPR/Cas9 *SUN1*-depleted THP-1 cells..... 92
Figure 43. HIV-1 infection is impaired in shRNA-reduced SUN2 U87MG CD4/CXCR4 cells..... 93

Figure 44. Jurkat Tag single-cell knockout clones for SUN1 or SUN2 genes..... 94
Figure 45. HIV-1 infection is not impaired in CRISPR/Cas9 *SUN1*- or *SUN2*-depleted Jurkat TAg cells..... 95
Figure 46. THP-1 CRISPR/Cas9 SUN1- or SUN2-depleted cells and the CypA restriction of HIVac capsids..... 97
Figure 47. Jurkat TAg CRISPR/Cas9 SUN1- or SUN2-depleted cells and the CypA restriction of HIVac capsids..... 98
Figure 48. GTP binding and hydrolysis are not important for anti-HIV-1 activity of MX2..... 100
Figure 49. HIV-1 CA mutants N74D and P90A have increased sensitivity to IFN-α-induced suppression in diverse cell types..... 101
Figure 50. HIV-1 CA mutants are sensitized to MX2-independent IFN-α-induced blocks in THP-1 cells..... 103
Figure 51. Hypersensitivity of the HIV-1 CA mutant N74D to IFN-α occurs at the stages of reverse transcription and nuclear import..... 105
Figure 52. The LINC complex connects nuclear structures to the cytoskeleton..... 107

10.2 Tables

Table 1. Classification of retroviruses by genera and genome type..... 4
Table 2. Equipment used in this work..... 28
Table 3. Materials used in this work..... 29
Table 4. Kits used in this work..... 30
Table 5. Chemical and reagents used in this work..... 30
Table 6. Buffer and solutions used in this work..... 32
Table 7. Bacterial culture media used in this work..... 33
Table 8. Cells used in this work..... 34
Table 9. Enzymes used in this work..... 35
Table 10. Plasmids used in this work..... 35
Table 11. Oligonucleotide sequences used in this study..... 38
Table 12. TaqMan qPCR primer/ probes/ standards..... 43
Table 13. Plasmids generated in this work..... 43
Table 14. Antibodies used in this work..... 47
Table 15. Software used in this work..... 48
Table 16. Membrane-associated NE proteins analyzed in the overexpression screen..... 64

11. Publications and contributions

11.1. Publications

Lorenzo Bulli, Luis Apolonia, Juliane Kutzner, Darja Pollpeter, Caroline Goujon, Nikolas Herold, Sarah-Marie Schwarz, Yannick Giernat, Oliver T. Keppler, Michael H. Malim, Torsten Schaller. *Complex interplay between HIV-1 Capsid and MX2-independent IFNα-induced antiviral factors.*
J Virol. 2016 Jul 27;90(16):7469-7480. DOI: 10.1128/JVI.00458-16

Nikolas Herold, Sean G Rudd, Linda Ljungblad, Kumar Sanjiv, Ida Hed Myrberg, Cynthia B J Paulin, Yaser Heshmati, Anna Hagenkort, Juliane Kutzner, Brent D G Page, José M Calderón-Montaño, Olga Loseva, Ann-Sofie Jemth, Lorenzo Bulli, Hanna Axelsson, Bianca Tesi, Nicholas C K Valerie, Andreas Höglund, Julia Bladh, Elisée Wiita, Mikael Sundin, Michael Uhlin, Georgios Rassidakis, Mats Heyman, Katja Pokrovskaja Tamm, Ulrika Warpman-Berglund, Julian Walfridsson, Sören Lehmann, Dan Grandér, Thomas Lundbäck, Per Kogner, Jan-Inge Henter, Thomas Helleday & Torsten Schaller. *Targeting SAMHD1 with the Vpx protein to improve cytarabine therapy for hematological malignancies*.

Nat Med. 2017 Feb;23(2):256-263. DOI: 10.1038/nm.4265.

Torsten Schaller, Lorenzo Bulli, Darja Pollpeter, Gilberto Betancor, Juliane Kutzner, Luis Apolonia, Nikolas Herold, Robin Burk, Michael H. Malim. *Effects of the inner nuclear membrane proteins SUN1/UNC-84A and SUN2/UNC-84B on the early steps of HIV-1 infection.*

J Virol. 2017 Sep 12;91(19). pii: e00463-17. DOI: 10.1128/JVI.00463-17.

Mirjam Schilling, Lorenzo Bulli, Sebastian Weigang, Laura Graf, Sebastian Naumann, Corinna Patzina, Valentina Wagner, Liane Bauersfeld, Caroline Goujon, Hartmut Hengel, Anne Halenius, Zsolt Ruzsics, Torsten Schaller, Georg Kochs. *Human MxB Protein Is a Pan-herpesvirus Restriction Factor.*

J Virol. 2018 Aug 16;92(17). pii: e01056-18. DOI: 10.1128/JVI.01056-18.

11.2. Conference contributions

Lorenzo Bulli, Darja Pollpeter, Gilberto Betancor, Juliane Kutzner, Luis Apolonia, Nikolas Herold, Robin Burk, Zeger Debyser, Lenard Vranckx, Irena Zurnic, Michael H. Malim and Torsten Schaller. Poster presentation: *The role of inner nuclear envelope associated proteins SUN1 and SUN2 in early HIV-1 infection steps.*

Retroviruses, Cold Spring Harbour Laboratory, NY, USA, 2018

12. References

1. Barasa, S.S., *True story about HIV: theory of viral sequestration and reserve infection.* HIV AIDS (Auckl), 2011. **3**: p. 125-33.

2. Sharp, P.M. and B.H. Hahn, *Origins of HIV and the AIDS pandemic.* Cold Spring Harb Perspect Med, 2011. **1**(1): p. a006841.

3. Barre-Sinoussi, F., et al., *Isolation of a T-lymphotropic retrovirus from a patient at risk for acquired immune deficiency syndrome (AIDS).* Science, 1983. **220**(4599): p. 868-71.

4. Gallo, R.C., et al., *Frequent detection and isolation of cytopathic retroviruses (HTLV-III) from patients with AIDS and at risk for AIDS.* Science, 1984. **224**(4648): p. 500-3.

5. Cohen, J. and M. Enserink, *Nobel Prize in Physiology or Medicine. HIV, HPV researchers honored, but one scientist is left out.* Science, 2008. **322**(5899): p. 174-5.

6. Morgan, D.A., F.W. Ruscetti, and R. Gallo, *Selective in vitro growth of T lymphocytes from normal human bone marrows.* Science, 1976. **193**(4257): p. 1007-8.

7. Wain-Hobson, S., et al., *LAV revisited: origins of the early HIV-1 isolates from Institut Pasteur.* Science, 1991. **252**(5008): p. 961-5.

8. Clavel, F., et al., *Isolation of a new human retrovirus from West African patients with AIDS.* Science, 1986. **233**(4761): p. 343-6.

9. (UNAIDS), J.U.N.P.o.H.A. *Unaids data 2018.* . Geneva: UNAIDS, 2018.

10. Arts, E.J. and D.J. Hazuda, *HIV-1 antiretroviral drug therapy.* Cold Spring Harb Perspect Med, 2012. **2**(4): p. a007161.

11. Weiss, R.A., *Retrovirus classification and cell interactions.* J Antimicrob Chemother, 1996. **37 Suppl B**: p. 1-11.

12. Weiss, R.A., *The discovery of endogenous retroviruses.* Retrovirology, 2006. **3**: p. 67.

13. Tazi, J., et al., *Alternative splicing: regulation of HIV-1 multiplication as a target for therapeutic action.* FEBS J, 2010. **277**(4): p. 867-76.

14. Temin, H.M. and S. Mizutani, *RNA-dependent DNA polymerase in virions of Rous sarcoma virus.* Nature, 1970. **226**(5252): p. 1211-3.

15. Baltimore, D., *RNA-dependent DNA polymerase in virions of RNA tumour viruses.* Nature, 1970. **226**(5252): p. 1209-11.

16. Taylor, B.S. and S.M. Hammer, *The challenge of HIV-1 subtype diversity.* N Engl J Med, 2008. **359**(18): p. 1965-6.

17. Faria, N.R., et al., *HIV epidemiology. The early spread and epidemic ignition of HIV-1 in human populations.* Science, 2014. **346**(6205): p. 56-61.

18. Worobey, M., et al., *Direct evidence of extensive diversity of HIV-1 in Kinshasa by 1960.* Nature, 2008. **455**(7213): p. 661-4.

19. Worobey, M., et al., *1970s and 'Patient 0' HIV-1 genomes illuminate early HIV/AIDS history in North America.* Nature, 2016. **539**(7627): p. 98-101.

20. Stephens, R.M., J.W. Casey, and N.R. Rice, *Equine infectious anemia virus gag and pol genes: relatedness to visna and AIDS virus.* Science, 1986. **231**(4738): p. 589-94.

21. Coffin, J.M. and N. Rosenberg, *Retroviruses. Closing the joint.* Nature, 1999. **399**(6735): p. 413, 415-6.

22. Pedersen, N.C., et al., *Isolation of a T-lymphotropic virus from domestic cats with an immunodeficiency-like syndrome.* Science, 1987. **235**(4790): p. 790-3.

23. Chakrabarti, L., et al., *Sequence of simian immunodeficiency virus from macaque and its relationship to other human and simian retroviruses.* Nature, 1987. **328**(6130): p. 543-7.

24. Franchini, G., et al., *Sequence of simian immunodeficiency virus and its relationship to the human immunodeficiency viruses.* Nature, 1987. **328**(6130): p. 539-43.

25. Fukasawa, M., et al., *Sequence of simian immunodeficiency virus from African green monkey, a new member of the HIV/SIV group.* Nature, 1988. **333**(6172): p. 457-61.

26. Tsujimoto, H., et al., *Sequence of a novel simian immunodeficiency virus from a wild-caught African mandrill.* Nature, 1989. **341**(6242): p. 539-41.

27. Yilmaz, A., C. Bolinger, and K. Boris-Lawrie, *Retrovirus translation initiation: Issues and hypotheses derived from study of HIV-1.* Curr HIV Res, 2006. **4**(2): p. 131-9.

28. Swanson, C.M. and M.H. Malim, *SnapShot: HIV-1 proteins.* Cell, 2008. **133**(4): p. 742, 742 e1.

29. Mattei, S., F.K. Schur, and J.A. Briggs, *Retrovirus maturation-an extraordinary structural transformation.* Curr Opin Virol, 2016. **18**: p. 27-35.

30. Hill, C.P., et al., *Crystal structures of the trimeric human immunodeficiency virus type 1 matrix protein: implications for membrane association and assembly.* Proc Natl Acad Sci U S A, 1996. **93**(7): p. 3099-104.

31. Murray, P.S., et al., *Retroviral matrix domains share electrostatic homology: models for membrane binding function throughout the viral life cycle.* Structure, 2005. **13**(10): p. 1521-31.

32. Gottlinger, H.G., J.G. Sodroski, and W.A. Haseltine, *Role of capsid precursor processing and myristoylation in morphogenesis and infectivity of human immunodeficiency virus type 1.* Proc Natl Acad Sci U S A, 1989. **86**(15): p. 5781-5.

33. Ono, A., et al., *Phosphatidylinositol (4,5) bisphosphate regulates HIV-1 Gag targeting to the plasma membrane.* Proc Natl Acad Sci U S A, 2004. **101**(41): p. 14889-94.

34. Saad, J.S., et al., *Point mutations in the HIV-1 matrix protein turn off the myristyl switch.* J Mol Biol, 2007. **366**(2): p. 574-85.

35. Saad, J.S., et al., *Structural basis for targeting HIV-1 Gag proteins to the plasma membrane for virus assembly.* Proc Natl Acad Sci U S A, 2006. **103**(30): p. 11364-9.

36. Dorfman, T., et al., *Role of the matrix protein in the virion association of the human immunodeficiency virus type 1 envelope glycoprotein.* J Virol, 1994. **68**(3): p. 1689-96.

37. Murakami, T. and E.O. Freed, *Genetic evidence for an interaction between human immunodeficiency virus type 1 matrix and alpha-helix 2 of the gp41 cytoplasmic tail.* J Virol, 2000. **74**(8): p. 3548-54.

38. Cosson, P., *Direct interaction between the envelope and matrix proteins of HIV-1.* EMBO J, 1996. **15**(21): p. 5783-8.

39. Campbell, E.M. and T.J. Hope, *HIV-1 capsid: the multifaceted key player in HIV-1 infection.* Nat Rev Microbiol, 2015. **13**(8): p. 471-83.

40. Franke, E.K., H.E. Yuan, and J. Luban, *Specific incorporation of cyclophilin A into HIV-1 virions.* Nature, 1994. **372**(6504): p. 359-62.

41. Mammano, F., et al., *Role of the major homology region of human immunodeficiency virus type 1 in virion morphogenesis.* J Virol, 1994. **68**(8): p. 4927-36.

42. Moore, M.D. and W.S. Hu, *HIV-1 RNA dimerization: It takes two to tango.* AIDS Rev, 2009. **11**(2): p. 91-102.

43. Levin, J.G., et al., *Nucleic acid chaperone activity of HIV-1 nucleocapsid protein: critical role in reverse transcription and molecular mechanism.* Prog Nucleic Acid Res Mol Biol, 2005. **80**: p. 217-86.

44. Scarlata, S. and C. Carter, *Role of HIV-1 Gag domains in viral assembly.* Biochim Biophys Acta, 2003. **1614**(1): p. 62-72.

45. Jacks, T., et al., *Characterization of ribosomal frameshifting in HIV-1 gag-pol expression.* Nature, 1988. **331**(6153): p. 280-3.

46. Freed, E.O., *HIV-1 assembly, release and maturation.* Nat Rev Microbiol, 2015. **13**(8): p. 484-96.

47. Sundquist, W.I. and H.G. Krausslich, *HIV-1 assembly, budding, and maturation.* Cold Spring Harb Perspect Med, 2012. **2**(7): p. a006924.

48. Pettit, S.C., et al., *The p2 domain of human immunodeficiency virus type 1 Gag regulates sequential proteolytic processing and is required to produce fully infectious virions.* J Virol, 1994. **68**(12): p. 8017-27.

49. Wiegers, K., et al., *Sequential steps in human immunodeficiency virus particle maturation revealed by alterations of individual Gag polyprotein cleavage sites.* J Virol, 1998. **72**(4): p. 2846-54.

50. de Marco, A., et al., *Structural analysis of HIV-1 maturation using cryo-electron tomography.* PLoS Pathog, 2010. **6**(11): p. e1001215.

51. Kohl, N.E., et al., *Active human immunodeficiency virus protease is required for viral infectivity.* Proc Natl Acad Sci U S A, 1988. **85**(13): p. 4686-90.

52. Peng, C., et al., *Role of human immunodeficiency virus type 1-specific protease in core protein maturation and viral infectivity.* J Virol, 1989. **63**(6): p. 2550-6.

53. Javanbakht, H., et al., *The interaction between HIV-1 Gag and human lysyl-tRNA synthetase during viral assembly.* J Biol Chem, 2003. **278**(30): p. 27644-51.

54. Bushman, F.D., T. Fujiwara, and R. Craigie, *Retroviral DNA integration directed by HIV integration protein in vitro.* Science, 1990. **249**(4976): p. 1555-8.

55. Walker, B.D., et al., *Inhibition of human immunodeficiency virus syncytium formation and virus replication by castanospermine.* Proc Natl Acad Sci U S A, 1987. **84**(22): p. 8120-4.

56. Willey, R.L., et al., *Biosynthesis, cleavage, and degradation of the human immunodeficiency virus 1 envelope glycoprotein gp160.* Proc Natl Acad Sci U S A, 1988. **85**(24): p. 9580-4.

57. Hallenberger, S., et al., *Inhibition of furin-mediated cleavage activation of HIV-1 glycoprotein gp160.* Nature, 1992. **360**(6402): p. 358-61.

58. McCune, J.M., et al., *Endoproteolytic cleavage of gp160 is required for the activation of human immunodeficiency virus.* Cell, 1988. **53**(1): p. 55-67.

59. Kowalski, M., et al., *Functional regions of the envelope glycoprotein of human immunodeficiency virus type 1.* Science, 1987. **237**(4820): p. 1351-5.

60. White, T.A., et al., *Molecular architectures of trimeric SIV and HIV-1 envelope glycoproteins on intact viruses: strain-dependent variation in quaternary structure.* PLoS Pathog, 2010. **6**(12): p. e1001249.

61. Labrijn, A.F., et al., *Access of antibody molecules to the conserved coreceptor binding site on glycoprotein gp120 is sterically restricted on primary human immunodeficiency virus type 1.* J Virol, 2003. **77**(19): p. 10557-65.

62. Mao, Y., et al., *Subunit organization of the membrane-bound HIV-1 envelope glycoprotein trimer.* Nat Struct Mol Biol, 2012. **19**(9): p. 893-9.

63. Doyle, T., C. Goujon, and M.H. Malim, *HIV-1 and interferons: who's interfering with whom?* Nat Rev Microbiol, 2015. **13**(7): p. 403-13.

64. Frankel, A.D. and J.A. Young, *HIV-1: fifteen proteins and an RNA.* Annu Rev Biochem, 1998. **67**: p. 1-25.

65. Wright, E.R., et al., *Electron cryotomography of immature HIV-1 virions reveals the structure of the CA and SP1 Gag shells.* EMBO J, 2007. **26**(8): p. 2218-26.

66. Briggs, J.A., et al., *Structure and assembly of immature HIV.* Proc Natl Acad Sci U S A, 2009. **106**(27): p. 11090-5.

67. Carlson, L.A., et al., *Three-dimensional analysis of budding sites and released virus suggests a revised model for HIV-1 morphogenesis.* Cell Host Microbe, 2008. **4**(6): p. 592-9.

68. Ganser-Pornillos, B.K., M. Yeager, and W.I. Sundquist, *The structural biology of HIV assembly.* Curr Opin Struct Biol, 2008. **18**(2): p. 203-17.

69. de Goede, A.L., et al., *Understanding HIV infection for the design of a therapeutic vaccine. Part I: Epidemiology and pathogenesis of HIV infection.* Ann Pharm Fr, 2015. **73**(2): p. 87-99.

70. Siliciano, R.F. and W.C. Greene, *HIV latency.* Cold Spring Harb Perspect Med, 2011. **1**(1): p. a007096.

71. Lever, A.M. and K.T. Jeang, *Replication of human immunodeficiency virus type 1 from entry to exit.* Int J Hematol, 2006. **84**(1): p. 23-30.

72. Jeang, K.T., H. Xiao, and E.A. Rich, *Multifaceted activities of the HIV-1 transactivator of transcription, Tat.* J Biol Chem, 1999. **274**(41): p. 28837-40.

73. Checkley, M.A., B.G. Luttge, and E.O. Freed, *HIV-1 envelope glycoprotein biosynthesis, trafficking, and incorporation.* J Mol Biol, 2011. **410**(4): p. 582-608.

74. Kutluay, S.B. and P.D. Bieniasz, *Analysis of the initiating events in HIV-1 particle assembly and genome packaging.* PLoS Pathog, 2010. **6**(11): p. e1001200.

75. Ono, A., *HIV-1 Assembly at the Plasma Membrane: Gag Trafficking and Localization.* Future Virol, 2009. **4**(3): p. 241-257.

76. von Schwedler, U.K., et al., *Functional surfaces of the human immunodeficiency virus type 1 capsid protein.* J Virol, 2003. **77**(9): p. 5439-50.

77. Luban, J., et al., *Human immunodeficiency virus type 1 Gag protein binds to cyclophilins A and B.* Cell, 1993. **73**(6): p. 1067-78.

78. Alce, T.M. and W. Popik, *APOBEC3G is incorporated into virus-like particles by a direct interaction with HIV-1 Gag nucleocapsid protein.* J Biol Chem, 2004. **279**(33): p. 34083-6.

79. Cen, S., et al., *The interaction between HIV-1 Gag and APOBEC3G.* J Biol Chem, 2004. **279**(32): p. 33177-84.

80. Douaisi, M., et al., *HIV-1 and MLV Gag proteins are sufficient to recruit APOBEC3G into virus-like particles.* Biochemical and Biophysical Research Communications, 2004. **321**(3): p. 566-573.

81. Luo, K., et al., *Amino-terminal region of the human immunodeficiency virus type 1 nucleocapsid is required for human APOBEC3G packaging.* J Virol, 2004. **78**(21): p. 11841-52.

82. Schafer, A., H.P. Bogerd, and B.R. Cullen, *Specific packaging of APOBEC3G into HIV-1 virions is mediated by the nucleocapsid domain of the gag polyprotein precursor.* Virology, 2004. **328**(2): p. 163-8.

83. Lifson, J.D., et al., *Induction of CD4-dependent cell fusion by the HTLV-III/LAV envelope glycoprotein.* Nature, 1986. **323**(6090): p. 725-8.

84. Feng, Y., et al., *HIV-1 entry cofactor: functional cDNA cloning of a seven-transmembrane, G protein-coupled receptor.* Science, 1996. **272**(5263): p. 872-7.

85. Alkhatib, G., et al., *CC CKR5: a RANTES, MIP-1alpha, MIP-1beta receptor as a fusion cofactor for macrophage-tropic HIV-1.* Science, 1996. **272**(5270): p. 1955-8.

86. Li, Q.J., et al., *CD4 enhances T cell sensitivity to antigen by coordinating Lck accumulation at the immunological synapse.* Nat Immunol, 2004. **5**(8): p. 791-9.

87. Lifson, J.D., et al., *AIDS retrovirus induced cytopathology: giant cell formation and involvement of CD4 antigen.* Science, 1986. **232**(4754): p. 1123-7.

88. Deng, H., et al., *Identification of a major co-receptor for primary isolates of HIV-1.* Nature, 1996. **381**(6584): p. 661-6.

89. Choe, H., et al., *The beta-chemokine receptors CCR3 and CCR5 facilitate infection by primary HIV-1 isolates.* Cell, 1996. **85**(7): p. 1135-48.

90. Liu, R., et al., *Homozygous defect in HIV-1 coreceptor accounts for resistance of some multiply-exposed individuals to HIV-1 infection.* Cell, 1996. **86**(3): p. 367-77.

91. Samson, M., et al., *Resistance to HIV-1 infection in caucasian individuals bearing mutant alleles of the CCR-5 chemokine receptor gene.* Nature, 1996. **382**(6593): p. 722-5.

92. Chan, D.C., et al., *Core structure of gp41 from the HIV envelope glycoprotein.* Cell, 1997. **89**(2): p. 263-73.

93. Miyauchi, K., et al., *HIV enters cells via endocytosis and dynamin-dependent fusion with endosomes.* Cell, 2009. **137**(3): p. 433-44.

94. Herold, N., et al., *HIV-1 entry in SupT1-R5, CEM-ss, and primary CD4+ T cells occurs at the plasma membrane and does not require endocytosis.* J Virol, 2014. **88**(24): p. 13956-70.

95. Wilen, C.B., J.C. Tilton, and R.W. Doms, *HIV: cell binding and entry.* Cold Spring Harb Perspect Med, 2012. **2**(8).

96. Rosa, A., et al., *HIV-1 Nef promotes infection by excluding SERINC5 from virion incorporation.* Nature, 2015. **526**: p. 212.

97. Usami, Y., Y. Wu, and H.G. Gottlinger, *SERINC3 and SERINC5 restrict HIV-1 infectivity and are counteracted by Nef.* Nature, 2015. **526**(7572): p. 218-23.

98. Yu, J., et al., *IFITM Proteins Restrict HIV-1 Infection by Antagonizing the Envelope Glycoprotein.* Cell Rep, 2015. **13**(1): p. 145-156.

99. Lu, J., et al., *The IFITM proteins inhibit HIV-1 infection.* J Virol, 2011. **85**(5): p. 2126-37.

100. Compton, A.A., et al., *IFITM proteins incorporated into HIV-1 virions impair viral fusion and spread.* Cell Host Microbe, 2014. **16**(6): p. 736-47.

101. Forshey, B.M., et al., *Formation of a human immunodeficiency virus type 1 core of optimal stability is crucial for viral replication.* J Virol, 2002. **76**(11): p. 5667-77.

102. Rasaiyaah, J., et al., *HIV-1 evades innate immune recognition through specific cofactor recruitment.* Nature, 2013. **503**(7476): p. 402-405.

103. Lahaye, X., et al., *The capsids of HIV-1 and HIV-2 determine immune detection of the viral cDNA by the innate sensor cGAS in dendritic cells.* Immunity, 2013. **39**(6): p. 1132-42.

104. Gao, D., et al., *Cyclic GMP-AMP synthase is an innate immune sensor of HIV and other retroviruses.* Science, 2013. **341**(6148): p. 903-6.

105. Yan, N., et al., *The cytosolic exonuclease TREX1 inhibits the innate immune response to human immunodeficiency virus type 1.* Nat Immunol, 2010. **11**(11): p. 1005-13.

106. Sokolskaja, E., D.M. Sayah, and J. Luban, *Target cell cyclophilin A modulates human immunodeficiency virus type 1 infectivity.* J Virol, 2004. **78**(23): p. 12800-8.

107. Hatziioannou, T., et al., *Cyclophilin interactions with incoming human immunodeficiency virus type 1 capsids with opposing effects on infectivity in human cells.* J Virol, 2005. **79**(1): p. 176-83.

108. Gamble, T.R., et al., *Crystal structure of human cyclophilin A bound to the amino-terminal domain of HIV-1 capsid.* Cell, 1996. **87**(7): p. 1285-94.

109. Thali, M., et al., *Functional association of cyclophilin A with HIV-1 virions.* Nature, 1994. **372**(6504): p. 363-5.

110. Bosco, D.A., et al., *Catalysis of cis/trans isomerization in native HIV-1 capsid by human cyclophilin A.* Proc Natl Acad Sci U S A, 2002. **99**(8): p. 5247-52.

111. Ptak, R.G., et al., *Inhibition of human immunodeficiency virus type 1 replication in human cells by Debio-025, a novel cyclophilin binding agent.* Antimicrob Agents Chemother, 2008. **52**(4): p. 1302-17.

112. Braaten, D., E.K. Franke, and J. Luban, *Cyclophilin A is required for an early step in the life cycle of human immunodeficiency virus type 1 before the initiation of reverse transcription.* J Virol, 1996. **70**(6): p. 3551-60.

113. Manel, N., et al., *A cryptic sensor for HIV-1 activates antiviral innate immunity in dendritic cells.* Nature, 2010. **467**(7312): p. 214-7.

114. Braaten, D., et al., *Cyclosporine A-resistant human immunodeficiency virus type 1 mutants demonstrate that Gag encodes the functional target of cyclophilin A.* J Virol, 1996. **70**(8): p. 5170-6.

115. Yoo, S., et al., *Molecular recognition in the HIV-1 capsid/cyclophilin A complex.* J Mol Biol, 1997. **269**(5): p. 780-95.

116. Colgan, J., et al., *Binding of the human immunodeficiency virus type 1 Gag polyprotein to cyclophilin A is mediated by the central region of capsid and requires Gag dimerization.* J Virol, 1996. **70**(7): p. 4299-310.

117. Fassati, A. and S.P. Goff, *Characterization of intracellular reverse transcription complexes of human immunodeficiency virus type 1.* J Virol, 2001. **75**(8): p. 3626-35.

118. Li, L., et al., *Role of the non-homologous DNA end joining pathway in the early steps of retroviral infection.* EMBO J, 2001. **20**(12): p. 3272-81.

119. Mangeat, B., et al., *Broad antiretroviral defence by human APOBEC3G through lethal editing of nascent reverse transcripts.* Nature, 2003. **424**(6944): p. 99-103.

120. Sheehy, A.M., et al., *Isolation of a human gene that inhibits HIV-1 infection and is suppressed by the viral Vif protein.* Nature, 2002. **418**(6898): p. 646-50.

121. Zhang, H., et al., *The cytidine deaminase CEM15 induces hypermutation in newly synthesized HIV-1 DNA.* Nature, 2003. **424**(6944): p. 94-8.

122. Laguette, N., et al., *SAMHD1 is the dendritic- and myeloid-cell-specific HIV-1 restriction factor counteracted by Vpx.* Nature, 2011. **474**(7353): p. 654-7.

123. Lahouassa, H., et al., *SAMHD1 restricts the replication of human immunodeficiency virus type 1 by depleting the intracellular pool of deoxynucleoside triphosphates.* Nat Immunol, 2012. **13**(3): p. 223-228.

124. Bukrinsky, M.I., et al., *A nuclear localization signal within HIV-1 matrix protein that governs infection of non-dividing cells.* Nature, 1993. **365**(6447): p. 666-9.

125. Gallay, P., et al., *HIV-1 infection of nondividing cells through the recognition of integrase by the importin/karyopherin pathway.* Proc Natl Acad Sci U S A, 1997. **94**(18): p. 9825-30.

126. Bouyac-Bertoia, M., et al., *HIV-1 infection requires a functional integrase NLS.* Mol Cell, 2001. **7**(5): p. 1025-35.

127. Vodicka, M.A., et al., *HIV-1 Vpr interacts with the nuclear transport pathway to promote macrophage infection.* Genes Dev, 1998. **12**(2): p. 175-85.

128. Fouchier, R.A., et al., *Interaction of the human immunodeficiency virus type 1 Vpr protein with the nuclear pore complex.* J Virol, 1998. **72**(7): p. 6004-13.

129. Heinzinger, N.K., et al., *The Vpr protein of human immunodeficiency virus type 1 influences nuclear localization of viral nucleic acids in nondividing host cells.* Proc Natl Acad Sci U S A, 1994. **91**(15): p. 7311-5.

130. Katz, R.A., et al., *Human immunodeficiency virus type 1 DNA nuclear import and integration are mitosis independent in cycling cells.* J Virol, 2003. **77**(24): p. 13412-7.

131. Case, S.S., et al., *Stable transduction of quiescent CD34(+)CD38(-) human hematopoietic cells by HIV-1-based lentiviral vectors.* Proc Natl Acad Sci U S A, 1999. **96**(6): p. 2988-93.

132. Naldini, L., et al., *Efficient transfer, integration, and sustained long-term expression of the transgene in adult rat brains injected with a lentiviral vector.* Proc Natl Acad Sci U S A, 1996. **93**(21): p. 11382-8.

133. Lewis, P., M. Hensel, and M. Emerman, *Human immunodeficiency virus infection of cells arrested in the cell cycle.* EMBO J, 1992. **11**(8): p. 3053-8.

134. Mehandru, S., et al., *Primary HIV-1 infection is associated with preferential depletion of CD4+ T lymphocytes from effector sites in the gastrointestinal tract.* J Exp Med, 2004. **200**(6): p. 761-70.

135. Weinberg, J.B., et al., *Productive human immunodeficiency virus type 1 (HIV-1) infection of nonproliferating human monocytes.* J Exp Med, 1991. **174**(6): p. 1477-82.

136. Yamashita, M., et al., *Evidence for direct involvement of the capsid protein in HIV infection of nondividing cells.* PLoS Pathog, 2007. **3**(10): p. 1502-10.

137. Yamashita, M. and M. Emerman, *Retroviral infection of non-dividing cells: old and new perspectives.* Virology, 2006. **344**(1): p. 88-93.

138. Yamashita, M. and M. Emerman, *Capsid is a dominant determinant of retrovirus infectivity in nondividing cells.* J Virol, 2004. **78**(11): p. 5670-8.

139. Hulme, A.E., et al., *Complementary Assays Reveal a Low Level of CA Associated with Viral Complexes in the Nuclei of HIV-1-Infected Cells.* J Virol, 2015. **89**(10): p. 5350-61.

140. Peng, K., et al., *Quantitative microscopy of functional HIV post-entry complexes reveals association of replication with the viral capsid.* Elife, 2014. **3**: p. e04114.

141. Schaller, T., et al., *HIV-1 capsid-cyclophilin interactions determine nuclear import pathway, integration targeting and replication efficiency.* PLoS pathogens, 2011. **7**(12): p. e1002439.

142. Bichel, K., et al., *HIV-1 capsid undergoes coupled binding and isomerization by the nuclear pore protein NUP358.* Retrovirology, 2013. **10**: p. 81.

143. Lin, D.H., et al., *Structural and functional analysis of the C-terminal domain of Nup358/RanBP2.* J Mol Biol, 2013. **425**(8): p. 1318-29.

144. Matreyek, K.A., et al., *Nucleoporin NUP153 phenylalanine-glycine motifs engage a common binding pocket within the HIV-1 capsid protein to mediate lentiviral infectivity.* PLoS Pathog, 2013. **9**(10): p. e1003693.

145. Hetzer, M.W., *The nuclear envelope.* Cold Spring Harb Perspect Biol, 2010. **2**(3): p. a000539.

146. Walther, T.C., et al., *The cytoplasmic filaments of the nuclear pore complex are dispensable for selective nuclear protein import.* J Cell Biol, 2002. **158**(1): p. 63-77.

147. Rout, M.P., et al., *The yeast nuclear pore complex: composition, architecture, and transport mechanism.* J Cell Biol, 2000. **148**(4): p. 635-51.

148. Labokha, A.A. and A. Fassati, *Viruses challenge selectivity barrier of nuclear pores.* Viruses, 2013. **5**(10): p. 2410-23.

149. Lim, R.Y., U. Aebi, and D. Stoffler, *From the trap to the basket: getting to the bottom of the nuclear pore complex.* Chromosoma, 2006. **115**(1): p. 15-26.

150. Strambio-De-Castillia, C., M. Niepel, and M.P. Rout, *The nuclear pore complex: bridging nuclear transport and gene regulation.* Nat Rev Mol Cell Biol, 2010. **11**(7): p. 490-501.

151. Fahrenkrog, B. and U. Aebi, *The nuclear pore complex: nucleocytoplasmic transport and beyond.* Nat Rev Mol Cell Biol, 2003. **4**(10): p. 757-66.

152. Brass, A.L., et al., *Identification of host proteins required for HIV infection through a functional genomic screen.* Science, 2008. **319**(5865): p. 921-6.

153. Konig, R., et al., *Global analysis of host-pathogen interactions that regulate early-stage HIV-1 replication.* Cell, 2008. **135**(1): p. 49-60.

154. Zhou, H., et al., *Genome-scale RNAi screen for host factors required for HIV replication.* Cell Host Microbe, 2008. **4**(5): p. 495-504.

155. Meehan, A.M., et al., *A cyclophilin homology domain-independent role for Nup358 in HIV-1 infection.* PLoS Pathog, 2014. **10**(2): p. e1003969.

156. Di Nunzio, F., et al., *Human nucleoporins promote HIV-1 docking at the nuclear pore, nuclear import and integration.* PLoS One, 2012. **7**(9): p. e46037.

157. Zhang, R., R. Mehla, and A. Chauhan, *Perturbation of host nuclear membrane component RanBP2 impairs the nuclear import of human immunodeficiency virus -1 preintegration complex (DNA).* PLoS One, 2010. **5**(12): p. e15620.

158. Di Nunzio, F., et al., *Nup153 and Nup98 bind the HIV-1 core and contribute to the early steps of HIV-1 replication.* Virology, 2013. **440**(1): p. 8-18.

159. Matreyek, K.A. and A. Engelman, *The requirement for nucleoporin NUP153 during human immunodeficiency virus type 1 infection is determined by the viral capsid.* J Virol, 2011. **85**(15): p. 7818-27.

160. Bhargava, A., X. Lahaye, and N. Manel, *Let me in: Control of HIV nuclear entry at the nuclear envelope.* Cytokine Growth Factor Rev, 2018. **40**: p. 59-67.

161. Ebina, H., et al., *Role of Nup98 in nuclear entry of human immunodeficiency virus type 1 cDNA.* Microbes Infect, 2004. **6**(8): p. 715-24.

162. Krishnan, L., et al., *The requirement for cellular transportin 3 (TNPO3 or TRN-SR2) during infection maps to human immunodeficiency virus type 1 capsid and not integrase.* J Virol, 2010. **84**(1): p. 397-406.

163. Lee, K., et al., *Flexible use of nuclear import pathways by HIV-1.* Cell Host Microbe, 2010. **7**(3): p. 221-33.

164. Price, A.J., et al., *CPSF6 defines a conserved capsid interface that modulates HIV-1 replication.* PLoS Pathog, 2012. **8**(8): p. e1002896.

165. Christ, F., et al., *Transportin-SR2 imports HIV into the nucleus.* Current biology : CB, 2008. **18**(16): p. 1192-202.

166. Lee, K., et al., *HIV-1 capsid-targeting domain of cleavage and polyadenylation specificity factor 6.* J Virol, 2012. **86**(7): p. 3851-60.

167. Valle-Casuso, J.C., et al., *TNPO3 is required for HIV-1 replication after nuclear import but prior to integration and binds the HIV-1 core.* J Virol, 2012. **86**(10): p. 5931-6.

168. Zhou, L., et al., *Transportin 3 promotes a nuclear maturation step required for efficient HIV-1 integration.* PLoS Pathog, 2011. **7**(8): p. e1002194.

169. De Iaco, A., et al., *TNPO3 protects HIV-1 replication from CPSF6-mediated capsid stabilization in the host cell cytoplasm.* Retrovirology, 2013. **10**: p. 20.

170. Ruegsegger, U., D. Blank, and W. Keller, *Human pre-mRNA cleavage factor Im is related to spliceosomal SR proteins and can be reconstituted in vitro from recombinant subunits.* Mol Cell, 1998. **1**(2): p. 243-53.

171. Shah, V.B., et al., *The host proteins transportin SR2/TNPO3 and cyclophilin A exert opposing effects on HIV-1 uncoating.* J Virol, 2013. **87**(1): p. 422-32.

172. De Iaco, A. and J. Luban, *Inhibition of HIV-1 infection by TNPO3 depletion is determined by capsid and detectable after viral cDNA enters the nucleus.* Retrovirology, 2011. **8**: p. 98.

173. Lahaye, X., et al., *Nuclear Envelope Protein SUN2 Promotes Cyclophilin-A-Dependent Steps of HIV Replication.* Cell Rep, 2016.

174. Schroder, A.R., et al., *HIV-1 integration in the human genome favors active genes and local hotspots.* Cell, 2002. **110**(4): p. 521-9.

175. Marini, B., et al., *Nuclear architecture dictates HIV-1 integration site selection.* Nature, 2015. **521**(7551): p. 227-31.

176. Ocwieja, K.E., et al., *HIV integration targeting: a pathway involving Transportin-3 and the nuclear pore protein RanBP2.* PLoS pathogens, 2011. **7**(3): p. e1001313.

177. Lelek, M., et al., *Chromatin organization at the nuclear pore favours HIV replication.* Nat Commun, 2015. **6**: p. 6483.

178. Krull, S., et al., *Protein Tpr is required for establishing nuclear pore-associated zones of heterochromatin exclusion.* EMBO J, 2010. **29**(10): p. 1659-73.

179. Rasheedi, S., et al., *The Cleavage and Polyadenylation Specificity Factor 6 (CPSF6) Subunit of the Capsid-recruited Pre-messenger RNA Cleavage Factor I (CFIm) Complex Mediates HIV-1 Integration into Genes.* J Biol Chem, 2016. **291**(22): p. 11809-19.

180. Sowd, G.A., et al., *A critical role for alternative polyadenylation factor CPSF6 in targeting HIV-1 integration to transcriptionally active chromatin.* Proc Natl Acad Sci U S A, 2016. **113**(8): p. E1054-63.

181. Cherepanov, P., et al., *HIV-1 integrase forms stable tetramers and associates with LEDGF/p75 protein in human cells.* J Biol Chem, 2003. **278**(1): p. 372-81.

182. Emiliani, S., et al., *Integrase mutants defective for interaction with LEDGF/p75 are impaired in chromosome tethering and HIV-1 replication.* J Biol Chem, 2005. **280**(27): p. 25517-23.

183. Llano, M., et al., *LEDGF/p75 determines cellular trafficking of diverse lentiviral but not murine oncoretroviral integrase proteins and is a component of functional lentiviral preintegration complexes.* J Virol, 2004. **78**(17): p. 9524-37.

184. Maertens, G., et al., *LEDGF/p75 is essential for nuclear and chromosomal targeting of HIV-1 integrase in human cells.* J Biol Chem, 2003. **278**(35): p. 33528-39.

185. Ciuffi, A., et al., *A role for LEDGF/p75 in targeting HIV DNA integration.* Nat Med, 2005. **11**(12): p. 1287-9.

186. Marshall, H.M., et al., *Role of PSIP1/LEDGF/p75 in lentiviral infectivity and integration targeting.* PLoS One, 2007. **2**(12): p. e1340.

187. Shun, M.C., et al., *LEDGF/p75 functions downstream from preintegration complex formation to effect gene-specific HIV-1 integration.* Genes Dev, 2007. **21**(14): p. 1767-78.

188. Lusic, M. and R.F. Siliciano, *Nuclear landscape of HIV-1 infection and integration.* Nat Rev Microbiol, 2017. **15**(2): p. 69-82.

189. Yoder, K.E. and F.D. Bushman, *Repair of gaps in retroviral DNA integration intermediates.* J Virol, 2000. **74**(23): p. 11191-200.

190. Delelis, O., et al., *Efficient and specific internal cleavage of a retroviral palindromic DNA sequence by tetrameric HIV-1 integrase.* PLoS One, 2007. **2**(7): p. e608.

191. Bonilla, F.A. and H.C. Oettgen, *Adaptive immunity.* J Allergy Clin Immunol, 2010. **125**(2 Suppl 2): p. S33-40.

192. Luckheeram, R.V., et al., *CD4(+)T cells: differentiation and functions.* Clin Dev Immunol, 2012. **2012**: p. 925135.

193. Berg, R.E. and J. Forman, *The role of CD8 T cells in innate immunity and in antigen non-specific protection.* Curr Opin Immunol, 2006. **18**(3): p. 338-43.

194. Brubaker, S.W., et al., *Innate immune pattern recognition: a cell biological perspective.* Annu Rev Immunol, 2015. **33**: p. 257-90.

195. Jin, X., H. Wu, and H. Smith, *APOBEC3G levels predict rates of progression to AIDS.* Retrovirology, 2007. **4**: p. 20.

196. Seissler, T., R. Marquet, and J.C. Paillart, *Hijacking of the Ubiquitin/Proteasome Pathway by the HIV Auxiliary Proteins.* Viruses, 2017. **9**(11).

197. Gaines, H., et al., *Immunological changes in primary HIV-1 infection.* AIDS, 1990. **4**(10): p. 995-9.

198. Stacey, A.R., et al., *Induction of a striking systemic cytokine cascade prior to peak viremia in acute human immunodeficiency virus type 1 infection, in contrast to more modest and delayed responses in acute hepatitis B and C virus infections.* J Virol, 2009. **83**(8): p. 3719-33.

199. Sandler, N.G., et al., *Type I interferon responses in rhesus macaques prevent SIV infection and slow disease progression.* Nature, 2014. **511**(7511): p. 601-5.

200. Li, G., et al., *Plasmacytoid dendritic cells suppress HIV-1 replication but contribute to HIV-1 induced immunopathogenesis in humanized mice.* PLoS Pathog, 2014. **10**(7): p. e1004291.

201. Schoggins, J.W., et al., *Pan-viral specificity of IFN-induced genes reveals new roles for cGAS in innate immunity.* Nature, 2014. **505**(7485): p. 691-5.

202. Pillai, S.K., et al., *Role of retroviral restriction factors in the interferon-alpha-mediated suppression of HIV-1 in vivo.* Proc Natl Acad Sci U S A, 2012. **109**(8): p. 3035-40.

203. Bosinger, S.E. and N.S. Utay, *Type I interferon: understanding its role in HIV pathogenesis and therapy.* Curr HIV/AIDS Rep, 2015. **12**(1): p. 41-53.

204. Goujon, C., et al., *Human MX2 is an interferon-induced post-entry inhibitor of HIV-1 infection.* Nature, 2013. **502**(7472): p. 559-62.

205. Kane, M., et al., *MX2 is an interferon-induced inhibitor of HIV-1 infection.* Nature, 2013. **502**(7472): p. 563-6.

206. Schoggins, J.W., et al., *A diverse range of gene products are effectors of the type I interferon antiviral response.* Nature, 2011. **472**(7344): p. 481-5.

207. Mildvan, D., et al., *Synergy, activity and tolerability of zidovudine and interferon-alpha in patients with symptomatic HIV-1 infection: AIDS Clincal Trial Group 068.* Antivir Ther, 1996. **1**(2): p. 77-88.

208. Torriani, F.J., et al., *Hepatitis C virus (HCV) and human immunodeficiency virus (HIV) dynamics during HCV treatment in HCV/HIV coinfection.* J Infect Dis, 2003. **188**(10): p. 1498-507.

209. Parrish, N.F., et al., *Phenotypic properties of transmitted founder HIV-1.* Proc Natl Acad Sci U S A, 2013. **110**(17): p. 6626-33.

210. Fenton-May, A.E., et al., *Relative resistance of HIV-1 founder viruses to control by interferon-alpha.* Retrovirology, 2013. **10**: p. 146.

211. Liu, Z., et al., *The interferon-inducible MxB protein inhibits HIV-1 infection.* Cell Host Microbe, 2013. **14**(4): p. 398-410.

212. Liu, Z., et al., *The highly polymorphic cyclophilin A-binding loop in HIV-1 capsid modulates viral resistance to MxB.* Retrovirology, 2015. **12**(1): p. 1.

213. Busnadiego, I., et al., *Host and viral determinants of Mx2 antiretroviral activity.* J Virol, 2014. **88**(14): p. 7738-52.

214. Bulli, L., et al., *Complex Interplay between HIV-1 Capsid and MX2-Independent Alpha Interferon-Induced Antiviral Factors.* J Virol, 2016. **90**(16): p. 7469-80.

215. Fricke, T., et al., *MxB binds to the HIV-1 core and prevents the uncoating process of HIV-1.* Retrovirology, 2014. **11**: p. 68.

216. Fribourgh, J.L., et al., *Structural insight into HIV-1 restriction by MxB.* Cell Host Microbe, 2014. **16**(5): p. 627-638.

217. Pavlovic, J., et al., *Resistance to influenza virus and vesicular stomatitis virus conferred by expression of human MxA protein.* J Virol, 1990. **64**(7): p. 3370-5.

218. Haller, O. and G. Kochs, *Human MxA protein: an interferon-induced dynamin-like GTPase with broad antiviral activity.* J Interferon Cytokine Res, 2011. **31**(1): p. 79-87.

219. Liu, S.Y., et al., *Systematic identification of type I and type II interferon-induced antiviral factors.* Proc Natl Acad Sci U S A, 2012. **109**(11): p. 4239-44.

220. Schilling, M., et al., *Human MxB Protein Is a Pan-herpesvirus Restriction Factor.* J Virol, 2018. **92**(17).

221. King, M.C., G. Raposo, and M.A. Lemmon, *Inhibition of nuclear import and cell-cycle progression by mutated forms of the dynamin-like GTPase MxB.* Proc Natl Acad Sci U S A, 2004. **101**(24): p. 8957-62.

222. Melen, K., et al., *Human MxB protein, an interferon-alpha-inducible GTPase, contains a nuclear targeting signal and is localized in the heterochromatin region beneath the nuclear envelope.* J Biol Chem, 1996. **271**(38): p. 23478-86.

223. Schulte, B., et al., *Restriction of HIV-1 Requires the N-Terminal Region of MxB as a Capsid-Binding Motif but Not as a Nuclear Localization Signal.* J Virol, 2015. **89**(16): p. 8599-610.

224. Kane, M., et al., *Nuclear pore heterogeneity influences HIV-1 infection and the antiviral activity of MX2.* Elife, 2018. **7**.

225. Dicks, M.D., et al., *Oligomerization Requirements for MX2-Mediated Suppression of HIV-1 Infection.* J Virol, 2016. **90**(1): p. 22-32.

226. Goujon, C., et al., *A triple-arginine motif in the amino-terminal domain and oligomerization are required for HIV-1 inhibition by human MX2.* J Virol, 2015. **89**(8): p. 4676-80.

227. Terry, L.J., E.B. Shows, and S.R. Wente, *Crossing the nuclear envelope: hierarchical regulation of nucleocytoplasmic transport.* Science, 2007. **318**(5855): p. 1412-6.

228. Schirmer, E.C., et al., *Nuclear membrane proteins with potential disease links found by subtractive proteomics.* Science, 2003. **301**(5638): p. 1380-2.

229. Burke, B. and K.J. Roux, *Nuclei take a position: managing nuclear location.* Dev Cell, 2009. **17**(5): p. 587-97.

230. Uzer, G., et al., *Cell Mechanosensitivity to Extremely Low-Magnitude Signals Is Enabled by a LINCed Nucleus.* Stem Cells, 2015. **33**(6): p. 2063-76.

231. Light, W.H. and J.H. Brickner, *Nuclear pore proteins regulate chromatin structure and transcriptional memory by a conserved mechanism.* Nucleus, 2013. **4**(5): p. 357-60.

232. Light, W.H., et al., *A conserved role for human Nup98 in altering chromatin structure and promoting epigenetic transcriptional memory.* PLoS Biol, 2013. **11**(3): p. e1001524.

233. Enninga, J., et al., *Role of nucleoporin induction in releasing an mRNA nuclear export block.* Science, 2002. **295**(5559): p. 1523-5.

234. Turgay, Y., et al., *SUN proteins facilitate the removal of membranes from chromatin during nuclear envelope breakdown.* J Cell Biol, 2014. **204**(7): p. 1099-109.

235. Malone, C.J., et al., *The C. elegans hook protein, ZYG-12, mediates the essential attachment between the centrosome and nucleus.* Cell, 2003. **115**(7): p. 825-36.

236. Chi, Y.H., et al., *Histone acetyltransferase hALP and nuclear membrane protein hsSUN1 function in de-condensation of mitotic chromosomes.* J Biol Chem, 2007. **282**(37): p. 27447-58.

237. Gonzalez-Aguilera, C., et al., *Genome-wide analysis links emerin to neuromuscular junction activity in Caenorhabditis elegans.* Genome Biol, 2014. **15**(2): p. R21.

238. Gonzalez-Aguilera, C., F. Palladino, and P. Askjaer, *C. elegans epigenetic regulation in development and aging.* Brief Funct Genomics, 2014. **13**(3): p. 223-34.

239. Wilson, K.L. and R. Foisner, *Lamin-binding Proteins.* Cold Spring Harb Perspect Biol, 2010. **2**(4): p. a000554.

240. Somech, R., et al., *The nuclear-envelope protein and transcriptional repressor LAP2beta interacts with HDAC3 at the nuclear periphery, and induces histone H4 deacetylation.* J Cell Sci, 2005. **118**(Pt 17): p. 4017-25.

241. Demmerle, J., A.J. Koch, and J.M. Holaska, *The nuclear envelope protein emerin binds directly to histone deacetylase 3 (HDAC3) and activates HDAC3 activity.* J Biol Chem, 2012. **287**(26): p. 22080-8.

242. Jacque, J.M. and M. Stevenson, *The inner-nuclear-envelope protein emerin regulates HIV-1 infectivity.* Nature, 2006. **441**(7093): p. 641-5.

243. Shun, M.C., et al., *Wild-type levels of human immunodeficiency virus type 1 infectivity in the absence of cellular emerin protein.* J Virol, 2007. **81**(1): p. 166-72.

244. Mulky, A., et al., *The LEM domain proteins emerin and LAP2alpha are dispensable for human immunodeficiency virus type 1 and murine leukemia virus infections.* J Virol, 2008. **82**(12): p. 5860-8.

245. De Andrea, M., et al., *The mouse interferon-inducible gene Ifi204 product interacts with the Tpr protein, a component of the nuclear pore complex.* Journal of interferon & cytokine research : the official journal of the International Society for Interferon and Cytokine Research, 2002. **22**(11): p. 1113-21.

246. Graham, F.L., et al., *Characteristics of a human cell line transformed by DNA from human adenovirus type 5.* J Gen Virol, 1977. **36**(1): p. 59-74.

247. Pear, W.S., et al., *Production of high-titer helper-free retroviruses by transient transfection.* Proc Natl Acad Sci U S A, 1993. **90**(18): p. 8392-6.

248. DuBridge, R.B., et al., *Analysis of mutation in human cells by using an Epstein-Barr virus shuttle system.* Mol Cell Biol, 1987. **7**(1): p. 379-87.

249. Ponten, J. and E.H. Macintyre, *Long term culture of normal and neoplastic human glia.* Acta Pathol Microbiol Scand, 1968. **74**(4): p. 465-86.

250. Princen, K., et al., *Establishment of a novel CCR5 and CXCR4 expressing CD4+ cell line which is highly sensitive to HIV and suitable for high-throughput evaluation of CCR5 and CXCR4 antagonists.* Retrovirology, 2004. **1**: p. 2.

251. Cavarelli, M., et al., *HIV-1 with multiple CCR5/CXCR4 chimeric receptor use is predictive of immunological failure in infected children.* PLoS One, 2008. **3**(9): p. e3292.

252. Kozak, S.L., et al., *Roles of CD4 and coreceptors in binding, endocytosis, and proteolysis of gp120 envelope glycoproteins derived from human immunodeficiency virus type 1.* J Biol Chem, 1999. **274**(33): p. 23499-507.

253. Kozak, S.L., J.M. Heard, and D. Kabat, *Segregation of CD4 and CXCR4 into distinct lipid microdomains in T lymphocytes suggests a mechanism for membrane destabilization by human immunodeficiency virus.* J Virol, 2002. **76**(4): p. 1802-15.

254. Princen, K., et al., *Inhibition of human immunodeficiency virus replication by a dual CCR5/CXCR4 antagonist.* J Virol, 2004. **78**(23): p. 12996-3006.

255. Foster, T.L., et al., *Resistance of Transmitted Founder HIV-1 to IFITM-Mediated Restriction.* Cell Host Microbe, 2016. **20**(4): p. 429-442.

256. Tsuchiya, S., et al., *Induction of maturation in cultured human monocytic leukemia cells by a phorbol diester.* Cancer Res, 1982. **42**(4): p. 1530-6.

257. Auwerx, J., *The human leukemia cell line, THP-1: a multifacetted model for the study of monocyte-macrophage differentiation.* Experientia, 1991. **47**(1): p. 22-31.

258. Kitano, K., et al., *Differentiating agents facilitate infection of myeloid leukemia cell lines by monocytotropic HIV-1 strains.* Blood, 1990. **76**(10): p. 1980-8.

259. Konopka, K., et al., *Long-term noncytopathic productive infection of the human monocytic leukemia cell line THP-1 by human immunodeficiency virus type 1 (HIV-1IIIB).* Virology, 1993. **193**(2): p. 877-87.

260. Ushijima, H., et al., *Characterization of cells of the myeloid-monocytic lineage (ML-1, HL-60, THP-1, U-937) chronically infected with the human immunodeficiency virus-1.* Pathobiology, 1993. **61**(3-4): p. 145-53.

261. Mikovits, J.A., et al., *Negative regulation of human immune deficiency virus replication in monocytes. Distinctions between restricted and latent expression in THP-1 cells.* J Exp Med, 1990. **171**(5): p. 1705-20.

262. Clapham, P.R., et al., *Human immunodeficiency virus infection of monocytic and T-lymphocytic cells: receptor modulation and differentiation induced by phorbol ester.* Virology, 1987. **158**(1): p. 44-51.

263. Meylan, P.R., et al., *In vitro differentiation of monocytoid THP-1 cells affects their permissiveness for HIV strains: a model system for studying the cellular basis of HIV differential tropism.* Virology, 1993. **193**(1): p. 256-67.

264. Konopka, K. and N. Duzgunes, *Expression of CD4 controls the susceptibility of THP-1 cells to infection by R5 and X4 HIV type 1 isolates.* AIDS Res Hum Retroviruses, 2002. **18**(2): p. 123-31.

265. Tsuchiya, S., et al., *Establishment and characterization of a human acute monocytic leukemia cell line (THP-1).* Int J Cancer, 1980. **26**(2): p. 171-6.

266. Goujon, C., et al., *Evidence for IFNalpha-induced, SAMHD1-independent inhibitors of early HIV-1 infection.* Retrovirology, 2013. **10**: p. 23.

267. Northrop, J.P., K.S. Ullman, and G.R. Crabtree, *Characterization of the nuclear and cytoplasmic components of the lymphoid-specific nuclear factor of activated T cells (NF-AT) complex.* J Biol Chem, 1993. **268**(4): p. 2917-23.

268. Usami, Y. and H. Gottlinger, *HIV-1 Nef responsiveness is determined by Env variable regions involved in trimer association and correlates with neutralization sensitivity.* Cell Rep, 2013. **5**(3): p. 802-12.

269. Pizzato, M., et al., *Dynamin 2 is required for the enhancement of HIV-1 infectivity by Nef.* Proc Natl Acad Sci U S A, 2007. **104**(16): p. 6812-7.

270. Nehls, J., et al., *HIV-1 replication in human immune cells is independent of TAR DNA binding protein 43 (TDP-43) expression.* PLoS One, 2014. **9**(8): p. e105478.

271. Zhang, X., et al., *Identification of SERINC5-001 as the Predominant Spliced Isoform for HIV-1 Restriction.* J Virol, 2017. **91**(10).

272. Zufferey, R., et al., *Multiply attenuated lentiviral vector achieves efficient gene delivery in vivo.* Nat Biotechnol, 1997. **15**(9): p. 871-5.

273. Ikeda, Y., et al., *The influence of gag on HIV-1 species specific tropism.* J Virol, 2004. **78**(21): p. 11816-11822.

274. Schaller, T., S. Hue, and G.J. Towers, *An active TRIM5 protein in rabbits indicates a common antiviral ancestor for mammalian TRIM5 proteins.* J Virol, 2007. **81**(21): p. 11713-21.

275. Schaller, T., et al., *Nuclear import of SAMHD1 is mediated by a classical karyopherin alpha/beta1 dependent pathway and confers sensitivity to VpxMAC induced ubiquitination and proteasomal degradation.* Retrovirology, 2014. **11**: p. 29.

276. Bainbridge, J.W., et al., *In vivo gene transfer to the mouse eye using an HIV-based lentiviral vector; efficient long-term transduction of corneal endothelium and retinal pigment epithelium.* Gene Ther, 2001. **8**(21): p. 1665-8.

277. Naldini, L., et al., *In vivo gene delivery and stable transduction of nondividing cells by a lentiviral vector.* Science, 1996. **272**(5259): p. 263-7.

278. Towers, G., et al., *A conserved mechanism of retrovirus restriction in mammals.* Proc Natl Acad Sci U S A, 2000. **97**(22): p. 12295-9.

279. Bock, M., et al., *Use of a transient assay for studying the genetic determinants of Fv1 restriction.* J Virol, 2000. **74**(16): p. 7422-30.

280. Strappe, P.M., et al., *Identification of unique reciprocal and non reciprocal cross packaging relationships between HIV-1, HIV-2 and SIV reveals an efficient SIV/HIV-2 lentiviral vector system with highly favourable features for in vivo testing and clinical usage.* Retrovirology, 2005. **2**: p. 55.

281. Poeschla, E.M., F. Wong-Staal, and D.J. Looney, *Efficient transduction of nondividing human cells by feline immunodeficiency virus lentiviral vectors.* Nat Med, 1998. **4**(3): p. 354-7.

282. Mitrophanous, K., et al., *Stable gene transfer to the nervous system using a non-primate lentiviral vector.* Gene Ther, 1999. **6**(11): p. 1808-18.

283. Ikeda, Y., et al., *Gene transduction efficiency in cells of different species by HIV and EIAV vectors.* Gene Ther, 2002. **9**(14): p. 932-8.

284. Negre, D., et al., *Characterization of novel safe lentiviral vectors derived from simian immunodeficiency virus (SIVmac251) that efficiently transduce mature human dendritic cells.* Gene Ther, 2000. **7**(19): p. 1613-23.

285. Johnston, E., et al., *Panel of prototypical infectious molecular HIV-1 clones containing multiple nucleoside reverse transcriptase inhibitor resistance mutations.* AIDS, 2005. **19**(7): p. 731-3.

286. Levy, D.N., et al., *Dynamics of HIV-1 recombination in its natural target cells.* Proc Natl Acad Sci U S A, 2004. **101**(12): p. 4204-9.

287. Popovic, M., et al., *Detection, isolation, and continuous production of cytopathic retroviruses (HTLV-III) from patients with AIDS and pre-AIDS.* Science, 1984. **224**(4648): p. 497-500.

288. Ochsenbauer, C., et al., *Generation of transmitted/founder HIV-1 infectious molecular clones and characterization of their replication capacity in CD4 T lymphocytes and monocyte-derived macrophages.* J Virol, 2012. **86**(5): p. 2715-28.

289. Schaller, T., et al., *Effects of Inner Nuclear Membrane Proteins SUN1/UNC-84A and SUN2/UNC-84B on the Early Steps of HIV-1 Infection.* J Virol, 2017. **91**(19).

290. Goodchild, R.E. and W.T. Dauer, *The AAA+ protein torsinA interacts with a conserved domain present in LAP1 and a novel ER protein.* J Cell Biol, 2005. **168**(6): p. 855-62.

291. Schindelin, J., et al., *Fiji: an open-source platform for biological-image analysis.* Nat Methods, 2012. **9**(7): p. 676-82.

292. Pizzato, M., et al., *A one-step SYBR Green I-based product-enhanced reverse transcriptase assay for the quantitation of retroviruses in cell culture supernatants.* J Virol Methods, 2009. **156**(1-2): p. 1-7.

293. Donahue, D.A., et al., *SUN2 Overexpression Deforms Nuclear Shape and Inhibits HIV.* J Virol, 2016. **90**(8): p. 4199-4214.

294. Donahue, D.A., et al., *SUN2 Silencing Impairs CD4 T Cell Proliferation and Alters Sensitivity to HIV-1 Infection Independently of Cyclophilin A.* J Virol, 2017. **91**(6).

295. Owens, C.M., et al., *Human and simian immunodeficiency virus capsid proteins are major viral determinants of early, postentry replication blocks in simian cells.* J Virol, 2003. **77**(1): p. 726-31.

296. Ganser-Pornillos, B.K., A. Cheng, and M. Yeager, *Structure of full-length HIV-1CA: a model for the mature capsid lattice.* Cell, 2007. **131**(1): p. 70-79.

297. Best, S., et al., *Positional cloning of the mouse retrovirus restriction gene Fv1.* Nature, 1996. **382**(6594): p. 826-9.

298. Bishop, K.N., et al., *Characterization of an amino-terminal dimerization domain from retroviral restriction factor Fv1.* J Virol, 2006. **80**(16): p. 8225-35.

299. Schaller, T., et al., *Fusion of cyclophilin A to Fv1 enables cyclosporine-sensitive restriction of human and feline immunodeficiency viruses.* J Virol, 2007. **81**(18): p. 10055-63.

300. Yap, M.W., et al., *The design of artificial retroviral restriction factors.* Virology, 2007. **365**(2): p. 302-14.

301. Haque, F., et al., *SUN1 interacts with nuclear lamin A and cytoplasmic nesprins to provide a physical connection between the nuclear lamina and the cytoskeleton.* Molecular and cellular biology, 2006. **26**(10): p. 3738-51.

302. Haque, F., et al., *Mammalian SUN protein interaction networks at the inner nuclear membrane and their role in laminopathy disease processes.* J Biol Chem, 2010. **285**(5): p. 3487-98.

303. Patel, J.T., et al., *Mitotic phosphorylation of SUN1 loosens its connection with the nuclear lamina while the LINC complex remains intact.* Nucleus, 2014. **5**(5): p. 462-73.

304. Malone, C.J., et al., *UNC-84 localizes to the nuclear envelope and is required for nuclear migration and anchoring during C. elegans development.* Development, 1999. **126**(14): p. 3171-81.

305. Hodzic, D.M., et al., *Sun2 is a novel mammalian inner nuclear membrane protein.* The Journal of biological chemistry, 2004. **279**(24): p. 25805-12.

306. Padmakumar, V.C., et al., *The inner nuclear membrane protein Sun1 mediates the anchorage of Nesprin-2 to the nuclear envelope.* J Cell Sci, 2005. **118**(Pt 15): p. 3419-30.

307. Sosa, B.A., et al., *LINC complexes form by binding of three KASH peptides to domain interfaces of trimeric SUN proteins.* Cell, 2012. **149**(5): p. 1035-47.

308. Starr, D.A. and H.N. Fridolfsson, *Interactions between nuclei and the cytoskeleton are mediated by SUN-KASH nuclear-envelope bridges.* Annu Rev Cell Dev Biol, 2010. **26**: p. 421-44.

309. Starr, D.A. and M. Han, *Role of ANC-1 in tethering nuclei to the actin cytoskeleton.* Science, 2002. **298**(5592): p. 406-9.

310. Scherthan, H., A. Sfeir, and T. de Lange, *Rap1-independent telomere attachment and bouquet formation in mammalian meiosis.* Chromosoma, 2011. **120**(2): p. 151-7.

311. Crabbe, L., et al., *Human telomeres are tethered to the nuclear envelope during postmitotic nuclear assembly.* Cell Rep, 2012. **2**(6): p. 1521-9.

312. Link, J., et al., *Analysis of meiosis in SUN1 deficient mice reveals a distinct role of SUN2 in mammalian meiotic LINC complex formation and function.* PLoS Genet, 2014. **10**(2): p. e1004099.

313. Ding, X., et al., *SUN1 is required for telomere attachment to nuclear envelope and gametogenesis in mice.* Dev Cell, 2007. **12**(6): p. 863-72.

314. Schmitt, J., et al., *Transmembrane protein Sun2 is involved in tethering mammalian meiotic telomeres to the nuclear envelope.* Proc Natl Acad Sci U S A, 2007. **104**(18): p. 7426-31.

315. Borrego-Pinto, J., et al., *Samp1 is a component of TAN lines and is required for nuclear movement.* J Cell Sci, 2012. **125**(Pt 5): p. 1099-105.

316. Wang, W., et al., *Structural insights into SUN-KASH complexes across the nuclear envelope.* Cell Res, 2012. **22**(10): p. 1440-52.

317. Luxton, G.W., et al., *TAN lines: a novel nuclear envelope structure involved in nuclear positioning.* Nucleus, 2011. **2**(3): p. 173-81.

318. Chang, W., et al., *Linker of nucleoskeleton and cytoskeleton (LINC) complex-mediated actin-dependent nuclear positioning orients centrosomes in migrating myoblasts.* Nucleus, 2015. **6**(1): p. 77-88.

319. Yu, J., et al., *KASH protein Syne-2/Nesprin-2 and SUN proteins SUN1/2 mediate nuclear migration during mammalian retinal development.* Hum Mol Genet, 2011. **20**(6): p. 1061-73.

320. Meinke, P., et al., *Muscular dystrophy-associated SUN1 and SUN2 variants disrupt nuclear-cytoskeletal connections and myonuclear organization.* PLoS Genet, 2014. **10**(9): p. e1004605.

321. Matsumoto, A., et al., *Global loss of a nuclear lamina component, lamin A/C, and LINC complex components SUN1, SUN2, and nesprin-2 in breast cancer.* Cancer Med, 2015. **4**(10): p. 1547-57.

322. Lv, X.B., et al., *SUN2 exerts tumor suppressor functions by suppressing the Warburg effect in lung cancer.* Sci Rep, 2015. **5**: p. 17940.

323. Hoffenberg, S., et al., *A novel membrane-anchored Rab5 interacting protein required for homotypic endosome fusion.* J Biol Chem, 2000. **275**(32): p. 24661-9.

324. Salazar-Gonzalez, J.F., et al., *Genetic identity, biological phenotype, and evolutionary pathways of transmitted/founder viruses in acute and early HIV-1 infection.* J Exp Med, 2009. **206**(6): p. 1273-89.

325. Liu, Z., et al., *The highly polymorphic cyclophilin A-binding loop in HIV-1 capsid modulates viral resistance to MxB.* Retrovirology, 2015. **12**: p. 1.

326. Billich, A., et al., *Mode of action of SDZ NIM 811, a nonimmunosuppressive cyclosporin A analog with activity against human immunodeficiency virus (HIV) type 1: interference with HIV protein-cyclophilin A interactions.* J Virol, 1995. **69**(4): p. 2451-61.

327. Price, A.J., et al., *Active site remodeling switches HIV specificity of antiretroviral TRIMCyp.* Nat Struct Mol Biol, 2009. **16**(10): p. 1036-42.

328. Turgay, Y., et al., *SUN proteins facilitate the removal of membranes from chromatin during nuclear envelope breakdown.* The Journal of cell biology, 2014. **204**(7): p. 1099-109.

329. Liu, Q., et al., *Functional association of Sun1 with nuclear pore complexes.* J Cell Biol, 2007. **178**(5): p. 785-98.

330. Li, P. and A.A. Noegel, *Inner nuclear envelope protein SUN1 plays a prominent role in mammalian mRNA export.* Nucleic Acids Res, 2015. **43**(20): p. 9874-88.

331. Zhou, L. and N. Pante, *The nucleoporin Nup153 maintains nuclear envelope architecture and is required for cell migration in tumor cells.* FEBS Lett, 2010. **584**(14): p. 3013-20.

332. Talamas, J.A. and M.W. Hetzer, *POM121 and Sun1 play a role in early steps of interphase NPC assembly.* The Journal of cell biology, 2011. **194**(1): p. 27-37.

333. Hulme, A.E., et al., *Identification of capsid mutations that alter the rate of HIV-1 uncoating in infected cells.* J Virol, 2015. **89**(1): p. 643-51.

334. Rihn, S.J., et al., *Extreme genetic fragility of the HIV-1 capsid.* PLoS Pathog, 2013. **9**(6): p. e1003461.

335. Chin, C.R., et al., *Direct Visualization of HIV-1 Replication Intermediates Shows that Capsid and CPSF6 Modulate HIV-1 Intra-nuclear Invasion and Integration.* Cell Rep, 2015. **13**(8): p. 1717-31.

336. Qi, M., R. Yang, and C. Aiken, *Cyclophilin A-dependent restriction of human immunodeficiency virus type 1 capsid mutants for infection of nondividing cells.* J Virol, 2008. **82**(24): p. 12001-8.

13. Acknowledgements

I would like to thank my primary supervisor Dr. Torsten Schaller for his support, ideas and discussions on this challenging project and to give me this big chance to work before in Frankfurt and later here, in Heidelberg. I am gratefull to my TAC committee members, Prof. Hans Georg Kräusslich, who revised this thesis thoroughly, and Dr. Marina Lusic. Thank you for constructive input during my annual progress all over this PhD, for providing excellent suggestions and feedback. I would also like to acknowledge Dr. Pierre-Yves Lozach and Dr. Freddy Frischknecht for being supportive and generous to be part of my defense committee.

I would also like to thank all the people in the department here in Heidelberg and in Frankfurt, who were always willing to provide help and suggestions and,

most of all, for always sharing laughter, big smiles and positive attitude. I thank especially Robin, Martin, Vojtech, Shawon and Annica from my office, Virginia and obviously Niko and Luca, who made me feel home often with their Mediterranean attitude.

A big huge thanks to friends who have supported me during this time. Especially the “Ziegler veterans” Dwain, Ivan, Gian Mario, Viktor and Francesco, my cool flatmate Romolo, Matthias, as well as Giuseppe and Matteo during my great experience in Frankfurt. Thank you guys for sharing so much together over these years and for your incredible patience, generosity, understanding, encouragement and humour.

I deeply thank you Mina, for your immense patience and trust in me, for your constant love and for always smiling and showing interest in everything around me…as well as reviewing this thesis.

Finally, a special thanks goes to my parents and my sister for their unconditional love and for having always supported and encouraged me to go through with ambitions.